

**RESILIN-LIKE POLYPEPTIDE-POLY(ETHYLENE GLYCOL) HYBRID  
HYDROGELS FOR MECHANICALLY-DEMANDING TISSUE  
ENGINEERING APPLICATIONS**

by

Christopher Leland McGann

A dissertation submitted to the Faculty of the University of Delaware in partial fulfillment of the requirements for the degree of Doctor of Philosophy in Materials Science and Engineering

Spring 2015

© 2015 Christopher Leland McGann  
All Rights Reserved

ProQuest Number: 3718357

All rights reserved

INFORMATION TO ALL USERS

The quality of this reproduction is dependent upon the quality of the copy submitted.

In the unlikely event that the author did not send a complete manuscript and there are missing pages, these will be noted. Also, if material had to be removed, a note will indicate the deletion.



ProQuest 3718357

Published by ProQuest LLC (2015). Copyright of the Dissertation is held by the Author.

All rights reserved.

This work is protected against unauthorized copying under Title 17, United States Code  
Microform Edition © ProQuest LLC.

ProQuest LLC.  
789 East Eisenhower Parkway  
P.O. Box 1346  
Ann Arbor, MI 48106 - 1346

**RESILIN-LIKE POLYPEPTIDE-POLY(ETHYLENE GLYCOL) HYBRID  
HYDROGELS FOR MECHANICALLY-DEMANDING TISSUE  
ENGINEERING APPLICATIONS**

by

Christopher Leland McGann

Approved: \_\_\_\_\_  
Darrin J. Pochan, Ph.D.  
Chair of the Department of Materials Science and Engineering

Approved: \_\_\_\_\_  
Babatunde A. Ogunnaike, Ph.D.  
Dean of the College of Engineering

Approved: \_\_\_\_\_  
James G. Richards, Ph.D.  
Vice Provost for Graduate and Professional Education

I certify that I have read this dissertation and that in my opinion it meets the academic and professional standard required by the University as a dissertation for the degree of Doctor of Philosophy.

Signed:

---

Kristi L. Kiick, Ph.D.  
Professor in charge of dissertation

I certify that I have read this dissertation and that in my opinion it meets the academic and professional standard required by the University as a dissertation for the degree of Doctor of Philosophy.

Signed:

---

Darrin J. Pochan, Ph.D.  
Member of dissertation committee

I certify that I have read this dissertation and that in my opinion it meets the academic and professional standard required by the University as a dissertation for the degree of Doctor of Philosophy.

Signed:

---

Xinqiao Jia, Ph.D.  
Member of dissertation committee

I certify that I have read this dissertation and that in my opinion it meets the academic and professional standard required by the University as a dissertation for the degree of Doctor of Philosophy.

Signed:

---

Robert E. Akins, Ph.D.  
Member of dissertation committee

## ACKNOWLEDGMENTS

The path through graduate school is long and challenging, but fortunately, it is not a path one walks alone. A community of people has supported me along the way and I am forever grateful for their help and guidance.

First, I would like to thank my advisor, Dr. Kristi Kiick, as she has been an outstanding educator and mentor. I am very grateful for the opportunity that she provided me and for her enthusiasm for this project. Dr. Kiick has established an excellent environment for the development of thoughtful, dynamic researchers and has helped me grow as a scientist and engineer. Additionally, I would also like to thank the current and past members of the Kiick laboratory for their kindness and support. I would like to thank Dr. Manoj Charati and Dr. Linqing Li for their help when I started working on resilin-like polypeptides and for designing the proteins used in this dissertation. I would also like to thank Dr. Aaron Baldwin, Dr. Sarah Grieshaber, Dr. Shuang Liu, Dr. Kenneth Koehler, Dr. Atsushi Mahara, Dr. Zhixiang Tong, Dr. Rebecca Scott, Nandita Bhagwat, Aidan Zerdoum and Dr. Eric Levenson for their thoughtful conversations regarding my work as well as for their friendship. In particular, I would like to thank Dr. Levenson for introducing a bewildered graduate student to proper laboratory technique when I first started working in the Kiick laboratory. I have had the great privilege of mentoring a number of undergraduate students whose work has been instrumental to my dissertation. I would like to thank Kevin Chang, Chris Black, Rebekah Dumm, Anna Jurusik and Nile Bunce.

My committee has been a great source of support and much of this dissertation would be impossible without their assistance. I would to thank Dr. Darrin Pochan for his helpful conversations and for his instruction in polymer physics. Dr. Xinqiao Jia has been incredibly gracious in providing me access to instrumentation in her laboratory that proved vital for this project. She has also been an excellent instructor in tissue engineering and polymer chemistry. Finally, I would like to thank Dr. Robert Akins for his invaluable advice and expertise concerning the cell biology of this project. He has been a strong supporter of my research and I am very grateful.

The Department of Materials Science & Engineering and the research community of the University of Delaware have been critical to my success as a graduate student. I would like to thank Robin Buccos, Charlies Garbini, Christine Williamson, Naima Hall and Kathleen Forwood for ensuring student safety and for creating a department whose environment which is productive and friendly. Dr. Shi Bai provided me with excellent instruction in NMR spectroscopy and has been outstanding in his stewardship of a superb NMR facility. I would like to thank the members of the Delaware Biotechnology Institute BioImaging Center, Michael Moore and Dr. Jeff Caplan, for their assistance with the confocal microscopy presented in this work. Additionally, I would like to thank Derrick Allen whose expertise in the Department of Chemistry and Biochemistry machine shop helped make possible the mechanical testing investigations presented in this dissertation.

Lastly, I would like to thank my friends and family for all of the love and support they provided me throughout graduate school. My mother, father and brother provided me with the care and emotional support that got me through and I am in their debt.

## **DEDICATION**

This dissertation is dedicated to my family and friends. Thank you for your support.

## TABLE OF CONTENTS

LIST OF TABLES .....	xi
LIST OF FIGURES .....	xii
ABSTRACT .....	xxi

### Chapter

1	INTRODUCTION .....	1
1.1	Tissue Engineering & Regenerative Medicine .....	1
1.2	Hydrogels for Tissue Engineering .....	2
1.2.1	Biomimetic PEG Hydrogels for Tissue Engineering .....	4
1.2.2	Biomimetic Protein Hydrogels for Tissue Engineering .....	8
1.3	Resilin and Resilin-like Polypeptides .....	10
1.3.1	Resilin Occurrence and Biosynthesis .....	10
1.3.1.1	Occurrence .....	10
1.3.1.2	Biosynthesis .....	12
1.3.2	General Properties of Natural Resilin .....	15
1.3.3	Development and Properties of Recombinant Resilins .....	18
1.3.4	Applications of Resilin-Like Polypeptides .....	23
1.4	Biosynthetic Protein-PEG Hybrid Hydrogels .....	30
1.5	Coronary Bypass Surgery and Cardiovascular Tissue Engineering .....	32
1.6	Dissertation Summary .....	34
2	RESILIN-BASED HYBRID HYDROGELS FOR CARDIOVASCULAR TISSUE ENGINEERING .....	36
2.1	Introduction .....	36
2.2	Experimental Section .....	41
2.2.1	Materials .....	41
2.2.2	Recursive Ligation and Mutagenesis .....	41
2.2.3	Expression, Purification, and Characterization of RLPs .....	44

2.2.4	Preparation of Reduced Proteins .....	45
2.2.5	Synthesis of PEG Vinyl Sulfone Cross-linker.....	46
2.2.6	Hydrogel Formation and Oscillatory Rheology .....	47
2.2.7	<i>In Vitro</i> Cell Culture of Aortic Adventitial Fibroblasts.....	48
2.3	Results and Discussion .....	50
2.3.1	Design of RLPs.....	50
2.3.2	Protein Expression, Purification, Characterization, and Reduction.....	53
2.3.3	Oscillatory Rheology Experiments.....	58
2.3.4	Encapsulated Cell Viability and Proliferation Assays.....	63
2.4	Conclusions .....	69
3	<b>THE RESILIENCE, DEGRADATION, CYTOTOXICITY AND LIQUID-LIQUID PARTITIONING OF RESILIN-PEG HYBRID HYDROGELS .....</b>	<b>70</b>
3.1	Introduction .....	70
3.2	Experimental Section.....	73
3.2.1	Materials .....	73
3.2.2	Expression and Purification of RLP24 .....	73
3.2.3	Preparation of Reduced RLP24 .....	74
3.2.4	Hydrogel Formation and Characterization of Swelling.....	75
3.2.5	Oscillatory Rheology.....	77
3.2.6	Tensile Testing .....	78
3.2.7	Biochemical Degradation of RLP24 and RLP24-PEG Hydrogels .....	83
3.2.8	Encapsulation, Viability and Proliferation of hMSCs.....	85
3.2.9	Analysis of Liquid-Liquid Partitioning Behavior.....	87
3.3	Results & Discussion.....	88
3.3.1	Design, Expression, Purification and Preparation of Reduced RLP24.....	88
3.3.2	Oscillatory Rheology.....	93
3.3.3	Swelling Measurements.....	97
3.3.4	Tensile Testing .....	99
3.3.5	Biochemical Degradation .....	107
3.3.6	Hydrogel Degradation .....	111
3.3.7	3D Encapsulation and Proliferation of hMSCs .....	114
3.3.8	Liquid-Liquid Partitioning Behavior .....	119

3.4	Conclusions .....	125
4	PHOTOCHEMICAL CROSS-LINKING OF RESILIN-LIKE POLYPEPTIDE/PEG HYBRID HYDROGELS USING THIOL-ENE CLICK CHEMISTRY .....	127
4.1	Introduction .....	127
4.2	Experimental Section.....	131
4.2.1	Materials .....	131
4.2.2	Expression and Purification of RLPX .....	131
4.2.3	Functionalization and Characterization of RLPXN .....	132
4.2.4	Cross-linking and Oscillatory Rheology of RLPXN-PEGSH Hydrogels .....	134
4.2.5	Photoencapsulation, Culture and Viability of hMSCs .....	135
4.3	Results & Discussion.....	136
4.3.1	Design, Expression and Purification of RLPX.....	136
4.3.2	Functionalization of RLPX.....	139
4.3.3	Oscillatory Rheology of Photopolymerized RLPXN-PEGSH Hydrogels .....	145
4.3.4	Photoencapsulation of hMSCs .....	150
4.4	Conclusions .....	152
5	CONCLUSIONS AND FUTURE DIRECTIONS .....	153
5.1	Conclusions and Significance.....	153
5.2	Future Directions .....	157
5.2.1	Expression and Purification of RLPs .....	157
5.2.2	<i>In vivo</i> Experiments and Immunogenicity.....	159
5.2.3	Expanded Analysis of RLPXN-PEGSH Hydrogels .....	159
5.2.3.1	ECM Biomimicry .....	160
5.2.3.2	Photopatterning.....	161
5.2.3.3	Solubility and Liquid-Liquid Partitioning Analysis ...	162
5.2.4	Liquid-Liquid Partitioning of RLP-PEG Hydrogels .....	164
5.2.5	A New RLP Family .....	164
	REFERENCES .....	166

Appendix

A LICENSES FOR COPYRIGHTED MATERIAL..... 187

## LIST OF TABLES

<b>Table 1.1</b> Selecting materials for hydrogel preparation. Comparison of natural and synthetic polymers typically used for preparation of cell compatible hydrogels – [15] – Published by The Royal Society of Chemistry. ....	4
<b>Table 1.2</b> Amino acid composition of resilin from wing-hinge and prealar arm of locust – Reproduced from Ref. [112] with permission from Elsevier. ...	14
<b>Table 1.3</b> Mechanical properties of structural proteins and synthetics. Reproduced from Ref. [87] with permission from Springer.....	16
<b>Table 1.4</b> Secondary structure analysis: a comparison of resilin-like polypeptides. Reproduced from Ref. [87] with permission from Springer. ....	20
<b>Table 2.1</b> Amino acid analysis of the RLPs.....	56
<b>Table 2.2</b> Resilin-like polypeptides molecular weights and yields .....	58
<b>Table 2.3</b> Summary of mechanical properties for RLP-PEG hydrogels.....	63
<b>Table 3.1</b> Summary of RLPL24-PEG Hydrogel Compositions and Precursor Properties.....	76
<b>Table 3.2</b> Dimensions of the Tensile Molds .....	79
<b>Table 3.3</b> Summary of the mechanical and physical properties of RLP24-PEG hydrogels at three cross-linking ratios.....	102
<b>Table 3.4</b> Summary of resilience calculations of RLP24-PEG hydrogels.....	103
<b>Table 4.1</b> Summary of reaction conditions investigated for RLPXN functionalization .....	133
<b>Table 4.2</b> Summary of the different reaction stiochiometries and their effect on the functionality of RLPXN .....	143

## LIST OF FIGURES

- Figure 1.1** The basic principle of tissue engineering is to utilize a rational combination of cells, signals and a material scaffold to help drive the regeneration of healthy, functional tissue..... 2
- Figure 1.2** Bioactive modification of a PEG hydrogel. Bioactivity can be incorporated through the addition of matrix degradable cross-links, cell adhesion peptides and growth factors..... 6
- Figure 1.3** (A) Location of dragonfly tendon and magnified image of resilin patch within tendon. Due to di- and trityrosine molecules resilin has a characteristic blue fluorescence under UV light (B) A schematic of the putative resilin gene, CG15920, derived from *Drosophila melanogaster*. Reproduced from Ref. [138] with permission from The Royal Society of Chemistry. .... 12
- Figure 1.4** Schematic illustrating a dityrosine cross-link. .... 15
- Figure 1.5** Chitin binding of a resilin-like polypeptide bearing the second exon of CG19520 analyzed via the SDS-PAGE of chromatographic eluents. The resilin without the domain (6H-res) does not bind to the chitin conjugated beads and elutes in the unbound (UB) fraction (or flow-through). However, the inclusion of second exon in the RLP (6H-resChBD) enables binding and the protein adheres to the chitin-bearing beads. It is removed in the bound (B) fraction. The ‘T’ fractions are purified protein for reference. Reprinted with permission from Ref. [169]. Copyright 2009 American Chemical Society. .... 21
- Figure 1.6** Purification of recombinant protein by cold-coacervation. (A) Green fluorescent protein (GFP) with resilin-like fusion tag in white light is shown as two phases following coacervation. (B) The sample is shown under blue light and illustrates how the GFP is concentrated in the bottom solution. (C) Following enzymatic cleavage the liberated GFP can be separated from resilin-like fusion tag. Reproduced from Ref. [174] with permission from John Wiley and Sons. .... 24

<b>Figure 1.7</b>	Schematic illustrating the modular RLP12 protein polymer which contains repetitive elastomeric domains (blue), cell adhesion domains (red), a degradation domain (magenta) and a heparin binding domain (yellow). A 6xHis tag (bright red) for affinity chromatography is present at the N-terminus. ....	26
<b>Figure 1.8</b>	Proliferation data and fluorescent microscopy for NIH-3T3 cells seeded on a control TCPS and on RLP12 films. Scale bars represent 100 $\mu\text{m}$ . Reproduced from Ref. [100] with permission from The Royal Society of Chemistry. ....	27
<b>Figure 1.9</b>	Tensile testing experiments of 20 wt% RLP-based hydrogels. The different ratios indicate the cross-linking conditions (lysine:hydroxyl). Minimal hysteresis indicates the resilience of the hydrogels. Reprinted with permission from Ref. [105]. Copyright 2011 American Chemical Society. ....	28
<b>Figure 1.10</b>	AFM of single molecules of the titin mimetic protein. As the protein is extended by the AFM tip the force curve increases as a GB1 domain unfolds. The schemes illustrate the structure of two different versions of the titin mimetic. GB1 are the immunoglobulin-like domains and R stands for the resilin sequence. (A) GB1-R-GB1-R-GB1-R-GB1-R. (B) GB1-R-(GB1) <sub>5</sub> -R(GB1) <sub>4</sub> -R. Reproduced from Ref. [180] with permission from the Nature Publishing Group. ....	30
<b>Figure 1.11</b>	A scheme illustrating how the bioinstructive scaffold would be utilized during coronary bypass surgery. ....	34
<b>Figure 2.1</b>	Scheme of the hydrogel formation and details of the cross-linking chemistry are presented alongside the amino acid sequence of the RLPs. Additionally, a legend indicating the resilin-like and biological domains is presented beneath the amino acid sequence. The parentheses indicate repeated sequences; in total, there are 12 repeats of the resilin sequence and two repeats of the integrin-binding domain within the larger brackets. The brackets indicate the repeated sequences of the higher molecular weight RLPs (RLP12 x = 1, RLP24 x=2, RLP36 x=3, RLP48 x=4). ....	39
<b>Figure 2.2</b>	Scheme depicting of the genetic engineering for recursive ligation of RLP12 gene and final mutagenesis. The construction of each gene (RLP24, RLP36, RLP48) was the same, but only the example of the cloning of RLP24 is illustrated in the figure. ....	42

<b>Figure 2.3</b>	H NMR of PEGVS Functionalization. This figure represents the complete H-NMR spectrum of the functionalized four-arm PEG vinyl sulfone (10 kDa), an insert depicts the 6.0-7.0 ppm region with the assignments for the olefin protons on the vinyl sulfone moiety and an image of the vinyl sulfone moiety. Integration of the olefin protons was based upon an assumed 909 protons present in the PEG backbone; the values indicate approximately four vinyl sulfone groups per polymer (quantitative functionalization).....	47
<b>Figure 2.4</b>	This image provides a visual representation of the recursive ligation and the location of the resulting cysteine residues. The blue 'c' represents the cysteine residues that were engineered via site-directed mutagenesis. The black 'c' represents the cysteine residues that were originally encoded in the RLP12 gene and doubled, tripled or quadrupled by recursive ligation. ....	51
<b>Figure 2.5</b>	(A) Agarose gel showing the BamHI/HindIII digestion of pET28aRLP48, pET28aRLP36, pET28aRLP24, pET28aRLP12, & pET28a (left to right). The linearized pET28a plasmid is clearly resolved between 5000 and 6000 bp while the RLP genes are represented by the bands migrating at approximately 800 bp to 3200 bp. (B) Coomassie stained SDS-PAGE gel (12%) showing the purified RLP proteins, RLP48, RLP36, RLP24 & RLP12 (left to right). ....	52
<b>Figure 2.6</b>	MALDI-MS Spectrum of the RLP proteins. The major peaks are as follows: 27509.27 for RLP12; 49389.46 for RLP24; 71315.64 for RLP36; and 93189.71 for RLP48.....	54
<b>Figure 2.7</b>	Oscillatory rheology time sweep of a 20wt% RLP24-PEG hydrogel cross-linked at 1:1 (gray) or 3:2 (black) molar ratios of vinyl sulfone to cysteine, at 37°C with an angular frequency of 6 rad/s and a strain of 1%. The inset demonstrates that the storage modulus ( $G'$ , solid squares) exceeds the loss modulus ( $G''$ , open squares) within a minute. ....	60
<b>Figure 2.8</b>	Oscillatory rheology frequency sweep experiments for RLP24-PEG hydrogels. Frequency sweeps were conducted over a range from 0.1 to 100 rad/s for 20wt% hydrogels cross-linked at 1:1 (red) or 3:2 (black) vinyl sulfone to cysteine at 37°C. The closed squares indicate the storage modulus ( $G'$ ) and the open circles indicate the loss modulus ( $G''$ ).....	61

**Figure 2.9** Fluorescent laser scanning confocal microscopy of human aortic adventitial fibroblasts (AoAF) encapsulated in 20wt% RLP24-PEG hydrogel cross-linked at a 3:2 vinyl sulfone to cysteine ratio, stained using Live/Dead stains.<sup>TM</sup> Calcein AM (Live) stain is shown in green and ethidium homodimer (Dead) stain is shown in red. Images are z-stacks of hydrogels (200  $\mu\text{m}$  thick) taken at 10x magnification using a water lens. Representative images from (A) Day 0, (B) Day 1, (C) Day 3 and (D) Day 7 are presented; the AoAFs remain viable throughout the entire experiment. Initially, the cells are rounded but as the experiment progresses they begin to adopt a spread morphology..... 65

**Figure 2.10** Proliferation data for encapsulated human aortic adventitial fibroblasts (AoAF) in RLP24-PEG hydrogels over seven days of cell culture. The bars represent the average number of living nuclei counted at a given timepoint; the error bars represent one standard deviation from the mean and the open circles represent the counts for each hydrogel analyzed ( $n = 3$ ). The number of living cells was determined by finding the difference between the number of nuclei stained by membrane-permeable Draq5 and the number of nuclei stained by membrane-impermeable ethidium homodimer. Fluorescent laser scanning microscopy was used to analyze four adjacent z-stacks that were 1800  $\mu\text{m}$  x 1800  $\mu\text{m}$  x 400  $\mu\text{m}$  (length x width x depth) for three different hydrogels at each timepoint. Volocity was used to count the cell nuclei for both the Draq5 and the ethidium homodimer channels. The results show that the number of nuclei remains relatively stable and that by day 7 the cells may be beginning to proliferate..... 67

**Figure 3.1** Image of the large and small Teflon molds. On the left is the mold used for cyclic strain testing and on the right is the mold for strain-to-break hydrogels. (A) Front side of the mold containing the indentation. (B) Reverse side of the mold for loading precursor solution. The mold on the left had one larger injection hole due to the size of the pipette tip used to fill the mold. .... 79

**Figure 3.2** Illustration of the process for making the RLP24-PEG hydrogels for tensile testing. (A) A glass slide is used to cover the mold which is then flipped over and (B) injected with the precursor solution (water + bromophenol blue is shown for contrast). The mold is filled with the precursor (C, D) and cross-linked in a humidified chamber, overnight at 37°C. (E) The cross-linked gel is removed from the mold and small rectangular pieces of steel mesh are placed at either end to provide friction for the DMA geometry. An actual RLP24-PEG gel is shown in final image. .... 80

<b>Figure 3.3</b>	Representative graph of how adjacent averaging was utilized to create curves for resilience measurements. The black dots represent the raw data for the extension, the red dots represent the raw data for the retraction, the black line represents the adjacent average curve for extension and the red line represents the retraction adjacent average curve. ....	82
<b>Figure 3.4</b>	Illustration of how the mechanical property testing under degradation experiments were performed. (A) The PTFE cup and bottom plate for the compression geometry shown individually and (B) assembled. Vacuum grease sealed the junction between cup and plate. (C) The entire assembly installed on the DMA including the top plate for the compression geometry. Not shown was a clear plastic covering that was used to prevent evaporation. ....	85
<b>Figure 3.5</b>	Representative chromatogram from a desalting preparation of reduced RLP24. The black curve indicates UV absorbance (mAU) at 280 nm and represents the protein component. The red curve indicates the conductivity (mS/cm) and represents the salt component. The blue curve is the temperature (°C).....	92
<b>Figure 3.6</b>	(A) Representative time sweeps of RLP24-PEG hydrogels cross-linked at different ratios of vinyl sulfone to cysteine thiol. (1% strain, 6 rad/s) (B) Representative frequency sweeps of RLP24-PEG hydrogels cross-linked at different ratios of vinyl sulfone to cysteine thiol (1% strain). All RLP24-PEG hydrogels were 20wt% and tested at 37°C.....	95
<b>Figure 3.7</b>	The summary of the effect the cross-linking ratio had on the storage modulus ( $G'$ )(Pa) for RLP24-PEG hydrogels as analyzed via oscillatory rheology.....	97
<b>Figure 3.8</b>	(A) Illustrates the effect cross-linking stoichiometry has on the swelling ratio and (B) equilibrium water content. The RLP24-PEG hydrogels with lower cross-linking ratios exhibited a greater degree of swelling as anticipated.....	98
<b>Figure 3.9</b>	Representative loading/unloading curves of the RLP24-PEG hydrogels strained to 60% at a rate 0.1 mm/s. The curves depict elastic materials that exhibit a small degree of hysteresis. This corresponds to the resilience in the 85-92% range of RLP24-PEG hydrogels.....	100

<b>Figure 3.10</b> Illustrates the deformation response at 20, 40 and 60% strain of RLP24-PEG hydrogels cross-linked at (A) 1:2, (B) 1:1 and (C) 3:2 ratios of vinyl sulfone to thiol. (D) The hydrogels demonstrated a small degree of hysteresis, but there was negligible plastic deformation as consecutive tensile cycles overlaid each other in panel (D). All hydrogels were strained at 0.1 mm/s. ....	103
<b>Figure 3.11</b> Representative strain-to-break curves for each of the RLP24-PEG cross-linking ratios. ....	106
<b>Figure 3.12</b> Representative gel electrophoresis of the incubation of RLP24 (7.3 $\mu$ M) without enzyme (A) and with the catalytic domain of human recombinant MMP1 (56 nM) (B). Over a 24-hour period MMP1 cleaved RLP24 which led to the development of lower molecular weight fragments. These fragments had molecular weights that roughly corresponded to the expected products given the position of the MMP domain in RLP24. ....	108
<b>Figure 3.13</b> Scheme illustrating the degradation of soluble RLP24 via MMP1. The degradation products will have molecular weights corresponding to the fragments in the image. The different biological domains of RLP24 are labeled. ....	109
<b>Figure 3.14</b> Densitometry of the RLP24 band degraded by MMP1. Each point represents the mean of three different samples; the error is the standard deviation of those samples. Major band indicates intact RLP24 band in gel. ....	111
<b>Figure 3.15</b> Normalized compressive storage modulus of RLP24-PEG hydrogels (20wt% 3:2 vinyl sulfone to thiol) incubated in MMP1 enzyme buffer without (BLACK) and with (RED) MMP1 enzyme. Data points were acquired every 15 minutes using 5% strain at a frequency of 1Hz. ....	113
<b>Figure 3.16</b> Analysis of viability of hMSCs encapsulated in RLP24-PEG hydrogels (20wt% 3:2 vinyl sulfone: thiol) at day 0 (A), day 5 (B), day 10 (C) and day 15 (D). Maximum intensity projections of z-stacks (200-250 $\mu$ m thick) are presented. Objective was 10x water lens and scale bar represents 200 $\mu$ m. ....	115

<b>Figure 3.17</b> Proliferation of hMSCs analyzed via Click-it™ Edu Assay and fluorescent microscopy. All cell nuclei are stained with DAPI (A) and proliferative cell nuclei stained with the Alexa Fluor™ 555 (B). The final panel (C) provides a merged image with the proliferative nuclei appearing purple. Maximum intensity projection of z-stacks are depicted. ....	118
<b>Figure 3.18</b> Phase contrast images of THP cross-linked RLP hydrogels (A, C) and RLP24-PEG hydrogels (B, D). Panels (A) and (B) are taken at 5x magnification (scale bar is 500 μm) and panels (C) and (D) are taken at 10x magnification (scale bar is 100 μm). ....	120
<b>Figure 3.19</b> Phase contrast image of RLP24-PEG hydrogels illustrating the deformation of the spherical phases due to mechanical stress; a behavior which implies an element of viscoelasticity. Air bubbles in the top right do not deform in the same way. ....	122
<b>Figure 3.20</b> Confocal microscopy of the fluorescently-labeled RLP24-PEGVS hydrogels. Panels depict the (A) fluorescein channel and the PEG component of the hydrogel, (B) the transmitted channel, and (C) the rhodamine channel and the RLP24 component of the hydrogel. Panel (D) provides a composite image of all three channels. Scale bar is 200 μm. ....	123
<b>Figure 3.21</b> Depicts slides from a z-stack confocal image of encapsulated hMSCs within an RLP24-PEG hydrogel. Faint outlines of the hydrogel heterogeneity can be identified via phase contrast and cells (represented in green) appear spread around and in between this heterogeneity. (Scale bar is 100 μm).....	125
<b>Figure 4.1</b> Scheme illustrating the sequence of RLPX and the attachment of the norbornene acid. (A) Scheme illustrating the cross-linking of the RLPXN-PEGSH hydrogels (B).....	130
<b>Figure 4.2</b> Representative SDS-PAGE gel of an RLPX purification. Lanes 1 is the cell-free lysate prior to incubation with Ni-NTA resin. Lane 2-3 are the cell-free lysate ‘flow-through’ fractions. Lanes 4-7 are wash buffer fractions and lane 8 is the elution fraction containing the RLPX. The benchmark protein ladder is in the final lane. ....	138
<b>Figure 4.3</b> <sup>1</sup> H NMR spectra of RLPXN (turquoise) and RLPX (red). The entire spectrum for both is depicted in (A) and a close up of the downfield region used for analysis is depicted in (B). ....	141

- Figure 4.4**  $^1\text{H}$  NMR spectrum of RLPXN functionalized with norbornene using a 3:4 reaction stoichiometry of norbornene acid to lysine residue. The five protons on eight phenylalanine benzyl rings will integrate to 40H and the integration of the alkene protons of norbornene (6.1 ppm) equals roughly 18.21 protons for this preparation. This equates to roughly 9.1 norbornenes per RLPX molecule. .... 142
- Figure 4.5**  $^1\text{H}$  NMR spectra of different preparations of RLPXN. By modulating the stoichiometric ratio of norbornene to lysine, RLPXN with different functionality could be attained. The decrease in functionality is reflected in the decrease in peak size at 6.1 ppm. A full spectrum is presented for the 1:1 (purple), 3:4 (blue), 1:2 (green), and 1:4 (yellow) reactions in panel (A) with a close up of the 6.0-8.0 ppm region in panel (B). The decrease in alkene peak size is clearly related to the change in stoichiometry. The control RLPX is presented as the red spectra. .... 144
- Figure 4.6** Effect of weight percent on the mechanical properties of RLPXN-PEGSH hydrogels. Oscillatory rheometry was used to investigate the gelation (A) and frequency dependence (B) of the hydrogels. A summary of the average storage moduli for the different weight percent gels is also presented (C). The oscillatory time sweep was conducted using 1% strain at 1 Hz and the frequency sweep was conducted between 0.01-10 Hz at 1% strain. The simple mean of at least three samples for a given concentration was used for the summary; the error represents the standard deviation. .... 147
- Figure 4.7** The effect of irradiation on RLPXN/PEGSH solutions is demonstrated via oscillatory rheology. (A) At the beginning of the experiment (solid symbols) the RLPX-PEGSH solution was a viscous liquid, but when irradiated to an intensity of  $1 \text{ mW/cm}^2$  for 30 seconds the solution began to cross-link (open symbols) as indicated by the increase in modulus. Switching off the light stopped the reaction which is reflected by the first plateau. The gelation was restarted for 60 seconds with irradiation set to  $1 \text{ mW/cm}^2$  before being switched off again. The result was another increase in modulus followed by a plateau. The gels were then cross-linked to completion. (B) The effect of irradiation intensity on gelation is depicted. Higher irradiation intensity led to faster gelation rates of the RLPXN-PEGSH hydrogel (6wt%). .... 149

<b>Figure 4.8</b>	Representative images of composite (‘live’, ‘dead’, and transmitted channels) z-stack maximum intensity projections at day 0, 5x <b>(A)</b> and 10x <b>(B)</b> magnification; at day 14, 5x <b>(C)</b> , 10x <b>(D)</b> magnification; and at day 28, 5x <b>(E)</b> , 10x <b>(F)</b> magnification. Z-stacks range from 100 to 300 $\mu\text{m}$ in depth. (Scale bar represents 200 $\mu\text{m}$ ).....	151
<b>Figure 5.1</b>	Schematic illustrating the different RLPs in the RLPX system and the ability to tailor the biological properties of the final hydrogels. Reproduced from Ref. [101] with permission from The Royal Society of Chemistry. ....	161
<b>Figure 5.2</b>	Depicts the oscillatory time sweep <b>(A)</b> and frequency sweep <b>(B)</b> of RLPXN-PEGSH hydrogels dissolved in pure water. The mechanical properties of these hydrogels were greater than for RLPXN-PEGSH gels dissolved in PBS. ....	163

## ABSTRACT

Over the past few decades, technological progress in the life sciences and engineering has combined with important insights in the fields of biology, biotechnology and materials science to make possible the design and synthesis of biological substitutes whose goal is the restoration dysfunctional tissue. The interdisciplinary field of tissue engineering has the explicit goal of developing methods and materials which aim to restore, maintain or improve the function of tissues and organs. Researchers believe that proper biological function of diseased or damaged tissue can be restored through a rational combination of biological signals, cells and material scaffolds. This has led to the development of numerous biomimetic matrices that attempt to drive regenerative processes through replicating or mimicking the biological cues present in the extracellular-matrix, the natural scaffolding of tissue. Hydrogels, which are water-swollen networks of macromolecules, have emerged as popular material for tissue engineering applications.

Often hydrogels are composed of synthetic or naturally-derived polymers, but a third category, biosynthetic protein polymers, has become a popular alternative. Recently, a number of recombinant protein polymers with sequences derived from natural protein elastomers have been investigated due to their outstanding mechanical properties. Resilin, a rubber-like protein found in specialized compartments of arthropods, is one such protein elastomer and possesses exceptional mechanical properties including: high resilience, long fatigue lifetime and superior extensibility. The Kiick laboratory has led the development of recombinant resilin-like polypeptides

(RLP) for tissue engineering applications by designing novel protein polymers which combine the sequences of natural resilin with biomimetic domains which confer cell-material interactivity. Previous studies by our laboratory introduced RLP hydrogels which were formed through a Mannich-type condensation reaction between hydroxymethyl phosphine cross-linkers and lysine residues contained within the RLP. These hydrogels proved to be cytocompatible, hydrated networks of protein that reproduced the rubber-like properties of native resilin

In this work, we introduce a hybrid material composed of RLP cross-linked with a synthetic polymer: poly(ethylene glycol) or PEG. These hybrid hydrogels combine the chemical flexibility and biocompatibility of PEG with the precise control, high fidelity and inherent bioactivity of biosynthetic proteins. Two versions of RLP-PEG hydrogels with different methods of cross-linking were investigated: the first is based upon a Michael-type addition reaction between the thiols of cysteine residues contained within RLP and vinyl sulfone moieties end-functionalized on a multi-arm PEG macromer; the second uses a norbornene-functionalized RLP to cross-link with a thiol-functionalized multi-arm PEG macromer via a photoinitiated thiol-ene step polymerization.

Recursive ligation of an RLP gene (RLP12) encoding for twelve repeats of a resilin-like sequence and including bioresponsive domains led to a family of high molecular weight RLPs: RLP24, RLP36, and RLP48. As characterized via oscillatory rheology, these RLPs could be cross-linked with a vinyl sulfone PEG macromer into elastic hydrogels. Subsequent encapsulation and three-dimensional culture of human aortic adventitial fibroblasts and human mesenchymal stem cells demonstrated the cytocompatibility of these RLP-PEG networks. Tensile testing of RLP24-PEG

hydrogels demonstrated that they were resilient, elastic hydrogels whose mechanical stiffness could be modulated by manipulating the cross-linking ratio of vinyl sulfone to cysteine thiol. The resilin-like polypeptides were susceptible to degradation by matrix metalloproteinase enzymes as both a soluble polypeptide and when cross-linked into hydrogels. Finally, the RLP24-PEG hydrogels demonstrated phase separation behavior that led to the formation of distinct micro-phases within the cross-linked hydrogel.

Photopolymerization of polymer hydrogels has the advantage of spatiotemporal control over the formation of network cross-links; a strategy which has been successfully applied to RLP-PEG hydrogels. RLPs were functionalized with a norbornene acid through simple amide bond coupling chemistry and the functionality of the RLP-norbornene conjugates were characterized via  $^1\text{H}$  NMR spectroscopy. The RLP conjugates were then photocross-linked with thiol-terminated PEG when exposed to ultra violet irradiation. The mechanical properties were analyzed through oscillatory rheology and the cytocompatibility was assessed through the three-dimensional photoencapsulation and culture of human mesenchymal stem cells.

These RLP-PEG hydrogels demonstrate the utility in hybrid materials that combine biosynthetic proteins with synthetic polymers. As versatile, mechanically resilient and cytocompatible materials, RLP-PEG hybrid hydrogels offer a unique and exciting strategy for the development of biomimetic tissue engineering scaffolds.

## Chapter 1

### INTRODUCTION

#### 1.1 Tissue Engineering & Regenerative Medicine

Recent advances in the life sciences and engineering has made possible the design and synthesis of biological substitutes which aim to restore, maintain or improve the function of native tissues and organs. The development and investigation of methods for the regeneration of dysfunctional tissues/organs is the domain of the interdisciplinary fields of tissue engineering and regenerative medicine.<sup>[1,2]</sup> The central hypothesis of these fields is that proper biological function can be restored through a rational combination of biological signals, cells and biomimetic matrices.<sup>[3,4]</sup> More specifically, provided with the correct biochemical and biophysical cues in addition to a supportive scaffold, cells with a degree of plasticity<sup>[5]</sup> will reestablish the structure and function of native tissue. The goal of tissue engineers is to draw upon knowledge from various disciplines, such as cell biology, chemistry, biomedical engineering and materials science, in the attempt to design materials or systems that promote this regenerative behavior.<sup>[1,2]</sup> Synthetic polymeric scaffolds have emerged as a promising technology in tissue engineering as they can be facilely designed and modified to mimic the natural microenvironment of cells and tissue.<sup>[6]</sup> In fact, mimicry of the extracellular matrix (ECM), the collection of molecules that provide structural and biochemical support to cells within tissue, is a well-established paradigm followed by many in the tissue engineering field.<sup>[7]</sup> In the pursuit of functional, biomimetic

scaffolds, hydrogels have emerged as a popular subset of tissue engineering scaffolds.<sup>[8-10]</sup>

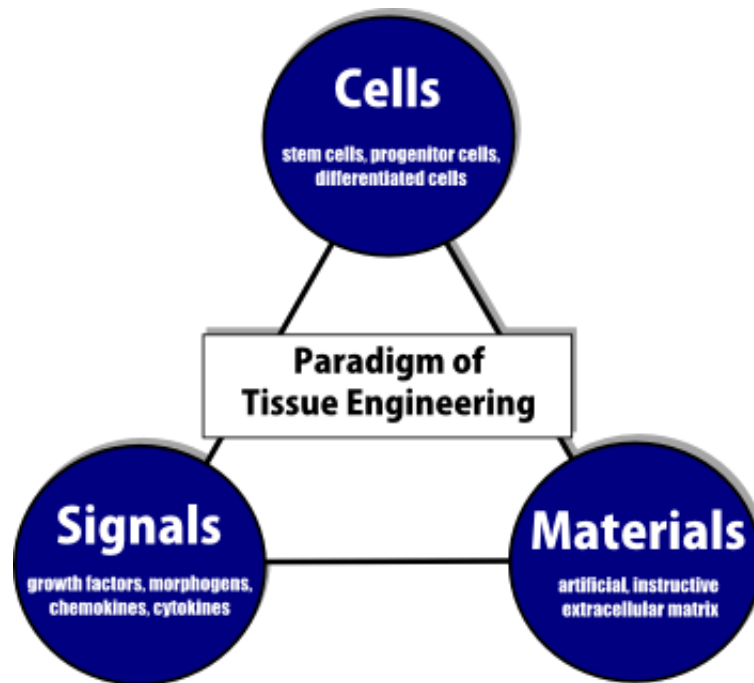


**Figure 1.1** The basic principle of tissue engineering is to utilize a rational combination of cells, signals and a material scaffold to help drive the regeneration of healthy, functional tissue.

## 1.2 Hydrogels for Tissue Engineering

Hydrogels are networks of macromolecules, chemically or physically cross-linked, which swell large quantities of water without dissolution;<sup>[9, 11]</sup> a property that allows for relatively flexible materials which resemble natural tissue.<sup>[12]</sup> Depending upon the specific polymer and method of implantation, hydrogels usually exhibit excellent biocompatibility and minimal thrombosis, inflammation or tissue damage.<sup>[9, 12]</sup> Furthermore, due to their swollen nature, they generally have high permeability for

oxygen, nutrients and other water-soluble metabolites.<sup>[12]</sup> These qualities make hydrogels an ideally suited method of delivering cells and signals to damaged tissue.

Hydrogels may be composed of either naturally-derived or synthetic polymers. Common naturally-derived polymers used for tissue engineering hydrogels include collagen/gelatin, hyaluronate, fibrin, alginate, agarose and chitosan.<sup>[9]</sup> In general, naturally-derived polymers are utilized because they are either components of native ECM or have macromolecular properties similar to ECM.<sup>[10]</sup> For example, collagen is the most abundant protein found in mammalian tissue<sup>[13]</sup> and is also major constituent of the extracellular matrix.<sup>[10]</sup> Naturally-derived polymers are advantageous due to their biocompatibility, innate bioactivity and cell-directed degradability.<sup>[9, 10]</sup> However, these polymers can exhibit batch variability, their hydrogels possess a limited range of mechanical properties and there are concerns over potential pathogen transmission as well as immunogenicity.<sup>[9, 14]</sup>

Synthetic polymers used for tissue engineering hydrogels can include poly(2-hydroxyethyl methacrylate), poly(*N*-isopropylacrylamide), poly(vinyl alcohol) and poly(ethylene glycol) or more commonly referred to as PEG.<sup>[9]</sup> In contrast to natural polymers, synthetics are appealing as hydrogel precursors since their chemistry and physical properties can be more precisely controlled and reproduced.<sup>[9, 10]</sup> By modulating the molecular weight, chemical identity, chain architecture and cross-linking functionality, one can control the gelation kinetics, mechanical properties and degradation kinetics of synthetic hydrogels.<sup>[10]</sup> While synthetic hydrogels benefit from a greater range of material properties, they usually display limited bioactivity and may require extensive purification from toxic byproducts that result from their synthesis.<sup>[9]</sup> Furthermore, the limited biodegradation of synthetics necessitates engineered

degradability usually through hydrolytic or proteolytic mechanisms.<sup>[8, 9]</sup> **Table 1.1** summarizes the differences between natural polymers and synthetics.<sup>[15]</sup>

**Table 1.1** Selecting materials for hydrogel preparation. Comparison of natural and synthetic polymers typically used for preparation of cell compatible hydrogels – [15] – Published by The Royal Society of Chemistry.

Feature/function	Natural polymers	Synthetic polymers
Biocompatibility	Polymer dependent	Polymer dependent
Bioactivity ( <i>i.e.</i> cell specific receptor)	Possible	Limited
Inherent biodegradability	✓✓	✓
Tunability of degradation kinetics	✓	✓✓
Degradation byproducts	Biocompatible	Potentially harmful
Flexibility for chemical modification	✓	✓✓
Flexibility of working range ( <i>i.e.</i> pH & ionic strength)	✓	✓✓
Tuning of mechanical properties	✓	✓✓
Commercial availability	✓	✓✓
Batch to batch variations	Likely	Controlled

### 1.2.1 Biomimetic PEG Hydrogels for Tissue Engineering

Hydrogels based upon the synthetic polymer, polyethylene glycol (PEG), have become especially attractive to biomedical researchers in the last decade.<sup>[8, 10]</sup> The polymer has been approved by the FDA for medical applications due to its biocompatibility, low toxicity, low immunogenicity and resistance to protein adsorption<sup>[8, 16, 17]</sup> The hydrophilic polymer can be synthesized through anionic or cationic polymerization<sup>[9]</sup> and into linear or branched (multiarm or star) chain architectures.<sup>[8]</sup> The hydroxyl end groups of PEG macromers can be easily converted into a variety of functional groups including: acetylene, acrylate, amine, azide, carboxyl, methyloxyl, methacrylate, norbornene, tetrazine, thiol, vinyl sulfone, *etc.*<sup>[8, 18, 19]</sup> Additionally, the end groups of an individual PEG molecule may be identical (homofunctional) or dissimilar (heterofunctional) depending upon the synthesis and

intended application.<sup>[8]</sup> The chemical flexibility of PEG allows it to be cross-linked into hydrogels using a wide range of chemistries. Furthermore, the macromers can be easily modified with bioactive molecules prior to or post gelation in order to incorporate greater functionality into the final material.<sup>[8, 20-27]</sup>

The chemical flexibility of PEG makes the polymer relatively ubiquitous in the field of tissue engineering, but its hydrophilicity and resistance to protein adsorption make the polymer especially important. The non-fouling, low immunogenic properties of the polymer in biological environments allow PEG hydrogels to effectively behave as ‘blank slates’ to which precise bioactivity may be incorporated through added biomolecules.<sup>[28, 29]</sup> Peptides, proteins, polysaccharides, *etc.* may be conjugated to or sequestered within what otherwise are inert materials in order to impart properties of cell adhesion, enzyme-sensitive degradation or the capacity to influence cell behavior (e.g. differentiation). In this way, PEG hydrogels offer a practical means of controlling cell-material interactions in a manner that mimics the function of natural ECM.<sup>[8]</sup>

For example, cell adhesion is an important prerequisite for a multitude of cellular functions including migration and proliferation.<sup>[30-33]</sup> The primary mode of cell attachment in native tissues is performed through cell-surface integrin binding to specific molecular domains present in ECM proteins such as fibronectin, laminin, elastin and collagen.<sup>[34-37]</sup> Integrin binding is crucial to tissue development and organization as it triggers important pathways which direct cell function and change cell phenotype.<sup>[38-41]</sup> The most prevalent means of introducing cell adhesive properties to PEG hydrogels is through the incorporation of short peptides which mimic these binding domains;<sup>[8]</sup> short peptides benefit from facile synthesis and higher stability in comparison to full-length proteins.<sup>[42-44]</sup> A variety of cell-adhesive peptides, derived

from ECM proteins, have been incorporated into PEG hydrogels,<sup>[8]</sup> but the RGD sequence found in fibronectin, laminin and collagen is by far the most common.<sup>[8, 42]</sup> The RGD sequence is useful for cell adhesion as it can bind to roughly half of the known integrins.<sup>[45]</sup> Often, a linear or cyclic RGD peptide is conjugated to the chain end of a PEG macromer incorporated into the hydrogel network. If provided with enough space cells will form focal adhesions with the peptide and bind to the material.<sup>[42, 46]</sup>

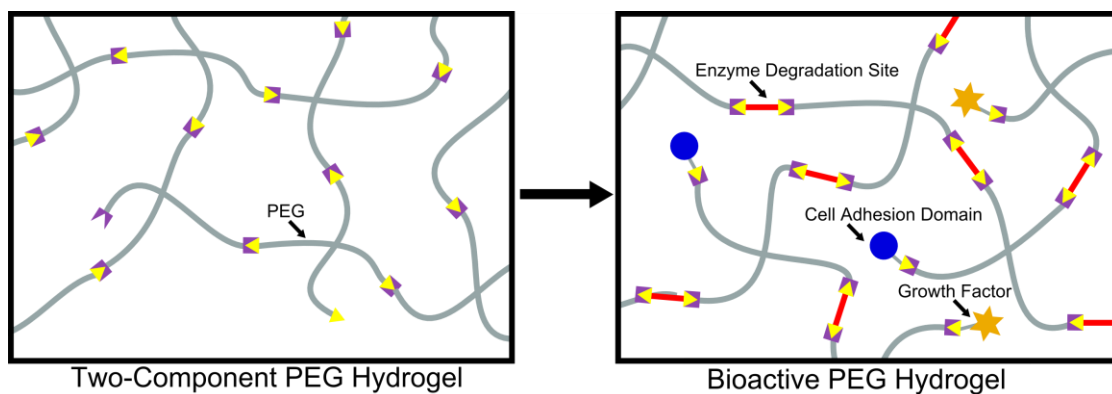


**Figure 1.2** Bioactive modification of a PEG hydrogel. Bioactivity can be incorporated through the addition of matrix degradable cross-links, cell adhesion peptides and growth factors.

Another important design criterion of tissue engineering scaffolds is degradability; as the defect site is regenerated with healthy, functional tissue, it is important that the scaffold simultaneously disappears to prevent the obstruction of the replacement tissue.<sup>[8]</sup> Since the polyether bonds which compose PEG polymers are relatively stable under physiological conditions,<sup>[47, 48]</sup> PEG hydrogels must incorporate a mechanism through which they are able to degrade. This can be either chemical

degradation<sup>[47-50]</sup> or it can be proteolytic degradation.<sup>[51-53]</sup> Proteolytic degradation is an important feature of natural ECM and plays a role in many biological processes including cell migration, tissue repair and matrix remodeling.<sup>[54-56]</sup> Many ECM proteins contain sequences which are selectively cleaved by proteolytic enzymes.<sup>[8]</sup> PEG hydrogels will often incorporate these cleavage domains, in the form of short peptides, into the backbone of the network in order to impart cell-directed degradability to the biomaterial.<sup>[8, 51-53, 57, 58]</sup> This approach allows PEG hydrogels to be selectively degraded by the cells driving the regeneration process.

The presentation of biological cues/signals is another crucial aspect of natural tissue development.<sup>[8]</sup> These signaling molecules consist of mitogens, responsible for cell division; morphogens, responsible for controlling tissue formation; and growth factors (GF).<sup>[59]</sup> Growth factors, which are a class of pro- or antiproliferative proteins, influence a variety of cell behavior including differentiation, migration, proliferation and gene expression.<sup>[60, 61]</sup> Native ECM serves an important role in regulating the activity of GF by sequestering the soluble forms through bound proteoglycans; this maintains the active conformation of the GF as well as its local concentration.<sup>[62]</sup> Recent study has demonstrated that bound GF may elicit a different biological response than soluble versions of the same molecule.<sup>[63]</sup> For example, bound vascular endothelial growth factor (VEGF) induces the sprouting of blood vessels while soluble VEGF encourages vessel dilation.<sup>[64-70]</sup> Mimicry of the dynamic relationship between ECM and GF has been attempted through the bioactive modification of PEG hydrogels using two different methods: (1) covalent attachment and (2) specific interaction. Covalent attachment of GF molecules to PEG hydrogels can be achieved through chemistries already present on the protein or through chemical modification of

the GF.<sup>[8]</sup> In some cases, researchers forgo full-length proteins in favor of short peptide sequences derived from the active domains of a particular GF.<sup>[43, 44, 71]</sup> Incorporating molecules with binding affinity for GF is another method of introducing this form of bioactivity to PEG hydrogels. For instance, research by the Kiick laboratory has utilized the growth factor binding property of the glycosaminoglycan (GAG), heparin, to sequester VEGF and other GFs within PEG hydrogels.<sup>[26, 27, 72, 73]</sup>

### **1.2.2 Biomimetic Protein Hydrogels for Tissue Engineering**

Over the past two decades a third class of macromolecules, biosynthetic protein polymers, have become an increasingly popular field of polymer research.<sup>[74]</sup> Protein polymers are polypeptides distinguished from other proteins, such as enzymes or cytokines, by their highly conserved and repetitive sequences. In addition, they generally serve a structural function for organisms rather than a strictly biological role. Discoveries in the field of biotechnology and protein engineering have made it possible to engineer mimetic polypeptides derived from natural proteins in addition to *de novo* sequences. The advantage of the biosynthetic approach is the high fidelity of synthesis and the precise control over chemical composition, chain length and structure. Gene sequences encoding for the protein polymer of interest can be easily synthesized, manipulated through genetic cloning and very effectively expressed in a variety of host organisms.<sup>[74]</sup> These technological developments have opened up a world of opportunity for the design of novel and highly functional materials.<sup>[75-77]</sup>

Tissue engineering has been quick to adopt protein engineering methods for the purpose of developing scaffolds composed of protein polymers;<sup>[78, 79]</sup> recombinant DNA technology has been applied to the production of collagens,<sup>[80-83]</sup> spider silks,<sup>[84-86]</sup> elastin-like polypeptides (ELPs),<sup>[87-90]</sup> and fibronectins.<sup>[91, 92]</sup> Additionally,

researchers have used these methods to combine the properties of two different proteins into a single macromolecule in order to impart the final material with enhanced bioactivity. These so-called ‘chimeric proteins’ illustrate the design flexibility and potential of protein-engineered materials.<sup>[79]</sup> For example, researchers fused spider silk sequences with antimicrobial domains derived from human neutrophil defensins and hepcidin peptides in an attempt to bestow the material with antibacterial activity.<sup>[84]</sup> In fact, many of the same biomimetic properties described in **Section 1.2.1** have been engineered into protein polymers.<sup>[93-101]</sup>

Biomimetic hydrogels derived from elastomeric proteins have been a particularly exciting subset of materials designed for tissue engineering applications. Elastomeric proteins occur naturally in a wide range of biological systems where their outstanding mechanical properties serve to provide organs/tissues with rubber-like elasticity.<sup>[102]</sup> Many elastomeric proteins have been studied including: abductin and byssus found in bivalve mollusks; gluten derived from wheat; elastin and titin found in vertebrate connective tissues; as well as resilin and silks found in arthropods.<sup>[102, 103]</sup> Elastin, resilin and flagelliform silk have been characterized as “intrinsically disordered proteins” due to the lack of long range structure. As cross-linked networks the proteins are able to withstand large deformation without rupture and will recover to their original state upon unloading of the external stress. The process is thought to be entropically-driven: disordered protein chains fall into a low entropy state when stretched (greater chain organization/less degrees of freedom) and are driven to regain a high entropy state (disorder) when the force is removed.<sup>[102]</sup> Recreating these properties in protein-engineered hydrogels for application in tissue engineering has been desirable especially for tissues that are mechanically-active and require

reversible elasticity.<sup>[99, 101, 104-107]</sup> As will be described in the following section, resilin is a particularly interesting material due its outstanding rubber elasticity and its hydrophilicity.

### **1.3 Resilin and Resilin-like Polypeptides**

Resilin is an elastomeric protein found in specialized compartments of arthropods and insects. The cross-linked, hydrophilic protein displays extraordinary elasticity, extensibility, fatigue resistance and resilience. Remarkably, the mechanical properties of this hydrated protein network are in near-agreement with classic rubber-elasticity theory. Facilitated by the advances made in recombinant DNA technologies and protein engineering, resilin has become an exciting topic of study for a new class of biomaterials that may see application in tissue engineering, drug delivery, biosensors and nanobiotechnology.<sup>[87]</sup> The following sections review the occurrence of resilin in nature and the development of resilin-like polypeptides. **Section 1.3.1** provides a brief description of the synthesis and significance of resilin in nature. **Section 1.3.2** covers the properties of natural resilin and the final two sections (**Section 1.3.3 & Section 1.3.4**) review the development of resilin-like materials as well as their role in the field of biomaterials.

#### **1.3.1 Resilin Occurrence and Biosynthesis**

##### **1.3.1.1 Occurrence**

The natural covering or integument of arthropods is a hardened, colored cuticle composed of a complex extracellular product made of chitin (a polysaccharide) and tanned or fibrous proteins.<sup>[108]</sup> In 1947, La Greca identified and described a colorless, clear material within the cuticle of locusts that sharply contrasted with the typical

hardened cuticle associated with insects. These elastic hyaline structures were named “rubber-like cuticle” and were largely ignored until Weis-Fogh’s investigations of arthropod flight in the 1950s.<sup>[109, 110]</sup> He reported that these colorless, swollen proteinaceous patches exhibited perfect long-range elasticity, superior extensibility and a unique amino acid composition; further the material could support rapid deformation in insect organs without hysteresis.<sup>[108, 109, 111, 112]</sup> The protein was named resilin, which is derived from the latin *resilire* meaning “to spring back.”<sup>[111, 112]</sup> Resilin was found to be an extremely stable cross-linked protein network and was insoluble in all solvents that did not break peptide bonds.<sup>[113]</sup> The protein is commonly found in insect tissue as part of a composite containing chitin.<sup>[109, 111]</sup>

Following the initial descriptions of resilin in dragonfly and locust [tendons of dragonflies (Odonata) and wing hinges of locusts (Orthoptera)]<sup>[109, 114]</sup> the protein was discovered in other arthropods where it generally serves as the function of an elastic spring.<sup>[113, 115-118]</sup> Examples of this include the salivary pump of assassin bugs as well as the feeding/pumping mechanisms of the tsetse fly, reduviid bug and honey bee.<sup>[113, 116-118]</sup> Resilin plays an important role in the sound production of a variety of arthropods.<sup>[119-124]</sup> In the tymbals of cicada, relatively thick patches of resilin (100-150  $\mu\text{m}$ ) experience stress-release cycles in the 1-10 kHz frequency, and despite this mechanically demanding environment the energy losses can be less than 20%.<sup>[113, 119, 122-124]</sup> This low energy dissipation serves a particularly important role in insect locomotion. The protein contributes to the mechanism of insect flight in locust and dragonfly,<sup>[114]</sup> but also damselflies,<sup>[125]</sup> beetles<sup>[126]</sup> and other species in the Dermapteran order.<sup>[127]</sup> Additionally, resilin appears to facilitate the jumping mechanism of fleas<sup>[128-133]</sup> and other leaping arthropods.<sup>[134-136]</sup> Finally, the remarkable

capacity of resilin to stretch is demonstrated by the swelling of the honey ant's abdomen, which enlarges considerably when the ant gorges on food.<sup>[137]</sup>

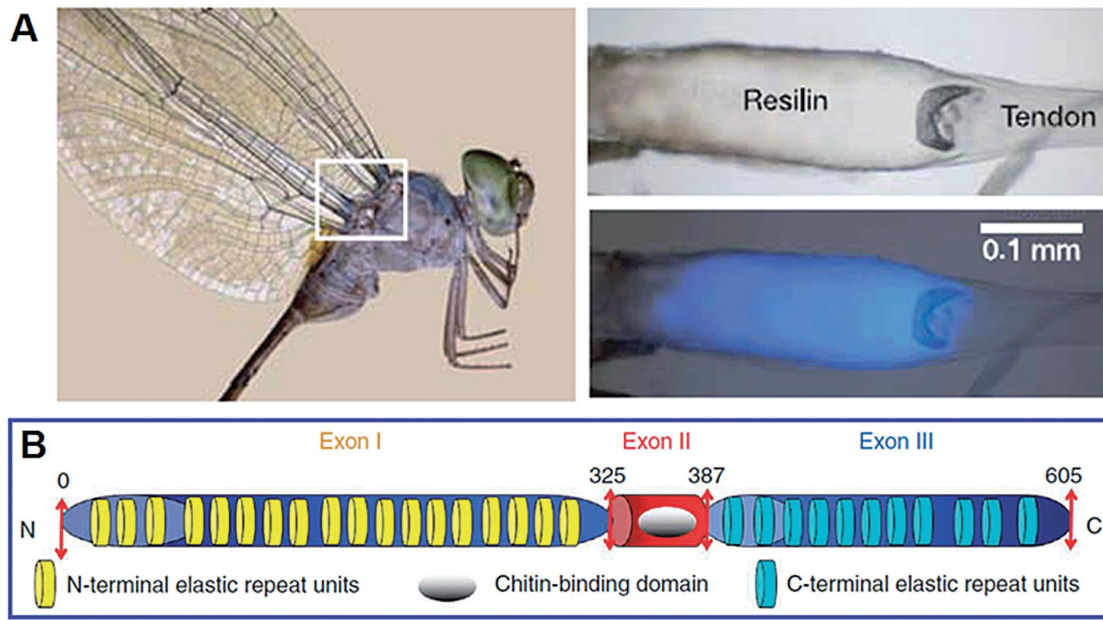


**Figure 1.3** (A) Location of dragonfly tendon and magnified image of resilin patch within tendon. Due to di- and trityrosine molecules resilin has a characteristic blue fluorescence under UV light (B) A schematic of the putative resilin gene, CG15920, derived from *Drosophila melanogaster*. Reproduced from Ref. [138] with permission from The Royal Society of Chemistry.

### 1.3.1.2 Biosynthesis

The amino acid composition of resilin was first reported in 1960;<sup>[112]</sup> however, it was not until the early 1990s that its primary structure was investigated. A study by Lombardi and Kaplan published resilin sequences which were acquired through the tryptic digests of cockroach resilin.<sup>[139]</sup> In 2001, Ardell and Andersen compared the cockroach sequences as well as sequences derived from locust resilin with the

*Drosophila melanogaster* genome. Their effort discovered two genes that would produce peptides homologous to the tryptic digest sequences from both species.<sup>[111, 140]</sup> One gene, CG15920, (*see* **Figure 1.3**) expressed a product that had an amino acid composition and isoelectric point that very closely resembled natural resilin.<sup>[140]</sup> The gene product also contained a signal peptide sequence at the N-terminus which indicates that it may be a secreted protein. Furthermore, the protein contained a variant of the Rebers-Riddiford consensus sequence that has been identified as a chitin-binding domain found in insect proteins.<sup>[140, 141]</sup> Perhaps the most important clue was the highly conserved and repetitive nature of the CG15920 gene product. In the first exon, a 15 amino acid long ‘motif’ sequence, GGRPSDSYGAPGGGN, is roughly repeated and in the third exon a sequence of 13 amino acids, GYSGGRPGGQDLG, is similarly repeated.<sup>[140]</sup> The first exon sequence has been utilized in a number of recombinant resilin-like polypeptides which demonstrate properties very similar to that of natural resilin.<sup>[105, 142-144]</sup>

The source of resilin’s hydrophilic properties is derived from its amino acid composition (*see* **Table 1.2**). Compared to collagen, elastin and silk fibroin, resilin contains a greater percentage of acidic residues and fewer non-polar residues.<sup>[109, 112]</sup> Resilin also contains a fair amount of tyrosine that is found to form two fluorescent amino acids: dityrosine and trityrosine. These two amino acids are responsible for the protein’s covalent cross-links (*see* **Figure 1.4**).<sup>[145-148]</sup> It is hypothesized that tyrosine cross-linking in natural resilin is the result of the coupling of two phenoxy radicals.<sup>[149, 150]</sup> The cross-linking and immobilization of resilin in the insect cuticle appears to occur very quickly; however, the exact mechanism is still largely unknown.<sup>[111, 151-154]</sup>

**Table 1.2** Amino acid composition of resilin from wing-hinge and prealar arm of locust – Reproduced from Ref. [112] with permission from Elsevier.

Amino acid	Resilin		Comparison		
	Residues/10 <sup>5</sup> g protein		Residues/10 <sup>5</sup> g protein		
	Average wing-hinge	Prealar arm	Collagen (ox-hide)	Elastin (ox ligamentum nuchae)	Silk fibroin ( <i>bombyx mori</i> )
Asp	113	122	52	4.5	16
Thr	35	34	19	8	12
Ser	91	91	41	8	160
Glu	53	54	76	14	14
Pro	87	89	125	156	5
Gly	448	414	354	398	590
Ala	129	120	116	212	389
Val	30	36	21	148	30
Met	Nil	Nil	6.5	(<1)	Nil
iLeu	20	19	14	31	9
Leu	26	27	28	66	7
Tyr	29	35	5	9	69
Phe	30	27	14	30	8
Amide N	(102)	-	(46)	(3)	-
Lys	6	-	27	3	4
His	8.5	-	4.5	0.5	2
Arg	40	-	47	5	6
<b>Tota</b>	1,145	1,128	1,063	1,093	1,321

Results of amino acid analysis performed on resilin from the locust *Schistocerca gregaria*, compared with values for collage, elastin and silk fibroin.

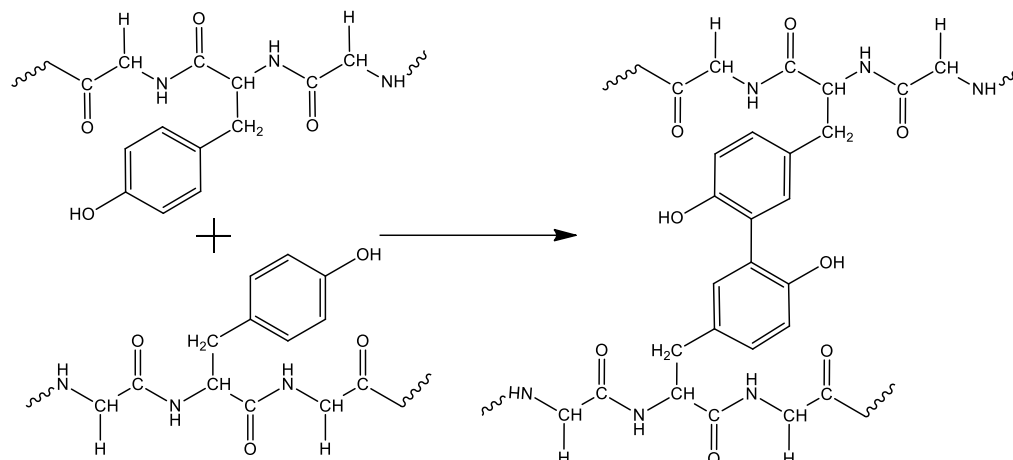


**Figure 1.4** Schematic illustrating a dityrosine cross-link.

### 1.3.2 General Properties of Natural Resilin

Natural resilin is a remarkably stable protein that is resistant to both high temperatures and protein coagulants. Degradation only occurs at 140-150°C and a number of fixatives, tanning agents and coagulants fail to alter the protein from its rubbery state. Only by drying or dehydrating in alcohol will the protein behave like a glassy polymer, but its rubber-like properties will return when reintroduced to water. The protein will only degrade in either extreme pH or in the presence of proteolytic enzymes. Natural resilin is a very concentrated material with a water-content near 50% at neutral pH and a refractive index that exceeds 1.4. Finally, due to its stable covalent cross-links, the protein is insoluble in all solvents and is resistant to common protein chaotropes.<sup>[109]</sup>

**Table 1.3** Mechanical properties of structural proteins and synthetics. Reproduced from Ref. [87] with permission from Springer.

Material	Modulus, $E_{init}$ (GPa)	Strength $\sigma_{max}$ (GPa)	Extensibility $\epsilon_{max}$	Toughness (MJ/m <sup>3</sup> )	Resilience (%)
Elastin (bovine ligament)	0.0011	0.002	1.5	1.6	90
Resilin (dragonfly tendon)	0.002	0.004	1.9	4	92
Collagen (mammalian tendon)	1.2	0.12	0.13	6	90
Mussel byssus, distal ( <i>M. californianus</i> )	0.87	0.075	1.09	45	28
Mussel byssus, proximal ( <i>M. californianus</i> )	0.016	0.035	2.0	35	53
Dragline silk ( <i>A. diadematus</i> )	10	1.1	0.3	160	35
Viscid silk ( <i>A. diadematus</i> )	0.003	0.5	2.7	150	35
Kelvar	130	3.6	0.027	50	-
Carbon fibre	300	4	0.013	25	-
High-tensile steel	200	1.5	0.008	6	-
Poly(glycerol-sebacate)	0.00028	-	2.67	-	-
Poly(PEG-citrate)	0.00191	0.00151	15.05	-	-
Natural rubber	0.002	0.030	9	-	-
Chloroprene rubber	0.003	0.022	10	-	-

Table summarizes the mechanical properties of structural proteins, high performance synthetic materials and synthetic elastomers.

Along with elastin, resilin is a structural protein which fulfills both definitions of an “elastic” material: (1) it is stretchy or flexible (i.e. extensible) and (2) it deforms in proportion to the magnitude of an applied stress without a loss of energy and it recovers completely (i.e. resilience).<sup>[155]</sup> Resilin from the dragonfly tendon was capable of stretching up to 400% of its resting length before breaking. Additionally, weeks of an applied tensile stress did not permanently deform the protein and it was still able to return to its original length following removal of the stress.<sup>[155]</sup> Dynamic mechanical analysis of resilin revealed very little energy loss to heat as a percentage of stored elastic energy: only 3.5% per half cycle when strained at 15-20 cycles/s. At

higher frequencies (200 cycles/s) the energy losses only crept up to 10% and as mentioned previously, the protein in cicada tymbals was similarly resilient.<sup>[113, 114, 119, 123, 124]</sup>

An interesting characteristic of resilin is the complete lack of long-range structure. No fine structure could be revealed through electron microscopy and zero crystallinity was detected by X-ray diffraction measurements conducted on natural resilin. Only when the protein was strained did any evidence for microcrystalline structure emerge and this was likely due to chain alignment.<sup>[156]</sup> The lack of structure might explain the near-ideal rubber elasticity of resilin. As a network of disordered protein chains, resilin would lose entropy when an external force is applied because the strain would limit the number of available chain conformations. Once the external force is removed, the protein chains are driven back to a high entropy (disordered) state and the material is restored.<sup>[111, 157, 158]</sup> Resilin was in remarkable agreement with rubber elasticity theory despite the fact that it was a hydrated protein that could participate in a variety of hydrophobic and electrostatic interactions.<sup>[111, 157]</sup>

The inherent disorder of the resilin network and its subsequent mechanical properties may be explained through its amino acid sequence and composition. Analysis of elastomeric protein sequences reveals a highly-conserved motif: the proline-glycine dyad. This amino acid dyad has been found in vertebrae elastins, molluscan byssus fibers, glutenin, and spider silks.<sup>[159-161]</sup> It has been suggested that the  $\beta$ -turn, a conformation of proline-glycine dyad, is responsible for elastomeric behavior of some of these proteins.<sup>[160, 161]</sup> One mechanism that has been proposed for elastin and glutenin is based upon the tendency for those proteins to form tandem  $\beta$ -turns. The dampening of internal chain dynamics upon extension of the resulting  $\beta$ -

spiral structure is considered to be responsible for the elasticity.<sup>[162]</sup> However, it should be mentioned that this is not necessarily settled within the literature. The presence of the proline-glycine dyad in resilin suggests some sort of structural importance, but investigations have provided very little evidence for the  $\beta$ -spiral model.<sup>[163]</sup> In fact, rigorous analysis of resilin-like polypeptides indicates an equilibrium between folded  $\beta$ -turns and extended structures which would suggest that resilin behaves like an entropic spring<sup>[164]</sup>. An interesting theory proposed by Rausher *et al.* speculates that the role of the proline glycine dyad is simply to prevent regular structure: prolines have the tendency to disrupt secondary structure due to their rigid conformation while glycines are too flexible to form secondary structures.<sup>[164, 165]</sup> The combination of both within the resilin sequence provides the protein with disordered polypeptide chains that behave like entropic springs.

### 1.3.3 Development and Properties of Recombinant Resilins

Following the discovery of the *Drosophila* resilin gene, CG15920, Elvin *et al.* cloned, expressed and purified the first exon of the gene as a soluble protein using an *Escherichia coli* host. This protein, named rec1-resilin, could form concentrated hydrogel networks (greater than 20 wt%) through the reaction of tyrosine residues using a Ru(II)-mediated photochemical method or by a peroxidase from *Arthomyces ramosus*. The protein was initially produced using isopropyl  $\beta$ -D-thiogalactopyranoside (IPTG)-induced expression, but yields of rec1-resilin were relatively low: 15 mg/L culture volume.<sup>[142]</sup> Later improvements using high cell density fermentation and a two-step induction method inspired by Studier auto-induction lead to higher yields of relatively pure rec1-resilin. Reported yields were as high as 300 mg/L culture volume.<sup>[166, 167]</sup> The purification of rec1-resilin was

improved by replacing affinity chromatography with a facile non-chromatographic “salting-out and heating” method. This method precipitated proteins from cell-free lysate using ammonium sulfate precipitation and was followed by a heating step that selectively precipitated bacterial proteins. Resilin’s extraordinary heat stability and hydrophilicity kept the protein soluble while other proteins denatured, aggregated, and precipitated out of solution. By separating the resilin from the aggregated protein via centrifugation relatively pure product could be obtained.<sup>[166]</sup>

Resilin-like polypeptides (RLPs) have been constructed using recursive ligation of short double stranded oligonucleotides which encode for the consensus motif sequence of different resilins. One such polypeptide, Dros16, contains sixteen repeats of the resilin consensus sequence, GGRPSDSYGAPGGGN, derived from rec1-resilin (the first exon of the CG19520 gene). Another polypeptide, An16, was synthesized using the same cloning technique, but the consensus sequence, AQTSSQYGAP, is a homolog found in *Anopheles gambiae* (African malaria mosquito). The *Anopheles* sequence contains a different amino acid composition from the *Drosophila* sequences, rec1-resilin and Dros16, but the YGAP motif is conserved.<sup>[168]</sup>

Investigations into the physical properties of recombinant resilins reveal behavior that closely matches natural resilin. Elvin *et al.* and Lyons *et al.* reported that as network hydrogels, the recombinant resilins (rec1, An16, Dros16) all exhibited blue fluorescence that is characteristic of the tyrosine cross-links.<sup>[142, 144]</sup> Additionally, the proteins demonstrated remarkable heat stability, which was another trait identified in natural resilin.<sup>[109, 166, 168]</sup> Structural investigations of the An16 resilin via Raman spectroscopy, 2D-NMR and small angle X-ray scattering indicated a lack of consistent

secondary structure when the protein was either a cross-linked gel or a soluble polypeptide.<sup>[163]</sup> Circular dichroism (CD) studies on all three recombinant resilins demonstrated a variety of different conformations, including  $\beta$ -sheets, turns, and poly (L-proline II) (PPII) structures. However, the vast majority, approximately 45-60% of the proteins, remain disordered.<sup>[144]</sup>

**Table 1.4** Secondary structure analysis: a comparison of resilin-like polypeptides. Reproduced from Ref. [87] with permission from Springer.

Resilin-like polypeptide and sequence motif	Technique	Helices (%)	Strands (%)	Turns (%)	Unordered (%) (or random coil)	Beta sheet (%)	PPII (%)
An16 - AQTPSSQYGAP	CD	5	-	11	64	10	10
Dros16 - GGRPSDSYGAPGGGN	CD	5.3	-	11.8	45.7	27.3	9.9
Rec1 resilin- GGRPSDSYGAPGGGN irregularly repeating	CD	2	-	11	58	18	11
Full-length <i>Drosophila</i> Resilin (two motifs)	FTIR	11.9	15.3	29.1	43.8	-	-
	CD	9.8	16.1	17.5	41.6	-	-
Cross-linked <i>Drosophila</i> resilin (two motifs)	FTIR	14.2	19.9	24.4	41.4	-	-
	CD	9.3	15.7	17.9	42.7	-	-

Table illustrates the preponderance of disorder or random coil structure for resilin-like polypeptides.

A critical test of a successfully designed resilin-like polypeptide is whether the mechanical properties of the protein match that of natural resilin. Mechanical testing of recombinant resilin has been conducted through tensile measurements or atomic force microscopy (AFM). Hydrogels comprising cross-linked rec1-resilin, An16, and Dros16 measured using AFM were found to have negligible hysteresis and resilience of  $97\pm 3\%$ ,  $98\pm 4\%$  and  $91\pm 5\%$ , respectively. The resilience was confirmed through tensile testing measurements which were also used to investigate the extensibility of

these materials. Rec1-resilin hydrogels had strain-to-break values of  $250\pm 43\%$  while An16 hydrogels could be stretched up to  $347\pm 61\%$  before breaking. A lower degree of cross-linking might explain the disparity in the strain-to-break values. The An16 hydrogels had only a 14.3% dityrosine content compared to the 18.8-21% dityrosine content of rec1-resilin. Finally, the tensile modulus was found to be  $26.9\pm 9$  kPa for rec1-resilin and  $5.7\pm 2$  kPa for An16.<sup>[142, 144]</sup>

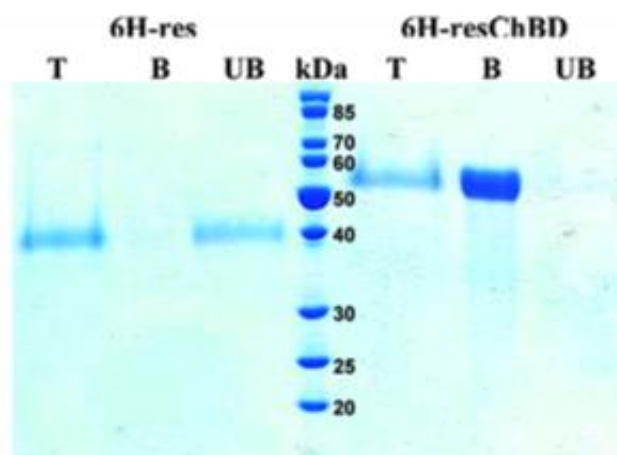


**Figure 1.5** Chitin binding of a resilin-like polypeptide bearing the second exon of CG19520 analyzed via the SDS-PAGE of chromatographic eluents. The resilin without the domain (6H-res) does not bind to the chitin conjugated beads and elutes in the unbound (UB) fraction (or flow-through). However, the inclusion of second exon in the RLP (6H-resChBD) enables binding and the protein adheres to the chitin-bearing beads. It is removed in the bound (B) fraction. The ‘T’ fractions are purified protein for reference. Reprinted with permission from Ref. [169]. Copyright 2009 American Chemical Society.

In a more recent investigation, Qin *et al.* cloned and expressed the full-length resilin protein derived from the *Drosophila* CG15920 gene (*see* **Figure 1.3B**); this

protein included all three of the exons contained in the gene. Two additional resilin proteins were produced in this study: one encoded for the first exon alone and a separate encoded the first two exons. The second exon contains the Rebers-Riddiford sequence variant that is important for chitin binding. Following purification, it was demonstrated that the inclusion of the second exon was necessary for the resilin protein to bind to chitin-conjugated beads (*see* **Figure 1.5**); the resilin which encoded only the first exon did not bind to beads.

Through infrared spectroscopy (FTIR) and CD analysis, it was found that the full-length protein exhibited structure in approximately 60% of the sequence (*see* **Table 1.4**). In both the soluble protein and in cross-linked gels this structure was composed of turns, strands and helical structures. The full-length resilin was cross-linked into hydrogels using horseradish peroxidase and the mechanical properties tested via AFM. It was found to contain very similar resilience to other RLPs and natural resilin.<sup>[169]</sup> In a separate study, the researchers compared a recombinant resilin protein derived from the first exon of the CG19520 gene to one derived from the third exon. Interestingly, both proteins were largely unstructured and both exhibited resilience, but the resilience of the first exon protein more closely matched that of natural resilin. Therefore, it was suggested that the first exon may be more important to the elastomeric behavior of resilin. In the same study, the researchers introduced a new way to cross-link the protein through a citrate-modified photo-Fenton system that uses a combination of citrate, iron, peroxide and UV light to initiate cross-linking.<sup>[170]</sup> A third report by Qin *et al.* attempted to describe the mechanism of resilin elasticity through analysis of the full-length *Drosophila* resilin protein. Based upon observations of resilin self-assembly, they believe that the first exon of the resilin protein transmits

elastic energy to the third exon sequence which then transforms into a highly ordered  $\beta$ -turn structure that behaves as a temporary energy depot. When the stress is removed or reduced the third exon region unravels and releases the potential energy back to the network via the first exon sequence.<sup>[171]</sup> This model for the elasticity of resilin is an interesting one, but further evidence, such as an exploration of naturally-derived resilin for this behavior, would be necessary for confirmation.

### 1.3.4 Applications of Resilin-Like Polypeptides

Thermo-responsive behavior is a characteristic of many polymers and often manifests itself through the presence of an upper or lower critical solution temperature (UCST or LCST, respectively). A mixture of polymers will lose miscibility and form separate phases when the temperature is raised/lowered past this critical temperature.<sup>[172]</sup> In 2005, Elvin *et al.* reported upon the thermo-responsive behavior of rec1-resilin: when cooled a resilin solution would separate into protein-rich and protein-poor phases.<sup>[142]</sup> Other recombinant resilin protein polymers demonstrated this cold coacervation behavior, which was also found to be reversible upon heating<sup>[168]</sup>. Following the initial descriptions of this behavior, Dutta *et al.* used dynamic light scattering measurements to precisely quantify what was reported to be the dual phase behavior of rec1-resilin. In other words, the protein appeared to have both UCST and LCST behavior.<sup>[173]</sup> Lyons *et al.*, took advantage of the UCST behavior by using resilin-like polypeptides as fusion tags for the purification of recombinant proteins. Purification through cold-coacervation led to pure, highly concentrated product.<sup>[174]</sup> This method mirrors the *inverse transition cycling* (ITC) method of purification that uses ELPs as thermo-responsive fusion tags to purify protein.<sup>[175]</sup> By incorporating

ELPs or RLPs as fusion tags in the design of biosynthetic proteins, one could expedite and improve the process of purification.<sup>[174]</sup>

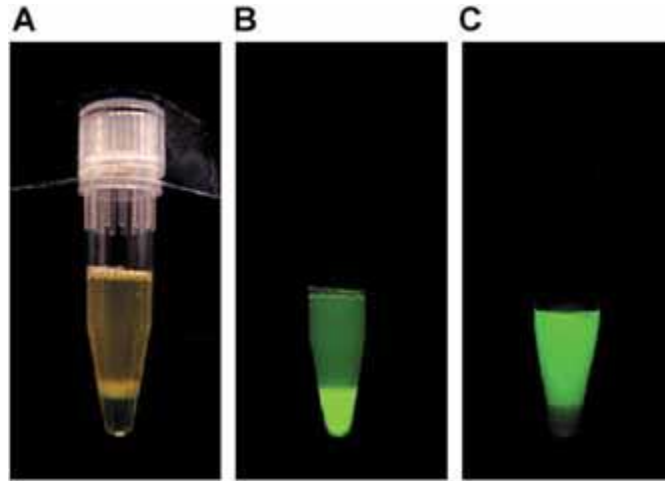


**Figure 1.6** Purification of recombinant protein by cold-coacervation. **(A)** Green fluorescent protein (GFP) with resilin-like fusion tag in white light is shown as two phases following coacervation. **(B)** The sample is shown under blue light and illustrates how the GFP is concentrated in the bottom solution. **(C)** Following enzymatic cleavage the liberated GFP can be separated from resilin-like fusion tag. Reproduced from Ref. [174] with permission from John Wiley and Sons.

Understanding and controlling protein adsorption to surfaces is crucial for any application where an artificial material is placed in a complex biological environment. Dutta *et al.* reported the fabrication of controlled nanostructures composed of rec1-resilin protein adsorbed to different substrates. By modulating pH and surface hydrophilicity, the researchers were able to assemble a variety of different morphologies of adsorbed resilin-like polypeptide.<sup>[176]</sup> In a different application of rec1-resilin, Truong *et al.* demonstrated that the protein adsorbed to the surface of a

gold substrate with different conformations and that the behavior was pH dependent. Adsorbed resilin could be induced into compact or brush-like conformations that formed quickly and were reversible. It is thought that such a property might have application in nanobiotechnology as either a biosensor or for control over cell behavior.<sup>[177]</sup> Vashi *et al.* found that rec1-resilin and the RLP, An16, were able to easily passivate tissue culture polystyrene (TCPS) through photochemical conjugation of the polypeptides to the surface. Normally adherent fibroblasts would lose the ability to bind to the plastic following this passivation. This method presented a fairly simple means of modifying TCPS and could potentially be used to introduce specific bioactive functionality to the surface.<sup>[178]</sup>

Driven by the excellent mechanical properties of resilin materials, a number of research groups have designed tissue engineering scaffolds composed of RLPs. In 2009, Charati *et al.* introduced a modular RLP (RLP12) that contained twelve repeats of a slightly modified resilin-like motif sequence: GGRPSDSFGAPGGGN. The tyrosine residues normally present in the resilin motif were replaced with phenylalanine to facilitate potential future studies involving photochemical crosslinking using non-canonical amino acids. In addition to the resilin sequences, the RLP12 polypeptide contained domains for cell binding, proteolytic degradation, and heparin immobilization. The cell binding domain was derived from the tenth type-III domain of fibronectin, RGDSP, and was incorporated in several locations along the polypeptide chain. The degradable domain was based upon a matrix metalloproteinase sensitive sequence, GPQG↓IWGQ, and the heparin-binding domain was composed of the following positively-charged sequence: KAAKRPKAAKDKQTK. The purpose of including a heparin-binding domain was to immobilize heparin which could in turn

bind growth factors such as vascular endothelial growth factor (VEGF) or basic fibroblast growth factor (bFGF).

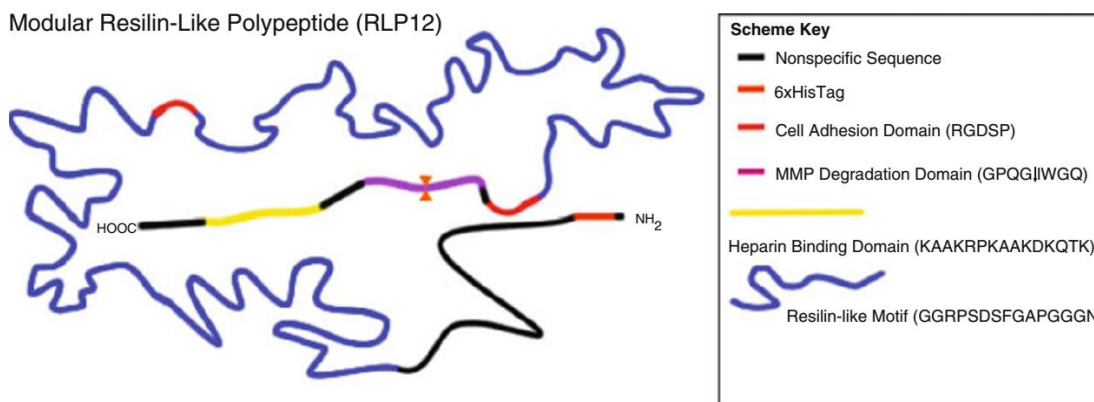


**Figure 1.7** Schematic illustrating the modular RLP12 protein polymer which contains repetitive elastomeric domains (blue), cell adhesion domains (red), a degradation domain (magenta) and a heparin binding domain (yellow). A 6xHis tag (bright red) for affinity chromatography is present at the N-terminus.

RLP12 was expressed using a BL21Star(DE3)/pET28a expression system and Studier auto-induction. Bacterial cell pellets were lysed and the cell free lysate could be purified using Ni-nitrilotriacetic acid (NTA) chromatography since the RLP12 incorporated a 6xHis fusion tag. The structure of RLP12 was investigated using CD and FTIR spectroscopy; the results demonstrated that the recombinant protein was largely unordered, but there was evidence for a small population of  $\beta$ -turns. Unlike the previously mentioned RLPs, RLP12 was crosslinked through the Mannich-type reaction between lysine residues and a hydroxymethyl phosphine cross-linker (THPP: b-[Tris(hydroxymethyl) phosphino] propionic acid). Hydrogels were cross-linked at

25 wt% precursor concentration and the mechanical properties were analyzed via oscillatory rheology and tensile testing. Two-dimensional culture of NIH-3T3 cells indicated initial evidence for the cyto-compatibility of the material. The cells appeared to adhere and proliferate on RLP12 scaffolds.<sup>[100]</sup>

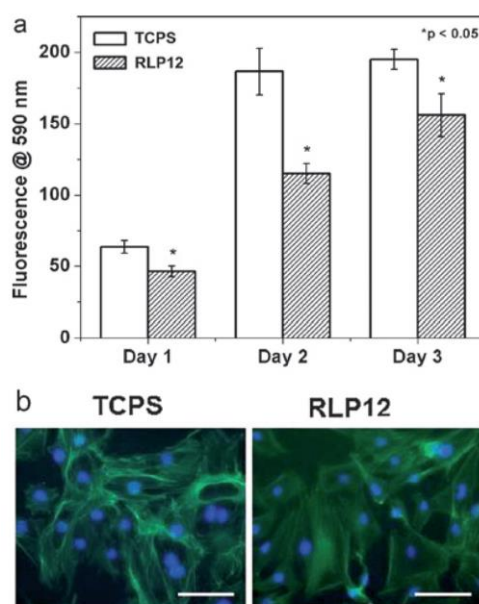


**Figure 1.8** Proliferation data and fluorescent microscopy for NIH-3T3 cells seeded on a control TCPS and on RLP12 films. Scale bars represent 100  $\mu\text{m}$ . Reproduced from Ref. [100] with permission from The Royal Society of Chemistry.

A more thorough analysis of the properties of the RLP12 gels demonstrated that the stiffness of the hydrogels could be modulated by adjusting the cross-linking ratio (lysine:hydroxyl). Further tensile testing demonstrated that the hydrogels were mechanically resilient (in excess of 90% resilience) and highly extensible (strain-to-breaks reaching 335%). Furthermore, the moduli of these hydrogels were comparable

to vocal fold tissue which would make the RLP12 hydrogels excellent candidate scaffolds for vocal fold tissue engineering. Even when the material was tested at high frequencies (30-150 Hz), its properties appeared suitable for that application.<sup>[105]</sup>

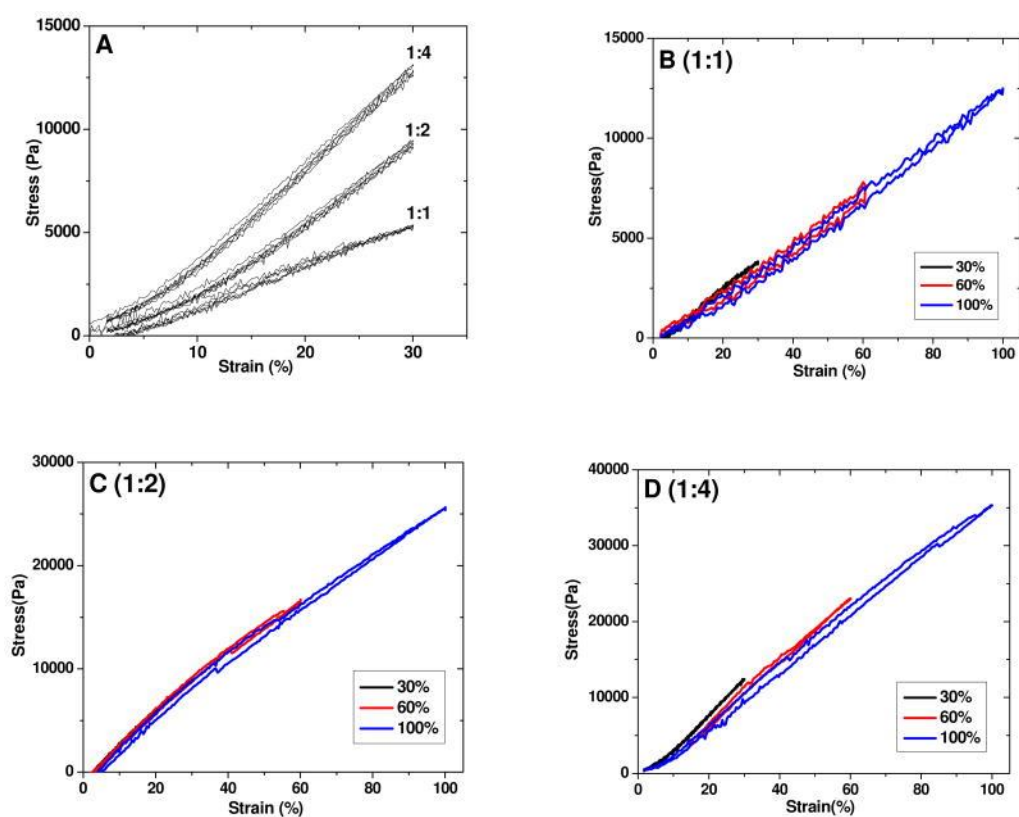


**Figure 1.9** Tensile testing experiments of 20 wt% RLP-based hydrogels. The different ratios indicate the cross-linking conditions (lysine:hydroxyl). Minimal hysteresis indicates the resilience of the hydrogels. Reprinted with permission from Ref. [105]. Copyright 2011 American Chemical Society.

Renner *et al.* has also pursued the development of modular RLPs for tissue engineering applications, but based the elastomeric domain off of the resilin sequence derived from *Anopheles gambiae* resilin (AQTSSQYGAP). Two RLPs were

synthesized: the first included repeats of the *A. gambiae* sequence and a cell binding domain; the second substituted the cell binding domain for a VEGF mimetic peptide. The expression of these RLPs proved to be difficult as only truncated or degraded RLP was produced using standard protocols. Only by lowering the expression temperature and protecting against ‘leaky’ expression were the researchers able to successfully produce the RLPs.<sup>[179]</sup> In a following publication, these resilin-like polypeptides were cross-linked using tris(hydroxymethyl)phosphine (THP), an analogue to THPP. Oscillatory rheology and compression testing demonstrated that the hydrogels exhibited stable, viscoelastic properties. Two dimensional culture of hMSCs demonstrated negligible cytotoxicity and the hMSCs appeared to bind to the resilin sequences containing cell adhesion domains.<sup>[99]</sup>

A final application of RLPs in tissue engineering materials was reported by Lv *et al.* In this report, a biomimetic of the giant muscle protein, titin, was constructed as block copolymer of immunoglobulin-like domains separated by resilin sequences. Native titin contains an alternating ordered/unordered structure which allows the protein to behave as a complex molecular spring. Under high stretching forces the immunoglobulin-like domains can unfold, dissipate energy and prevent damage. The mechanical properties of the biomimetic were analyzed through AFM techniques: the AFM tip pulled on single molecules of the protein while the researchers monitored the stress response. As shown in **Figure 1.10**, this AFM method could demonstrate the sequential unfolding of the ordered domains. Additionally, the titin-mimetic could be cross-linked into a hydrated biomaterial via a  $[\text{Ru}(\text{bpy})_3]^{2+}$  photochemical strategy.<sup>[180]</sup>

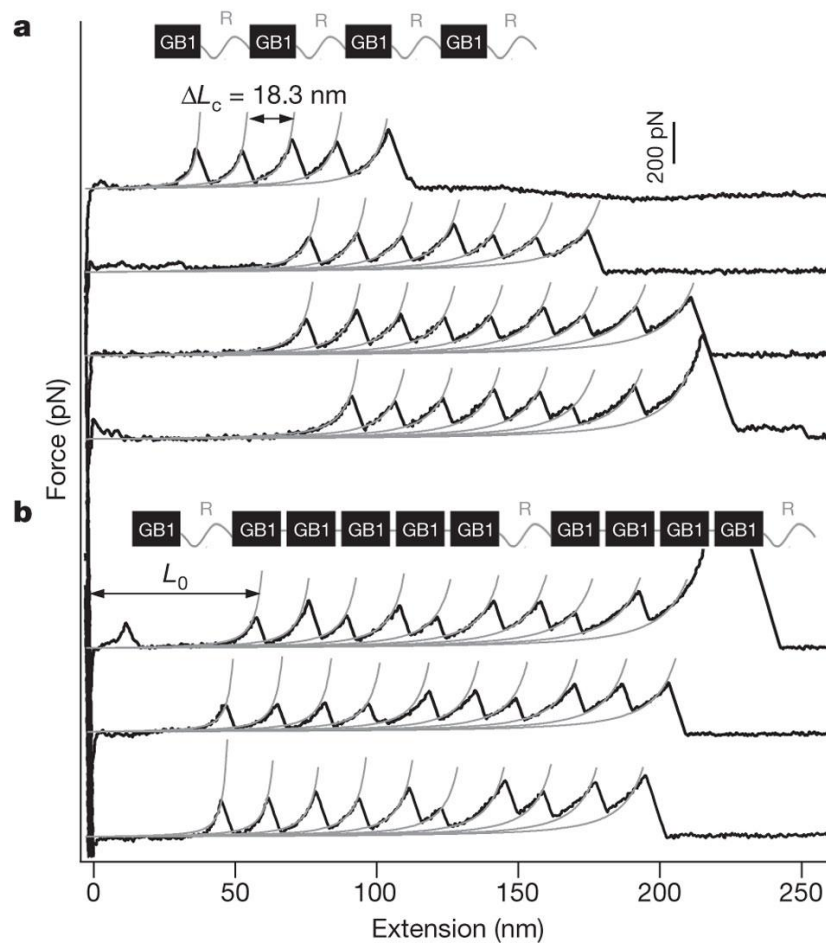


**Figure 1.10** AFM of single molecules of the titin mimetic protein. As the protein is extended by the AFM tip the force curve increases as a GB1 domain unfolds. The schemes illustrate the structure of two different versions of the titin mimetic. GB1 are the immunoglobulin-like domains and R stands for the resilin sequence. **(A)** GB1-R-GB1-R-GB1-R-GB1-R. **(B)** GB1-R-(GB1)<sub>5</sub>-R(GB1)<sub>4</sub>-R. Reproduced from Ref. [180] with permission from the Nature Publishing Group.

#### 1.4 Biosynthetic Protein-PEG Hybrid Hydrogels

As discussed in **Section 1.2.1** and **Section 1.2.2**, many hydrogel materials for biomedical applications have been developed using PEG macromers or biosynthetic proteins. The chemical flexibility and biocompatibility of PEG as well as the precise

control and high fidelity of biosynthetic proteins make these precursor macromolecules ideally suited for tissue engineering applications. It should come as little surprise that hybrid materials, which see to combine the advantages offered by both macromolecules, have also been investigated. In 2002, Halstenberg, *et al.* reported upon hydrogels that were constructed using a protein-*graft*-PEG macromer cross-linked through photopolymerization. Briefly, a recombinant protein containing fibrinogen and ATIII-mimetic domains was engineered and expressed in *E. coli*. Purified protein was conjugated with PEG-acrylate chains that were subsequently photopolymerized to form cross-linked hydrogels. These hydrogels were found to cross-link instantly upon exposure to light as well support the culture and migration of neonatal human foreskin fibroblasts (hFF).<sup>[95]</sup> In two publications, Rizzi *et al.* explored hybrid hydrogels consisting of vinyl sulfone functionalized PEG macromers and recombinant protein mimetics based upon fibrinogen and collagen. These hydrogels were cross-linked using a mild Michael-type addition reaction between thiols of cysteine residues contained within the polypeptide and vinyl sulfone moieties present at the chain ends of PEG macromers. The mechanical and swelling properties of the hydrogels could be modulated through precursor concentration while the degradability was controlled through the inclusion of proteolytic domains within the polypeptide sequence. The author demonstrated that hFF cells could adhere to the hybrid hydrogels and that encapsulated cells migrated within the material. Finally, in a rat calvarial defect model, only the hydrogels sensitive to proteolytic degradation were found to support bone regeneration.<sup>[96, 97]</sup>

Despite this apparent success of the hybrid hydrogel approach there were not any other reports of such materials in the tissue engineering field for many years. To

this author's knowledge, the initial work by the Hubbell laboratory described above was the extent of research into recombinant protein/PEG hydrogels for tissue engineering applications. Fortunately, there has been renewed interest in this approach by the Kiick laboratory<sup>[104]</sup> and the Heilshorn laboratory.<sup>[181]</sup> Both research groups have created hydrogels composed of PEG and a recombinant elastomeric protein. The Heilshorn laboratory uses ELPs and PEG while our laboratory has pursued RLP-based hybrid materials.<sup>[104, 181]</sup> As will be demonstrated in the following chapters, RLP-PEG hydrogels are cytocompatible, bioactive, and mechanically resilient networks that support three-dimensional cell culture. RLP-PEG hydrogels are promising materials that may serve as cell-instructive scaffolds for mechanically-demanding tissue engineering applications such as vocal fold<sup>[101, 106]</sup> or cardiovascular tissue.

## **1.5 Coronary Bypass Surgery and Cardiovascular Tissue Engineering**

Cardiovascular diseases are the leading cause of mortality in the world with an estimated 17.3 million deaths caused by disorders of the heart and blood vessels in 2008 alone.<sup>[182]</sup> Of those deaths, coronary heart disease was responsible for an estimated 7.3 million.<sup>[183]</sup> By 2030 the number of deaths caused by cardiovascular diseases will climb to 23.3 million and most will be the result of heart disease or stroke.<sup>[182, 184]</sup> Currently, the principal treatment for coronary artery disease is to utilize angioplasty to open blockages or to surgically place bypass grafts derived from saphenous vein tissue. Unfortunately, these grafts are susceptible to failure due to maladaptive remodeling of the vein graft in response to the elevated mechanical stresses characteristic of arterial tissue.<sup>[185]</sup>

Grafts derived from synthetic materials, such as PTFE or Dacron<sup>TM</sup>, are vulnerable to thrombosis or even infection; additionally, synthetics lack growth

potential which limits their use in the pediatric population.<sup>[186]</sup> Tissue-engineered blood vessels (TEBVs) offer promise as completely biological, living, autologous vessels produced *in vitro* for application as small-diameter conduits for bypass surgery.<sup>[187-189]</sup> TEBVs are artificial vessels which are fabricated using cells from patient tissue; they may be fabricated by seeding a tube-shaped scaffold which degrades leaving a mature vessel or by rolling 2D cell-sheets into tubes which are then assembled into a vessel. Unfortunately, an autologous source of cells must be expanded *ex vivo* for the creation of the construct and extensive culture is required for the vessel to mature; both requirements mean long lead times (months) for the bypass surgery, a condition that may be unacceptable for the patient. Decellularization of the TEBV would allow for long-term storage, but acellular grafts have their own challenges. They often fail if their diameter is less than 6 mm due to thrombosis and they often need mechanical support from synthetic materials.<sup>[189]</sup>

A third approach would use hydrogels as a therapeutic agent for saphenous vein bypass graft surgery. By themselves vein grafts may have unsuitable mechanical properties to function as arterial tissue. However, cell-instructive hydrogels applied to the exterior of the vein graft could provide mechanical support while potentially guiding the development of healthy neo-adventitium as well as attenuating the maladaptive responses which ultimately lead to graft failure. Such an approach would negate the need for long periods of *ex vivo* vessel growth and maturation as the material could be readily applied during surgery. Hybrid hydrogels based upon recombinant resilin-like polypeptides and PEG macromers are well suited for this application for several reasons: (1) they can be cross-linked quickly following injection; (2) they can be easily engineered for bioactivity through inclusion of different

biological domains and (3) the sharpness the reversible elasticity of resilin that would help the material deal with the repetitive forces associated with blood flow.

### Instructive Hydrogel Application in Coronary Bypass Surgery

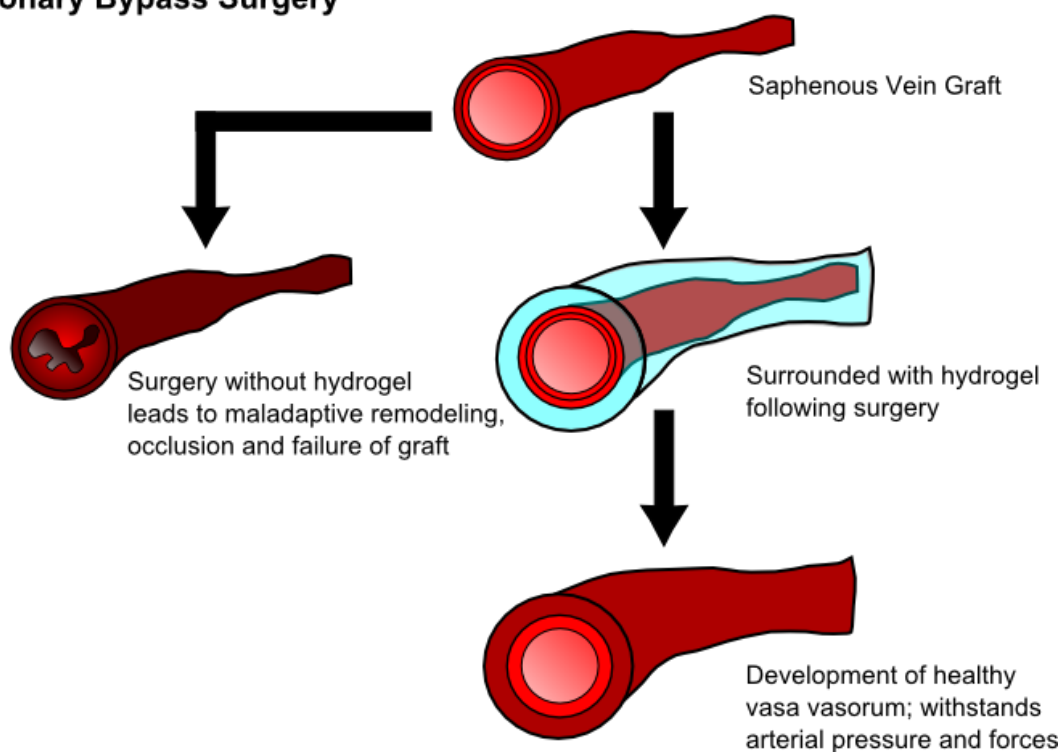


**Figure 1.11** A scheme illustrating how the bioinstructive scaffold would be utilized during coronary bypass surgery.

### 1.6 Dissertation Summary

This dissertation reports the investigation of the mechanical and biological properties of hybrid hydrogels composed of biosynthetic resilin-like polypeptides and PEG macromers. This introduction, **Chapter 1**, reviewed several topics important to this project including: the types and properties of hydrogels used for tissue

engineering, resilin and resilin-like materials, recombinant protein-PEG hybrid hydrogels and the motivation for this project, cardiovascular tissue engineering. In **Chapter 2**, the first description of resilin-PEG hybrid hydrogels is presented. This chapter covers the initial cloning, expression and purification of RLP, the characterization of the gelation of RLP with PEG and some initial cytocompatibility testing in the form of 3D cell encapsulation experiments. **Chapter 3** will introduce additional rheological testing of the RLP-PEG hydrogels, tensile testing for assessing mechanical resilience, experiments demonstrating the proteolysis of the RLP via incorporated MMP-sensitive domains and the 3D cell culture of encapsulated human mesenchymal stem cells (hMSC). Additionally, liquid-liquid partitioning behavior of these hydrogels and its implications are discussed. In **Chapter 4**, a novel cross-linking chemistry based upon the photoinitiated thiol-ene click chemistry is introduced to RLP-PEG hybrid hydrogels. This chemistry is applied to a new RLP designed to include a more flexibly edited gene sequence. The chapter reports the conjugation of photochemical groups to the RLP and its characterization via  $^1\text{H}$  NMR. In addition, the mechanical properties of the hybrid gels and their cyto-compatibility with encapsulated hMSCs were investigated and reported. **Chapter 5** will conclude the document by summarizing the major discoveries of this work, their impact on the tissue engineering field and future directions for RLP-PEG hybrid hydrogels.

## Chapter 2

# RESILIN-BASED HYBRID HYDROGELS FOR CARDIOVASCULAR TISSUE ENGINEERING

### 2.1 Introduction

The development of materials for regenerative medicine can be especially challenging when the target tissues or organs undergo periodic loading forces as a part of proper function. Materials designed for these mechanically active environments must be able to withstand these forces without a loss in performance while additionally serving as a guide for tissue repair and regeneration. Cardiovascular tissue, in particular, has distinct elastomeric properties<sup>[14]</sup> where elastic fibers, such as collagen and elastin, serve as critical structural components.<sup>[190-193]</sup> Therefore, it is important that cardiovascular biomaterials incorporate elasticity into their design to ensure proper function.<sup>[190-192]</sup>

Biosynthetic approaches to the design of biomaterials for regenerative medicine have been widely studied owing to their exceptional control over the properties of the resulting recombinant polypeptides.<sup>[74, 194, 195]</sup> Biomimetic domains or biological recognition sequences derived from components of the extracellular matrix (ECM) may be directly engineered into these polymers in an attempt to confer cell-instructive signals that guide tissue repair and regeneration.<sup>[6, 7, 98]</sup> Utilizing sequences from elastomeric proteins as the structural domains in these recombinant polypeptides offers a particularly exciting strategy given the outstanding mechanical properties of the protein polymers when cross-linked into gels.<sup>[107, 155]</sup> Elastin-like polypeptides

(ELP) in particular have garnered much focus as potential materials for tissue engineering,<sup>[89, 196]</sup> and cross-linked ELPs have shown promise as injectable scaffolds for tissue repair.<sup>[90, 197-199]</sup> In addition, polypeptides based on the insect structural protein resilin have also emerged as potential candidates for material-based regenerative therapies for mechanically demanding applications.<sup>[100, 105]</sup> Resilin is an elastomeric protein found in specialized compartments of arthropods where it provides the rubber elasticity necessary for flight,<sup>[126]</sup> sound production,<sup>[119]</sup> and feeding.<sup>[117]</sup> This highly disordered, cross-linked protein is rich in proline and glycine residues that may work mutually to confer chain disorder by providing conformation-restricted rigidity and chain flexibility, respectively.<sup>[109, 156, 165, 200]</sup> The resulting randomly coiled, isotropic three-dimensional network has been shown to behave as an ideal rubber with near-perfect reversible long-range elasticity.<sup>[156, 200]</sup>

Following the identification of a resilin-like motif sequence by Ardell and Andersen,<sup>[140]</sup> there have been numerous recent reports of recombinant resilin-like polypeptides (RLPs), but these studies have focused largely on the physiochemical properties or the structure-function properties of the protein.<sup>[142-144, 163, 164, 166, 168-170, 173, 176, 177, 201, 202]</sup> After our initial reports describing the excellent elastomeric properties of RLPs explicitly designed for regenerative medicine applications,<sup>[100]</sup> there have been a handful of additional reports exploring engineered RLPs for biomedical applications.<sup>[100, 105, 179, 180]</sup> These RLP-based materials have also inspired the development of highly resilient synthetic hydrogels composed of poly(ethylene glycol) PEG and PDMS.<sup>[203]</sup> The novel RLP (RLP12) designed and reported by our group has a modular sequence that incorporates 12 repeats of the resilin-like consensus sequence in addition to domains for cell adhesion, cell-directed degradation, and heparin

binding. Our previous work has demonstrated that, when cross-linked into hydrogels by reaction with an amine-reactive phosphine-based cross-linker, the hydrogels were highly resilient (>90%) and recovered reversibly following deformation,<sup>[105]</sup> a characteristic trait of natural resilin.<sup>[105, 109, 157, 200]</sup>

In order to further expand the versatility of these RLP materials, we have investigated the production of RLP-PEG hybrid hydrogels that are cross-linked through a Michael-type addition reaction between the thiols of cysteine residues on the polypeptide and a vinyl sulfone-terminated four-arm star PEG cross-linker (*see Figure 2.1*). The reaction between the cysteine thiol and vinyl sulfone has been shown to be highly selective at relatively mild pH<sup>[97, 204]</sup> and has been widely applied as a cross-linking mechanism for biomaterial hydrogels.<sup>[52, 96, 97, 205-218]</sup> The use of multicomponent PEG hydrogels has been widely employed owing to the fact that PEG macromers are nonimmunogenic, resist protein adsorption and may utilize a variety of cross-linking chemistries and chain architectures.<sup>[8]</sup> The development of protein-PEG hybrid hydrogels combines the advantages of PEG macromers with those of biosynthetic polypeptides, namely the cross-linking chemistry and chain architecture flexibility of the PEG macromers and the specificity and inherent bioactivity of the polypeptide component.<sup>[96, 97, 177]</sup> In early reports by the Hubbell and co-workers,<sup>[96, 97, 177]</sup> PEG macromers were used to cross-link recombinant polypeptides through either vinyl sulfone-based Michael-type addition<sup>[96, 97, 177]</sup> or photoinitiated polymerization of acrylate groups.<sup>[95]</sup> Sequences derived from fibrinogen, collagen and anti-thrombin III were utilized in the recombinant polypeptide component and provided cell-matrix interactivity.<sup>[95-97]</sup> In addition, Ehrbar and co-workers<sup>[25, 219-221]</sup> have demonstrated that enzymatically cross-linking hydrogels via the activity of transglutaminase factor XIIIa

offers a promising strategy for mild and specific cross-linking of multicomponent PEG hydrogels. Other strategies include the photoinitiated thiol-ene chemical cross-linking of peptides and PEG macromers developed by Anseth and co-workers.<sup>[18, 222]</sup>

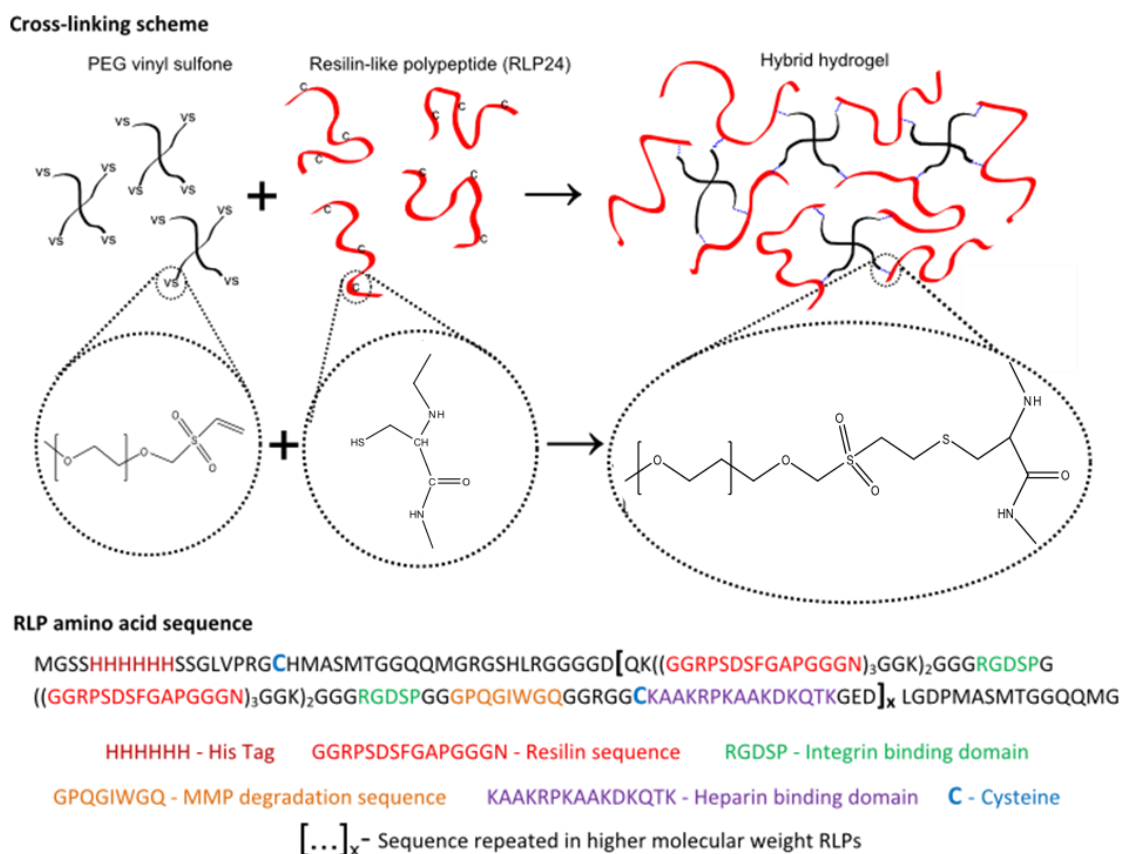


**Figure 2.1** Scheme of the hydrogel formation and details of the cross-linking chemistry are presented alongside the amino acid sequence of the RLPs. Additionally, a legend indicating the resilin-like and biological domains is presented beneath the amino acid sequence. The parentheses indicate repeated sequences; in total, there are 12 repeats of the resilin sequence and two repeats of the integrin-binding domain within the larger brackets. The brackets indicate the repeated sequences of the higher molecular weight RLPs (RLP12  $x = 1$ , RLP24  $x = 2$ , RLP36  $x = 3$ , RLP48  $x = 4$ ).

The production of RLP–PEG hydrogels is motivated by these previous reports with the incorporation of resilin-like sequences intended to confer elastomeric properties to hybrid matrices containing cell-instructive domains. Reversible elasticity would be particularly advantageous in cardiovascular applications where the biomaterial would be subjected to hemodynamic cyclic loading forces<sup>[192]</sup> A compliant, cell-instructive biomaterial could serve as a beneficial therapeutic material in vascular grafts, angioplasties, or other cardiovascular surgeries. Adventitial fibroblasts, which are located in the tunica adventitia of blood vessels,<sup>[223]</sup> have emerged as an important regulator of vessel health and thus serve as an appropriate model for assessing the viability of RLP–PEG hydrogels as potential three-dimensional matrices for cardiovascular applications. This work reports the development of higher molecular weight RLPs with increasing numbers of cysteines to permit their incorporation into PEG-based hybrid materials. The cross-linking and mechanical properties of these RLP–PEG hydrogels were assessed via dynamic oscillatory rheology; homogeneous, stable networks are rapidly formed upon mixing of the two components. In addition, the encapsulation of adventitial fibroblasts demonstrates the cytocompatibility of these matrices for primary cells derived from human cardiovascular tissue. These RLP–PEG hydrogels are thus exciting biomaterials with potential as an injectable tissue engineering scaffold for cardiovascular applications.

## 2.2 Experimental Section

### 2.2.1 Materials

All chemicals were purchased from Sigma-Aldrich (St. Louis, MO) or Fisher Scientific (Waltham, MA) and used as received unless otherwise noted. Ni-NTA agarose resin was purchased from Qiagen (Valencia, CA). Water was deionized and filtered through a ThermoFisher Barnstead NANOpure Diamond water purification system. The RLP12 gene<sup>[100, 105]</sup> in a pUC57 plasmid was obtained from Genscript Corporation (Piscataway, NJ) and the cloning plasmid pGEM-3z was purchased from Promega (Madison, WI). The expression plasmid, pET28a, was obtained from Novagen (EMD Chemicals, Gibbstown NJ). Restriction enzymes, phosphatases, and ligases were purchased from New England Biolabs (Ipswich, MA). Electroporation was performed using a Gene Pulser Xcell Microbial System from Bio-Rad Laboratories (Hercules, CA). Three *Escherichia coli* strains utilized for cloning included DH5 $\alpha$  chemically competent cells and ElectroMax DH10B electrocompetent cells purchased from Life Technologies (Carlsbad, CA) as well as *dam-/dcm-* SCS110 cells purchased from Agilent Technologies (Santa Clara, CA). BL21Star<sup>TM</sup>(DE3) cells from Life Technologies served as the expression strain, as previously reported.<sup>[100, 105]</sup>

### 2.2.2 Recursive Ligation and Mutagenesis

Recursive ligation methods were employed to construct the higher molecular weight RLPs through the use of the flanking restrictions sites BglII and BclI as depicted in **Figure 2.2**. Due to the methylation sensitivity of the BclI enzyme, *dam-/dcm-* SCS110 cells had to be utilized to produce plasmid DNA from which the RLP12 gene could be wholly digested. The RLP12 gene was initially supplied in a pUC57a plasmid as reported in Charati, *et. al.*;<sup>[100]</sup> the RLP12 gene was digested and

purified from this plasmid using the BamHI and HindIII restriction sites (represented in blue). It was then ligated into a pGEM-3z plasmid for the recursive ligation procedure.

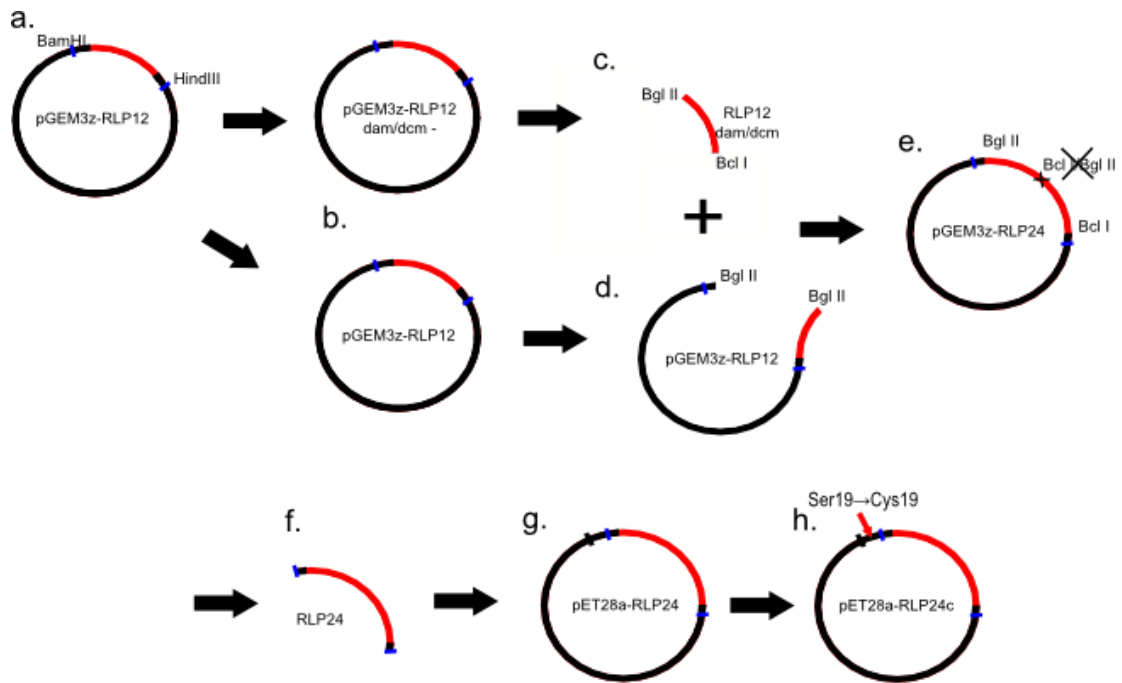


**Figure 2.2** Scheme depicting of the genetic engineering for recursive ligation of RLP12 gene and final mutagenesis. The construction of each gene (RLP24, RLP36, RLP48) was the same, but only the example of the cloning of RLP24 is illustrated in the figure.

The pGEM-RLP12 plasmid is represented in step (a) of **Figure 2.2**.

Transformation into SCS110 cells and DH5 $\alpha$  cells provided stocks of *dam/dcm* negative (unmethylated) and *dam/dcm* positive (methylated) pGEM3zRLP12 plasmid as represented in step (b). As shown in step (c) the *dam/dcm* negative the RLP12 gene

was digested and purified from the plasmid using BglII restriction enzyme and the methylation sensitive Bcl I restriction enzyme. The *dam/dcm* positive pGEM3z-RLP12 was linearized using the Bgl II restriction enzyme as shown in step (d). The cohesive ends created by the digestion of the Bgl II and Bcl I restriction enzymes were complimentary to the Bgl II site on the linearized pGEM-RLP12 plasmid in step (d). This allowed for the ligation of the RLP12 gene into that restriction site which effectively doubled the length of the RLP12 gene to create pGEM3z-RLP24 [step (e)]. The pGEM3z-RLP36 & pGEM3z-RLP48 were prepared in the same manner, but the linearized pGEM3z-RLP12 plasmid was swapped for either linearized pGEM3z-RLP24 or linearized pGEM3z-RLP36. The ligation of the sticky ends representing the Bcl I site on the RLP12 gene and the Bgl II site on the plasmid led to the elimination of both of the sites as represented by the 'X' in step (e). To move the entire gene (RLP12, RLP24, RLP36 or RLP48) into an expression plasmid, the BamHI and HindIII sites (again, indicated in blue) were used to digest the gene from the cloning plasmid and to ligate the gene into the expression plasmid, pET28a(+), as shown in steps (f) and (g). In step (g), the black hash mark on the pET28a-RLP24 plasmid indicates the start codon of the protein. Site-directed mutagenesis of the Ser19 residue is represented in step (h) by the red arrow; each RLP was subjected to a mutagenesis step to introduce a cysteine residue at the N-terminus of the expressed proteins.

Standard molecular biology techniques were used to complete the recursive ligation of the RLPs.<sup>[224]</sup> Gene sequencing (Delaware Biotechnology Institute, Newark, DE) and DNA gel electrophoresis confirmed each stage of cloning as well as the final recombinant genes: RLP24, RLP36 & RLP48. The Ser19 residue of the RLPs was mutated to a cysteine using site-directed mutagenesis via the QuikChange II XL

Site-Directed Mutagenesis Kit from Agilent Technologies (Santa Clara, CA). Gene sequencing confirmed the successful mutation. Chemically competent BL21Star™(DE3) cells were transformed with the mutated pET28aRLP plasmids to yield the host strains used for expression.

### **2.2.3 Expression, Purification, and Characterization of RLPs**

As previously reported,<sup>[100, 105]</sup> protein expression was achieved via Studier auto-induction techniques<sup>[167]</sup> using ZYP-5052 media, with cultures grown at 37 °C for 4 h before the temperature was lowered to 24 °C for an additional 24 h of expression.

Following expression, cells were harvested via centrifugation and the cell pellets stored at -20°C. The frozen cell pellets were thawed and resuspended in native lysis buffer (50 mM NaH<sub>2</sub>PO<sub>4</sub>, 300 mM NaCl, 10 mM imidazole, 10 mM β-mercaptoethanol, 0.1% Tween 20) under stirring at 4°C. Lysozyme was added at a concentration of 1 mg/mL to the lysed cells for 30 minutes to an hour before the lysate was further disrupted by using a Fisher Scientific Sonic Dismembrator 500 equipped with a 10 mm tapered probe. The lysate was sonicated until there was a noticeable decrease in lysate viscosity and the lysate developed a darker color. The cell lysate was then centrifuged at 30000g for 60 minutes and the soluble extract decanted; additional β-mercaptoethanol was added to the soluble extract to raise its concentration to 20 mM. The cell-free extract was then heated to 90°C in a water bath for 10 minutes or until a white precipitate formed in solution. This precipitate was spun out via centrifugation (3000g, 10 min) and the soluble lysate was diluted using additional native lysis buffer chilled at 4°C. The pH of cell lysate was adjusted to approximately 8.0 before incubation for several hours with the Ni-NTA resin

(QIAGEN). The mixture was loaded onto gravitational flow columns and washed with 10 column volumes of native lysis buffer followed by 10 column volumes of native wash buffer (50 mM NaH<sub>2</sub>PO<sub>4</sub>, 300 mM NaCl, 20 mM imidazole, 10 mM β-mercaptoethanol). The RLP was eluted with 2-3 column volumes of native elution buffer (50 mM NaH<sub>2</sub>PO<sub>4</sub>, 300 mM NaCl, 250 mM imidazole) and dialyzed (MW10000) first against 4L of 1 M NaCl and then against 4L of pure water (5x). Following dialysis the protein solution was filtered, frozen and lyophilized to a white fluffy solid. The introduction of a heating step and the incorporation of the β-mercaptoethanol were found to enhance the purity of the product. Depending upon the protein expressed, yields ranged between 50-100 mg of protein per liter of expression culture.

Protein expression was confirmed and monitored via sodium dodecyl sulfate polyacrylamide gel electrophoresis (SDS-PAGE) and visualized via Coomassie blue staining. The molecular weight of the RLPs was confirmed by MALDI-TOF analysis conducted at the W.M. Keck Biotechnology Resource Laboratory at Yale University (New Haven, CT). Amino acid analysis confirmed the composition of the polypeptides and was performed by the Molecular Structure Facility at the University of California, Davis (Davis, CA) using a Hitachi L-800 sodium citrate-based amino acid analyzer (Tokyo, Japan).

#### **2.2.4 Preparation of Reduced Proteins**

Pure lyophilized RLP was reduced using tris(2-carboxyethyl)phosphine hydrochloride (TCEP-HCl) in a 10 mM MES, 500 mM NaCl buffer (pH 5.6) and desalted using a Zeba™ Spin desalting column (7 kDa MWCO, Pierce Rockford, IL). The flow-through was immediately frozen in liquid N<sub>2</sub> and lyophilized. The free thiol

content of protein was measured using the Ellman's assay protocol (in 100 mM Tris, 2.5 mM sodium acetate, 40  $\mu$ M DTNB, pH 8.0);<sup>[225, 226]</sup> the colorimetric change of the solution upon reduction of the DTNB by the RLPs was monitored using an Agilent 8453 UV–Vis spectrophotometer.

### 2.2.5 Synthesis of PEG Vinyl Sulfone Cross-linker

Hydroxyl-terminated four-arm star PEG (10 kDa) was purchased from JenKem Technology USA (Allen, TX) and functionalized with vinyl sulfone following previously established protocols by Lutolf and Hubbell.<sup>[52]</sup>  $^1\text{H}$  NMR (400 MHz,  $\text{CDCl}_3$ ) confirmed quantitative functionalization (**Figure 2.3**):  $\delta = 3.6$  ppm (PEG backbone), 6.1 ppm ( $\text{CH}_2=\text{CH-SO}_2$ , d, 1H), 6.4 ppm ( $\text{CH}_2=\text{CH-SO}_2$ , d, 1H), 6.8 ppm ( $\text{CH}_2=\text{CH-SO}_2$  dd, 1H).

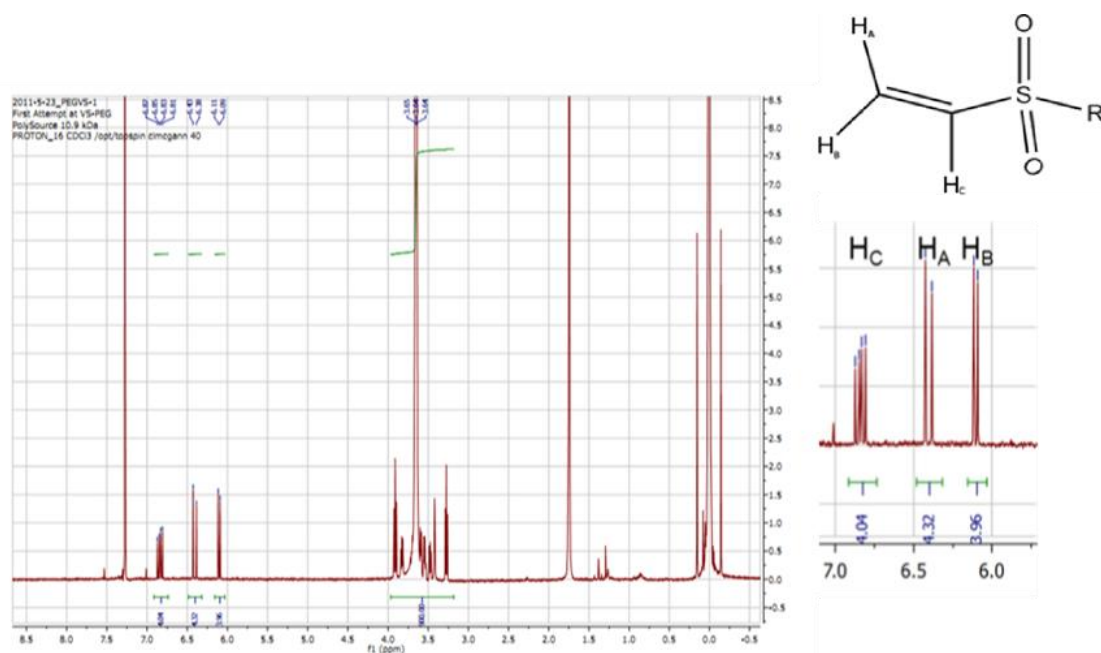


**Figure 2.3**  $^1\text{H}$  NMR of PEGVS Functionalization. This figure represents the complete  $^1\text{H}$ -NMR spectrum of the functionalized four-arm PEG vinyl sulfone (10 kDa), an insert depicts the 6.0-7.0 ppm region with the assignments for the olefin protons on the vinyl sulfone moiety and an image of the vinyl sulfone moiety. Integration of the olefin protons was based upon an assumed 909 protons present in the PEG backbone; the values indicate approximately four vinyl sulfone groups per polymer (quantitative functionalization)

## 2.2.6 Hydrogel Formation and Oscillatory Rheology

RLP-PEG hydrogels were formed by simple mixing of precursor solutions of the PEG and RLP under specific conditions described below. Oscillatory rheology experiments conducted on a stress-controlled AR-G2 rheometer (TA Instruments, New Castle, DE) were used to characterize the cross-linking and subsequent mechanical properties of the RLP-PEG hydrogels. Experiments were conducted at 37 °C using a 20 mm diameter cone-on-plate geometry with 1° cone angle and 25  $\mu\text{m}$  gap distance. Time and frequency sweeps were performed on all hydrogels. The RLP and

PEG precursors were dissolved separately in PBS buffer (pH 7.4); a 0.2  $\mu\text{L}$  drop of concentrated NaOH was used to adjust the pH of RLP solution to approximately 8.0 and both precursors were kept on ice prior to the experiment. The precursors were then combined, vortexed briefly, and loaded onto the rheometer stage maintained at a temperature of 4  $^{\circ}\text{C}$ . This slowed the cross-linking reaction so that the geometry could be lowered into place prior to gelation. Once the experiment was started, the temperature was quickly increased to and maintained at 37  $^{\circ}\text{C}$ ; mineral oil was used to seal the hydrogel and prevent evaporation. The RLP–PEG hydrogels were prepared at concentrations of 20 wt% and were cross-linked at vinyl sulfone to cysteine residue (VS:CYS) ratios of 1:1 and 3:2. Experiments were repeated on three to four samples and representative data presented.

### **2.2.7 *In Vitro* Cell Culture of Aortic Adventitial Fibroblasts**

Human aortic adventitial fibroblasts (AoAF) were a generous gift of Dr. Robert Akins (Nemours, Wilmington, DE). The cells were cultured according to protocols provided by Lonza (Basel, Switzerland) and using the Lonza SCGM<sup>TM</sup> BulletKit<sup>TM</sup> media system. The cells for the encapsulation experiments were between passage numbers 7 and 11. Prior to the encapsulation, the AoAF cells were lifted, counted, and resuspended in stromal cell growth media (SCGM) at a concentration of 5,000,000 cells per mL. Aliquots of 50,000 cells (10  $\mu\text{L}$ ) were prepared in microcentrifuge tubes for each of the gels. A solution of the PEG precursor was prepared in 10  $\mu\text{L}$  of PBS buffer (pH 7.4) while the RLP24 was dissolved into 30  $\mu\text{L}$  of PBS buffer (pH 7.4) with phenolphthalein (1 mM) included as a pH indicator. The pH of the RLP solution was adjusted using 0.2  $\mu\text{L}$  drops of 2 N NaOH until a slight pink hue was observed indicating the pH was approximately 8.2. Hydrogels were

produced at 20 wt% concentration and cross-linked at a 3:2 ratio (VS:CYS) to ensure sufficient cross-linking in the presence of cells. The precursors were mixed and briefly vortexed before being gently triturated with the 10  $\mu$ L of media containing the cells. This solution was then loaded onto a glass-bottom dish (MatTek Corporation Ashland, MA) and placed into a cell culture incubator where the hydrogels were cross-linked at 37  $^{\circ}$ C; media (3 mL) was added to the gels after 3 min of cross-linking. Hydrogels were lifted from the glass-bottom dish after an hour of incubation to facilitate diffusion of media into the hydrogel; media was exchanged every 3 d. Cell viability and proliferation analysis were performed on three sample hydrogels at days 0, 1, 3, and 7. Hydrogels were costained with Calcein AM and Ethidium homodimer-1 (Live/Dead<sup>®</sup> Life Technologies Carlsbad, CA) and DRAQ5<sup>™</sup> stain (BioStatus Limited Shepshed, United Kingdom) to assess the viability of encapsulated cells and the total number of cell nuclei, respectively. Hydrogels were washed 2-3x with approximately 5 mL of PBS and then incubated at 37  $^{\circ}$ C in a 5% CO<sub>2</sub> incubator for 30 min in 700  $\mu$ L of PBS containing: 5  $\mu$ M DRAQ5, 2  $\mu$ M Calcein AM, and 4  $\mu$ M Ethidium homodimer-1. Cell viability and nuclei number were visualized using fluorescence laser scanning confocal microscopy (Zeiss LSM 510 NLO multiphoton, Carl Zeiss, Inc., Thornwood, NY). To ascertain proliferation of the aortic fibroblasts in the PEG–RLP gels, microscopy data were acquired, in each hydrogel, from four adjacent regions approximately 1800  $\mu$ m in length and width and 400  $\mu$ m in depth. The numbers of cells in each tile were determined via image analysis (see below). Three hydrogels were imaged in this manner for each time point; the center of the four tiles was chosen to be the middle of the hydrogel and the tiles were independently assigned. In total, approximately 5 mm<sup>3</sup> (5  $\mu$ L) of each hydrogel (50  $\mu$ L) was imaged

and analyzed. These data were processed using Velocity 3D Image Analysis Software (PerkinElmer, Waltham, MA) to determine numbers of cell nuclei for both the membrane-permeable Draq5 stain as well as the membrane-impermeable ethidium homodimer-1 stain; the number of living cells was calculated as the difference between the two counts.

## 2.3 Results and Discussion

### 2.3.1 Design of RLPs

The sequences of all the RLPs, with the detailed amino acid sequences of the various domains, are presented in **Figure 2.1**. As previously reported,<sup>[100, 105]</sup> these constructs utilized a slightly modified version of the putative resilin-like sequence (GGRPSDSFGAPGGGN) derived from the first exon of the *Drosophila melanogaster* CG15920 gene.<sup>[140]</sup> The tyrosine residue included in the original motif was substituted with a phenylalanine residue (shown in bold) for the potential future incorporation of nonnatural amino acids that would confer photocross-linking properties. Tensile testing and oscillatory rheology have shown that this substitution does not affect the mechanical properties of the RLP12 hydrogels.<sup>[100, 105]</sup> Additionally, the RLP includes sequences for cell-matrix interactions including an integrin-binding domain for cell adhesion (GRGDSPG),<sup>[42]</sup> a matrix metalloproteinase (MMP) sensitive sequence (GPQG↓IWGQ)<sup>[227]</sup> for cell-directed matrix degradation, and a heparin-binding domain (HBD) (KAAKRPKAAKDKQTK)<sup>[228]</sup> for the sequestration of heparin and growth factors.

RLPs of higher molecular weight were produced to yield polypeptides with multiple cysteine residues, which would permit cross-linking of these RLP sequences

into a network using Michael-type addition reactions. Recursive ligation of the original RLP12 gene yielded RLP24, RLP36, and RLP48 with cysteine functionalities of two, three, and four, respectively (*see Figure 2.4*). A restriction digestion using BamHI and HindIII of the four pET28a/RLP genes and a pET28a plasmid, followed by DNA gel electrophoresis, was performed; results are shown in **Figure 2.5A**. As illustrated in the figure, bands are present at approximately 800, 1500, 2200, and 2900 bp; these lengths correspond to the expected base-pair length of the four RLP genes. (The band at 5300 bp results from the linearized expression plasmid.) These results confirm the success of the recursive ligation of the RLP genes and their insertion into the pET28a expression plasmid. Further confirmation of these results was provided by gene sequencing (data not shown).

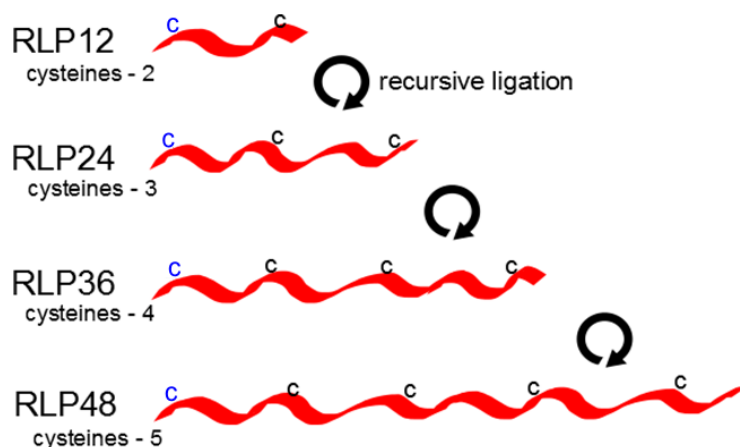


**Figure 2.4** This image provides a visual representation of the recursive ligation and the location of the resulting cysteine residues. The blue 'c' represents the cysteine residues that were engineered via site-directed mutagenesis. The black 'c' represents the cysteine residues that were originally encoded in the RLP12 gene and doubled, tripled or quadrupled by recursive ligation.

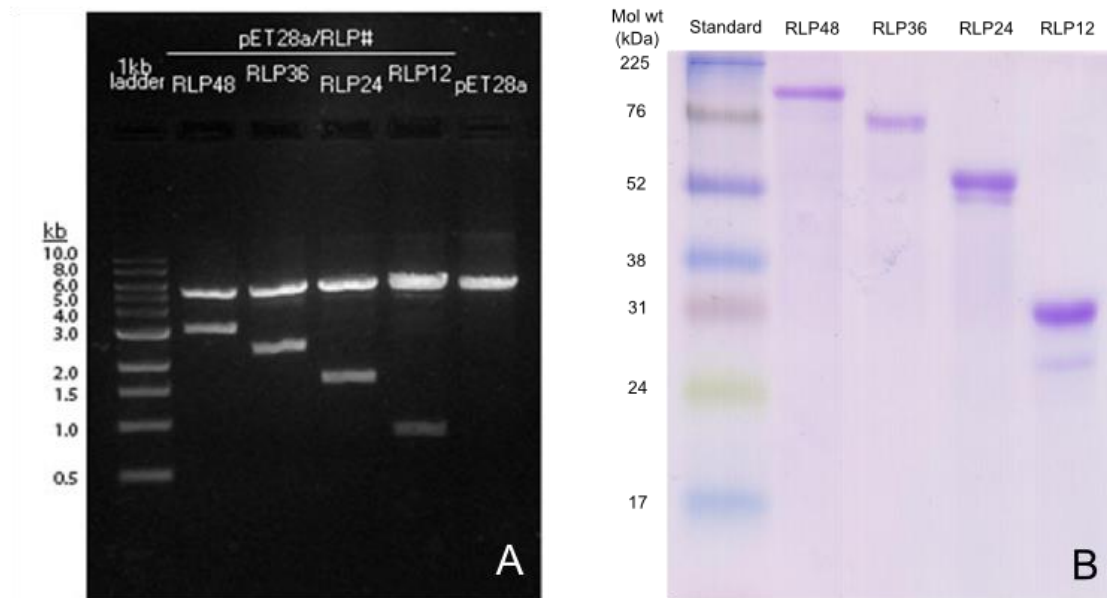


**Figure 2.5** (A) Agarose gel showing the BamHI/HindIII digestion of pET28aRLP48, pET28aRLP36, pET28aRLP24, pET28aRLP12, & pET28a (left to right). The linearized pET28a plasmid is clearly resolved between 5000 and 6000 bp while the RLP genes are represented by the bands migrating at approximately 800 bp to 3200 bp. (B) Coomassie stained SDS-PAGE gel (12%) showing the purified RLP proteins, RLP48, RLP36, RLP24 & RLP12 (left to right).

The original RLP12 gene encoded for a single cysteine residue that was located near the C-terminus of the polypeptide; recursive ligation introduced polypeptides with higher functionality, but with cysteine residues that were located only toward the C-terminal end of the domains (**Figure 2.4**) rather than throughout the full polypeptide, which caused a significant fraction of the N-terminal end of the RLP to not be cross-linked into the network. Initial rheological characterization of RLP-PEG hydrogels using these original RLP constructs yielded materials with moduli far below predicted values and too low for practical use in clinical application (data not shown). In order to permit effective crosslinking of the N-terminal end of each

polypeptide chain and minimize any deleterious effect of dangling chain ends,<sup>[158]</sup> the Ser19 residue at the N-terminus of each polypeptide was mutated to a cysteine via site-directed mutagenesis (data not shown). The polypeptides with this S19C mutation have been used for all further characterization and application.

### **2.3.2 Protein Expression, Purification, Characterization, and Reduction**

Each of the RLPs was expressed using Studier auto-induction techniques and purified under native conditions using Ni-NTA affinity chromatography. SDS-PAGE analysis was conducted on the purified RLP fractions (**Figure 2.5B**). The bands on the gel are present at 30, 52, 76, and approximately 100 kDa, consistent with the expected molecular weights of the RLP12, RLP24, RLP36, and RLP48 proteins, respectively. The lack of any other significant bands in the SDS-PAGE analysis indicates the purity of the RLPs. In this analysis, the RLPs migrate slightly higher than their theoretical values, but this is consistent with our previous results for RLP12<sup>[100]</sup> as well as with results from RLPs expressed by other laboratories.<sup>[142, 168]</sup> Atypical SDS-binding has been described as cause for this discrepancy and has been noted for proteins with unusual amino acid composition.<sup>[22, 168]</sup>

Matrix-assisted laser desorption/ionization (MALDI-TOF) analysis of intact RLPs was performed to confirm the exact molecular weights of the proteins; analysis shows that the major peaks fall within 1% of the theoretical molecular weights. The MALDI mass spectrometry results obtained for the RLP12, RLP24, RLP36 and RLP48 are presented in **Figure 2.6**. Lyophilized samples were dissolved in an appropriate volume of 50% acetonitrile, 0.1% TFA at a concentration of 100 pmol/ $\mu$ L. A 1  $\mu$ l aliquot of the sample was then diluted 10-fold into matrix solution (10mg/ml sinapinic acid in 50% acetonitrile/0.1% TFA), and 1  $\mu$ l was spotted on the MALDI

target. The final concentration of the sample was 10 pmol/spot. Data were acquired on an Applied Biosystems/MDS SCIEX 4800 MALDI TOF/TOF Analyzer with external calibration.

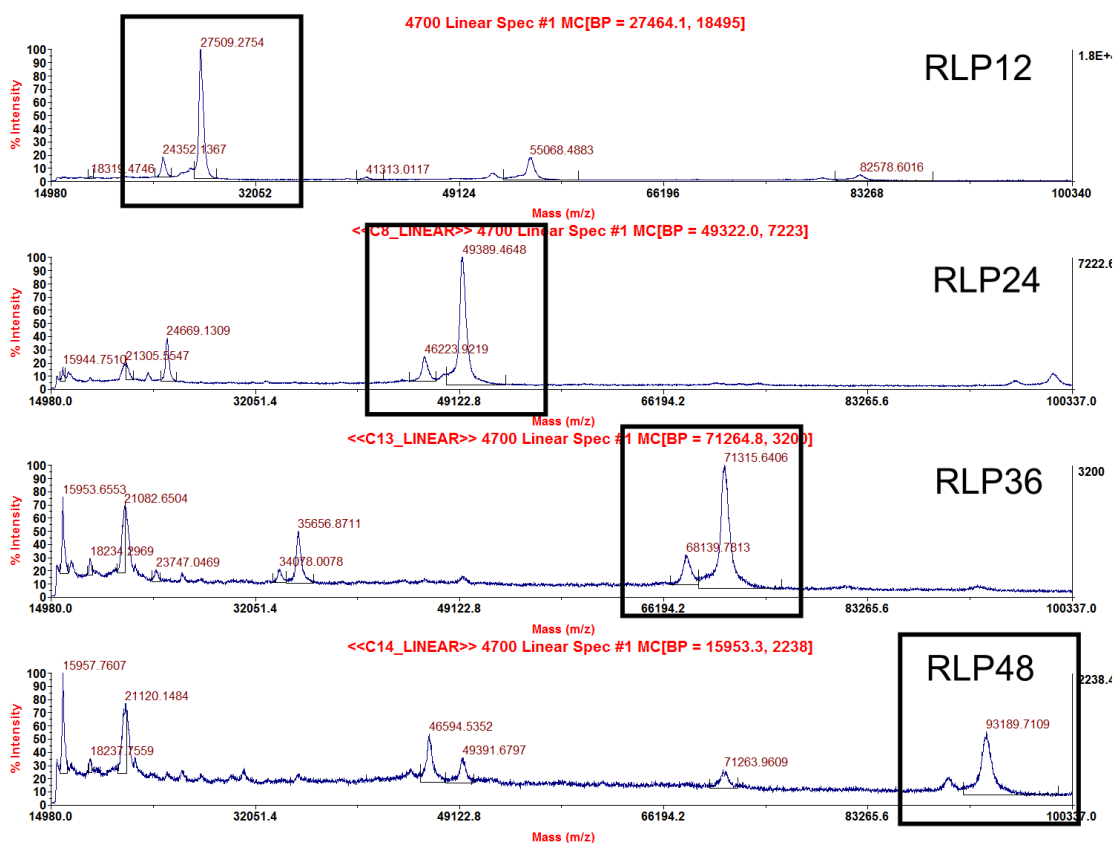


**Figure 2.6** MALDI-MS Spectrum of the RLP proteins. The major peaks are as follows: 27509.27 for RLP12; 49389.46 for RLP24; 71315.64 for RLP36; and 93189.71 for RLP48.

RLP12 exhibits a major peak at 27509 with a possible truncation product at 24352. Each of the RLP proteins exhibited a small truncation product which was on average 3167Da less in molecular weight. This has been observed in other resilin-like

polypeptide systems and is possibly early termination of transcription or translation.<sup>[179]</sup> In the RLP12 spectrum, other peaks include dimers at 55068Da (homodimer of main peak) and 51912 (heterodimer), trimers at 82575, as well as a doubly-charged trimer at 41313. RLP24 exhibits a major peak at 49389 with a possible truncation product at 46223. Other peaks include dimers at 98780 Da (homodimer of main peak) and 95621, as well as doubly-charged monomers at 24669. The peaks in the 70K-74K range are doubly-charged trimers. RLP36 exhibits a major peak at 71315 with a possible truncation product at 68139. The peaks at 35656 and 34078 are doubly-charged monomers. RLP48 exhibits a major peak at 93187 with a possible truncation product at 90023. The peaks at 46594 and 45025 are the doubly-charged monomers, while the peak at 31061 is probably a triple charged monomer. The peaks at 16000 and 21100 appear in RLP24, RLP36 and RLP48 with various intensities. It is possible that these are contaminating proteins or degraded RLP, but it is important to note that that peak intensity does not correlate with quantity as different species have different ionization efficiencies and lower molecular weight species usually have a stronger signal. Additionally, these species do not have corresponding bands in the SDS-PAGE gels and therefore, probably exist in negligible quantities.

Amino acid analysis of the RLPs demonstrated that the composition of the purified proteins was within 10% of the expected values (**Table 2.1**). Given that the composition of the protein is consistent with that expected theoretically, the existence, in low percentages, of a slightly lower molecular weight product probably results from truncation or degradation as has been described in other reports of RLP expression.<sup>[166, 169, 179]</sup> Isolation of products that lack these lower molecular weight contaminants can

be achieved by lowering the temperature of the expression culture and by harvesting during the exponential phase of the expression.<sup>[179]</sup> Since the small overall percentage of sample comprising truncated product was small, such optimization was not conducted in these studies and the polypeptides were used without further purification.

**Table 2.1** Amino acid analysis of the RLPs

Amino Acid	RLP12			RLP24			RLP36			RLP48		
	Measured	Theor.		Measured	Theor.		Measured	Theor.		Measured	Theor.	
	[nmol]	[%]	[%]									
Cysteic Acid	0.039	0.19		0.037			0.041			0.028		
Cystine	0.020	0.10		0.024			0.000			0.023		
Cys		0.38	0.70		0.49	0.50		0.21	0.50		0.36	0.50
Asp +Asn	2.144	10.33	10.00	1.889	10.80	10.60	2.133	11.13	10.80	2.340	11.29	11.00
Thr	0.200	0.96	1.00	0.110	0.63	0.70	0.110	0.57	0.60	0.122	0.59	0.60
Ser	2.046	9.86	10.90	1.693	9.68	10.80	1.857	9.69	10.70	1.969	9.50	10.70
Glu + Gln	0.722	3.48	2.90	0.467	2.67	2.60	0.474	2.47	2.40	0.567	2.73	2.30
Pro	1.961	9.45	9.90	1.781	10.19	10.60	2.283	11.91	10.90	2.345	11.31	11.00
Gly	7.846	37.81	37.70	6.775	38.75	38.90	7.330	38.25	39.40	8.062	38.89	39.60
Ala	1.297	6.25	6.00	1.056	6.04	6.20	1.165	6.08	6.30	1.293	6.24	6.40
Val	0.156	0.75	0.30	0.060	0.34	0.20	0.028	0.15	0.10	0.042	0.20	0.10
Met	0.145	0.70	2.30	0.068	0.39	1.30	0.041	0.21	0.90	0.045	0.22	0.70
Ile	0.079	0.38	0.30	0.065	0.37	0.40	0.107	0.56	0.40	0.092	0.44	0.40
Leu	0.213	1.03	1.00	0.091	0.52	0.50	0.107	0.56	0.40	0.111	0.54	0.30
Tyr	0.020	0.10	0.00	0.000	0.00	0.00	0.000	0.00	0.00	0.000	0.00	0.00
Phe	0.869	4.19	4.00	0.820	4.69	4.40	0.891	4.65	4.50	0.993	4.79	4.60
His	0.542	2.61	2.60	0.294	1.68	1.50	0.289	1.51	1.00	0.270	1.30	0.80
Lys	0.764	3.68	3.60	0.806	4.61	4.00	0.907	4.73	4.20	0.939	4.53	4.20
Trp	0.265	1.28	0.30	0.234	1.34	0.40	0.109	0.57	0.40	0.049	0.24	0.40
Arg	1.422	6.85	6.30	1.191	6.81	6.40	1.289	6.73	6.40	1.419	6.84	6.50

Amino acid composition analysis was performed by the Molecular Structure Facility at the University of California, Davis (Davis, CA) using a Hitachi L-8800 sodium citrate-based amino acid analyzer (Tokyo, Japan). Protein samples were cleaved by HCl hydrolysis, separated with ion exchange chromatography and detected using a ninhydrin reaction. The results indicate that the protein sample compositions closely match the expected compositions.

With molecular weights of 71.1 kDa and 92.9 kDa, the RLP36 and RLP48 proteins represent the highest molecular weight RLPs reported to date; additionally, these RLPs represent some of the highest yielding RLPs expressed outside of high-cell density fermentation.<sup>[105, 166, 179, 180]</sup> As shown in **Table 2.2**, each of the RLPs could be expressed and purified in significant quantities ranging from 50 to 100 mg/L culture depending on the specific polypeptide. RLP24 yielded the greatest quantity per liter of expression (100 mg/L culture), which although less than values reported for elastin-like polypeptides (1.6 g/L of expression media),<sup>[229]</sup> is greater than yields often reported for other protein polymers.<sup>[95, 97]</sup> The high yields under native conditions for purification suggest that these RLPs are highly soluble and easily expressed by their bacterial hosts. Natural resilin and RLPs have been shown to be relatively heat stable<sup>[109, 166, 168]</sup> and this property has proven useful in the purification of RLPs including the RLPs described in this work.<sup>[166, 168]</sup> Purification of RLPs was improved through the inclusion of  $\beta$ -mercaptoethanol to the purification buffers to prevent disulfide formation and through the addition of a heating step to selectively precipitate non-resilin bacterial proteins from the cell-free lysate. RLPs with free thiol were prepared by first reducing the cysteine residues of the RLP via treatment with TCEP-HCl in an acidic buffer, followed by desalting, freezing and lyophilization. Using this method, RLPs with approximately 90%–100% free thiol content could routinely be produced.

**Table 2.2** Resilin-like polypeptides molecular weights and yields

RLP	Theoretical Molecular Weight [Da]	Protein Yield <sup>a)</sup> [[mg/ L expression]	Specific Yield <sup>a)</sup> [mg/g cell pellet mass]
RLP12	27590.0	77.2	3.96
RLP24	49389.7	99.6	5.20
RLP36	71189.3	79.0	4.05
RLP48	92989.0	53.2	2.65

<sup>a)</sup> values are mean of at least two separate purifications.

### 2.3.3 Oscillatory Rheology Experiments

The gelation and mechanical properties of the RLP–PEG hydrogels play an important role in determining whether the materials could be potentially useful in a desired clinical capacity. *In situ* oscillatory rheology offers a practical approach to elucidating the gelation kinetics and the ultimate mechanical properties of the RLP–PEG hydrogels, and also provides direct correlation to our previous work on PEG-based hydrogels and their impact on cardiovascular cell phenotypes. Thorough evaluation of the tensile properties of these materials, to permit comparison of the elastomeric behavior of these RLP–PEG hydrogels versus the highly elastomeric behavior of RLP-only hydrogels, is currently underway. For the oscillatory rheology experiments, RLP–PEG hydrogels prepared in PBS at a 20 wt% concentration were characterized via dynamic oscillatory rheology using a cone-on-plate geometry at either a 1:1 or 3:2 ratio of vinyl sulfone groups to cysteine residues. **Figure 2.7** shows representative time sweeps for the cross-linking of RLP24-PEG hydrogels at the two cross-linking ratios investigated. These data demonstrate that the 3:2 cross-linking ratio leads to higher moduli and more rapid cross-linking than the 1:1 cross-linking ratio; the final moduli of the 3:2 hydrogels were consistently in the 12–13 kPa range while the 1:1 hydrogels had final moduli in the 8–9 kPa range. As the inset in **Figure 2.7** shows, gelation took place in under a minute [as indicated here by the crossover of

the storage modulus ( $G'$ ) and loss modulus ( $G''$ )], although the storage modulus did not reach a plateau until much later, which may suggest that the reaction of the thiol and vinyl sulfone groups is incomplete at shorter timescales during gelation. While we did not explicitly evaluate the extent of reaction in these gels in this initial report, such evaluation will be a part of future studies. *In situ* oscillatory rheology for RLP-PEG hydrogels cross-linked with RLP12, RLP36, or RLP48 indicated similar results (data not shown). These data are consistent with the gelation profiles of other multicomponent-PEG hydrogel networks cross-linked via Michael-type additions,<sup>[52, 97]</sup> although are in contrast to the gelation profiles of RLP12 hydrogels (25 wt%) cross-linked with  $\beta$ -[tris(hydroxymethyl)phosphino]propionic acid (THPP) (which reached plateaus within 10 min).<sup>[105]</sup> This disparity is likely due to the difference in the cross-linker; the diffusion of small molecule cross-linkers such as THPP is not as restricted as macromolecules such as the PEG-VS.

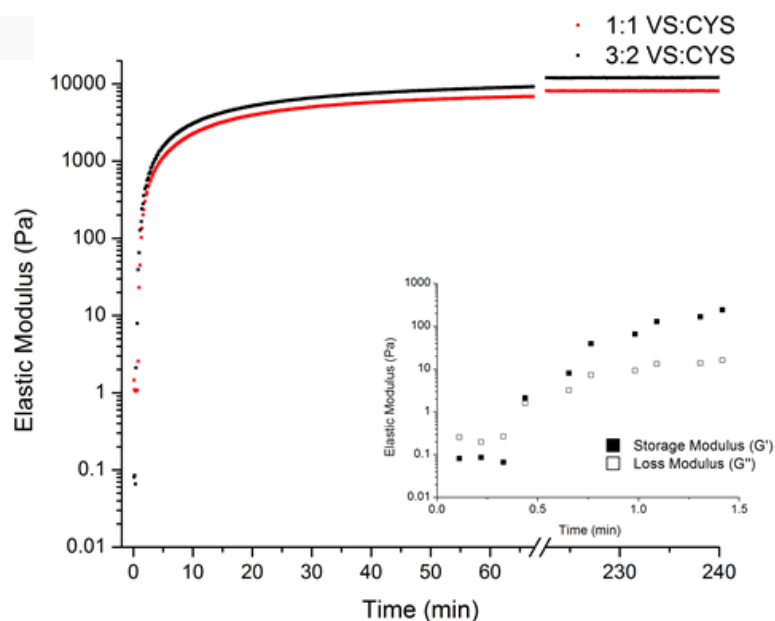


**Figure 2.7** Oscillatory rheology time sweep of a 20wt% RLP24-PEG hydrogel cross-linked at 1:1 (gray) or 3:2 (black) molar ratios of vinyl sulfone to cysteine, at 37°C with an angular frequency of 6 rad/s and a strain of 1%. The inset demonstrates that the storage modulus ( $G'$ , solid squares) exceeds the loss modulus ( $G''$ , open squares) within a minute.

To assess the stability of the RLP-PEG hydrogels across a range of shear rates, dynamic oscillatory frequency sweeps ranging from 0.1 to 100  $\text{rad s}^{-1}$  were employed; **Figure 2.8** provides representative data from experiments with the RLP24-PEG hydrogels. The values of the storage modulus were insensitive to frequency over the frequencies investigated, indicating that the hydrogels behave as elastic solid-like materials expected of permanently cross-linked networks. Similar insensitivity to angular frequency was observed for the RLP-PEG hydrogels cross-linked with RLP12, RLP36, and RLP48 (data not shown) and for the previously reported RLP hydrogels cross-linked with THPP.<sup>[100, 105]</sup> Interestingly, at higher angular frequencies

the RLP-PEG networks behaved more elastically than other recombinant protein-PEG hydrogels cross-linked by the same chemistry,<sup>[97]</sup> the recombinant protein-PEG hydrogels reported by Rizzi *et al.* demonstrated increasing phase angle and loss modulus starting at angular frequencies beginning in the 2–5 Hz range, which was attributed to network structure relaxations at those higher frequencies. The relative insensitivity of the RLP-PEG hydrogels at high angular frequencies indicates a robust network with a potential wider range of clinical applications.

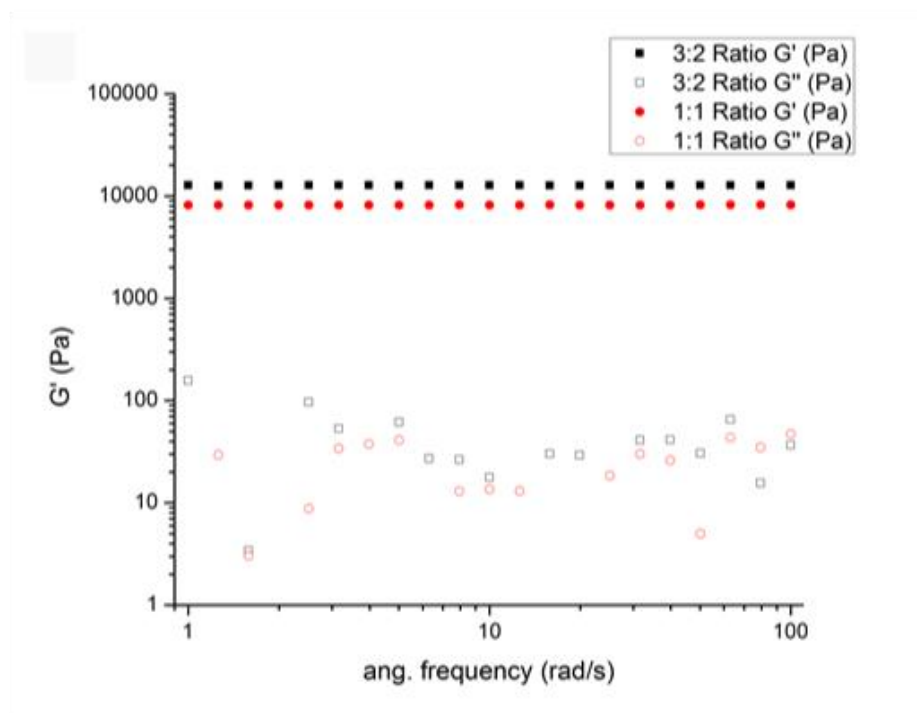


**Figure 2.8** Oscillatory rheology frequency sweep experiments for RLP24-PEG hydrogels. Frequency sweeps were conducted over a range from 0.1 to 100 rad/s for 20wt% hydrogels cross-linked at 1:1 (red) or 3:2 (black) vinyl sulfone to cysteine at 37°C. The closed squares indicate the storage modulus ( $G'$ ) and the open circles indicate the loss modulus ( $G''$ ).

**Table 2.3** provides a summary of the observed final elastic moduli for hydrogels cross-linked with all four of the RLPs. With the exception of RLP12, there was little change in the final elastic moduli of the RLP–PEG hydrogels regardless of the number of cysteines on the RLP, owing to the fact that the molecular weight between cross-links does not change between the various RLP constructs.<sup>[100, 158]</sup> Hydrogels cross-linked using RLP24, RLP36, and RLP48 had elastic moduli in the 7–9 kPa range when cross-linked in a 1:1 ratio and of approximately 11–12 kPa when cross-linked in a 3:2 ratio of vinyl sulfone to cysteine thiol. The reason that RLP12, which contains only two cysteine residues, does not follow this trend is likely due to its propensity to form network defects; the failure of one cysteine to react with a load bearing part of the network would result in the formation of a dangling chain end.<sup>[52, 158, 230]</sup> Nevertheless, the final mechanical properties of these hydrogels fall within 5–10 kPa, a suitable range for cardiovascular applications.<sup>[73, 231]</sup>

**Table 2.3** Summary of mechanical properties for RLP-PEG hydrogels

RLP	Number of Cysteines <sup>a)</sup>	Cross-linking Ratio[VS:CYS] <sup>b)</sup>	
		1:1	3:2
		Storage Modulus (Pa) <sup>c)</sup>	Storage Modulus (Pa) <sup>c)</sup>
RLP12	2	2628.0 ± 620.8	7187.3 ± 378.9
RLP24	3	8038.0 ± 1383.6	12297.5 ± 1571.3
RLP36	4	7769.6 ± 394.4	11930.6 ± 1631.9
RLP48	5	8947.5 ± 730.4	11480.9 ± 361.7

<sup>a)</sup> number of cysteines contained on the polypeptide; <sup>b)</sup> the ratio of vinyl sulfone groups to cysteine residues in a 20wt% hydrogel; <sup>c)</sup> value for storage modulus is an average of at least three samples and the (±) error is equal to the one standard deviation.

### 2.3.4 Encapsulated Cell Viability and Proliferation Assays

Human aortic adventitial fibroblasts (AoAF) were mixed at room temperature into a solution containing RLP24 and PEG-VS at a 3:2 ratio of vinyl sulfone to cysteine; the resulting hydrogels were cultured at 37 °C in a 5% CO<sub>2</sub> incubator in SCGM growth media. Cell viability was analyzed several hours following encapsulation, out to 7 d of culture, using fluorescent laser scanning confocal imaging via live/dead staining. Representative images shown in **Figure 2.9** illustrate the great excess of the calcein-AM stain (green) and relative absence of ethidium homodimer-1 (red), indicating that the majority of cells survive encapsulation and remain viable out to 7 d; indeed, the AoAFs not only survive encapsulation but also begin to spread out and adopt a spindle-shaped morphology by day 7. **Figure 2.9A** presents day 0 data for the AoAFs a few hours following encapsulation and shows viable cells with a rounded

morphology that are small in size. Twenty-four hours following encapsulation (**Figure 2.9B**), the majority of the AoAFs remain rounded, but a few appear to begin spreading in the hydrogel. By day 3 (**Figure 2.9C**), these extensions become more clearly defined and more cells adopt this phenotype; additionally, the cells have also increased in size. By day 7 (**Figure 2.9D**), a majority of the AoAFs has adopted a spread phenotype and the cells have also grown considerably larger in comparison to those analyzed immediately following encapsulation (Day 0). The data clearly show that the RLP-PEG matrices can support encapsulated fibroblasts, but it also suggests that the cells may be interacting with the biological cues engineered into the RLP. The transition from a rounded to extended morphology over the course of a week suggests that these cells may be locally degrading the RLP-PEG matrix and perhaps are forming focal adhesions to the integrin binding domains.<sup>[52, 96, 221]</sup> It is well documented the inclusion of matrix degradation sequences and cell adhesion domains facilitates cell spreading in 3D<sup>[18, 52, 96, 222]</sup> and that the absence of these domains results in cells that remain rounded.<sup>[90, 197]</sup> Therefore, due to the clear morphological change of the AoAFs and the fact that it took several days for this transformation to occur, it is reasonable to suggest that the cells are remodeling and adhering to the RLP-PEG matrix. RLPs that lack the cell-binding domains and MMP-sensitive sequences are currently under investigation.

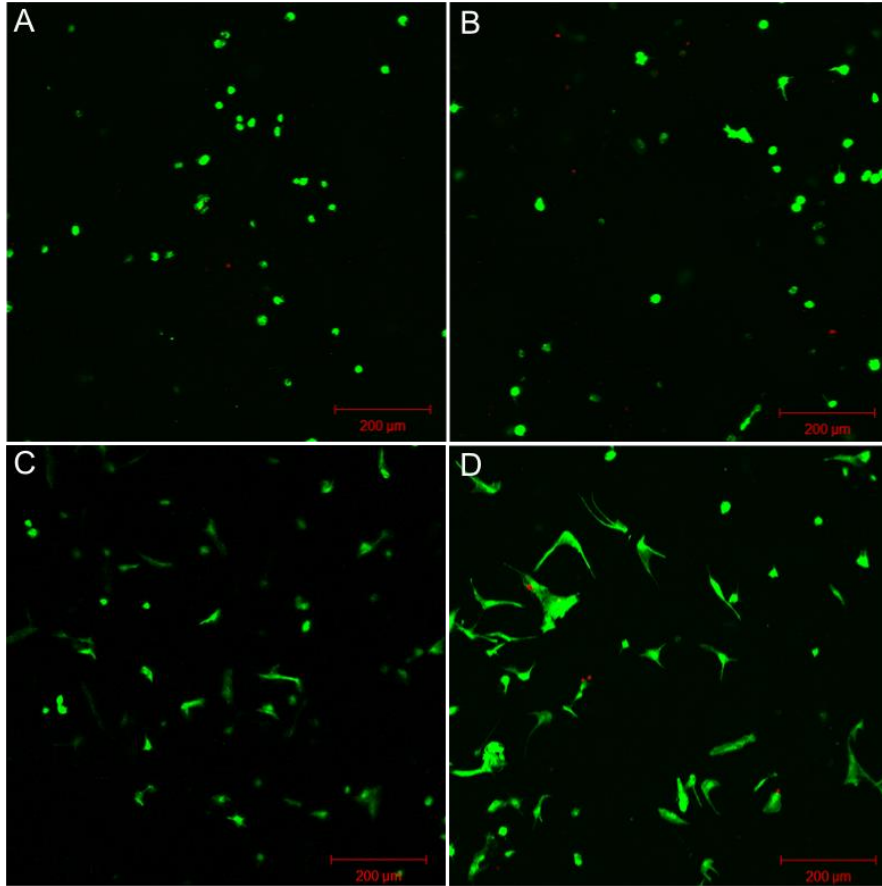


**Figure 2.9** Fluorescent laser scanning confocal microscopy of human aortic adventitial fibroblasts (AoAF) encapsulated in 20wt% RLP24-PEG hydrogel cross-linked at a 3:2 vinyl sulfone to cysteine ratio, stained using Live/Dead stains.<sup>TM</sup> Calcein AM (Live) stain is shown in green and ethidium homodimer (Dead) stain is shown in red. Images are z-stacks of hydrogels (200  $\mu\text{m}$  thick) taken at 10x magnification using a water lens. Representative images from (A) Day 0, (B) Day 1, (C) Day 3 and (D) Day 7 are presented; the AoAFs remain viable throughout the entire experiment. Initially, the cells are rounded but as the experiment progresses they begin to adopt a spread morphology

To determine whether the fibroblasts were proliferating, cell nuclei were stained with Draq 5 in addition to Live/Dead stains and imaged using fluorescent laser scanning confocal microscopy; the number of nuclei was counted using Volocity 3D

Image Analysis Software imaging software. Three individual hydrogels were imaged per time point and a significant area of each hydrogel was imaged ( $\approx 5 \mu\text{L}$ ) in an effort to prevent bias. It is assumed that all nuclei would be stained with the membrane permeable Draq 5 and that only the membrane-compromised cells would be stained with the ethidium homodimer, therefore the difference between the two counts represents the number of living cells. **Figure 2.10** reports the average number of living cells at each time point in approximately a  $5 \mu\text{L}$  volume of RLP-PEG hydrogel. In the figure, the bars represent the average of three gels with the error bars indicating one standard deviation; the open circles provide the actual numbers of living cells recorded for an individual hydrogel. The general trend of the data indicate that the number of living cells drops initially, as has been reported for other 3D cell constructs,<sup>[222, 232]</sup> but recovers by the final time point at day 7. Unfortunately, there is a large spread in the data (particularly for days 0 and 7), which most likely results from an initial lack of homogeneity of cell dispersion in these gels during gelation. Despite this experimental error, the number of living cells remains stable, and perhaps increases with time, providing further evidence that the RLP-PEG matrices can successfully support encapsulated fibroblasts.

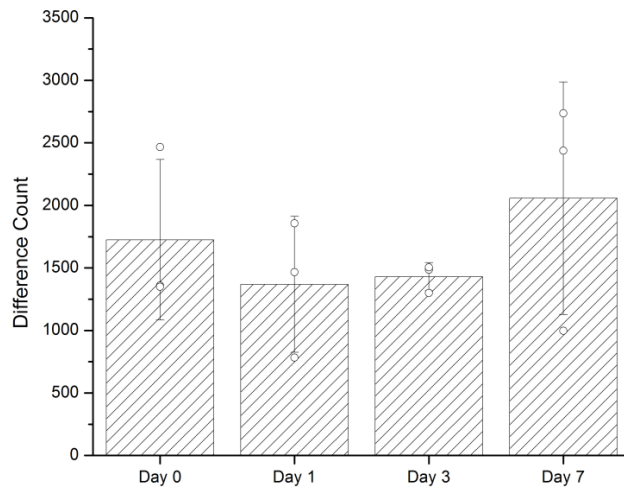


**Figure 2.10** Proliferation data for encapsulated human aortic adventitial fibroblasts (AoAF) in RLP24-PEG hydrogels over seven days of cell culture. The bars represent the average number of living nuclei counted at a given timepoint; the error bars represent one standard deviation from the mean and the open circles represent the counts for each hydrogel analyzed ( $n = 3$ ). The number of living cells was determined by finding the difference between the number of nuclei stained by membrane-permeable Draq5 and the number of nuclei stained by membrane-impermeable ethidium homodimer. Fluorescent laser scanning microscopy was used to analyze four adjacent z-stacks that were  $1800 \mu\text{m} \times 1800 \mu\text{m} \times 400 \mu\text{m}$  (length x width x depth) for three different hydrogels at each timepoint. Volocity was used to count the cell nuclei for both the Draq5 and the ethidium homodimer channels. The results show that the number of nuclei remains relatively stable and that by day 7 the cells may be beginning to proliferate.

Hybrid hydrogels consisting of protein and PEG offer a strategy to designing tissue engineering materials that combine the inherent bioactivity of proteins with the versatility of synthetic systems. Seliktar and co-workers<sup>[233]</sup> have employed PEGylated-fibrinogen/fibronectin copolymers that could be cross-linked into hybrid

hydrogels through the photoinitiated polymerization of acrylate moieties on the PEG chains. These hydrogels demonstrated utility in the three-dimensional cell culture of cardiomyocytes,<sup>[234]</sup> neonatal human foreskin fibroblasts,<sup>[235]</sup> and smooth muscle cells.<sup>[236]</sup> Although the fibrinogen/fibronectin conferred the hydrogels with cell adhesive and cell-mediated degradation properties,<sup>[233-236]</sup> there was still little to no control over the size and sequence of the protein component of these hydrogels and therefore cell-matrix interactions could not be adapted to specific biological applications.<sup>[97]</sup> Halstenberg *et al.*<sup>[95]</sup> and Rizzi *et al.*<sup>[96, 97]</sup> demonstrated that protein polymers, in which size and amino acid sequence are exactly controlled, could be cross-linked using PEG cross-linkers into elastic hybrid matrices using photopolymerization and Michael-type addition, respectively. The protein polymers contained sequences derived from extracellular matrix (ECM) proteins that conferred enzyme-degradable and cell adhesive properties. Encapsulated neonatal foreskin fibroblasts demonstrated the ability to migrate through the matrices which contained the degradable sequences suggesting that the cells were actively remodeling and interacting with their microenvironment.<sup>[95-97]</sup>

The results presented here indicate the potential of RLP-PEG matrices as tissue engineering materials for cardiovascular tissue engineering. Future work will investigate the role of the MMP-sensitive domain and the presence of integrin-binding domains in the development of the spindle-like AoAF morphology. Additionally, matrix stiffness has previously been indicated by our group as having an impact on the proliferation and phenotypes of AoAFs,<sup>[73, 237]</sup> and the use of RLP-PEG hydrogels for 3D encapsulation of these cells may provide a more physiologically relevant analysis of the effects of matrix elasticity on these cells.

## **2.4 Conclusions**

This study reports the development and production of three high-molecular-weight RLPs, which can be cross-linked into elastic hybrid hydrogels via a Michael-type addition reaction with a PEG-vinyl sulfone cross-linker. These hydrogels can be cross-linked under benign conditions and successfully encapsulate human aortic adventitial fibroblast cells. The encapsulated cells remained viable over 7 d of culture and began to adopt a spread morphology consistent with the natural fibroblast phenotype. These hybrid hydrogels present a promising strategy to the development of tissue engineering materials for cardiovascular applications.

## Chapter 3

### THE RESILIENCE, DEGRADATION, CYTOCOMPATIBILITY AND LIQUID-LIQUID PARTITIONING OF RESILIN-PEG HYBRID HYDROGELS

#### 3.1 Introduction

One of the primary motivations behind the design of elastomeric protein hydrogels is to recreate the flexible, reversible elasticity of native soft tissues. In tissue engineering applications, the hydrogel scaffold needs to serve as a temporary substitute while healthy tissue regenerates and it is therefore important to engineer a durable scaffold that may withstand the repetitive mechanical forces characteristic of some soft tissues.<sup>[196]</sup> Research into “intrinsically disordered proteins” (IDP) such as elastin, resilin and flagelliform spider silk have become increasingly important as these proteins display remarkable elasticity and fatigue resistance.<sup>[102]</sup> Recombinant protein polymers based upon the characteristic sequences of IDPs have demonstrated mechanical properties comparable to the natural proteins.<sup>[102]</sup> Previously mentioned in **Chapter 1**, our laboratory has recently developed resilin-like polypeptides (RLPs) for mechanically-demanding tissue engineering applications. RLP hydrogels cross-linked using a small amine-reactive molecule formed elastic hydrogels that were shown to be stable, resilient and highly extensible via tensile testing and oscillatory rheology.<sup>[105, 107, 238]</sup> Hybrid hydrogels, composed of RLPs cross-linked with PEG macromers, were introduced in the following chapter (*see Figure 2.1*) and were found to be stable, viscoelastic materials as characterized by oscillatory rheology. However, it was left undetermined as to whether the RLP-PEG hydrogels shared the rubber elasticity of

their amine cross-linked counterparts. To address this shortcoming, tensile testing of these hydrogels was employed using a dynamic mechanical analyzer and the results are reported in this chapter.

For tissue engineering scaffolds to perform well as temporary substitutes, they must have suitable mechanical properties, such as rubber elasticity, but also need to contain a mechanism through which they are eventually removed and replaced by the new tissue. Degradation of the scaffold through either chemical<sup>[49, 50, 218]</sup> or biological means<sup>[53, 58, 96, 214]</sup> is absolutely essential. However, it is important that the material degrade in synchrony with the formation of new tissue so as to prevent either the failure of the scaffold prior to tissue maturation or the obstruction of regenerating tissue.<sup>[8]</sup> Cell-mediated degradation has been proposed as one method of achieving this type of control; as cells proliferate and populate the scaffold, the matrix is degraded through the digestion of proteolytic cross-links.<sup>[52, 214]</sup> Essentially the scaffold is remodeled ‘on-demand’ by infiltrating or encapsulated cells. Numerous materials have employed this paradigm including recombinant protein polymers.<sup>[95-97, 100, 101, 104]</sup> In fact, since proteolytic sequences can be directly engineered into the backbone of protein polymers, it is quite easy to introduce the functionality to these materials.<sup>[74, 101]</sup> A number of elastin-like, silk-like and resilin-like polypeptides have been engineered with proteolytic domains.<sup>[93, 101, 107, 239]</sup> The RLPs described in **Chapter 2** (*see Figure 2.1*) were engineered with matrix metalloproteinase (MMP) sensitive domains as MMPs have been implicated the remodeling of ECM and structural proteins.<sup>[227, 240]</sup> Matrix remodeling by MMP is an important function of tissue morphogenesis and repair.<sup>[241]</sup> This chapter reports the degradation of both soluble RLP and RLP-PEG hydrogels by MMP.

In the previous chapter, the cyto-compatibility of the RLP-PEG hydrogels was demonstrated through encapsulation experiments of human aortic adventitial fibroblasts. These cells remained viable following a week of culture within the RLP-PEG hydrogels and after a few days the cells began to spread and adopt a spindle-like morphology not present in other hydrogels constructed from recombinant, elastomeric proteins.<sup>[90, 101, 197]</sup> In the present chapter, the survival and behavior of encapsulated human mesenchymal stem cells (hMSCs) is investigated. Stem cells are an important aspect of tissue engineering. Their capacity for self-renewal and potential for differentiation are traits that researchers seek to incorporate into tissue engineered materials.<sup>[5]</sup> Adult hMSCs are a particularly useful subset of stem cells that are easily expanded, relatively nonimmunogenic and can be differentiated into several different types of tissue.<sup>[242]</sup> In cardiovascular tissue engineering applications, it has been found that populations of hMSCs express endothelial markers while others express smooth muscle markers. It has also been hypothesized that hMSCs may function as vascular progenitors,<sup>[243-245]</sup> which may have important applications in the development of healthy vascular tissue following coronary bypass surgery.

Finally, this chapter reports on the liquid-liquid partitioning behavior which unexpectedly occurred upon the mixing of precursor solutions to form the RLP-PEG hydrogels. Liquid-liquid partitioning is well known behavior for macromolecular solutions of PEG and protein,<sup>[246, 247]</sup> but previous recombinant protein-PEG hydrogels make no mention of the phenomenon.<sup>[95-97, 181]</sup>

## 3.2 Experimental Section

### 3.2.1 Materials

All chemicals or reagents were purchased from Sigma-Aldrich (St. Louis, MO) or Fisher Scientific (Waltham, MA) and used as received unless otherwise noted. Ni-NTA agarose used for protein purification was purchased from Qiagen (Valencia, CA) or Thermo Scientific (Rockford, IL). Water for buffers or media was deionized and filtered using either a ThermoFisher Barnstead NANOpure Diamond water purifier or a Purelab *Classic* (Siemens, Munich, Germany). The synthesis and characterization of the 4-arm PEG vinyl sulfone cross-linker was previously described<sup>[104]</sup> and used established protocols.<sup>[52]</sup> The vinyl sulfone functionality of the PEG macromer was found to be ~4 based upon <sup>1</sup>H NMR analysis reported previously.<sup>[104]</sup>

### 3.2.2 Expression and Purification of RLP24

All the studies described in this chapter were performed using a single resilin-like polypeptide, RLP24, (*see* **Figure 2.1**) derived from the previously reported family of RLPs constructed by the Kiick laboratory. The RLP24 polypeptide was found to cross-link as effectively as higher molecular weight RLPs, but RLP24 expressed in higher yields. For these studies, RLP24 was expressed and purified using the same methods reported on in the earlier publication.<sup>[104]</sup> In brief, Studier auto-induction and ZYP-5052 media was used for the expression;<sup>[167]</sup> a 4-hour growth period at 37°C was followed with a 24-hour 24°C expression period. Cells were pelleted via centrifugation and frozen at -20°C. Sonication and detergent-containing lysis buffer was used to disrupt the cell walls and centrifugation cleared the lysate of insoluble debris. As reported previously, a heating step under reducing conditions improved the

final purity of the RLP24 polypeptide. The protein contained a 6xHis fusion tag for affinity chromatography purification and the protein was dialyzed against pure water to remove salts prior to lyophilization. The purity of the protein was confirmed using sodium dodecyl sulfate polyacrylamide gel electrophoresis (SDS-PAGE) visualized with Coomassie blue staining. The characterization of the RLP24 polypeptide via amino acid analysis and mass spectroscopy was previously reported.<sup>[104]</sup>

### **3.2.3 Preparation of Reduced RLP24**

Pure lyophilized protein was reduced using tris(2-carboxyethyl)phosphine hydrochloride (TCEP-HCl) in a 10 mM MES, 500 mM NaCl buffer (pH 5.5). Depending upon the initial free thiol content of the RLP, the TCEP-HCl to thiol ratio and the incubation time was modulated. However, conditions usually consisted of a 1-3x TCEP-HCl to thiol ratio and an incubation period of approximately one hour at room temperature with mixing. The protein was reduced at a 20 mg/mL concentration, but was diluted to 10 mg/mL by additional MES buffer in preparation for the desalting process.

Two methods were employed for the removal of salts and TCEP-HCl prior to freezing and lyophilization. The first method utilized Zeba™ Spin desalting columns (7 kDa MWCO, ThermoFisher, Rockford, IL). The flow through was collected and immediately frozen using liquid N<sub>2</sub> and lyophilized.<sup>[104]</sup> This method proved suitable for the production of reduced protein, but inconsistent results required multiple attempts that proved expensive and resulted in lost protein. Fast protein liquid chromatography (FPLC) was employed to improve upon the desalting process and to track the differential elution of protein and salt. A GE Life Sciences AKTA™ Explorer100 and Purifier 10 high performance FPLC (Delaware Biotechnology

Institute, Newark, DE) equipped with a HiPrep<sup>TM</sup> 26/10 Desalting column was used. RLP24 protein was reduced using the same conditions as described above and was pumped to the column at a rate of 8-10 mL/min using a mobile phase of chilled, deionized and filtered water. The UV/vis detector set at 280 nm monitored the flow of protein in the mobile phase while the conductivity detector was used to measure salt concentration. The RLP24 protein eluent was collected, immediately frozen in liquid N<sub>2</sub> and lyophilized.

The free thiol content of lyophilized protein was determined using an Ellman's colorimetric assay and UV/vis spectroscopy. A sample of reduced protein was weighed and a theoretical thiol content was estimated using the molecular weight and sequence of RLP24. The sample was dissolved in a solution containing the Ellman's reagent (100 mM Tris, 2.5 mM sodium acetate and 40 μM DTNB, pH 8.0) and the absorbance at 412 nm was measured using an Agilent 4853 UV-vis spectrophotometer. The free thiol content of the sample was calculated using the absorbance and the extinction coefficient of TNB<sup>2-</sup> ion.<sup>[225, 226]</sup>

### **3.2.4 Hydrogel Formation and Characterization of Swelling**

All of the RLP24-PEG hydrogels in this study were cross-linked using a 20 wt% precursor solution including both RLP and PEG; however, three different cross-linking ratios were explored: 3:2, 1:1 and 1:2 of vinyl sulfone to cysteine thiol. Since the weight percent remained constant but the cross-linking ratios differed the final composition of the hydrogels changed slightly as summarized in **Table 3.1**.

**Table 3.1** Summary of RLPL24-PEG Hydrogel Compositions and Precursor Properties

<b>Vinyl Sulfone:Cysteine Cross-linking Ratio</b>	<b>Mass %</b>		<b>Mole Ratio</b>
	<b>RLP24</b>	<b>PEGVS</b>	<b>RLP24:PEGVS</b>
<b>3:2</b>	81.45	18.55	2.67
<b>1:1</b>	86.82	13.18	1.33
<b>1:2</b>	92.94	7.06	0.89

<b>Precursor</b>	<b>Molecular Weight (Da)</b>	<b>Functionality</b>
<b>PEG-Vinyl Sulfone</b>	10,000	4
<b>RLP24</b>	49,389	3

To prepare cross-linked RLP-PEG hydrogels, the precursors were first dissolved separately in PBS buffer (pH 7.4). For mechanical testing and swelling studies, the RLP24 was dissolved in enough PBS to equal 80% of the final volume of the hydrogel solution. For example, a 100 uL hydrogel would have been cross-linked using an 80 uL RLP solution and a 20 uL PEG solution regardless of the cross-linking ratio. A pH sensitive dye, phenolphthalein (1 mM), was included in the RLP solution and 0.2 uL drops of concentrated NaOH were used to adjust the final pH to ~8.2. This was indicated by a color change in the solution to a slightly pinkish hue which corresponds to the color change phenolphthalein (colorless → pink) undergoes at pH 8.2.

To create hydrogels for the swelling investigations, 40 uL hydrogels were prepared on Parafilm<sup>TM</sup> substrates and cross-linked overnight at 37°C in a humidified chamber. The gels were swelled for 120 hours at 37°C in a PBS buffer containing a solution of 1mM ethylenediaminetetraacetic acid (EDTA), 0.002% sodium azide and antibiotic/antimycotic (Life Technologies, Carlsbad, CA) to prevent enzymatic degradation or microorganism contamination. The swollen hydrogels were removed from the buffer, carefully blotted dry using a Kimwipe and measured gravimetrically

on a microbalance. To measure the dry weight of the RLP-PEG hydrogel the hydrogels were frozen in liquid N<sub>2</sub> and lyophilized. The swelling ratio and water content were calculated using the following equations:<sup>[93, 101, 105]</sup>

$$q = \frac{m_s}{m_d}$$
$$WC = \frac{m_s - m_d}{m_s} \times 100\%$$

where  $q$  is the swelling ratio at equilibrium,  $WC$  is the water content at equilibrium,  $m_s$  is the mass of the swollen hydrogel and  $m_d$  is the mass of the dried hydrogel. The data reported are the simple mean of five samples with the error reported as the standard deviation.

### 3.2.5 Oscillatory Rheology

The oscillatory rheology experiments were conducted on a stress-controlled AR-G2 rheometer (TA Instruments, New Castle, DE) using a 20 mm diameter stainless steel cone-on-plate geometry with a 1° cone angle and a 25 μm gap distance. The precursor solutions were prepared as described above. To slow the rate of cross-linking, the precursors were chilled on ice prior to being briefly mixed using a vortex mixer. Quickly, the RLP-PEG solution was deposited onto a prechilled (4°C) rheometer stage while the cone-on-plate geometry was brought to the appropriate gap. Mineral oil sealed the geometry and prevented evaporation; the temperature was then quickly raised to 37°C where it was maintained for the remainder of the experiment. The formation of elastic hydrogels was monitored using a time sweep conducted at 1% strain and an angular frequency of 6 rad/s. This experiment was followed with a frequency sweep from 0.1 rad/s to 100 rad/s conducted at 1% strain. Experiments were repeated on three to four samples for each cross-linking ratio and the shear modulus

was reported as the simple mean. The error was the corresponding standard deviation of the samples tested.

### **3.2.6 Tensile Testing**

The tensile testing of the RLP24-PEG hydrogels was carried out on an RSA-G2 dynamic mechanical analyzer (DMA) (TA Instruments) using the axial tensile geometry and immersion chamber. Previously, hydrogel films of cross-linked RLP were cast in a contact lens molds and a stainless steel dye was used to cut dog-bone shaped specimens.<sup>[100, 105, 238]</sup> However, this method proved to be unsuitable for the RLP-PEG hydrogels as the instrument could not measure these smaller hydrogels. Instead, polytetrafluoroethylene (PTFE) molds (prepared courtesy of Derrick Allen, Department of Chemistry & Biochemistry, University of Delaware, Newark, DE) were used to cast comparatively larger RLP-PEG hydrogels. Two different formats were used for these experiments: large gels for uniaxial cyclic strain testing and smaller gels for strain-to-break measurements.

To construct the molds small rectangular indentations were carved/drilled into a block of PTFE (Industrial Plastic Supply, Anaheim, CA) and on the reverse side two injection holes were drilled at either end of the rectangular indentation. **Figure 3.1** provides an image of the two types of molds. The dimensions of the mold are provided in **Table 3.2**.

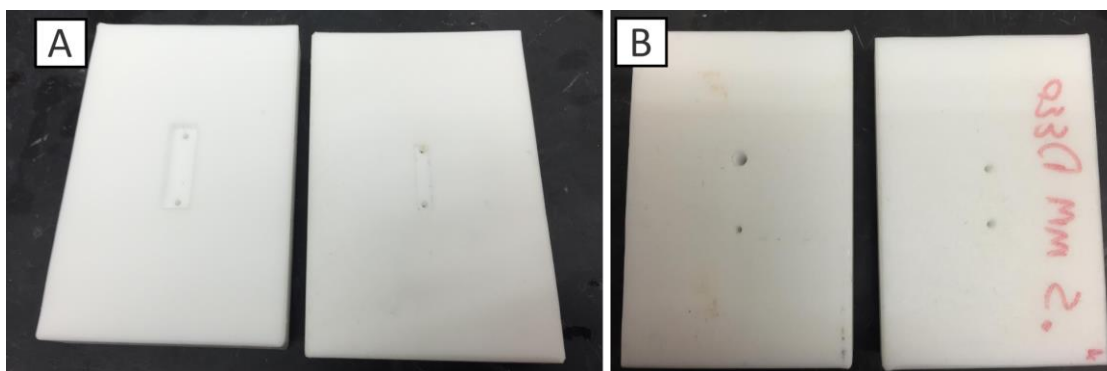


**Figure 3.1** Image of the large and small Teflon molds. On the left is the mold used for cyclic strain testing and on the right is the mold for strain-to-break hydrogels. **(A)** Front side of the mold containing the indentation. **(B)** Reverse side of the mold for loading precursor solution. The mold on the left had one larger injection hole due to the size of the pipette tip used to fill the mold.

**Table 3.2** Dimensions of the Tensile Molds

Mold Type	Length (mm)	Width (mm)	Depth (mm)
Cyclic Testing	20.0	6.3	1.5
Strain to Break	15.0	3.5	0.75

To create the hydrogels, a glass slide was placed over the indentation and sealed using vacuum grease. The RLP24 and PEGVS precursors (again, prepared as described in **Section 3.2.3**) would be mixed on a vortex mixer and then pipetted into the mold through the injection holes. **Figure 3.2** provides an illustration of this process using water dyed with bromophenol blue for contrast.

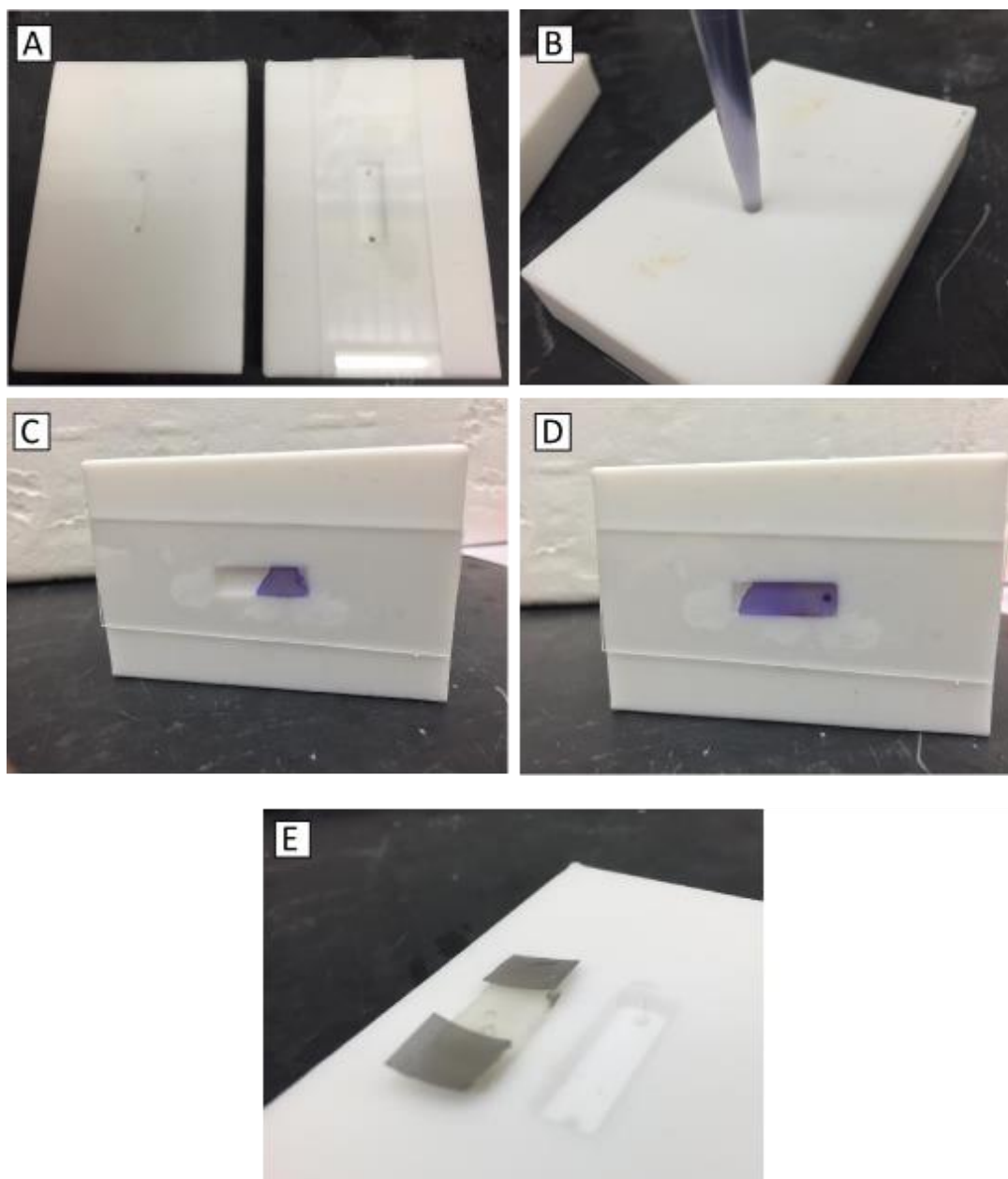


**Figure 3.2** Illustration of the process for making the RLP24-PEG hydrogels for tensile testing. (A) A glass slide is used to cover the mold which is then flipped over and (B) injected with the precursor solution (water + bromophenol blue is shown for contrast). The mold is filled with the precursor (C, D) and cross-linked in a humidified chamber, overnight at 37°C. (E) The cross-linked gel is removed from the mold and small rectangular pieces of steel mesh are placed at either end to provide friction for the DMA geometry. An actual RLP24-PEG gel is shown in final image.

The mold would then be placed in a humidified chamber and cross-linked overnight at 37°C. The following day gels would be carefully removed in a bath of water to provide lubrication and to prevent the gel from tearing. The gels were then swelled under the conditions described above for a minimum of 48 hours before testing. Gels were stored at 4°C in sealed containers with a small amount of the PBS buffer containing antimicrobial reagents. The dimensions of the swollen hydrogel were measured using calipers before testing.

Small pads of steel mesh (McMaster-Carr, Elmhurst, IL) were cut and placed at either end of the rectangular gels. These helped provide friction and prevented slipping when the gels were placed in the axial tensile geometry of the DMA. An immersion chamber kept the gels hydrated in PBS buffer during the experiments. For the cyclic strain experiments the hydrogels were strained to 20%, 40% and 60% strain at a constant rate of 0.1 mm/s for five cycles per sample. The gels used for the strain-to break measurements were similarly strained at a 0.1 mm/s strain rate.

The raw data were entered into Origin™ 8.5.1 (OriginLab Corporation, Northampton, MA) for analysis. In order to calculate the resilience of these materials the raw data points were converted into smooth curves using a Signaling Processing function, “Adjacent Averaging.” This function generated a curve based upon the average of a five data point window for each raw data point gathered by the DMA. An example of this is presented in **Figure 3.3**. To determine the resilience of the material the adjacent average extension and retraction curves were integrated to find the corresponding area beneath the curve. Resilience is measured as the percent of energy recovered following deformation and was calculated by dividing the area of the retraction curve by the area of the extension curve.<sup>[105, 238]</sup> The resilience for a

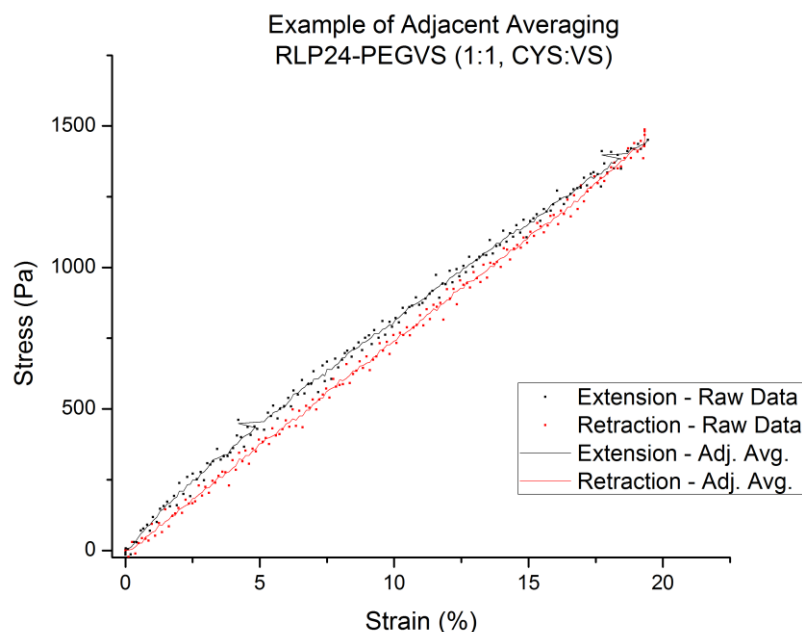


**Figure 3.3** Representative graph of how adjacent averaging was utilized to create curves for resilience measurements. The black dots represent the raw data for the extension, the red dots represent the raw data for the retraction, the black line represents the adjacent average curve for extension and the red line represents the retraction adjacent average curve.

particular sample was the simple mean for all five cycles at one of the strains (20, 40, or 60% strain). The final resilience for a given cross-linking ratio and strain was calculated as the average of three or four samples. The Young's modulus for a particular sample was found by taking a linear fit of the extension curve (up to 10% strain) for each cycle of a 60% strain experiment. The slope for each curve was averaged to give the modulus.<sup>[203]</sup> The Young's modulus for a given cross-linking ratio was the simple mean of a three or four samples. For the strain-to-break measurements, an adjacent average curve was generated using the same procedure. The strain-to-break was determined to be the percent strain at which the stress dropped by 20% or

more (tearing was considered breaking). The final strain-to-break values reported were the simple mean of three or four samples for each cross-linking ratio. The error for all of the reported data is the standard deviation of three or four samples.

### 3.2.7 Biochemical Degradation of RLP24 and RLP24-PEG Hydrogels

The RLP24 protein was engineered to contain two MMP sensitive domains for matrix degradation (*see* **Figure 2.1**). The biochemical degradation of RLP24 was analyzed by incubating free polypeptide with MMP enzyme and sampling the reaction over a 24-hour period. These samples were then characterized using SDS-PAGE and densitometry. The effect MMP had on the mechanical properties of RLP-PEG hydrogels was also investigated. Hydrogel degradation was monitored *in situ* by compression testing on the DMA over a 10-hour time period.

The soluble degradation experiments was carried out in triplicate at 37°C by degrading a 7.3  $\mu\text{M}$  (0.36  $\mu\text{g/mL}$ ) concentration of RLP24 in a buffer (50 mM HEPES, 2 mM  $\text{CaCl}_2$ , 0.05% Brij-35) containing 56 nM (1.1 mg/L) of recombinant catalytic domain of the human MMP-1 enzyme (rhMMP1) (Enzo Life Sciences, Farmingdale, NY). The temperature was maintained using a Mastercycler<sup>TM</sup> PCR thermal cycler (Eppendorf, Hamburg, Germany). Over a 24 hour time period 20  $\mu\text{L}$  samples were removed from a 320  $\mu\text{L}$  reaction volume and were mixed with SDS sample buffer to neutralize the enzymatic activity. The samples were then immediately frozen to await further analysis via gel electrophoresis (12% SDS-PAGE).<sup>[248]</sup> The gels were stained with Coomassie Blue and densitometry analysis was performed on scanned images of dried gels (NIH ImageJ software, Bethesda, MA).

The mechanical properties of RLP24-PEG hydrogels incubated in the presence of the rhMMP1 enzyme were monitored using compression testing via the RSA-G2

DMA. Using the same cross-linking protocol described in the sections above, cylinder shaped RLP24-PEG hydrogels (50  $\mu$ L, 20wt%, 3:2 ratio of vinyl sulfone to cysteine thiol) were cross-linked using modified syringes. These gels were swelled for ~3 days in the antimicrobial/EDTA PBS buffer at 37°C and stored at 4°C. Gels were allowed to come to room temperature prior to the start of the experiment. The immersion chamber provided by TA Instruments had a volume of ~35mL and would require a significant amount of enzyme. Therefore, a smaller chamber with a volume of 1.5 mL was constructed from a cylinder of PTFE (courtesy of Derrick Allen). Essentially, the chamber was a small PTFE cup with a hole to fit the compressive geometry (**Figure 3.4**). The bottom plate would be sealed using vacuum grease to prevent the enzyme buffer from leaking and a clear plastic covering was used to reduce evaporation.

The dimensions of the hydrogel were measured using calipers and loaded on to the bottom plate of the geometry. The top plate was brought into contact with the top of the gel and then pre-strained another 10% to prevent detachment during the experiment. For the first 12 hours of the experiment, the enzyme buffer contained no enzyme; this period of testing served as the control. After the initial phase of the experiment the buffer was carefully removed via pipet and replaced with buffer containing the rhMMP1 enzyme at a 171 nM (3.33 mg/L) concentration. The experiment was monitored for another 10 hours. The DMA was set to an oscillatory time sweep experiment where gels were compressed to 5% strain at a frequency of 1 Hz; data points were collected in 15 minute intervals. The raw data were normalized to the initial modulus and a simple average of the normalized data points of three separate samples was used to generate curves; error is the standard deviation.

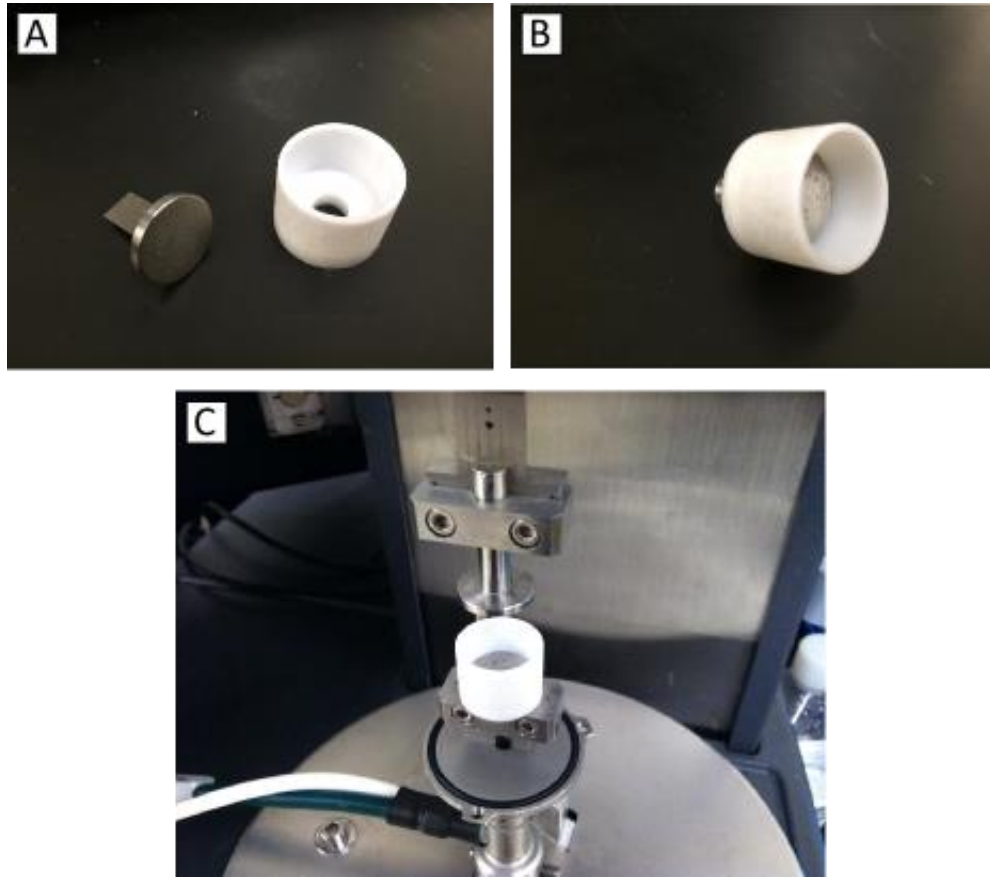


**Figure 3.4** Illustration of how the mechanical property testing under degradation experiments were performed. (A) The PTFE cup and bottom plate for the compression geometry shown individually and (B) assembled. Vacuum grease sealed the junction between cup and plate. (C) The entire assembly installed on the DMA including the top plate for the compression geometry. Not shown was a clear plastic covering that was used to prevent evaporation.

### 3.2.8 Encapsulation, Viability and Proliferation of hMSCs

Bone-derived human mesenchymal stem cells (Lonza, Basel, Switzerland) were cultured according to the manufacturer's specifications at 37°C, 5% CO<sub>2</sub> and using the BulletKit™ hMSC growth medium sold by Lonza. The cell passage number for these experiments ranged between P5 and P10; confluency was kept below 80%.

The encapsulation of hMSCs was performed using the same protocol as reported previously for the encapsulation of human aortic adventitial fibroblast in RLP24-PEG hydrogels.<sup>[104]</sup> The hydrogel composition remained 20wt% with a 3:2 cross-linking ratio (vinyl sulfone:thiol). For cell viability and proliferation imaging, hydrogels with a volume of 50  $\mu$ L were seeded at a density of 200,000 per mL (10,000 per hydrogel).

Over a two week period, cell viability within the RLP24-PEG hydrogels was analyzed via laser scanning confocal microscopy (Delaware Biotechnology Institute, Newark, DE) and Live/Dead® staining (Life Technologies). Hydrogels were placed in PBS buffer containing 2  $\mu$ M Calcein AM and 4  $\mu$ M Ethidium homodimer-1 for 30 minutes prior to imaging on the confocal (Zeiss LSM 510 NLO multiphoton, Carl Zeiss, Inc., Thornwood, NY). Experiments were run in triplicate with several z-stacks acquired from every sample for each time point. Representative maximum intensity projections were reported here.

Proliferation of encapsulated cells was investigated using a Click-iT EdU cell proliferation assay (Life Technologies). Cell-gels were pulsed for 48 hours with a 20 mM concentration of 5-ethynyl-2'-deoxyuridine (EdU) on day 3 of culture. The gels were then fixed with paraformaldehyde (day 5) and reacted, according to the manufacturer's instructions, with Alexa Fluor® 555. Following a destaining procedure to remove the Alexa dye, the cell nuclei were stained with 4',6-diamidino-2-phenylindole (DAPI) and the gels were imaged using a Eclipse Ti-E fluorescent microscope (Nikon, Tokyo, Japan). Experiments were run in triplicate and several z-stacks were acquired.

### 3.2.9 Analysis of Liquid-Liquid Partitioning Behavior

Initially, to investigate the liquid-liquid partitioning behavior of RLP24-PEG hydrogels (20 wt%, 3:2 VS:CYS) phase contrast imaging was employed on the Eclipse fluorescence microscope. RLP24-PEG hydrogels were compared to pure RLP hydrogels cross-linked with an amine-reactive small molecule, tris(hydroxymethyl)phosphine, at a 3:1 ratio of hydroxyl group to lysine in 20wt% solutions of RLP24. The gelation of the pure RLP hydrogels was performed at 37°C for a period of a few hours. Images of the hydrogels were taken immediately following cross-linking using 5x and 10x magnification.

Fluorescent confocal microscopy was also used to investigate the phase separation of the RLP24-PEG hydrogels. For this analysis, RLP24 and PEGVS were labelled with tetramethylrhodamine isothiocyanate (TRITC) (Thermo Fisher) and 5-((2-(and-3)-S-(acetylmercapto) succinoyl) amino) fluorescein, (SAMSA fluorescein, Life Technologies), respectively. RLP24 was dissolved in a sodium carbonate buffer (100 mM pH 9.0) at a 5 mg/mL concentration and was reacted at 4°C overnight with the TRITC fluorophore at a 1:250 ratio of isothiocyanate to lysine. The protein was then desalted using a Zeba™ Spin desalting column (MWCO 7kDa) to remove the unreacted fluorophore. The protein would later be reduced and lyophilized using the protocols described above. The PEGVS was labelled through the reaction of the vinyl sulfone group with the thiol present on the SAMSA fluorescein (1:250 thiol:vinyl sulfone): the SAMSA was prepared according the manufacturer protocol and was reacted with the PEGVS (150 mg) for 1 hour at room temperature in 10.5 mL of buffer (20 mM sodium phosphate, pH 7.5). The PEGVS was similarly desalted to remove residual fluorophore and lyophilized to a dry powder. The fluorescently-tagged precursors were diluted into unlabeled precursors at a 1:100 ratio to form the RLP24-

PEGVS hydrogels. Hydrogels were cross-linked at 37°C within CoverWell™ perfusion chambers (Grace Bio-Labs, Bend, OR) on glass slides and imaged directly.

### 3.3 Results & Discussion

#### 3.3.1 Design, Expression, Purification and Preparation of Reduced RLP24

The design and cloning of the RLP24 gene has already been described in **Chapter 2**.<sup>[104]</sup> The gene was the result of recursive ligation of the original RLP12 gene reported in previous publications.<sup>[100, 105]</sup> A number of high molecular weight RLPs were created using the same method,<sup>[104]</sup> but only RLP24 was chosen for the following studies. This was due to its superior expression and the negligible change in hydrogel mechanical properties for the higher molecular weight RLPs.<sup>[104]</sup> The RLP24 protein contains 24 repeats of a slightly modified resilin-like sequence (GGRPSDSFGAPGGGN) derived from the *Drosophila melanogaster* CG15920 gene.<sup>[100, 104, 140]</sup> As indicated in bold, a phenylalanine residue was incorporated in lieu of a tyrosine residue for potential incorporation of non-canonical amino acids that would confer photocross-linking properties. While this tyrosine→phenylalanine substitution removes the amino acid responsible for the cross-links of natural resilin,<sup>[142, 148]</sup> it does not affect the elastomeric behavior of cross-linked RLP hydrogels.<sup>[105, 238]</sup> To impart the RLP24 with cell adhesion properties, four integrin binding domains (RGDSP) were included in regular intervals along the polypeptide chain.<sup>[34, 104]</sup> Additionally, RLP24 includes two heparin binding domains (KAAKRPKAAKDKQTK) for the potential sequestration of heparin and growth factor.<sup>[104, 249]</sup> Two matrix metalloproteinase (MMP) sensitive sequences (GPQGIWGQ) were included toward the middle and near the C-terminus of the

RLP24 protein. Finally, three cysteine residues are present along the polypeptide chain for cross-linking with the PEG vinyl sulfone.<sup>[104]</sup>

RLP24 was expressed using Studier auto-induction and purified under native conditions using affinity chromatography as previously reported.<sup>[104]</sup> The yield of the protein following purification could vary significantly: between 40-100 mg/L of expression culture and in terms of specific yield from 2.5-5.6 mg/g of cell pellet mass. This is partially attributed to the reuse of the Ni-NTA resin, which appeared less effective at binding RLP after a number of purifications. Another potential source of low protein yields may be due to the scaling of the expression media from 3L to 4.5L. The additional volume was intended to increase yield, but may have limited aeration or gas exchange in the shaker cultures and hampered the expression of RLP24. Batch fermentation of RLPs has proven effective at increasing product with reported yields as high as 450 mg/L for a resilin-like polypeptide based upon the *Anopheles gambiae*.<sup>[144]</sup> Under optimized conditions, elastin-like polypeptides have been expressed at an astounding 1.6 g/L expression culture.<sup>[229]</sup> However, the expression and purification of RLPs is not necessarily trivial. Renner *et al.* struggled to express an RLP based upon the same resilin-like motif (AQTSSQYGAP) from the *A. gambiae* gene. Only through reduced culture temperatures and early harvesting could non-degraded RLP be attained.<sup>[179]</sup> RLP24 has been the most successful RLP produced by our laboratory in terms of yield, but there is room for improvement and quantity will always be important for the use of RLP as a material.

The purity of RLP24 preparations could be improved through the inclusion of  $\beta$ -mercaptoethanol (5-20 mM) in the lysis and wash buffers during purification. This prevented the formation disulfide bridges with bacterial proteins that would

contaminate the final product. Unfortunately, it left an unreactive mercaptoethanol adduct on the purified protein. Unless removed, the protein could not be cross-linked with the PEG vinyl sulfone. As demonstrated in **Chapter 2**, the mercaptoethanol adduct was reduced using TCEP-HCl and subsequently removed via a centrifugal desalting column.<sup>[104]</sup> This method was successful in producing reduced RLP24 protein, but the disposable columns and the low throughput made the process very expensive. Furthermore, there no way of tracking successful separation of TCEP, salt and protein.

Rizzi *et al.* found success in preparing reduced fibrinogen-collagen mimetic proteins using TCEP-HCl and dialysis at low temperatures over a period of ~9 hours.<sup>[97]</sup> However, this method could not be applied successfully to the RLP24 protein due to the number of basic residues (lysine and arginine) on the polypeptide and the potential for electrostatic interactions with the TCEP molecule. Despite being one of the more effective reducing agents available,<sup>[250]</sup> TCEP suffers from the disadvantage that it made up of three carboxylic acid groups which may form salt-bridges with positively charged residues in the absence of charge-screening. Therefore, it was not uncommon to find that a prep of RLP24 had a free thiol content greater than 100% of the total number of cysteine residues; some preparations of RLP24 were retaining unreacted TCEP. This residual TCEP had to be removed because it potentially interfered with mass measurements of lyophilized protein and it may also be detrimental to cell viability within RLP-PEG hydrogels. The dialysis procedure, even one that included a concentrated salt step to screen TCEP, proved insufficient at producing reduced RLP24.

Fast protein liquid chromatography (FPLC) equipped with a desalting column was employed as a means of improving throughput, lowering cost and providing on-line monitoring of component elution. RLP24 protein was reduced in a high salt buffer (10mM MES, 500 mM NaCl) with an acidic pH of ~5.5 for an hour at room temperature. The lower pH was intended to prevent the reformation of disulfide bonds. An even lower pH may have been desirable, but the protein precipitated in buffers with a pH lower than ~5.3. The salinity of the buffer would help screen charges and prevent TCEP from co-eluting with the protein. After an hour of reduction, protein solutions were diluted and promptly processed on the FPLC with chilled, ddH<sub>2</sub>O serving as the mobile phase.

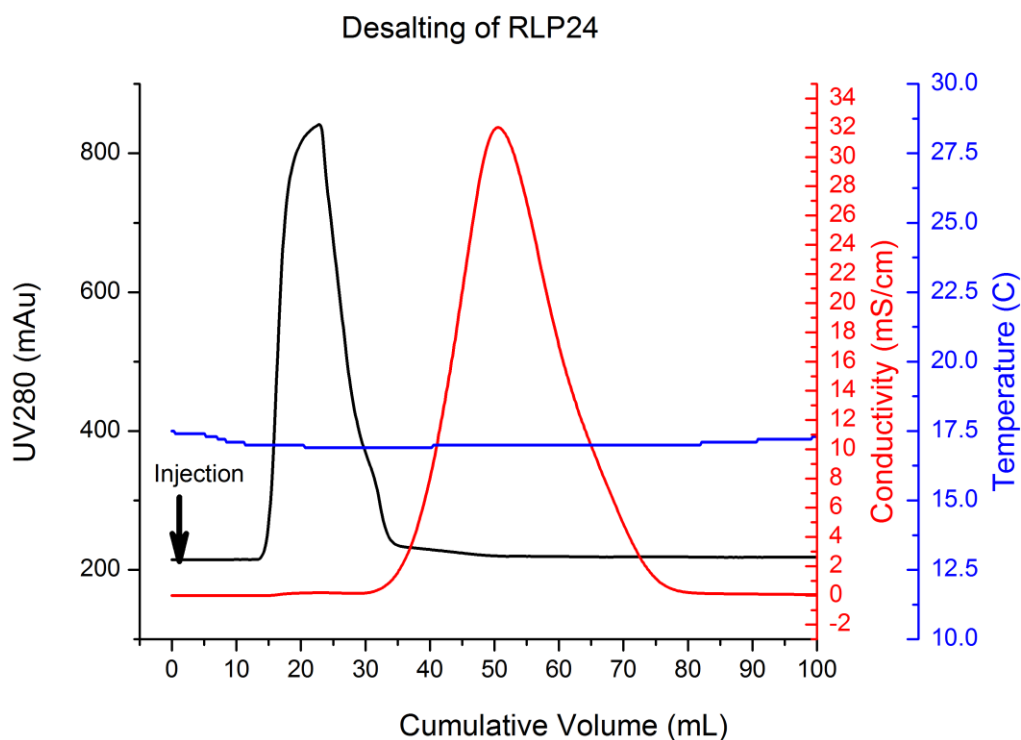


**Figure 3.5** Representative chromatogram from a desalting preparation of reduced RLP24. The black curve indicates UV absorbance (mAU) at 280 nm and represents the protein component. The red curve indicates the conductivity (mS/cm) and represents the salt component. The blue curve is the temperature (°C).

**Figure 3.5** depicts the chromatogram from a representative desalting preparation. At pumping rates of ~9 mL/min, the protein, indicated by the black curve, was well-separated from the salts, indicated by the red curve, and the entire process was complete in less than 15 minutes. The eluted protein was captured, immediately frozen in liquid N<sub>2</sub> and lyophilized to a dry powder. This method was able to produce reduced RLP24 with functionality ranging between 85% and 95% of total thiol content as determined via an Ellman's assay.<sup>[104, 226]</sup> The FPLC method proved to be a fast,

reliable and cost-effective way of obtaining reduced RLP. As much as ~500 mg could be processed in a 2-3 hour period and since the column was reusable the method was less costly than disposable centrifugal columns. Furthermore, the online detectors provided a means of tracking progress, which was not available in either the dialysis or centrifugal desalting methods.

### 3.3.2 Oscillatory Rheology

To determine the gelation and mechanical properties of RLP24-PEG hydrogels, *in situ* oscillatory rheology was employed. As previously reported in **Chapter 2**, the mechanical properties of RLP-PEG hydrogels did not change significantly with increasing RLP molecular weight and functionality. Recursive ligation of the original gene increased the size and functionality of the RLPs, but the number of cysteines per unit of chain length remained roughly equivalent for each polypeptide. Therefore, the cross-link density in the final RLP-PEG hydrogel stayed the same regardless of the RLP molecular weight.<sup>[104]</sup> In order to modulate the mechanical properties of these hydrogels, it was decided to use only the RLP24 construct and instead to vary the vinyl sulfone to cysteine thiol stoichiometry. The following reports the gelation and mechanical properties of three cross-linking ratios used to form RLP24-PEG hydrogels: 3:2, 1:1, and 1:2 (vinyl sulfone:thiol). The 3:2 ratio was included due to the observation that in order to achieve optimal mechanical properties a slight stoichiometric imbalance is necessary to overcome non-ideal cross-linking behavior in polymer networks.<sup>[97, 251, 252]</sup>

In **Figure 3.6A** and **Figure 3.6B**, representative oscillatory time sweeps and frequency sweeps are presented. Regardless of reactive group stoichiometry, RLP24-PEG hydrogels cross-linked rapidly (<5 min) and had storage moduli that were

insensitive to the strain rate (angular frequency). The gelation time was comparable other recombinant protein-PEG hydrogels cross-linked using the same chemistry and similar conditions;<sup>[97]</sup> furthermore, the relatively quick gelation of RLP24-PEG hydrogels indicates the potential for application as an injectable material. The stable storage modulus over a range of strain frequencies is a characteristic of elastic, solid-like materials with permanently cross-linked networks. This is an important property that is not universally found in protein-PEG hydrogels<sup>[97]</sup> and it represents the formation of a robust material that can withstand a variety of strain conditions.

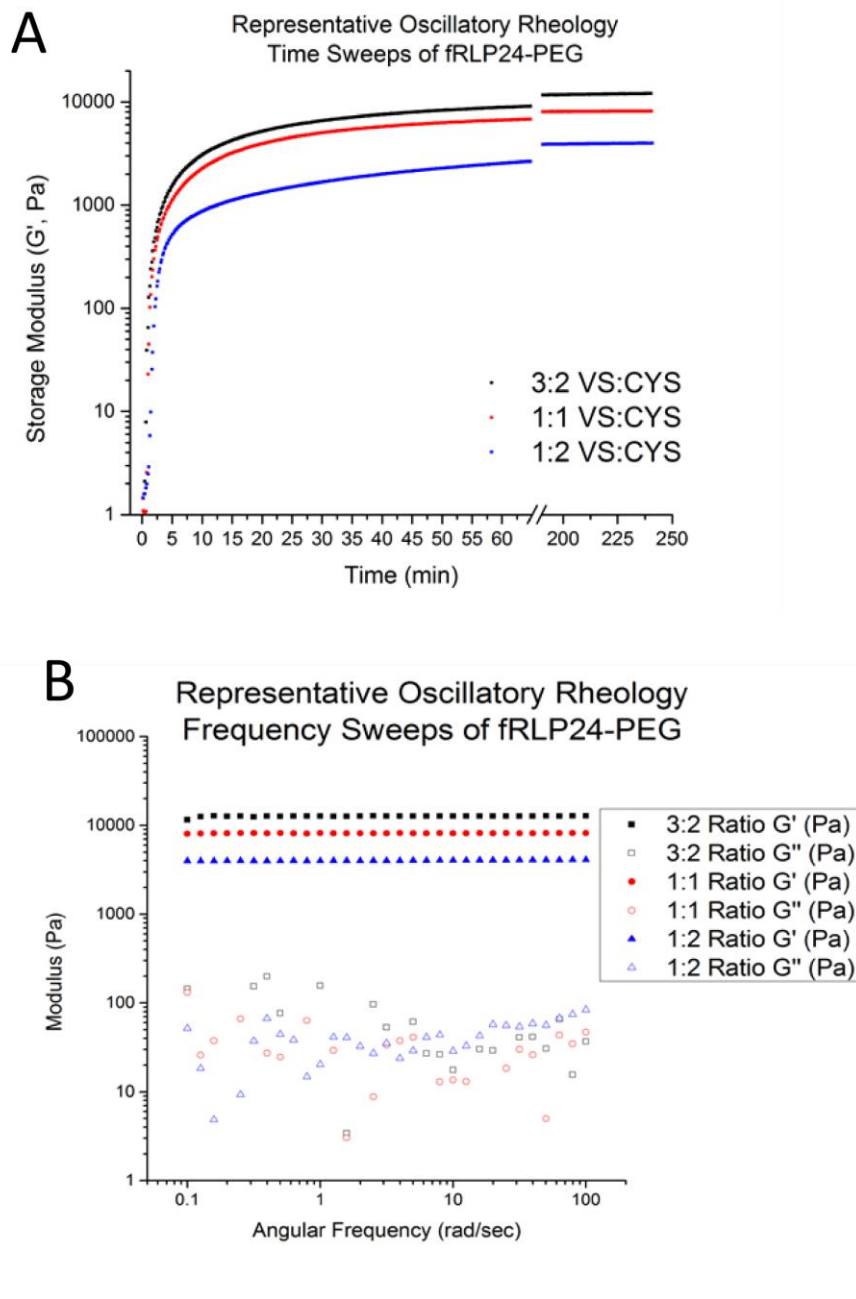


**Figure 3.6** (A) Representative time sweeps of RLP24-PEG hydrogels cross-linked at different ratios of vinyl sulfone to cysteine thiol. (1% strain, 6 rad/s) (B) Representative frequency sweeps of RLP24-PEG hydrogels cross-linked at different ratios of vinyl sulfone to cysteine thiol (1% strain). All RLP24-PEG hydrogels were 20wt% and tested at 37°C.

The average storage moduli for the RLP24-PEG hydrogels are presented in **Figure 3.7**. RLP24-PEG hydrogels cross-linked at a 3:2 ratio of vinyl sulfone to cysteine thiol formed hydrogels with stiffness in the 12-13 kPa range while the hydrogels cross-linked at 1:1 and 1:2 had moduli in the 8-9 kPa and 3-4 kPa ranges, respectively. The upward trend in stiffness with respect to the cross-linking stoichiometry was observed in other protein-PEG hydrogels<sup>[97]</sup> and was also observed in RLP hydrogels cross-linked using small molecules.<sup>[105]</sup> As mentioned previously, this behavior indicates the formation of network defects which have to be compensated for through the inclusion of additional cross-linker. The higher concentration of precursors (20wt% compared to 9 wt% in Rizzi *et al.*)<sup>[97]</sup> undoubtedly contributed to the overall higher stiffness and wider range of attainable moduli. However, it should be noted that this actually reveals an important and useful trait of RLP24-PEG hydrogels. The RLP24 precursor was soluble in concentrations as high as 40 wt% (during precursor preparation) and this highlights the ability of resilin-based materials to overcome a potential design constraint: protein polymer solubility. Secondary and tertiary structure effects complicate the prediction of protein solubility and proteins that are insoluble under physiological conditions would not be useful as hydrogel precursors.<sup>[97]</sup> Proteins based upon resilin-like sequences do not appear to be susceptible to this constraint and it is likely due to the inherent disorder and hydrophilicity of resilin.

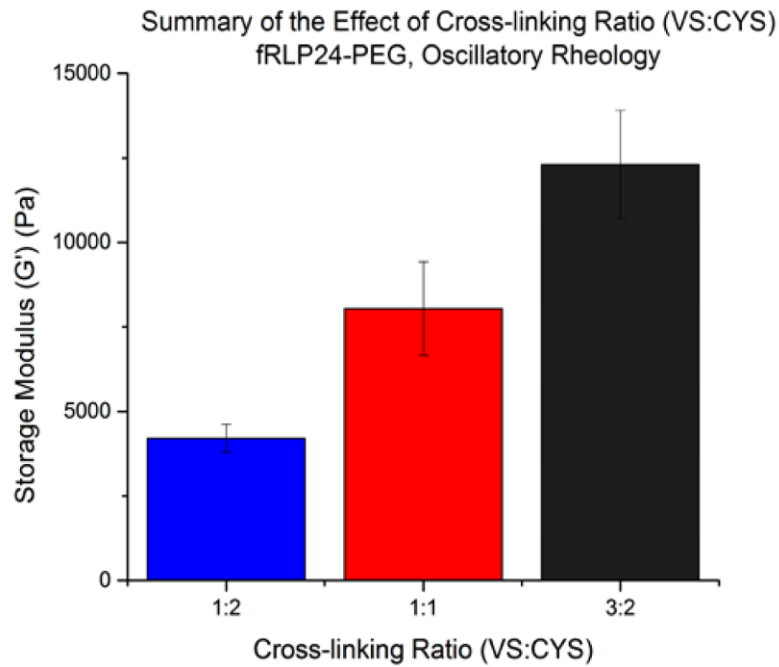


**Figure 3.7** The summary of the effect the cross-linking ratio had on the storage modulus ( $G'$ )(Pa) for RLP24-PEG hydrogels as analyzed via oscillatory rheology.

### 3.3.3 Swelling Measurements

The swelling behavior for all three RLP24-PEG hydrogel compositions was investigated using simple gravimetric methods. Following gelation, the hydrogels were immersed in PBS buffer containing EDTA, sodium azide and antibiotic/antimycotic for a period of five days at 37°C. The addition of EDTA was a preventative measure against protease activity and the inclusion of sodium azide and antibiotic/antimycotic was simply to inhibit the growth of microorganisms. The swollen hydrogel weight was measured on a microbalance and then compared to the dry weight following lyophilization.

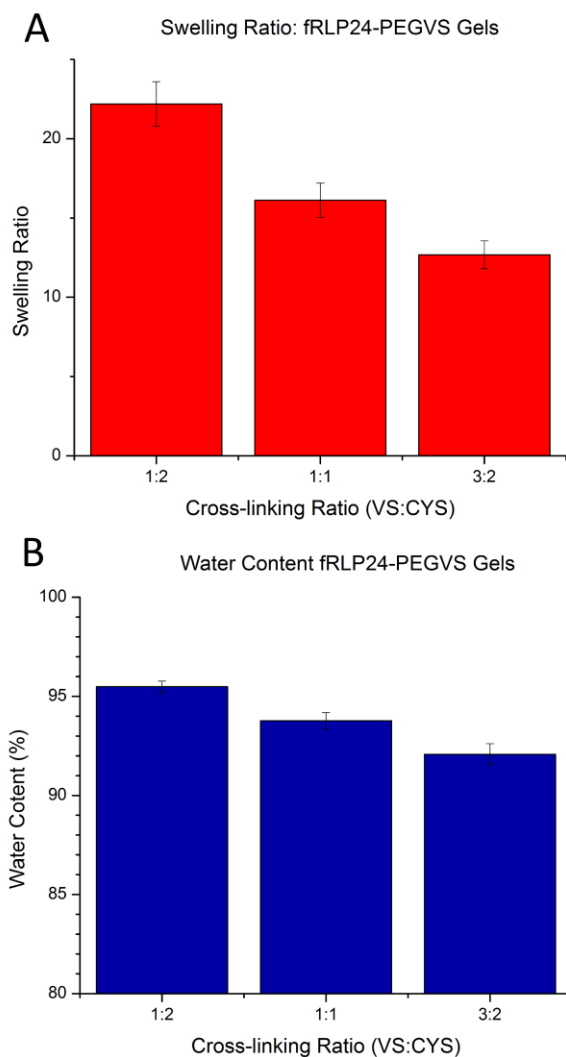


**Figure 3.8** (A) Illustrates the effect cross-linking stoichiometry has on the swelling ratio and (B) equilibrium water content. The RLP24-PEG hydrogels with lower cross-linking ratios exhibited a greater degree of swelling as anticipated.

The results of the analysis are presented in the terms of the swelling ratio in **Figure 3.8A** and the equilibrium water content in **Figure 3.8B**. The swelling ratio and subsequent water content decreased with an increasing stoichiometry of vinyl sulfone

to thiol. This evidence supports the rheometry data that the cross-linking density of the hydrogels could be controlled by modulating the ratio of vinyl sulfone to thiol. Overall, the RLP24-PEG hydrogels were swollen materials. The initial precursor concentration was 20 wt%, but following swelling the water content was as high as 95% for the 1:2 cross-linked hydrogels and over 90% for the other two compositions. These results are in stark comparison to other reports by our laboratory where RLP is cross-linked through lysine residues using small molecule hydroxymethyl phosphines. In one report, 20 wt% RLP12 hydrogels had water contents that ranged from 80-90% over the cross-linking ratios investigated.<sup>[105]</sup> In another report, a recently introduced RLP protein, RLPX, exhibited no swelling behavior when cross-linked into hydrogels. The equilibrium water content of the RLPX hydrogels was 80% when the polypeptide was cross-linked in a 20 wt% precursor concentration (1:1 ratio of lysine to hydroxymethyl).<sup>[101]</sup> Additionally, elastin-like polypeptides cross-linked through small molecules exhibited a similar low degree of swelling.<sup>[90, 93, 197]</sup> However, other protein-PEG hydrogels displayed swelling that was more comparable to what was found in the RLP24-PEG hydrogels.<sup>[95, 97]</sup>

### **3.3.4 Tensile Testing**

Tensile testing of RLP24-PEG hydrogels was used to investigate the mechanical properties of the swollen hydrogels under uniaxial strain. Samples representing all three cross-linking ratios were placed under repeated cycles of extension and contraction at different percent strain in order to determine the elasticity and resilience of the networks. The hydrogels were formed overnight using PTFE molds and were swelled in PBS buffer for a period of at least two days prior to testing. Hydrogels were immersed in PBS buffer at room temperature and tested using a RSA-

G2 DMA equipped with an axial tensile geometry; a small pad of wire mesh affixed to the hydrogel helped provide friction at the contact point with the geometry and prevented slipping. Cyclic strain measurements were performed at 20, 40 and 60% strain for each sample and multiple samples were analyzed for each cross-linking ratio.

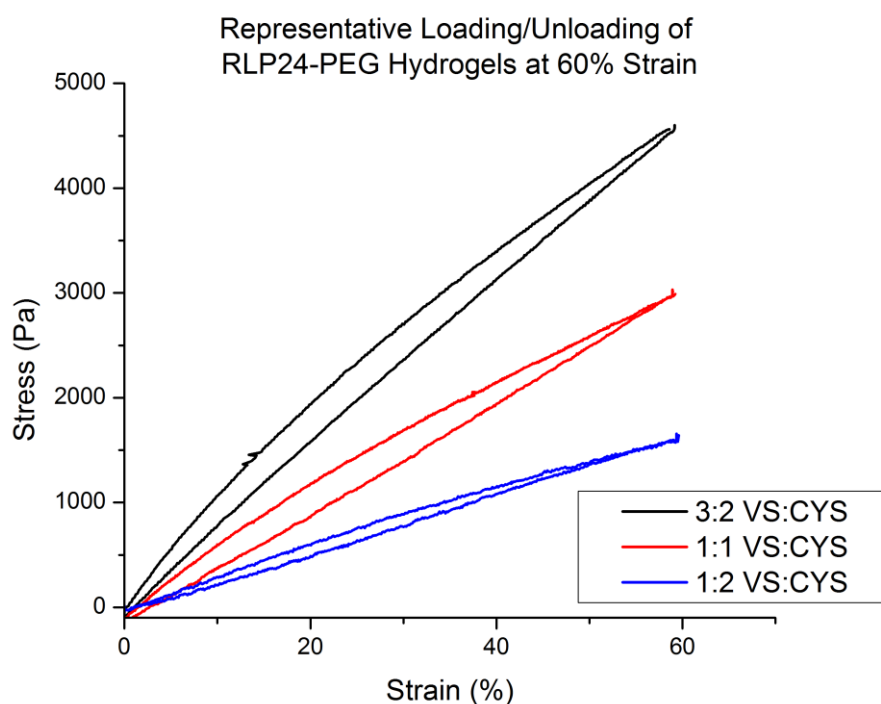


**Figure 3.9** Representative loading/unloading curves of the RLP24-PEG hydrogels strained to 60% at a rate 0.1 mm/s. The curves depict elastic materials that exhibit a small degree of hysteresis. This corresponds to the resilience in the 85-92% range of RLP24-PEG hydrogels.

**Figure 3.9** depicts representative loading and unloading cycles at 60% strain for all three hydrogel cross-linking ratios. As anticipated, the more tightly cross-linked

hydrogels exhibited steeper extension/contraction curves which reflected their greater stiffness. **Table 3.3** reports the Young's modulus for each cross-linking ratio as determined from the slope of the first 10% strain of the extension curve. Overall, the tensile moduli were lower than expected based upon the shear modulus data from rheological testing. For homogeneous isotropic materials the Young's modulus is related to the shear modulus through the following equation:

$$E = 2G(1 + \nu)$$

where  $E$  is the Young's (tensile) modulus,  $G$  is the shear modulus and  $\nu$  is the Poisson ratio.<sup>[253]</sup> Since rubber materials are assumed to have a Poisson ratio of  $\sim 0.5$ ,<sup>[254]</sup> the Young's modulus ought to be  $\sim 36.9$  kPa for the 3:2 cross-linked RLP24-PEG hydrogel whose shear modulus is  $\sim 12.3$  kPa. This discrepancy with theory is likely due to the different experimental conditions of the two mechanical testing methods. The rheology was not conducted on swollen hydrogels as it was performed *in situ* to analyze the properties of gelation. However, it has been shown that the RLP24-PEG hydrogels swell considerably and therefore, it is reasonable to assume that the network structure of the hydrogels has changed. The swollen gels analyzed via tensile testing will have lower cross-link densities and fewer chain entanglements which will correlate to softer materials. This observation is supported by the lack of disparity between theory and experiment for the RLP12 and RLPX hydrogels cross-linked by small molecules. As discussed, these hydrogels did not swell to the same degree as the RLP24-PEG hydrogels and therefore, the mechanical properties remained similar for both the tensile and rheological measurements.<sup>[101, 238]</sup>

**Table 3.3** Summary of the mechanical and physical properties of RLP24-PEG hydrogels at three cross-linking ratios

Cross-linking Ratio (VS:CYS)	Water Content (%)	Shear Modulus (Pa)	Youngs Modulus (Pa)	Strain to Break (%)
3:2	92.1 ± 0.5	12300 ± 1601 <sup>a</sup>	11530 ± 2340	68.1 ± 7.9
1:1	93.8 ± 0.4	8040 ± 1385 <sup>a</sup>	7070 ± 1350	85.6 ± 9.0
1:2	95.5 ± 0.3	4205 ± 415	4250 ± 1250	173.4 ± 34.9

<sup>a</sup> previously reported data.<sup>[104]</sup>

**Figure 3.10A-C** represents the deformation response of a single loading/unloading cycle at the three tested strains for each hydrogel composition. Each curve represents the fourth of five consecutive stress/release cycles at 20, 40 or 60% strain for a representative sample. These graphs show that hysteresis, or the difference between the loading and unloading curve, increased with higher strain, but overall, the hydrogels remained elastic. **Figure 3.10D** shows all five cycles to 60% strain experienced by a representative 3:2 cross-linked hydrogel. The cycles overlay each other very closely which illustrates the lack of plastic deformation experience by the RLP24-PEG hydrogels. Consecutive strain cycles did not appear to have deleterious effects on the properties of these hydrogels. The hysteresis of the RLP24-PEG gels was larger than for the small molecule cross-linked RLP hydrogels,<sup>[105, 238]</sup> but resilience calculations determined that RLP-PEG hydrogels were between 87-98% resilient depending upon the strain. **Table 3.4** summarizes the resilience calculations; each cross-linking value represents the mean of three samples.

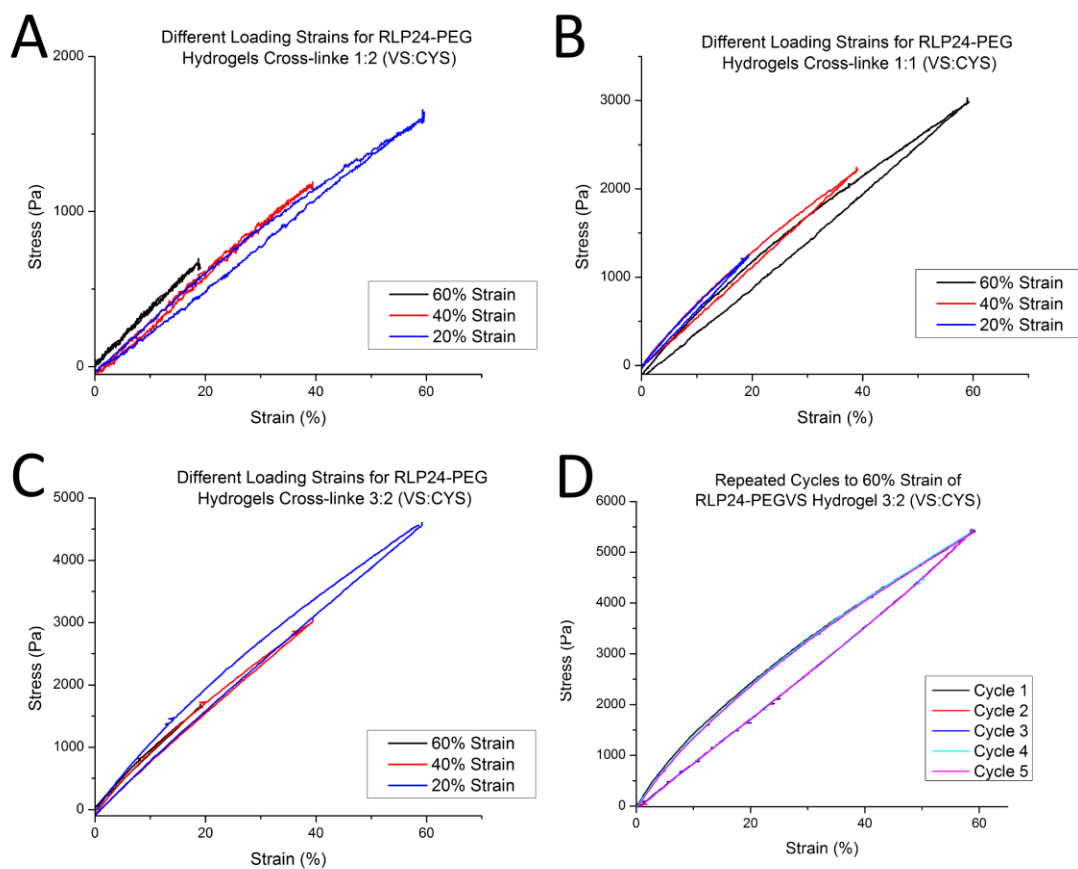


**Figure 3.10** Illustrates the deformation response at 20, 40 and 60% strain of RLP24-PEG hydrogels cross-linked at (A) 1:2, (B) 1:1 and (C) 3:2 ratios of vinyl sulfone to thiol. (D) The hydrogels demonstrated a small degree of hysteresis, but there was negligible plastic deformation as consecutive tensile cycles overlaid each other in panel (D). All hydrogels were strained at 0.1 mm/s.

**Table 3.4** Summary of resilience calculations of RLP24-PEG hydrogels

Cross-linking Ratio (VS:CYS)	Resilience at percent strain (%)		
	20%	40%	60%
3:2	93 ± 4	90 ± 4	88 ± 4
1:1	90 ± 4	89 ± 3	87 ± 3
1:2	98 ± 2	92 ± 1	89 ± 1

Each value represents the simple mean of 3 samples; error is the standard deviation.

At 60% strain the resilience of the RLP24-PEG hydrogels was greater than 87% for each cross-linking ratio and slightly lower than the hydroxymethyl phosphine cross-linked RLPs. The resilience of those hydrogels was in the 90-96% range at 60% strain using a similar strain rate.<sup>[105, 238]</sup> In general, RLP-based hydrogels, when tested under similar conditions, exhibit resilience in the 90-98% range.<sup>[142, 144]</sup> RLP24-PEG hydrogels still represent an improvement in resilience compared to polybutadiene rubber (~80%),<sup>[142]</sup> and some elastin-like polypeptide materials.<sup>[255-257]</sup> Available data on physically and covalently cross-linked ELP films demonstrates mechanical resilience only in the 50-60% range.<sup>[255-257]</sup> Recently, silk/elastin-like materials have improved upon the mechanical properties of ELP films, but even these materials have resilience in only the 80-90% range.<sup>[258, 259]</sup> Interestingly, the resilience of aortic elastin is ~ 77%<sup>[260]</sup> indicating that the resilience of RLP24-PEG hydrogels falls within a favorable regime in terms of potential application.

In addition to the cyclic strain measurements, the RLP24-PEG hydrogels were subject to strain-to-break experiments in order to explore the extensibility of the gels. **Figure 3.11** depicts representative strain-to-break measurements for the three RLP24-PEG cross-linking ratios and **Table 3.3** summarizes the results of the experiments. As was the case with other RLP hydrogels the more densely cross-linked networks proved to be the least extensible.<sup>[105]</sup> The 3:2 cross-linked RLP24-PEG hydrogels exhibited strain-to-break of ~68% while the 1:2 cross-linked gels could be strained to 175% before breaking. Pure RLP hydrogels exhibited maximum strain that was far higher than the hybrid hydrogels.<sup>[105, 144, 238]</sup> This was a perplexing development for two reasons: (1) the pure RLP hydrogels usually had a higher cross-link density; (2) the resilience of the hybrid networks was comparable to the pure RLP hydrogels. One

explanation for the lower strain-to-break might be the experimental set up and the relatively soft RLP24-PEG hydrogels. The hydrogels were more susceptible to microfracture that occurred upon sample loading especially when compressed by the metal clamps which held the gel to the axial tensile geometry. Another explanation for the difference in extensibility may be attributed to how swollen the RLP24-PEG hydrogels were as compared to the pure RLP hydrogels. Absorption of large quantities of solvent diminishes the mechanisms that lead to tough elastomers: first, fewer network chains occupy the cross-sectional area of the hydrogel, which implies fewer chains need to be fractured to propagate a crack; second, separation between segments of the network mean less opportunity for crystallization and viscoelastic energy dissipation.<sup>[261]</sup>

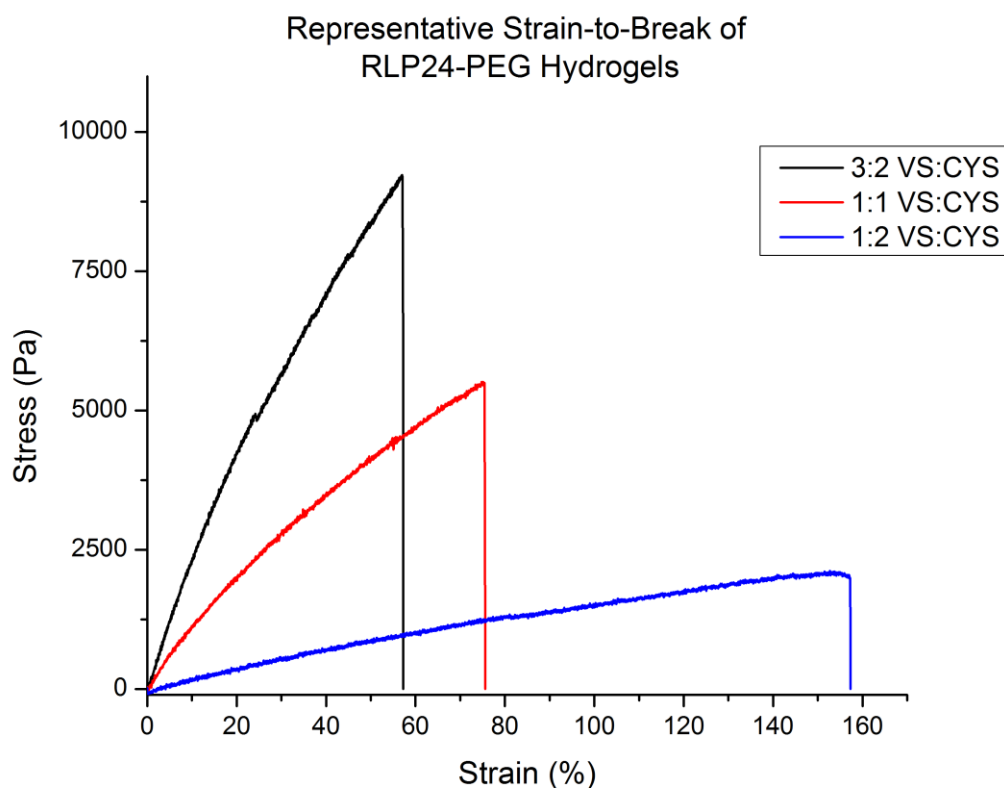


**Figure 3.11** Representative strain-to-break curves for each of the RLP24-PEG cross-linking ratios.

The network architecture of the RLP24-PEG hydrogels would not immediately suggest this disparity in extensibility. In fact, a report by Cui, *et al.* demonstrated that wholly PEG hydrogels formed through step-polymerized cross-linking had outstanding mechanical resilience and extensibility.<sup>[203]</sup> However, the use of PEG to form these hydrogels offers another potential explanation; it was discovered that the RLP24-PEG hydrogels contained a high level of heterogeneity not present in the other RLP gels. This heterogeneity may have contributed to the propagation of gel fracture

at high strains. The liquid-liquid partitioning behavior of the RLP24-PEG hydrogels that gave rise to this heterogeneity is further discussed in **Section 3.3.8**.

### **3.3.5 Biochemical Degradation**

The RLP24 gene encoded for two short domains which are sensitive to cleavage by MMP enzymes. The GPQGIWGQ domain, derived from human  $\alpha$ (I) collagen,<sup>[227]</sup> was incorporated into the RLPs in order to impart cell-directed degradability to the polypeptides. Since MMPs play an active role in tissue remodeling,<sup>[227, 240]</sup> incorporating these short peptide domains into synthetic polymeric biomaterials as labile cross-links has been an important tissue engineering strategy. Hydrogels with this design improve the migration and proliferation of encapsulated cells.<sup>[52, 58, 96, 222]</sup> The degradation properties of RLP24 were first analyzed without being cross-linked into hydrogels. Soluble RLP24 was incubated at 37°C for a 24-hour period with a recombinant enzyme representing the catalytic domain of human MMP-1. At regular intervals small samples of the biochemical reaction were removed for analysis via gel electrophoresis (SDS-PAGE). The enzyme concentration (56 nM) was not chosen based upon any *in vivo* observation, but merely provided a degradation rate that could be easily monitored over the 24 hour time period. Likewise, the concentration of RLP24 (7.3  $\mu$ M) was chosen based upon effective protein visualization via Coomassie staining following gel electrophoresis. For a negative control, RLP24 was incubated at 37°C in the enzyme buffer without MMP1 and samples were taken over the same time period.

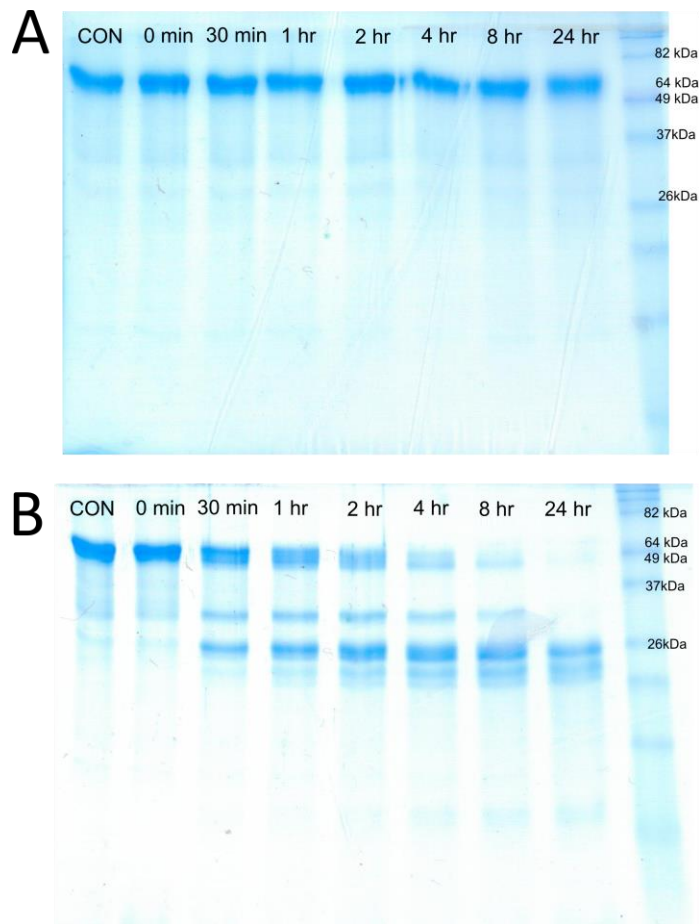


**Figure 3.12** Representative gel electrophoresis of the incubation of RLP24 (7.3  $\mu\text{M}$ ) without enzyme (**A**) and with the catalytic domain of human recombinant MMP1 (56 nM) (**B**). Over a 24-hour period MMP1 cleaved RLP24 which led to the development of lower molecular weight fragments. These fragments had molecular weights that roughly corresponded to the expected products given the position of the MMP domain in RLP24.

**Figure 3.12** presents representative gel electrophoresis of the degradation studies: **Figure 3.12A** depicts the control and **Figure 3.12B** depicts the degradation experiment. As shown in the gels, the RLP24 is clearly degraded when incubated with the MMP1 enzyme. The full-length protein represented by the top band in the control lane (CON) disappears over the course the experiment and is replaced by lower

molecular weight fragments. Additionally, the absence of the enzyme in the control results in intact RLP24 throughout the entire experimental time period. More importantly, the molecular weights of the degraded fragments roughly correspond to the theoretical sizes based upon the location of the MMP domains within RLP24. **Figure 3.13** provides a scheme of the degradation products and their molecular weights.

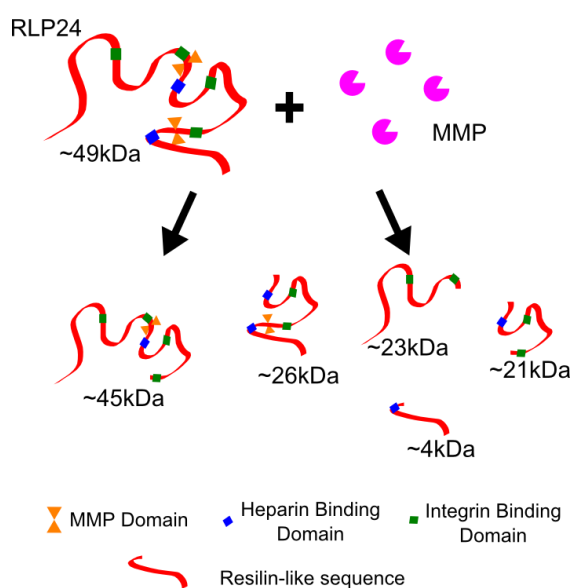


**Figure 3.13** Scheme illustrating the degradation of soluble RLP24 via MMP1. The degradation products will have molecular weights corresponding to the fragments in the image. The different biological domains of RLP24 are labeled.

It has been well-documented that RLP proteins, including RLP24, run higher than their theoretical molecular weight in SDS-PAGE.<sup>[104, 142, 168]</sup> This behavior was also noticed in the RLP24 degradation fragments. However, the protein bands' pattern and their general vicinity within a lane made clear the identity of the degradation

products. The first clear evidence of degradation product appears at 30 minutes. Upon close inspection, the 45 kDa fragment is present at this time point, but its band was slightly obscured by the full length protein. It is more apparent at the 4-hour and 8-hour time points. The lower molecular weight fragments (26, 23 and 21 kDa) were more obvious at the earlier time points. The 26 kDa fragment can be distinguished from the other two as it only makes a temporary appearance over the course of the experiment. This fragment contains a degradation domain and therefore, it was not a permanent species. At 24 hours there is no longer any presence of the fragment in the SDS-PAGE gel. At the conclusion of the experiment, the only remaining species were the 23 and 21 kDa bands as well as the faintest evidence of a 4 kDa band.

Densitometry was used to quantify the disappearance of the major band over the 24-hour time period of the experiment. This was done in triplicate using SDS-PAGE gels from three different experiments. The results are depicted in **Figure 3.14**. The degradation of the major band occurs very rapidly with more than 50% of the band disappearing within the first few hours. In another report by our laboratory, an RLP containing a single MMP domain was degraded by the enzyme, but it occurred more slowly than for RLP24. However, this may have been due to a higher ratio of substrate to enzyme in that study: 410:1 for the RLP as compared to 260:1 for RLP24. In addition, the RLP24 degradation used a specific MMP1 enzyme buffer whereas the other RLP was degraded in PBS which may have affected the efficacy of the enzyme.<sup>[101]</sup> Regardless, these soluble studies confirmed the reports made by others that protein polymers can be engineered with site-specific degradability.<sup>[93, 101]</sup>

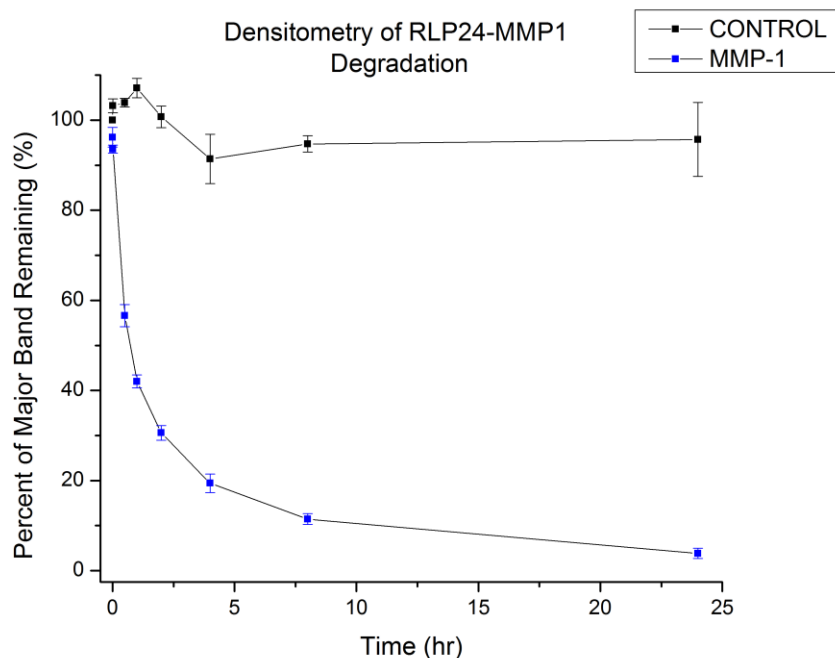


**Figure 3.14** Densitometry of the RLP24 band degraded by MMP1. Each point represents the mean of three different samples; the error is the standard deviation of those samples. Major band indicates intact RLP24 band in gel.

### 3.3.6 Hydrogel Degradation

The degradation of RLP24-PEG hydrogels by MMP1 was investigated by measuring the change in the mechanical properties of hydrogels exposed to the enzyme. However, rather than testing the hydrogels at regular intervals, a method was employed that continuously monitored the hydrogel's mechanical properties while it was incubated with MMP1 enzyme. This *in situ* method of analyzing hydrogel degradation was successfully demonstrated by Baldwin *et al.* who used rheometry to investigate the reverse gelation of PEG hydrogels.<sup>[50]</sup> For the RLP24-PEG hydrogels, unconfined compression testing using a DMA was chosen due to the greater hydrogel surface area available to the enzyme. Initially, hydrogels were loaded on to the DMA

and immersed in enzyme buffer without the MMP1 enzyme. Oscillatory compressive testing (1 Hz, 5% strain) was conducted on the hydrogels for a period of approximately 12 hours with data points collected every 15 minutes. The buffer was then replaced with buffer containing the enzyme (171 nM, 1.5 mL total volume) and the testing was continued for another 10 hours. The experiment was carried out in triplicate and the raw storage modulus data were normalized to the initial compressive modulus. **Figure 3.15** depicts the simple mean and the error (standard deviation) of those samples.

The black squares in **Figure 3.15** depict the compressive modulus of the hydrogel during the 12-hour testing period when it was not exposed to the enzyme. The initial decrease of ~20% in the storage modulus of the material is likely due to the swelling of RLP24-PEG hydrogel. During storage the hydrogels were not immersed in buffer and were only briefly washed with the enzyme buffer prior to loading onto the DMA. Therefore, the hydrogels were probably not at equilibrium swelling for the first few hours of testing. However, the modulus did stabilize after the first 200 minutes, which indicates that, absent any other stimulus, the mechanical properties of the hydrogels were stable. Only when the buffer was exchanged and the MMP enzyme was exposed to the hydrogels did the normalized storage modulus decrease. The red squares depict the period when hydrogel was incubated with the enzyme and the resulting difference in the mechanical properties is quite clear. In the first two hours the normalized storage modulus dropped from ~80 to ~50% and continued until the hydrogels were only ~20% of their original elasticity.

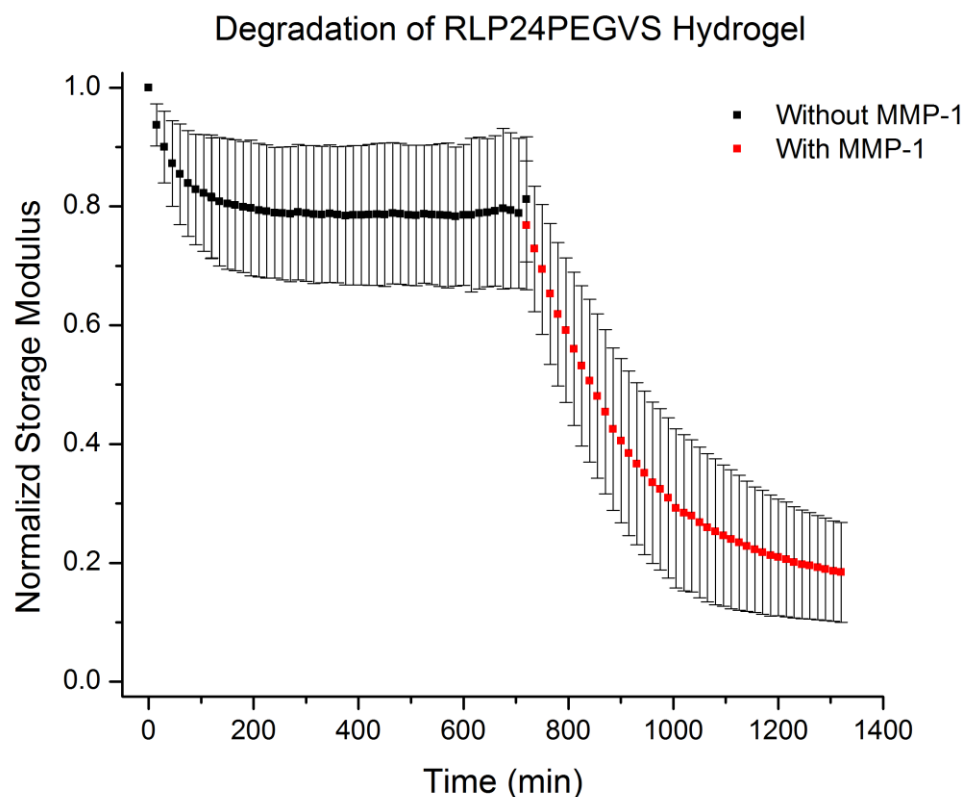


**Figure 3.15** Normalized compressive storage modulus of RLP24-PEG hydrogels (20wt% 3:2 vinyl sulfone to thiol) incubated in MMP1 enzyme buffer without (BLACK) and with (RED) MMP1 enzyme. Data points were acquired every 15 minutes using 5% strain at a frequency of 1Hz.

This dramatic change in the normalized storage modulus of the hydrogels in the presence of MMP1 is demonstrable proof that the hydrogels, like the soluble RLP, were susceptible to enzymatic cleavage. This result indicates the availability of the MMP domain to proteolysis and to the ability for cells that express MMP to potentially remodel and degrade the RLP24-PEG hydrogels. The *in situ* method of monitoring gel degradation is a powerful technique that is not fully explored in this work. For example, Baldwin *et al.* was able to determine degradation kinetics of the

PEG gels using rheometry data and standard rubber elasticity theory.<sup>[50]</sup> This type of analysis was outside the scope of the current work, but it illustrates how this method could be applied to the investigation and optimization of the degradation properties of tissue engineering scaffolds like RLP24-PEG hydrogels.

### **3.3.7 3D Encapsulation and Proliferation of hMSCs**

The cytocompatibility of RLP24-PEG hydrogels was investigated through the three-dimensional encapsulation and culture of hMSCs. As potential injectable scaffolds for tissue engineering, the RLP24-PEG hydrogels must have the capacity to deliver viable cells to target tissues. Previously, it was demonstrated that human aortic adventitial fibroblasts survived encapsulation within RLP24-PEG hydrogels and could be successfully cultured in 3D for a week.<sup>[104]</sup> In this study, bone-derived hMSCs were chosen for encapsulation as stem cells have two valuable traits for tissue engineering: the capacity for self-renewal and for differentiation<sup>[5]</sup> as well as their vascular differentiation potential.<sup>[262]</sup> By demonstrating cytocompatibility with stem cells, the RLP24-PEG hydrogels would clear an important benchmark for application as tissue engineering scaffolds.

The hMSCs were encapsulated using the same procedure that was performed with the fibroblasts.<sup>[104]</sup> The RLP24 and PEG precursors were prepared separately in PBS buffer and were briefly mixed before triturated with a small amount of cell media containing the hMSCs. The RLP24-PEG solutions containing cells were quickly deposited into glass wells and allowed to cross-link at 37°C for 5 to 10 minutes. The cell-gels were then immersed in media and cultured for up to 15 days. To assess the cell viability, the gels were fluorescently stained via Live/Dead<sup>TM</sup> and imaged using confocal microscopy.

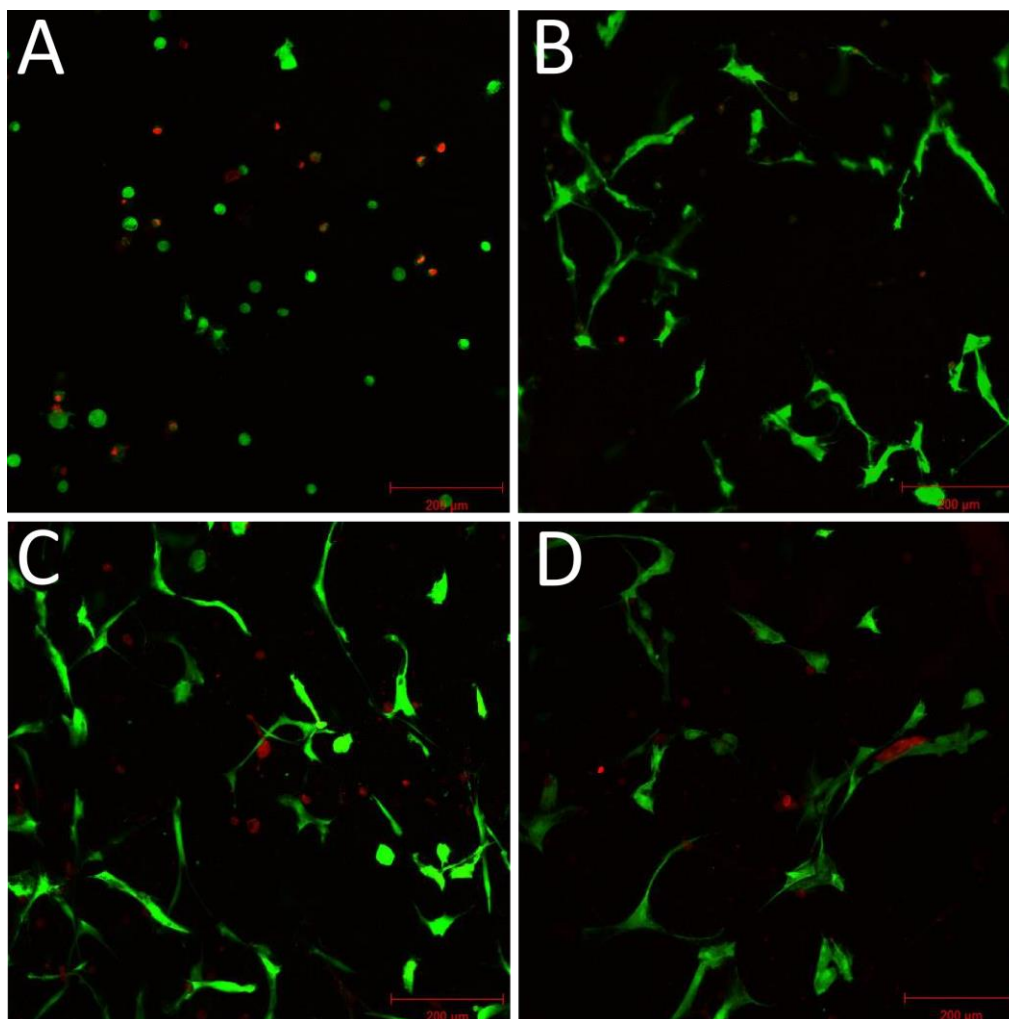


**Figure 3.16** Analysis of viability of hMSCs encapsulated in RLP24-PEG hydrogels (20wt% 3:2 vinyl sulfone: thiol) at day 0 (**A**), day 5 (**B**), day 10 (**C**) and day 15 (**D**). Maximum intensity projections of z-stacks (200-250 μm thick) are presented. Objective was 10x water lens and scale bar represents 200 μm.

**Figure 3.16** depicts the results of the viability imaging experiments. The day 0 image, depicted by **Figure 3.16A**, represents the viability of the hMSCs immediately following encapsulation. Panels **B**, **C** and **D** of **Figure 3.16** represent days: 5, 10, and

15, respectively. Following encapsulation the hMSCs demonstrated great viability. A large number of the cells were stained green indicating intact, metabolically active cells. The bright red spots are nuclei stained with ethidium homodimer-1 and represent cells with compromised membranes that are likely undergoing cell death. While the number of dying cells was greater for the hMSCs than for the adventitial fibroblasts,<sup>[104]</sup> it was clear from the day 0 image that a majority of the cells survived. Furthermore, as depicted in the subsequent time points (**Figure 3.16B-D**), the hMSCs remained viable throughout the entire culture period indicating successful encapsulation.

Importantly, the hMSCs were able to spread out and adopt 3D spindle-like morphologies when encapsulated in the RLP24-PEG gels. This behavior was an exciting development as it had not been previously reported in RLP or ELP hydrogels cross-linked via small molecules.<sup>[101, 197]</sup> Adventitial fibroblasts also spread into the RLP24-PEG hydrogels following 3-5 days of culture.<sup>[104]</sup> Taken together, these data suggests the cells are interacting with the engineered biological domains of the RLP24 protein. The cells appear to be adhering to the matrix and may even be locally degrading the hydrogel via MMP. A variety of MMP enzymes, including MMP1, are known to be expressed by hMSCs.<sup>[222]</sup> Furthermore, Anderson, *et al.* demonstrated that hMSCs encapsulated in PEG hydrogels with MMP-sensitive cross-links would degrade the gels and spread out in the matrices.<sup>[222]</sup> In other studies, cells encapsulated within recombinant protein-PEG hydrogels have demonstrated similar spreading and migration behavior.<sup>[96]</sup> The difference in cell behavior between the pure RLP hydrogels and protein-PEG gels may have to do with the mesh-size of the respective hydrogel network. The cross-links in RLP24-PEG gels are separated by long chains of

PEG and polypeptide that would provide ample space for cleavage by enzymes such as MMP. Visual inspection of the hydrogels at day 10 and day 15 revealed materials that were much softer and beginning to lose their shape; an observation that supports the cell-directed degradation of these hydrogels. By day 15, the gels were becoming viscous and had swelled considerably. This would explain why there appears to be fewer cells in the day 15 image (**Figure 3.16D**) as the expansion of the hydrogel pushed hMSCs outside the microscope field of view.

The proliferation of hMSCs encapsulated within the RLP24-PEG hydrogels was analyzed through fluorescent microscopy. Cell-gels were incubated for two days with a BrDU-type compound (EdU) which would be incorporated into the DNA of dividing cells. The EdU could then be selectively stained with an Alexa Fluor<sup>TM</sup> dye and visualized using a fluorescent microscope. The RLP24-PEG gels were incubated with the EdU on day 3 and were imaged on day 5. DAPI was used as a counterstain to reveal both proliferative and non-proliferative cell nuclei. **Figure 3.17** depicts the results from a representative cell-gel analyzed for proliferation. In panels **A** and **B**, the cell nuclei are represented by DAPI and the Alexa Fluor<sup>TM</sup> 555 dye, respectively. Panel **C** depicts a merged image. All of the nuclei in this particular location of the gel are stained with DAPI, but only a handful of nuclei were stained with the Alexa Fluor<sup>TM</sup> 555 dye. The presence of these red nuclei indicates that those hMSCs had recently divided. In the composite image (panel **C**) the purple nuclei provide a clear representation of the proliferative cells in relation to the other cells.

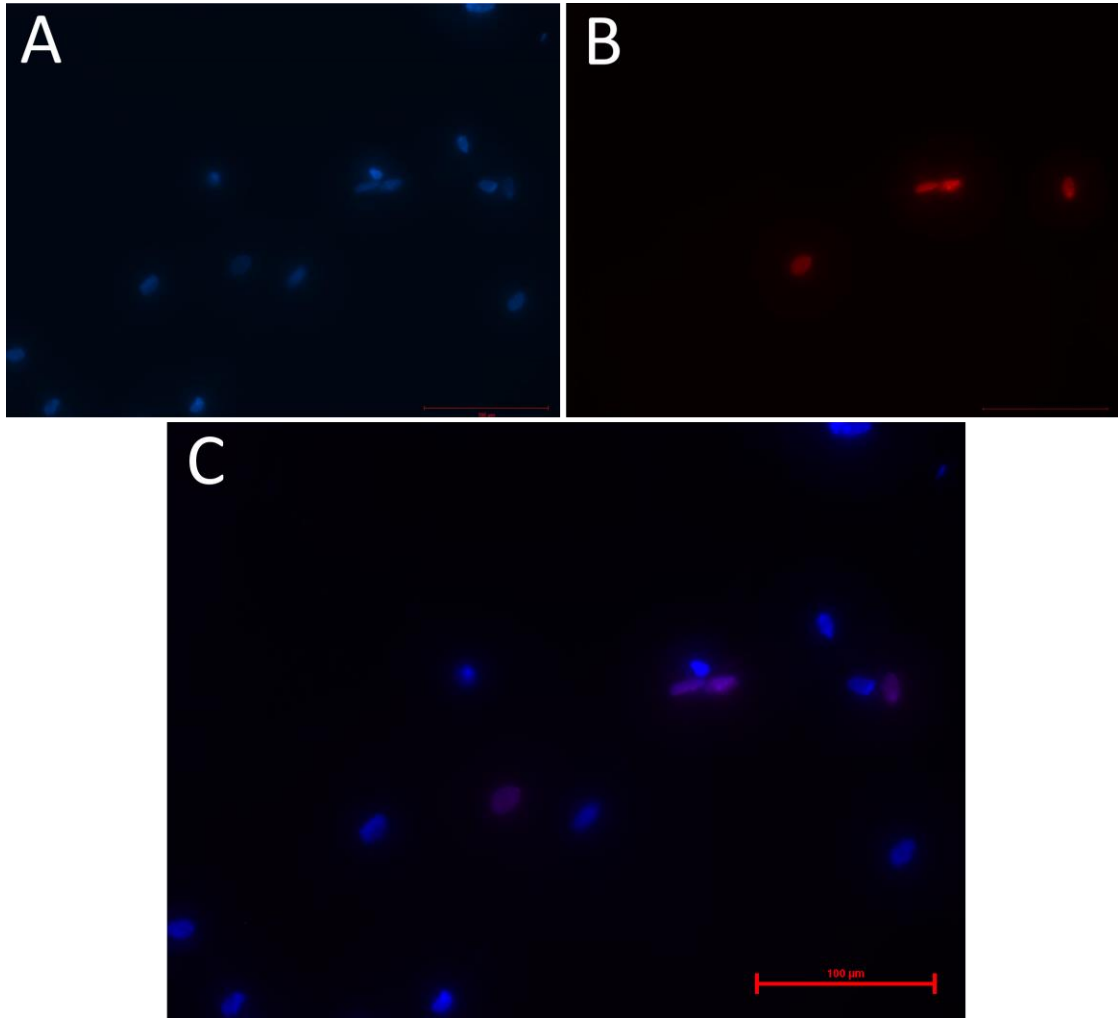


**Figure 3.17** Proliferation of hMSCs analyzed via Click-it™ Edu Assay and fluorescent microscopy. All cell nuclei are stained with DAPI (A) and proliferative cell nuclei stained with the Alexa Fluor™ 555 (B). The final panel (C) provides a merged image with the proliferative nuclei appearing purple. Maximum intensity projection of z-stacks are depicted.

The images presented in **Figure 3.17** clearly demonstrate that the hMSCs are proliferating within the RLP24-PEG hydrogels. In panel **B**, two of the proliferative nuclei were found in very close proximity to each other. These nuclei may represent daughter cells which recently underwent division. However, proliferative nuclei were

generally found further away from each other ( $>100\ \mu\text{m}$ ); it is possible that this is due to cell migration within the hydrogel. Similar distributions of proliferative nuclei were observed in PEG hydrogels.<sup>[222]</sup> Regardless, the presence of proliferating hMSCs is an important sign of cell viability and it also implies that the hMSCs have not reached terminal differentiation within these hydrogels.<sup>[222]</sup> ‘Stem-like’ hMSCs within RLP24-PEG hydrogels could be coaxed down a number of differentiation lineages for a variety of tissue engineering applications by incorporating specific biological cues into these encapsulation experiments.

### **3.3.8 Liquid-Liquid Partitioning Behavior**

An interesting phenomenon was discovered during the preparation of the RLP24-PEG hydrogels. Upon mixing, transparent precursor solutions of RLP24 and PEG would instantly turn opaque before gradually regaining optical clarity as the hydrogels cross-linked. Using phase contrast microscopy, the RLP24-PEG hydrogels were found to be composed of a heterogeneous structure filled with spherical domains that were tens to hundreds of microns in size. The cause of this heterogeneity was attributed to the liquid-liquid partitioning behavior of RLP and PEG.

The partitioning of two different polymers in aqueous solutions has been a well-known phenomenon for more than a century.<sup>[263]</sup> The behavior is most simply explained using the statistical mechanical treatment of polymer solutions in Flory-Huggins theory.<sup>[264, 265]</sup> Essentially, the theory indicates that due to the high molecular weight nature of polymer chains the Gibbs free energy of mixing is dominated by polymer-polymer interactions. Two dissimilar polymers are likely to interact unfavorably which will lead to phase separation even at low concentrations of polymer solute.<sup>[246, 247, 264, 265]</sup> Aqueous mixtures of PEG and protein have been a popular

system to study as the interactions between the two macromolecules prove important to protein crystallization,<sup>[266, 267]</sup> separation/purification strategies<sup>[268-270]</sup> and the analysis of disease progression.<sup>[271]</sup>

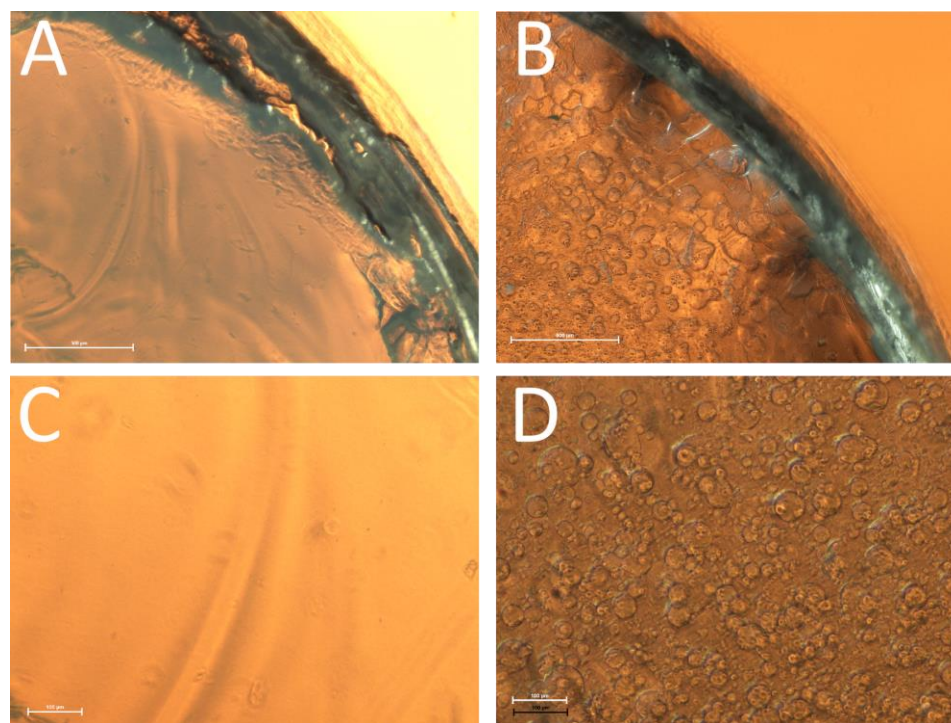


**Figure 3.18** Phase contrast images of THP cross-linked RLP hydrogels (**A, C**) and RLP24-PEG hydrogels (**B, D**). Panels (**A**) and (**B**) are taken at 5x magnification (scale bar is 500  $\mu\text{m}$ ) and panels (**C**) and (**D**) are taken at 10x magnification (scale bar is 100  $\mu\text{m}$ ).

The partitioning behavior of RLP24-PEG hydrogels was initially analyzed through phase contrast microscopy. **Figure 3.18** presents images of RLP24-PEG hydrogels and pure RLP24 hydrogels cross-linked via tris(hydroxymethyl)phosphine (THP). In **Figure 3.18A**, the edge of the pure RLP24 hydrogel under 5x magnification

depicts a material that is slightly opaque but absent of any heterogeneity. There is evidence of some particulate matter, but this was typical of lyophilized RLP24 attracting dust during hydrogel preparation. The dark arc intersecting the image was the edge of the hydrogel and coincides with the edge of a well in which the hydrogel was formed. **Figure 3.18B** represents the RLP24-PEG hydrogel in the same location at the edge of the gel and under the same magnification. The image illustrates the dense heterogeneous structure that comprises the RLP24-PEG hydrogels. These spherical domains are the result of the liquid-liquid partitioning behavior caused by the introduction of PEG into the RLP24 precursor solution. Panels **C** and **D** provide images within the main-body of the hydrogels at 10x magnification. The difference between the two types of hydrogels is very clear even under phase-contrast microscopy. The small molecule cross-linked hydrogels are perfectly homogeneous with only a few contaminating artifacts, while the RLP24-PEG gels are rich in spherical bodies of many sizes.

It would be reasonable to suspect that the RLP24-PEG hydrogels are filled with air bubbles, but when the hydrogels were temporarily deformed with a mechanical force the image shown in **Figure 3.19** was acquired. **Figure 3.19A** shows the RLP24-PEG hydrogel prior to deformation while panel **B** depicts the same hydrogel depressed with a pipet tip. The spherical domains deform under the stress while air bubbles (present in the top right) remain rigid and spherical.

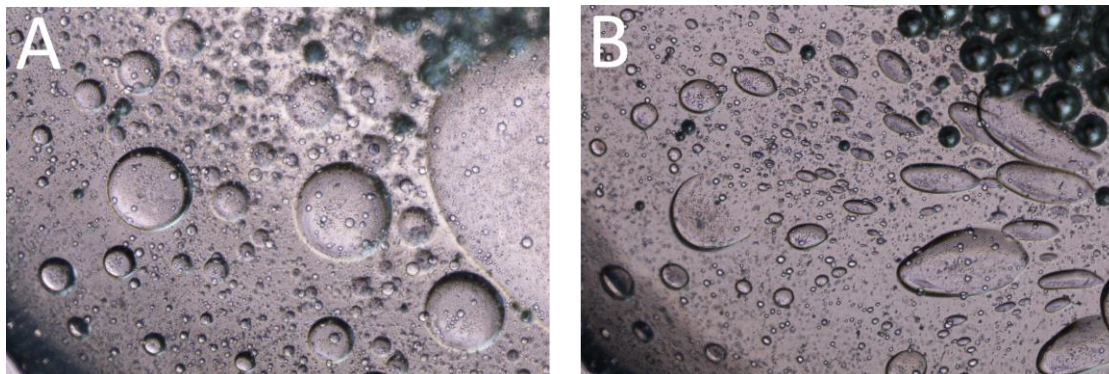


**Figure 3.19** Phase contrast image of RLP24-PEG hydrogels illustrating the deformation of the spherical phases due to mechanical stress; a behavior which implies an element of viscoelasticity. Air bubbles in the top right do not deform in the same way.

Further evidence for the formation of separate phases is presented via fluorescent confocal microscopy. The RLP24 and PEGVS precursors were labeled with different fluorophores and then cross-linked into hydrogels. The different phases within the hydrogel could then be illuminated through the fluorophores. **Figure 3.20** depicts all three channels and a composite acquired from imaging a fluorescent RLP24-PEG hydrogel. PEG was labeled with a fluorescein-type molecule and is depicted in green by panel **A**. The RLP24 was labeled with rhodamine and is represented by the red in panel **C**. Panel **B** displays the transmitted channel. In panel **D**, a composite image of all three channels is presented. From this image, it is very clear that the two precursors have separated into protein-rich and PEG-rich phases. However, the separation is not complete: the spheres appear to contain more RLP24 but are not devoid of PEG. Likewise, there is RLP in the interstitial space that is dominated by the PEG component. The incomplete separation is characteristic of protein-PEG partitioning systems. Unless precipitation occurs, there is not total

exclusion of one macromolecule from a particular phase.<sup>[247, 271, 272]</sup> Of course, this is beneficial for the RLP24-PEG system as it ensures the cross-linking of the macromolecules and subsequent gelation.

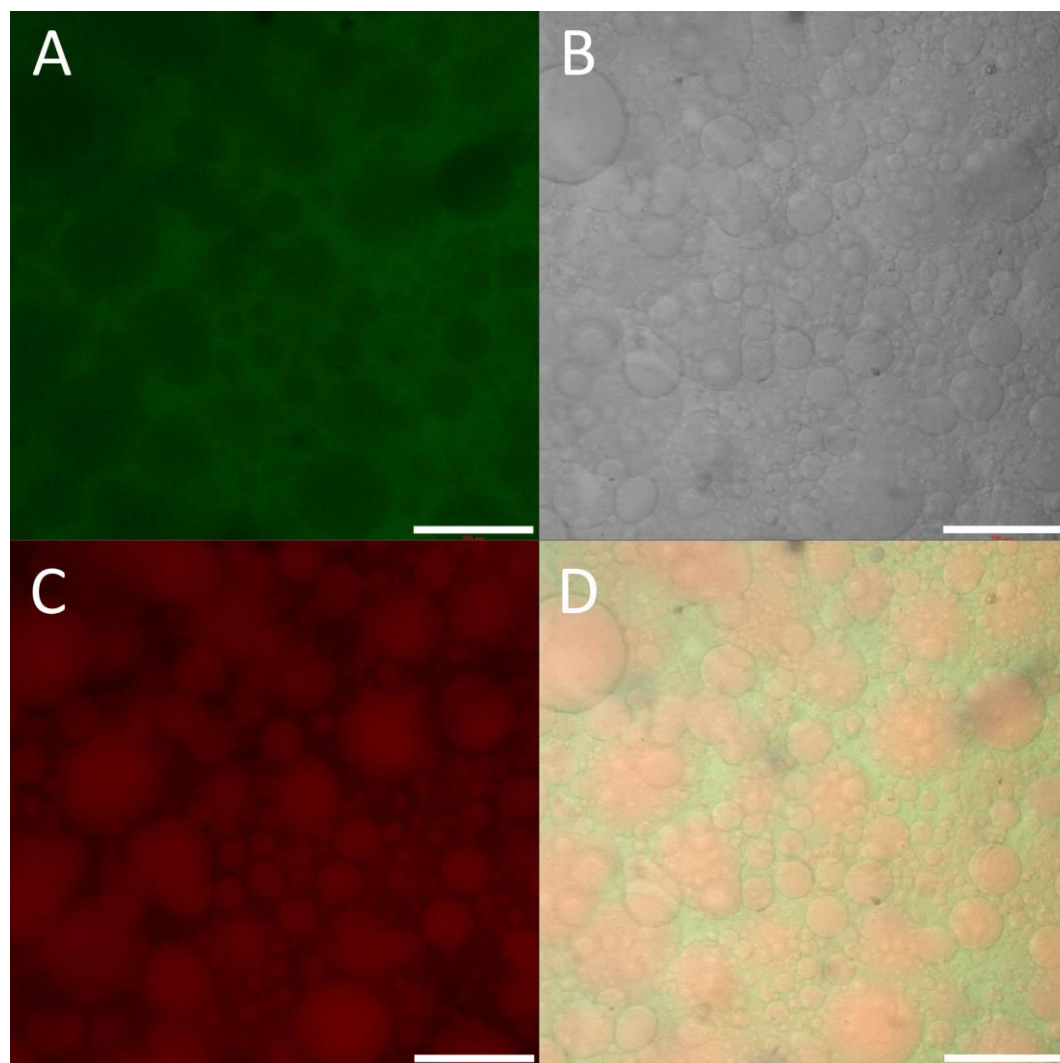


**Figure 3.20** Confocal microscopy of the fluorescently-labeled RLP24-PEGVS hydrogels. Panels depict the (A) fluorescein channel and the PEG component of the hydrogel, (B) the transmitted channel, and (C) the rhodamine channel and the RLP24 component of the hydrogel. Panel (D) provides a composite image of all three channels. Scale bar is 200  $\mu\text{m}$ .

The truly interesting aspect of this behavior is how it relates to other protein-PEG liquid-liquid partitioning systems. Normally, the protein-rich and PEG-rich phases continue to agglomerate resulting in the formation of two macroscopic phases.<sup>[247, 271]</sup> In fact, this would occur when hydroxyl-terminated PEG was mixed with RLP (data not shown). However, the cross-linking reaction competes with the process of agglomeration in mixtures of RLP24 and PEG vinyl sulfone. The result is that the phase separated domains become kinetically trapped within the material. In others, incomplete phase separation is what causes the hydrogel's heterogeneity.

This entrapped phase separation might explain the relatively low extensibility of the RLP24-PEG hydrogels. Under high extension, the interface between the spherical domains and interstitial space may propagate fractures within the hydrogel and cause premature failure. Despite the deleterious effect the partitioning may have on the mechanical properties, there is some evidence that it may be beneficial to 3D cell culture. In **Figure 3.21**, hMSCs are depicted as spreading around and onto the phase separated domains. This suggests that a degree of heterogeneity within hydrogel materials facilitates important cell behavior such as attachment and migration. More work will be necessary to fully characterize both the partitioning behavior and the resulting heterogeneity of the hydrogels. However, it is clear that hybrid hydrogels composed of RLP and PEG lead to interesting materials with useful physical and biological properties that are well-suited for application in tissue engineering.

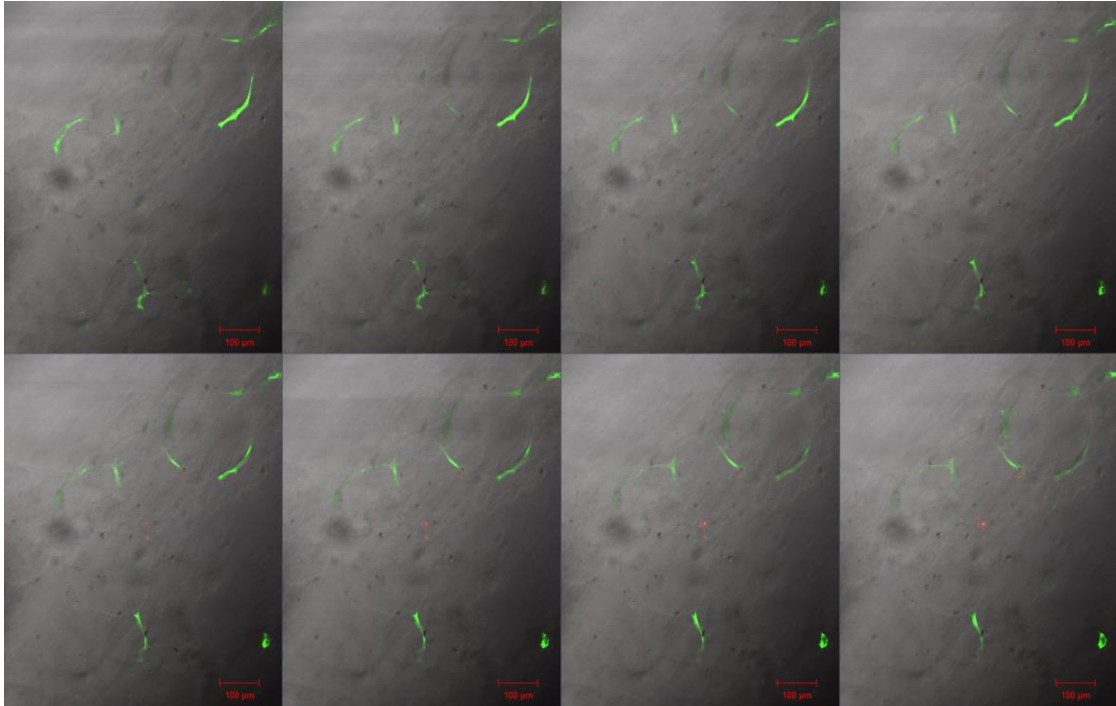


**Figure 3.21** Depicts slides from a z-stack confocal image of encapsulated hMSCs within an RLP24-PEG hydrogel. Faint outlines of the hydrogel heterogeneity can be identified via phase contrast and cells (represented in green) appear spread around and in between this heterogeneity. (Scale bar is 100  $\mu\text{m}$ )

### 3.4 Conclusions

Hybrid hydrogels composed of a resilin-like polypeptide, RLP24, and vinyl sulfone functionalized PEG macromer are elastic, resilient materials capable of the successful encapsulation and 3D culture of hMSCs. Cross-linked via a Michael-type addition between vinyl sulfone and thiols of cysteine residues, these hydrogels rapidly form and have rubber-like properties that would be useful for mechanically-demanding tissue engineering applications. The resilin-like polypeptides are sensitive to degradation via MMP1 both as soluble polypeptide and as cross-linked hydrogels. Encapsulated hMSCs remain viable and proliferate within the hydrogels over a 15 day

time period and adopt a spread, spindle-like morphology. Finally, the RLP24-PEG hydrogels demonstrate liquid-liquid partitioning behavior that gives rise to heterogeneous microstructure which might have implications for the mechanical and biological properties of these hydrogels.

## Chapter 4

### PHOTOCHEMICAL CROSS-LINKING OF RESILIN-LIKE POLYPEPTIDE/PEG HYBRID HYDROGELS USING THIOL-ENE CLICK CHEMISTRY

#### 4.1 Introduction

Photopolymerization has become increasingly important to the biomedical and tissue engineering fields over the last few decades. The use of visible or UV light to initiate polymerization or cross-linking reactions has several advantages over conventional chemistries. Photopolymerized materials often have very fast cure rates under physiological conditions, generate very little heat and can be performed using aqueous precursors that are relatively biocompatible.<sup>[12]</sup> However, the most significant advantage comes from the spatial and temporal control over the cross-linking, which provides unparalleled control over the final properties of a material.<sup>[12, 18, 20, 273, 274]</sup> One of the most familiar applications of photopolymerization has been in the dentistry field where it has been widely applied in dental sealants and restorations.<sup>[275, 276]</sup>

In the tissue engineering field, photo-initiated reactions have primarily been employed as a method of cross-linking macromolecules into networks<sup>[8, 10, 12, 18, 277, 278]</sup> and patterning materials to add functionality.<sup>[20, 21, 24, 273, 274, 279, 280]</sup> The ability to control the degree of polymerization via exposure time or irradiation intensity allows an operator a greater degree of control as compared to conventional cross-linking chemistries. For example, in a conventionally cross-linked hydrogel, the mechanical properties are often manipulated through reactive group stoichiometry, precursor

concentration and precursor molecular weight; or, effectively, the cross-linking density.<sup>[281, 282]</sup> A photochemically cross-linked hydrogel introduces one further controllable variable: the extent of reaction. By simply switching off or altering the intensity of light, the reaction kinetics of photoinitiation may be altered affecting the extent of reaction and the resulting cross-link density.<sup>[18, 283]</sup> An advantage of light-mediated cross-linking for clinicians is that the precursors may be premixed and positioned prior to gelation.<sup>[18]</sup> The spatial control over the reaction is another advantage of photocross-linkable materials. By directing the geometry of light exposure, a material can be formed into a variety of complex shapes that conform and adhere to tissue structures.<sup>[12]</sup> More recently, researchers have used light to pattern photoreactive hydrogels with fluorescent tags and biomolecules in order to impart enhanced bioactivity to the scaffolds. Several laboratories have demonstrated that PEG hydrogels may be patterned to create specific two and three dimensional geometries of conjugated molecules.<sup>[20, 21, 24, 273, 274, 279, 280]</sup> Culver *et al.* has demonstrated that the 3D patterning of adhesion molecules via two-photon laser scanning lithography led to the migration of cells and the development of vascular-like structures within the patterned hydrogel.<sup>[280]</sup>

Synthetic polymers, such as PEG, often serve as the macromolecular precursors for photocross-linkable hydrogels. However, biosynthetic protein polymers have emerged as an exciting alternative precursor for use in tissue engineering scaffolds. Recombinant protein polymers offer the advantages of precise control over composition, sequence and molecular weight as well as the ability to engineer biological activity directly into the polypeptide backbone.<sup>[74, 93, 100, 101, 104]</sup> Unfortunately, there has been a limited exploration of introducing photoreactive

chemistries to biosynthetic protein polymers for the creation of tissue engineering scaffolds.<sup>[95, 279, 284, 285]</sup> Instead research has focused on the acrylation/methacrylation of naturally-derived proteins (e.g. gelatin, fibrinogen) and creating materials from these modified proteins.<sup>[233, 234, 236, 286-299]</sup>

In this chapter, we introduce a photocross-linkable recombinant protein-PEG hybrid hydrogel composed of a resilin-like polypeptide (RLP) and a multiarm star PEG macromer. Lysine residues present in regular intervals along the RLP chain have been modified with a norbornene acid via amide bond coupling chemistry (*see Figure 4.1*). This norbornene can be reacted with a thiol-functionalized PEG through a highly efficient and selective step-polymerization reaction: thiol-ene click chemistry.<sup>[300]</sup> Thiol-ene reactions have been an important part of polymer chemistry for the better part of a century.<sup>[301]</sup> However, more recently, the chemistry has been applied to formation of PEG-based hydrogels for tissue engineering and drug delivery applications.<sup>[18, 53, 222, 232]</sup> Traditional photoreactive chemistries, such as the acrylate/methacrylate systems mentioned above, differ from thiol-ene chemistries in that the cross-linking is driven by radical chain-growth polymerization. This results in networks with heterogeneous structures consisting of poly(meth)acrylate chains of varying size.<sup>[18, 302]</sup> As a step-growth polymerization, thiol-ene chemistry forms cross-links between complementary reactive groups and results in more homogeneous network shown to possess superior mechanical properties than chain-growth networks.<sup>[18, 22]</sup> Further, it has recently been demonstrated that thiol-ene chemistry made be more cyto-comptabile than radical chain growth mechanisms.<sup>[303]</sup>

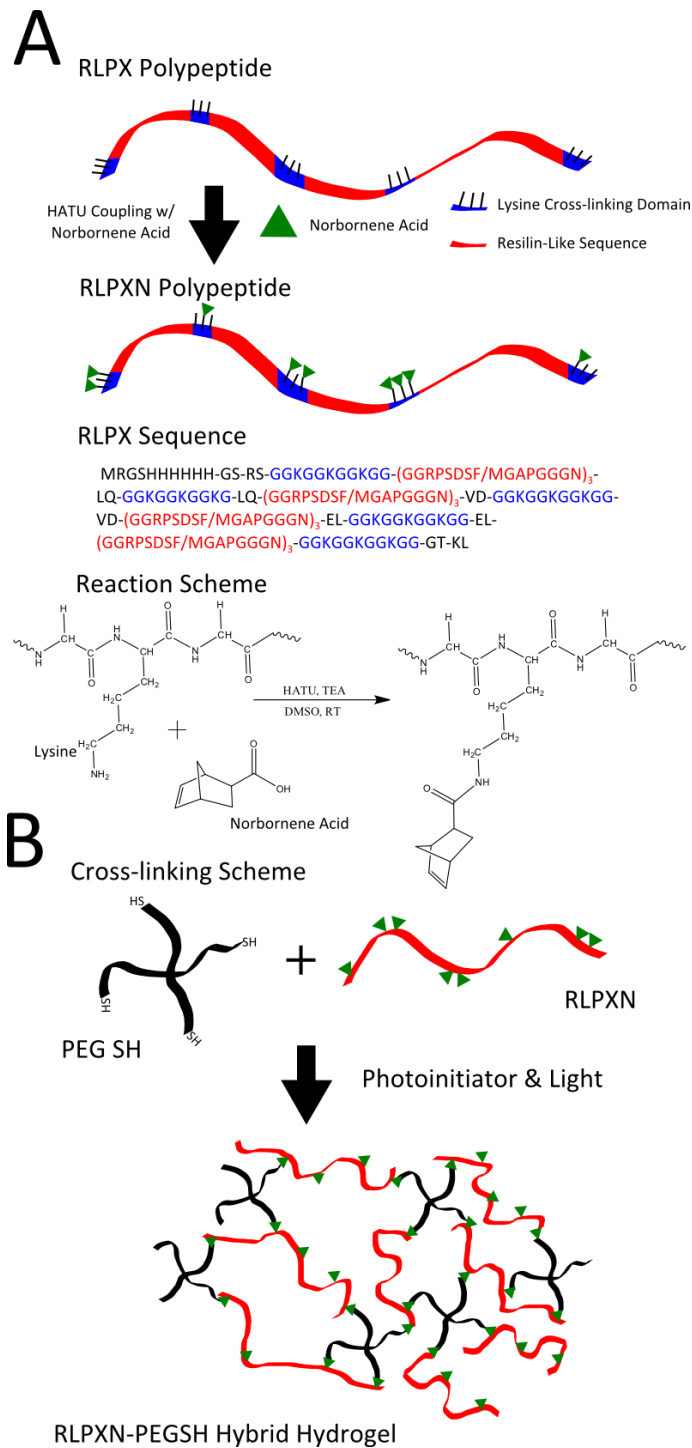


**Figure 4.1** Scheme illustrating the sequence of RLPX and the attachment of the norbornene acid. **(A)** Scheme illustrating the cross-linking of the RLPXN-PEGSH hydrogels **(B)**.

Here, we report the functionalization of the RLP with norbornene and its characterization via  $^1\text{H}$  NMR. The mechanical properties of these hybrid hydrogels are analyzed via oscillatory rheology. Initial cyto-compatibility measurements are performed through the encapsulation and culture of human mesenchymal stem cells within these hydrogels. To our knowledge, this is the first application of thiol-ene photocross-linking to the formation of recombinant protein hydrogels for tissue engineering applications.

## **4.2 Experimental Section**

### **4.2.1 Materials**

All chemicals or reagents were purchased from Sigma-Aldrich (St. Louis, MO) or Fisher Scientific (Waltham, MA) and used as received unless otherwise noted. Ni-NTA agarose used for protein purification was purchased from Qiagen (Valencia, CA) or Thermo Scientific (Rockford, IL). Water for buffers or media was deionized and filtered using either a ThermoFisher Barnstead NANOpure Diamond water purifier or a Purelab *Classic* (Siemens, Munich, Germany). The thiol-terminated 4-arm star PEG (10 kDa) was purchased from JenKem Technology USA (Plano, TX). The photoinitiator, lithium phenyl-2,4,6-trimethylbenzoylphosphinate (LAP), was kindly prepared by Dr. Kenneth C. Koehler.

### **4.2.2 Expression and Purification of RLPX**

The design and cloning of the RLPX protein has been previously reported elsewhere.<sup>[101, 238]</sup> Expression was performed using the QIAexpress® expression system (QIAGEN, Valencia, CA). Briefly, *E. coli* M15[pREP4] was transformed with a pQE-80L plasmid containing the RLPX gene. To express the RLPX protein, the *E.*

*coli* host was grown in 2xYT medium containing proper antibiotics to an O.D. of ~0.6. These cultures were then induced to express the protein through the addition of isopropyl  $\beta$ -D-thiogalactopyranoside (IPTG) to a 1 mM final concentration. The cultures were then allowed to express for four hours at 37°C. Cells were pelleted via centrifugation and frozen at -20°C. Purification was performed using native conditions according to the manufacturer's guidelines for Ni-NTA affinity chromatography.<sup>[304]</sup> The eluent containing the RLPX product was dialyzed against 1 M NaCl once and then against ddH<sub>2</sub>O (5x). The dialyzed solutions were subsequently frozen and lyophilized to a dry powder. The purification was monitored via gel electrophoresis (SDS-PAGE).<sup>[248]</sup> Amino acid analysis and mass spectroscopy characterization for RLPX has been previously reported.<sup>[101]</sup>

#### 4.2.3 Functionalization and Characterization of RLPXN

The RLPX protein was functionalized with norbornene through regularly occurring lysine residues on the polypeptide chain (*see* **Figure 4.1A**). Simple amide bond coupling chemistry conjugated *exo*-5-norbornenecarboxylic acid (Sigma Aldrich) to the amine side chain of the lysine residues. First, RLPX was dissolved using heat and sonication into dimethyl sulfoxide (DMSO) at a 5 mg/mL concentration; the drop-wise addition of triethylamine (TEA) assisted with the dissolution. The norbornene acid was separately dissolved in DMSO with TEA added in a 1:1 ratio. The total molar ratio of TEA to lysine for any given reaction was never greater than 10:1. To initiate the reaction the coupling reagent, ((1-[bis(dimethylamino)methylene]-1H-1,2,3-triazolo[4,5-b]pyridinium 3-oxid hexafluorophosphate), or HATU, was dissolved in DMSO, combined with the norbornene/DMSO/TEA mixture and promptly added to the RLPX/DMSO/TEA

solution. The reaction ran at room temperature for approximately 2 hours. The ratio of norbornene acid to lysine residue varied depending upon the desired functionality of the RLPX conjugate. However, the ratio of HATU to norbornene was kept at 1:1 stoichiometry to avoid side reactions. The following table illustrates the different reactions performed and the corresponding ratios of all the reagents:

**Table 4.1** Summary of reaction conditions investigated for RLPXN functionalization

<b>Reaction</b>	<b>HATU:NORBORNENE:LYSINE</b>
<b>A</b>	1.00 : 1.00 : 1.00
<b>B</b>	0.75 : 0.75 : 1.00
<b>C</b>	0.50 : 0.50 : 1.00
<b>D</b>	0.25 : 0.25 : 1.00

Due to the efficiency of the reaction, the norbornene did not need to be included in excess. The reaction was terminated through the addition of an equal volume of water containing a 100  $\mu\text{M}$  concentration of ammonium hydroxide. This solution was promptly dialyzed (Snakeskin<sup>TM</sup>, 10 kDa, Thermo Scientific) against ddH<sub>2</sub>O for two hours in a 20:1 volumetric ratio of buffer to dialysate; this removed most of the DMSO. In later stages of dialysis, precipitation was prevented by adding a minute concentration (<10  $\mu\text{M}$ ) of sodium hydroxide to the dialysis buffer. However, in the final step of dialysis, the protein was always returned to pure water. Finally, the RLPXN solution was filtered, frozen in liquid N<sub>2</sub> and lyophilized.

The functionality of the RLPX protein was characterized via <sup>1</sup>H NMR. Samples were prepared in a ~5mg/mL concentration of functionalized RLPX dissolved in D<sub>2</sub>O with ~0.2% NaOD (Cambridge Isotope Laboratories, Tewksbury, MA). They were analyzed using either a AVIII 600 MHz NMR spectrometer equipped

with a 5-mm Bruker SMART probe or a AV400 NMR spectrometer equipped with a cryogenic QNP probe (Bruker, Billerica, MA) courtesy of Dr. Shi Bai (Department of Chemistry and Biochemistry, University of Delaware, Newark, DE). Water suppression was employed in the analysis. As an engineered protein, the sequence of RLPX was known and the presence of eight phenylalanine residues per RLPX molecule was used as a reference for the quantification of norbornene. The integration of the phenyl ring protons (7.15-7.35 ppm) could be compared to the integration of the olefin protons present on the norbornene (6.00-6.15 ppm).

#### **4.2.4 Cross-linking and Oscillatory Rheology of RLPXN-PEGSH Hydrogels**

Characterization of gelation and the mechanical properties was conducted using an AR-G2 Rheometer (TA Instruments, New Castle, DE) equipped with an OmniCure® S1000 UV lamp assembly for photocuring applications; a stainless steel 8mm diameter parallel plate geometry was used for these experiments. RLPXN and PEGSH were dissolved separately in PBS buffer (pH 7.4) that included the LAP photoinitiator at a 0.067 wt% concentration. Different weight percentages of precursor (RLP and PEG included together) were analyzed, but the cross-linking stoichiometry of norbornene to thiol was kept constant at 1:1 ratio. Precursor solutions were briefly mixed on a vortex mixer and deposited on to a quartz crystal that would guide UV light to the solution and serve as the rheometer stage during the experiment. Unless otherwise noted, the solutions were cured using 365 nm light at an intensity of 5 mW/cm<sup>2</sup>. Oscillatory time sweeps were conducted using 1% strain at 1 Hz and frequency sweeps from 0.01 – 10 Hz used 1% strain. The composition of the each RLPXN-PEGSH hydrogel was always ~50% protein, ~50% PEG. The elastic moduli

were reported as a simple mean of three experiments and the error is the standard deviation.

#### **4.2.5 Photoencapsulation, Culture and Viability of hMSCs**

The viability of bone-derived human mesenchymal stems encapsulated within RLPXN-PEG hydrogels was analyzed through confocal microscopy. The hMSCs (Lonza, Basel, Switzerland) were cultured according to the manufacturer's specifications at 37°C, 5% CO<sub>2</sub> and using the BulletKit™ hMSC growth medium sold by Lonza. The passage number for these cells ranged between P5 and P10 and confluency was kept below 80%. The RLPXN-PEGSH hydrogels used for the encapsulation experiments were 6wt% (RLPXN and PEGSH) and had a final volume of 50 µL.

Initially, the LAP initiator was dissolved in PBS buffer at a 0.084% concentration to compensate for the lack of photoinitiator in the cell media. RLPXN and PEGSH were dissolved separately in this PBS buffer; usually, a few drops (0.2 µL) of 2N NaOH were needed to help solubilize the protein. Prior to the encapsulation, the hMSCs were lifted via trypsin/EDTA (Lonza), counted using a hemocytometer and separated into 10 µL aliquots of 20,000 cells. The precursors were vortex mixed and then triturated with the cells before deposited on to a glass-bottom dish (MatTek Corporation, Ashland, MA). These dishes were then placed under 365nm UV light (B-100 High Intensity Long Wave Length Lamp, UltraViolet Products, Upland, CA) at ~6 mW/cm<sup>2</sup> for 30 seconds. Immediately following, 3 mL of growth media was added to the dishes and the cell-gels were placed in an incubator (37 °C, 5% CO<sub>2</sub>); lifting the gels encouraged diffusion to the bottom edge and improved viability.

Live/Dead® stain (Life Technologies) was utilized to determine the viability of the hMSCs over a 28 day time period. Prior to imaging, hydrogels were placed in PBS buffer containing 2  $\mu$ M Calcein AM and 4  $\mu$ M Ethidium homodimer-1 for 30 minutes. The cell-gels were then imaged using laser scanning confocal microscopy on a Zeiss LSM 510 NLO multiphoton microscope (Carl Zeiss, Inc., Thornwood, NY) courtesy of the Delaware Biotechnology Institute (Newark, DE) Bioimaging Center. Z-stack images were acquired from several sample gels for a given time point. Representative maximum intensity projections were reported.

### **4.3 Results & Discussion**

#### **4.3.1 Design, Expression and Purification of RLPX**

The design, expression and purification of RLPX has been previously reported by Li *et. al.*, but a summary of the important details will be provided here.<sup>[101]</sup> The RLPX protein consists of 12 repeats of a resilin-like sequence based upon the consensus sequence (GGRPSDSYGAPGGGN) derived from the first exon of *Drosophila melanogaster* gene, CG15920.<sup>[140]</sup> One major difference between the RLPX sequence and the one found in the *Drosophila* gene was the substitution of tyrosine residues for phenylalanine or methionine (GGRPSDSF/MGAPGGGN). This substitution enabled future incorporation of non-canonical amino acids with side-chain chemistries that could serve as potential cross-linking sites. The resilin-like motifs were organized in four groups of three repeats along the RLPX sequence. These resilin domains were flanked by five ‘cross-linking domains’ containing three lysine residues for a total of 15 lysines per RLPX molecule. The cross-linking domains also contained two glycine spacers between each lysine residue to form the following sequence:

GGKGGKGGKGG. **Figure 4.1** provides an illustration of the RLPX polypeptide and its sequence. The cross-linking domains were important to this work because they enabled the functionalization of the RLPX protein through amide bond coupling chemistry. It should be noted that the RLPX gene is so named because of its flexible gene sequence which can incorporate bioactive domains, such as integrin-binding, with great specificity and relative ease. Therefore, the 'X' in RLPX, denotes both the variability of the sequence as well as its lack of bioactive domains. Other bioactive versions of RLPX (RLP-RGD, RLP-MMP, *etc.*) have been constructed,<sup>[101]</sup> but the addition of photoreactive chemistries to these species was outside the scope of this work.

The expression of RLPX was performed using the QIAexpress system and the protocols set forth by the manufacturer.<sup>[304]</sup> Briefly, overnight cultures of transformed *E. coli* were used to inoculate six Fernbach flasks containing 500 or 750 mL of 2xYT medium. These were allowed to grow in shaker incubators at 37°C until they achieved an O.D. of ~0.6. The cultures were then induced using a 1 mM concentration of IPTG and allowed to express for four hours at 37°C. Purification was performed under native conditions using Ni-NTA affinity chromatography; the product eluent was dialyzed against pure water, frozen and lyophilized. The yield for expression ranged between 10-30 mg/L of expression media and between 1.90-5.03 mg/g of cell paste. Although the protein yield differed between preparations it was still consistent with previous reports.<sup>[101]</sup> Characterization of RLPX preparations was performed using gel electrophoresis. **Figure 4.2** depicts a representative SDS-PAGE gel containing samples from a purification.

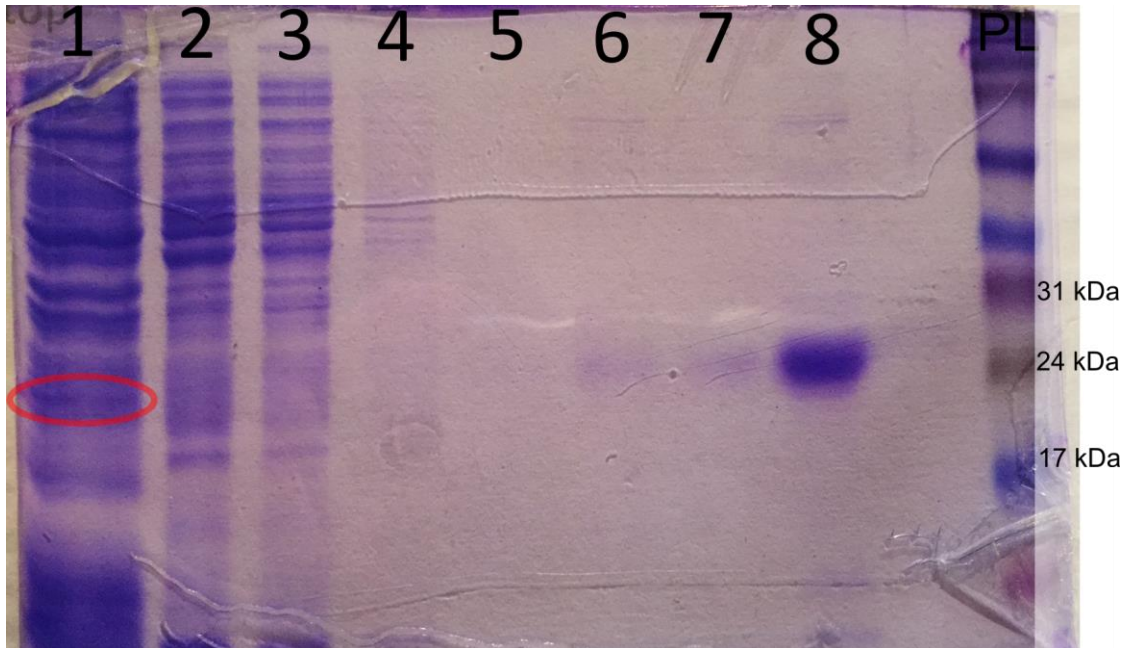


**Figure 4.2** Representative SDS-PAGE gel of an RLPX purification. Lanes 1 is the cell-free lysate prior to incubation with Ni-NTA resin. Lane 2-3 are the cell-free lysate ‘flow-through’ fractions. Lanes 4-7 are wash buffer fractions and lane 8 is the elution fraction containing the RLPX. The benchmark protein ladder is in the final lane.

Lane 1 in **Figure 4.2** represents the cell-free lysate prior to incubation with the Ni-NTA resin. This fraction contains all of the soluble bacterial proteins and RLPX. The band denoting the RLPX protein can be identified in this fraction by its approximate molecular weight and the disappearance of the band in lanes 2 & 3. The second and third lanes of the gel represent the ‘flow-through’ fractions and consist of only proteins that do not bind to the resin. Subsequent wash steps removed contaminating proteins and in lane 8 the RLPX protein is eluted using a high concentration of imidazole. As indicated by the gel, the RLPX protein is fairly pure at this step. Dialysis of the protein elution removed buffer salts and the RLPX was

lyophilized to a dry powder. Previously, Li *et al.* reported the mass spectroscopy and amino acid composition analysis of RLPX preparations that further confirmed the production of the protein.<sup>[101]</sup>

### **4.3.2 Functionalization of RLPX**

To impart photoreactivity to the RLPX protein, norbornene acid was conjugated to the polypeptide through the lysine residues. Since the protein was found to be soluble in DMSO, it was decided to use the highly efficient peptide coupling reagent, HATU, to perform the conjugation. The HATU coupling resulted in high conversion of lysine residues at stoichiometrically equivalent ratios of reactive groups, a factor that simplified purification. Lyophilized RLPX protein was dissolved into a solution of DMSO. Separately, a solution of DMSO, norbornene acid, HATU and TEA were combined to pre-activate the carboxylic acid. The activated norbornene and RLPX solutions were then mixed and allowed to react for two hours at room temperature. At the end of the two-hour period, water containing a small concentration of ammonium hydroxide (< 0.1 mM) was added to the reaction. Initially, dialysis against pure water was used to remove the DMSO and any byproducts of the reaction. To prevent precipitation of the protein, the dialysis buffer was switched to water containing a small concentration of sodium hydroxide (<0.1 mM). Before the protein solution was frozen and lyophilized, a final dialysis step against pure water was performed to remove any remaining salt. The decision to switch from ammonium hydroxide to sodium hydroxide was empirical and based upon the finding that lyophilized RLP dissolved more easily when previously dialyzed against water containing NaOH. One concern was that the electrostatic interactions between TEA and the protein could potentially drag the RLPX out of solution when transferred to

the aqueous phase. The addition of the hydroxide bases to the dialysis steps was intended to mitigate these interactions by swapping the TEA for smaller counter ions. The yields for conjugation reaction varied between 59 and 79%. Following the conjugation reaction, the protein was denoted RLPXN for RLPX-norbornene.

To determine the functionality of RLPXN, samples of the protein were dissolved into D<sub>2</sub>O containing a small concentration of NaOD (0.2% w/v) and analyzed using <sup>1</sup>H NMR. **Figure 4.3** depicts representative NMR spectra of RLPXN and unconjugated RLPX. The NMR spectra were very complex in the upfield region due to the number of different amino acids that made the RLPX sequence. The number of potential chemical shifts and their tendency to overlap complicated the analysis in this region. Fortunately, the 6.0-8.0 ppm region was far less complex and could be utilized to determine norbornene functionality. Three important chemical shifts were present in the downfield region of the RLPX NMR spectra. The inclusion of a 6xHis fusion tag on the RLPX protein for purification gave rise to the peaks at ~6.75 and ~7.6 ppm. These peaks corresponded to the two protons present on the imidazole ring of the histidine side chain. However, it was the inclusion of eight phenylalanine residues in RLPX sequence that proved to be critical for the calculation of norbornene functionality. The phenylalanine side chain, a benzyl ring, contains five protons which appear very characteristically around 7.4 ppm. This region could be integrated and used to compare integrations in the 6.1 ppm region for the alkene protons of the norbornene.<sup>[18]</sup> **Figure 4.3A** displays the entire spectra of RLPXN (turquoise) and RLPX (red). Panel **B** provides a close up of the downfield region of the spectra.

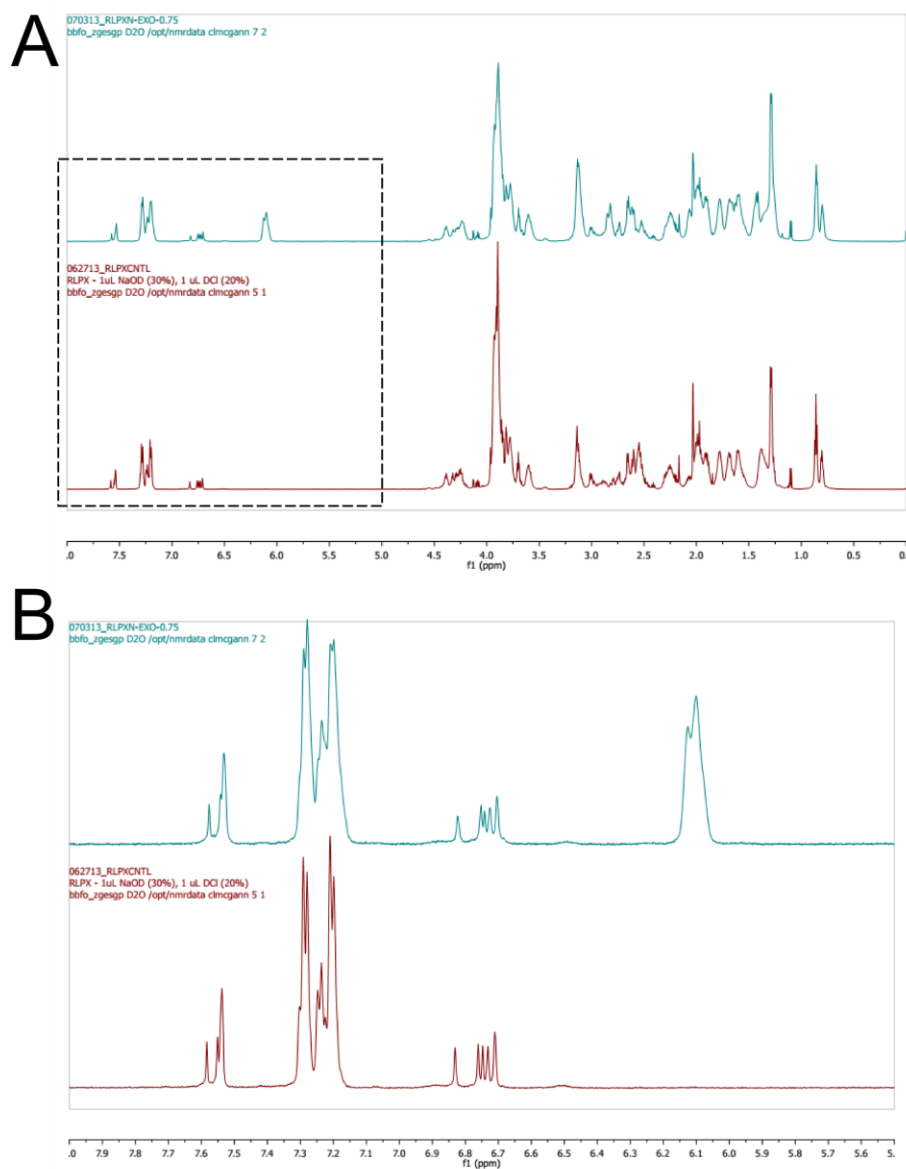


**Figure 4.3**  $^1\text{H}$  NMR spectra of RLPXN (turquoise) and RLPX (red). The entire spectrum for both is depicted in (A) and a close up of the downfield region used for analysis is depicted in (B).

**Figure 4.4** displays the integration calculation for determining the functionality of an RLPXN preparation. Additionally, the protons used in the analysis

are shown in their corresponding chemical structures. For this particular preparation of RLPXN the norbornene acid was reacted with lysine in a 3:4 (0.75:1) ratio. The benzyl ring proton region was integrated to equal 40 protons based upon 8 phenylalanine residues per RLPX molecule and 5 protons per ring. The region at 6.1 ppm, which corresponds to the two alkene protons on the norbornene, was integrated to be 18.21 protons and the functionality was determined to be ~9.1 norbornenes per RLPX molecule.

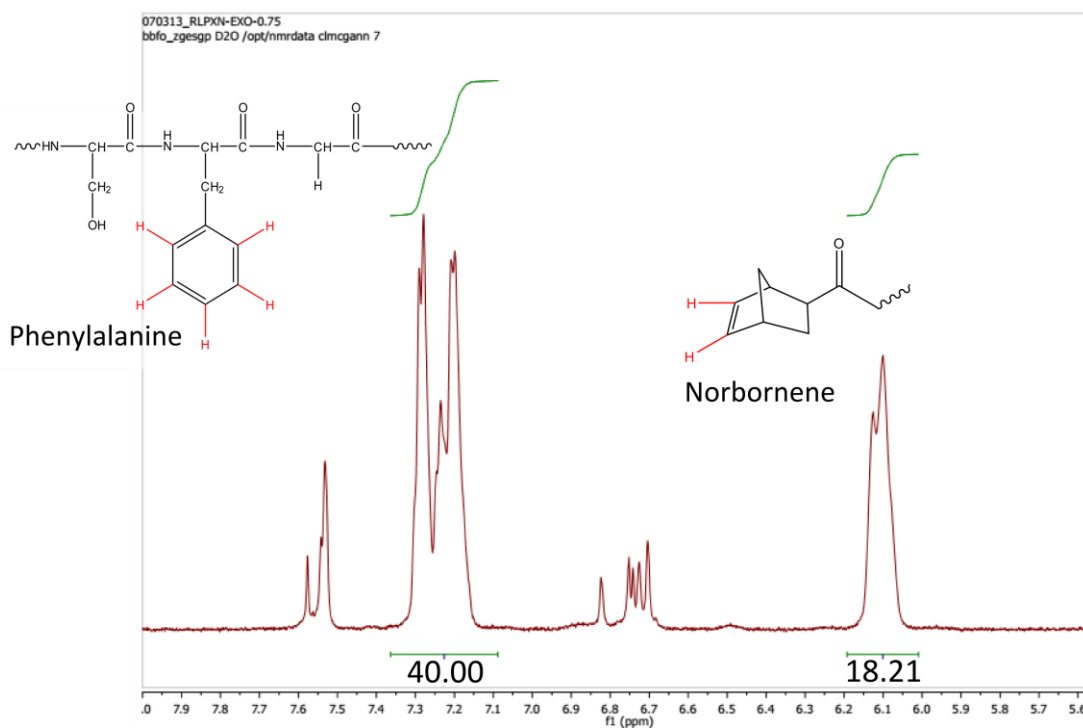


**Figure 4.4** <sup>1</sup>H NMR spectrum of RLPXN functionalized with norbornene using a 3:4 reaction stoichiometry of norbornene acid to lysine residue. The five protons on eight phenylalanine benzyl rings will integrate to 40H and the integration of the alkene protons of norbornene (6.1 ppm) equals roughly 18.21 protons for this preparation. This equates to roughly 9.1 norbornenes per RLPX molecule.

The functionality of the RLPXN protein could be modulated by altering the reaction stoichiometry. As mentioned previously, the efficient HATU conjugation meant that it was not necessary to exceed a 1:1 reaction stoichiometry of norbornene acid to lysine. High functionalities could be attained without including excess reagent. Four different reaction stoichiometries outlined in **Table 4.1** were investigated and analyzed using  $^1\text{H}$  NMR. The results of the NMR are presented in **Figure 4.5**. The functionality of each preparation was determined through NMR and the results are presented in **Table 4.2**.

**Table 4.2** Summary of the different reaction stiochiometries and their effect on the functionality of RLPXN

Norbornene:Lysine	$^1\text{H}$ Integration	Functionality	% of Lysine
1.00 : 1.00	25.78	12.9	85.9
0.75 : 1.00	18.21	9.1	60.9
0.50 : 1.00	14.79	7.4	49.3
0.25 : 1.00	7.68	3.3	22.0

As illustrated by the table, the functionality of RLPXN was easily tailored through modification of the reaction stoichiometry. RLPXN with low or high functionality could be easily produced. However, the reaction efficiency at the 1:1 and 0.75:1 ratios was lower due to the precipitation of highly conjugated RLPXN as it was transferred to aqueous solutions. The addition of large hydrophobic norbornene moieties and the simultaneous removal of charged lysine residues were detrimental to the solubility of the RLPX. A larger degree of precipitation nearly always occurred in the preparations pursuing a higher functionality. For this reason, it was chosen to use a 3:4 (0.75:1) ratio of norbornene acid to lysine for future experiments. RLPXN with 9.1 norbornenes appeared to strike a balance between functionality and solubility.

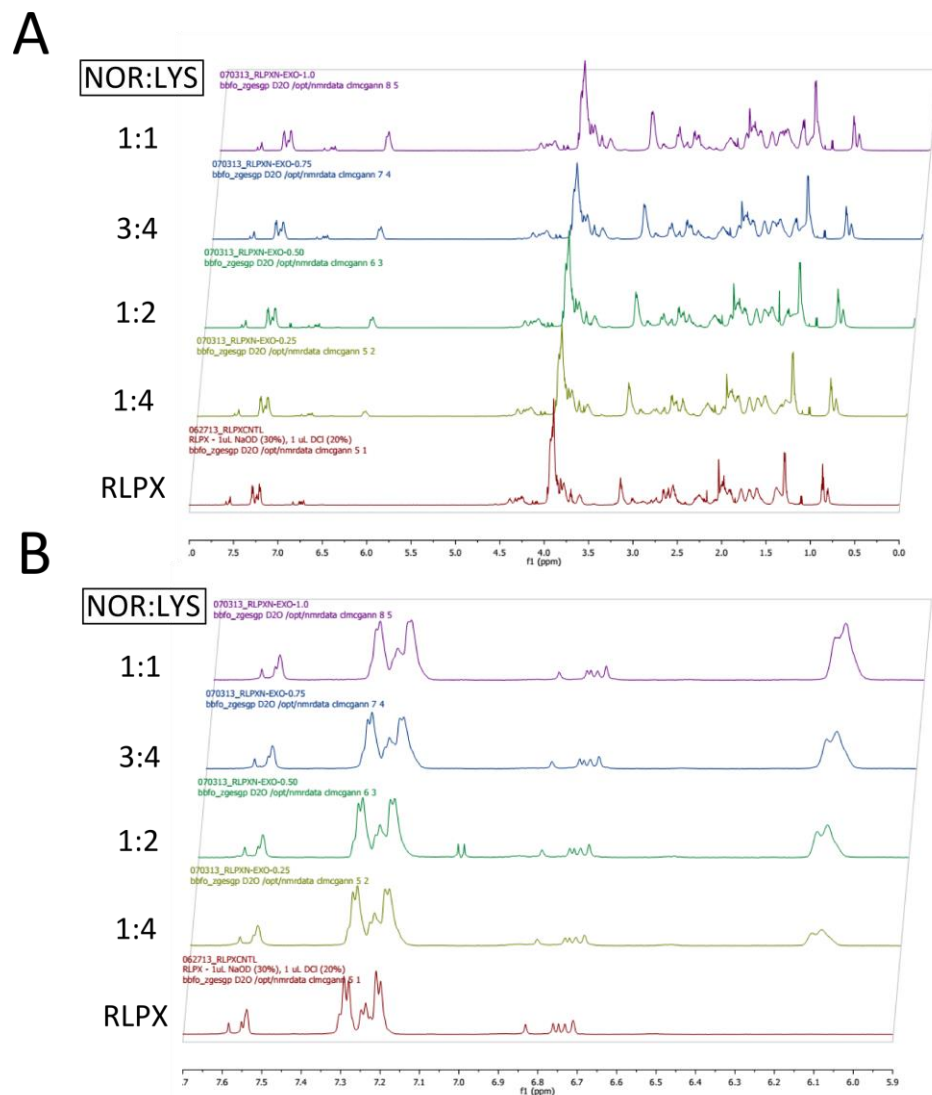


**Figure 4.5**  $^1\text{H}$  NMR spectra of different preparations of RLPXN. By modulating the stoichiometric ratio of norbornene to lysine, RLPXN with different functionality could be attained. The decrease in functionality is reflected in the decrease in peak size at 6.1 ppm. A full spectrum is presented for the 1:1 (purple), 3:4 (blue), 1:2 (green), and 1:4 (yellow) reactions in panel (A) with a close up of the 6.0-8.0 ppm region in panel (B). The decrease in alkene peak size is clearly related to the change in stoichiometry. The control RLPX is presented as the red spectra.

### 4.3.3 Oscillatory Rheology of Photopolymerized RLPXN-PEGSH Hydrogels

To form hydrogels, RLPXN was cross-linked with thiol-terminated PEG macromer using a photo-initiated thiol-ene step polymerization. The precursors were prepared separately by dissolving RLPXN or PEG thiol into PBS solutions containing 0.067wt% LAP photoinitiator. The solutions were promptly combined and exposed to UV light at 365 nm to initiate the cross-linking reaction. A few photoinitiators were explored, but the LAP initiator demonstrated the best water solubility and had the greatest reactivity when exposed to light at 365 nm.<sup>[305]</sup> The mechanical properties of the RLPXN-PEGSH hydrogels were explored through oscillatory rheology with *in situ* photopolymerization of the precursors using a photocuring accessory attached to the rheometer. The mechanical stiffness of the hydrogels was modulated by controlling the weight percent of the precursor solutions while maintaining a 1:1 ratio of thiol to norbornene. Precursors of RLPXN and PEG thiol were prepared at the following concentrations: 6, 4 and 3wt%. **Figure 4.6A** depicts representative oscillatory time sweeps of RLPXN-PEGSH gelation and the effect that weight percent had on the final mechanical properties. As illustrated by the figure, gelation was nearly instantaneous for the precursor solutions when cross-linked using a 5 mW/cm<sup>2</sup> irradiation intensity. Further, the gelation time was independent of the precursor concentration. **Figure 4.6B** depicts the frequency dependence of RLPXN-PEGSH hydrogels at different precursor concentrations. For strain frequencies approaching 5 Hz the RLPXN-PEGSH hydrogels demonstrated behavior consistent with permanently cross-linked networks. However, there was an upward trend in the storage and loss modulus at the higher strain frequencies. This was likely due to physical chains entanglements constraining the network and causing it to behave more elastically.<sup>[306]</sup> The source of these entanglements may be related to the proximity of the network junctions within

these hydrogels. Each cross-linking domain contains three lysine residues separated by only two glycines. Once conjugated with norbornene and reacted with the PEG macromer, several chains of synthetic polymer and polypeptide would be in close proximity. Thus, the potential for physical entanglement increases and the chains would not be able to behave viscously at higher testing frequencies. Other RLP-PEG hydrogels with better cross-link distribution did not demonstrate this frequency dependence.<sup>[104]</sup>

**Figure 4.6C** depicts the range of mechanical properties that could be attained by the hydrogels at the investigated precursor concentrations. The moduli of the RLPXN-PEGSH hydrogels could be very low in the 400-500 Pa at 3wt% or more elastic in 3000-4000 Pa range at 6wt%. The elasticity of RLPXN-PEGSH hydrogels compared well with PEG hydrogels using the same chemistry as well as with a number of tissues within the body, an important attribute for potential tissue engineering scaffolds.<sup>[18]</sup> An important advantage of the RLPXN-PEGSH hydrogels is that they use far less polypeptide than other RLP hydrogels. Usually, RLP hydrogels are cross-linked at 20wt% or 25wt% concentration, which creates a huge requirement for the polypeptide especially when performing a multitude of experiments. For the 6wt% RLPXN-PEGSH hydrogels, only 3 mg of protein would be necessary for a 100  $\mu$ L hydrogel while 20 mg would be necessary for a pure RLPX hydrogel cross-linked with a small molecule.

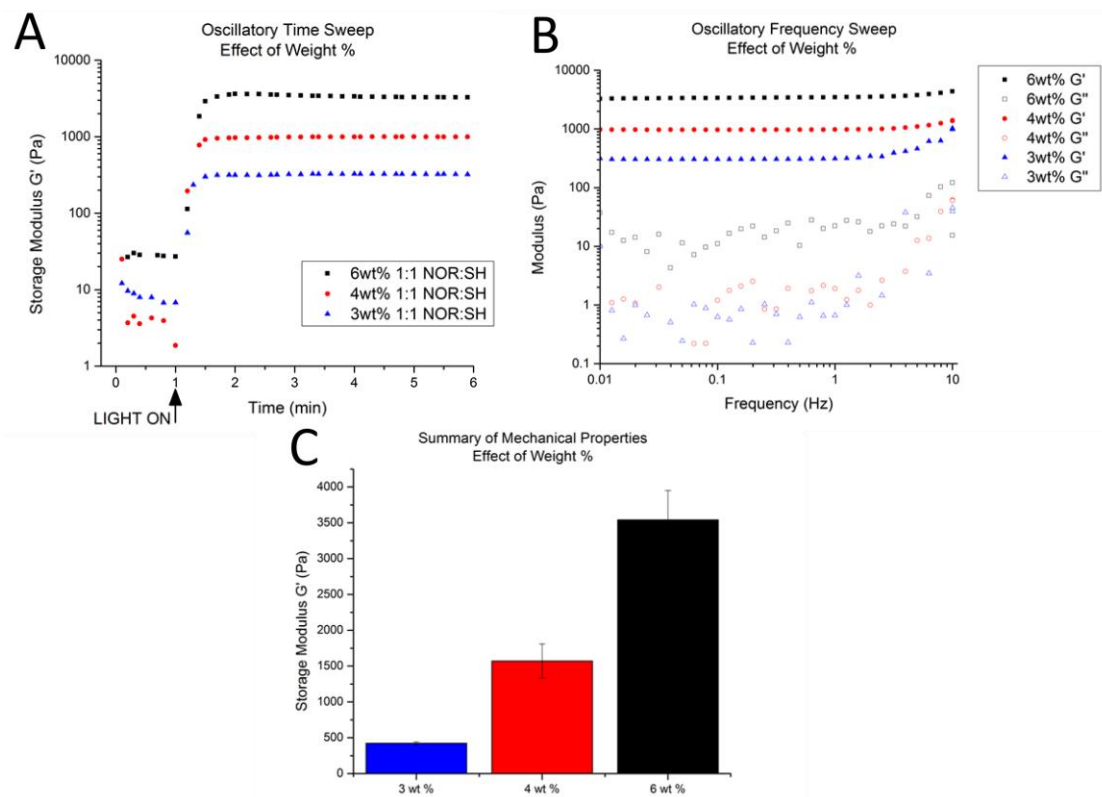


**Figure 4.6** Effect of weight percent on the mechanical properties of RLPXN-PEGSH hydrogels. Oscillatory rheometry was used to investigate the gelation (**A**) and frequency dependence (**B**) of the hydrogels. A summary of the average storage moduli for the different weight percent gels is also presented (**C**). The oscillatory time sweep was conducted using 1% strain at 1 Hz and the frequency sweep was conducted between 0.01-10 Hz at 1% strain. The simple mean of at least three samples for a given concentration was used for the summary; the error represents the standard deviation.

Spatiotemporal control over cross-linking was the major motivation behind the development of the RLPXN-PEGSH hydrogels. The effect that light had on the cross-linking of the hydrogels was investigated using oscillatory rheology. One experiment, depicted in **Figure 4.7A**, exposed the precursor solutions for only brief periods and at low irradiation intensity. The open symbols represent when the UV light was turned

on while the closed symbols represent when the UV light was turned off. As indicated by the figure, the cross-linking reaction and corresponding increase in the storage modulus (black symbols) only occurred when the precursor solution was exposed to light. When the light was switched off, the photoinitiation reaction did not occur and the step polymerization ceased. An important implication of this experiment is that control over the gelation and subsequent mechanical properties of RLPXN-PEGSH hydrogels can be achieved by altering its exposure to light. A single precursor composition may be used to create photocross-linked hydrogels with a range of different mechanical properties. Additionally, it was demonstrated that the irradiation intensity could modulate cross-linking rate. At lower intensities, the photoinitiation proceeded more slowly and as depicted in **Figure 4.7B** the gelation correspondingly occurred more slowly. The mechanical testing of the RLPXN-PEGSH hydrogels demonstrates a high degree of control over the final properties of these materials. The cross-linking/gelation of these hydrogels is clearly light-dependent and at the discretion of the operator.

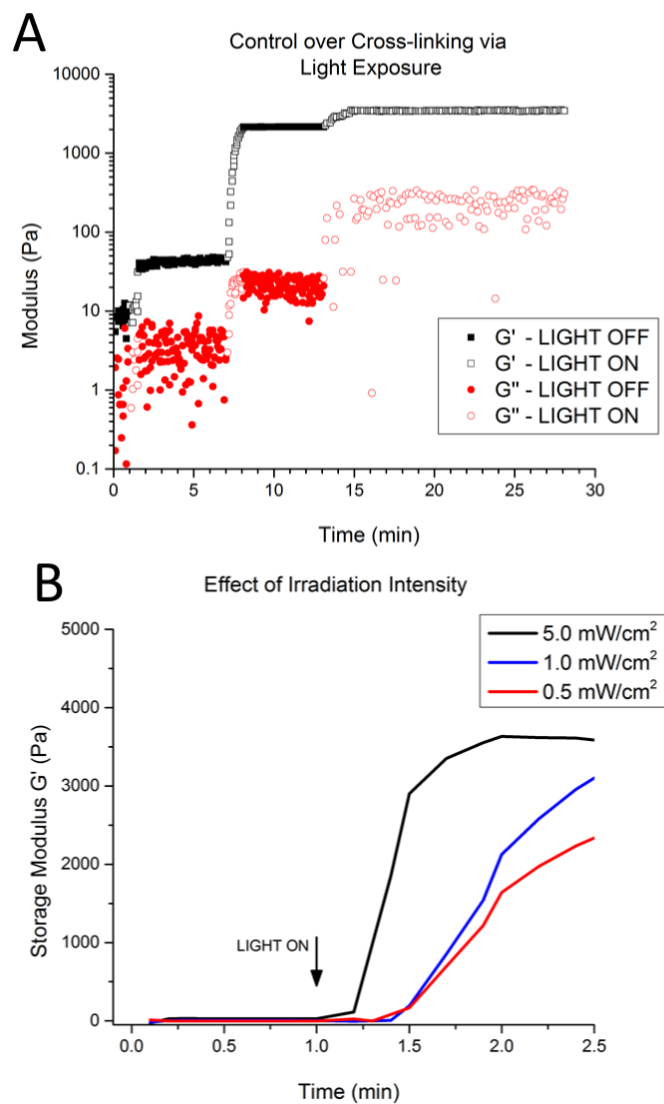


**Figure 4.7** The effect of irradiation on RLPXN/PEGSH solutions is demonstrated via oscillatory rheology. **(A)** At the beginning of the experiment (solid symbols) the RLPX-PEGSH solution was a viscous liquid, but when irradiated to an intensity of 1 mW/cm<sup>2</sup> for 30 seconds the solution began to cross-link (open symbols) as indicated by the increase in modulus. Switching off the light stopped the reaction which is reflected by the first plateau. The gelation was restarted for 60 seconds with irradiation set to 1 mW/cm<sup>2</sup> before being switched off again. The result was another increase in modulus followed by a plateau. The gels were then cross-linked to completion. **(B)** The effect of irradiation intensity on gelation is depicted. Higher irradiation intensity led to faster gelation rates of the RLPXN-PEGSH hydrogel (6wt%).

#### 4.3.4 Photoencapsulation of hMSCs

The photoencapsulation and culture of human mesenchymal stem cells was used to demonstrate the cytocompatibility of the RLPXN-PEGSH hydrogels (6wt% 1:1 ratio of norbornene to thiol). The hMSCs were cultured within the gels for a period of 28 days and their viability was determined via Live/Dead<sup>TM</sup> staining and confocal microscopy. The encapsulation process was fairly straightforward: RLPXN and PEG precursors were dissolved in PBS buffer containing LAP initiator and then mixed into cell media containing the hMSCs. Small aliquots were deposited on to glass plates and cross-linked using a UV lamp ( $\sim 6 \text{ mW/cm}^2$ , 30 seconds). The entire encapsulation procedure was performed within a biosafety cabinet to prevent contamination. The hydrogels were then immersed in cell media and analyzed at day 0, day 14 and day 28 for cell viability. **Figure 4.8** depicts composite images containing the ‘live’ channel, the ‘dead’ channel and the transmitted channel. Each image represents the maximum intensity projection of z-stacks a few 100  $\mu\text{m}$  in depth. Panels **A** and **B** represent 5x and 10x magnification of day 0 acquisitions; panels **C** and **D** represent day 14 and panels **E** and **F** represent day 28. The viability of the hMSCs was analyzed directly following encapsulation for a day 0 time point. Immediately, it was clear that the hMSCs survived the photocross-linking reaction and that there were few, if any, dead cells. In fact, cell viability remained excellent throughout the entire experimental time period. There did not appear to be a loss in viability or even a change in the number of the encapsulated hMSCs. To date, the culture of hMSCs to 28 days is the longest reported period of encapsulated cell culture within RLP hydrogels. By the final time point, the gels had started to lose their elasticity possibly due to the degradation of the hydrogels by the cells. In the transmitted channel, the hydrogels appeared ‘rougher’ and texturized in a way that was unlike earlier time points.

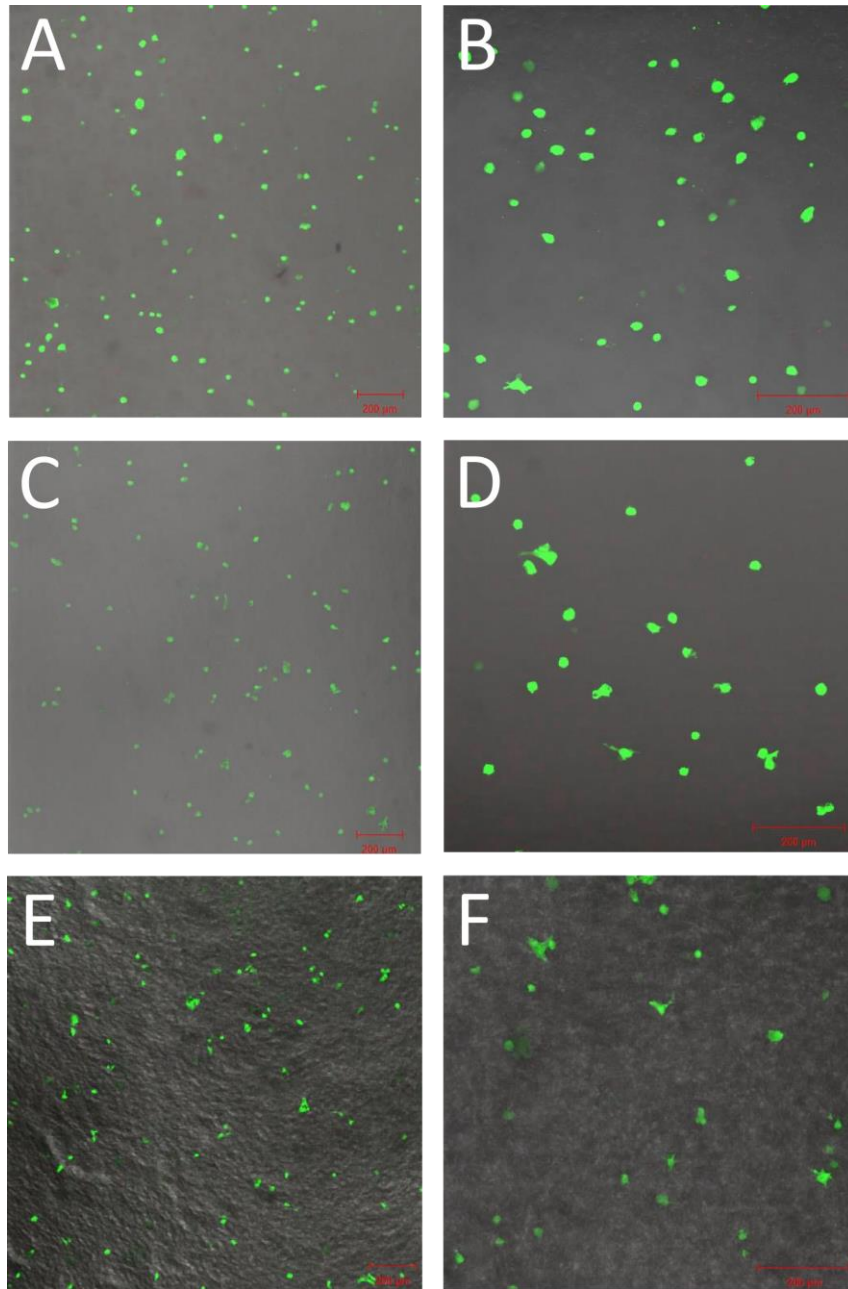


**Figure 4.8** Representative images of composite (‘live’, ‘dead’, and transmitted channels) z-stack maximum intensity projections at day 0, 5x (**A**) and 10x (**B**) magnification; at day 14, 5x (**C**), 10x (**D**) magnification; and at day 28, 5x (**E**), 10x (**F**) magnification. Z-stacks range from 100 to 300  $\mu\text{m}$  in depth. (Scale bar represents 200  $\mu\text{m}$ ).

As noted earlier, the RLPX protein did not include any biological domains conferring degradability or cell binding properties. This is reflected by the lack of interaction between the cells and the matrix. A few hMSCs extended processes into the matrix, but the majority remained rounded. Other RLP-PEG hydrogels that incorporated both degradation and cell adhesion domains, such as those described in **Chapter 2** and **Chapter 3**, were clearly interacting with encapsulated cells. Within those hydrogels, the cells spread and formed spindle-like morphologies. The promising viability, however, of the RLPXN-PEGSH hydrogels warrants further investigation especially with bioactive RLPs.

#### **4.4 Conclusions**

Recombinant resilin-like polypeptides were expressed, purified and conjugated with photoreactive molecules in order to photocross-link the protein into a hybrid hydrogel containing a PEG macromer. Lysine residues included in the polypeptide were functionalized with norbornene acid using HATU coupling and the degree of functionality could be assessed using  $^1\text{H}$  NMR. The resulting RLPXN was then cross-linked using the photoinitiator, LAP, and thiol terminated PEG to create elastic hybrid hydrogels. The mechanical properties of these thiol-ene step polymerized hydrogels were investigated via oscillatory rheology. The cytocompatibility of the materials was demonstrated through the viable encapsulation and 3D culture of hMSCs. The RLPXN-PEGSH hybrid hydrogels demonstrate that click chemistries may be simply and effectively applied to materials composed of biosynthetic protein polymers.

## Chapter 5

### CONCLUSIONS AND FUTURE DIRECTIONS

#### 5.1 Conclusions and Significance

Over the past few decades, the design of materials for tissue engineering and regenerative medicine has started to reflect the biological complexity of tissue development. It has become clear that new materials must incorporate a wide range of biological cues and signals in order to spur regenerative processes. The extracellular-matrix has proven to be an important source of these signals and mimicry of the ECM has led to scaffolds with enhanced cell-material interaction. Many tissue engineering materials incorporate bioactive moieties for cell adhesion, enzymatic cleavage and growth factor sequestration. Both naturally-derived and synthetic polymers serve as valuable precursors for hydrogel scaffolds due to their relative biocompatibility and hydrophilicity. However, more recently, biosynthetic protein polymers have emerged as an alternative macromolecular precursor for the development of tissue engineering materials. Recombinant protein polymers are valuable due to the precise control and high fidelity over the sequence afforded by Nature's highly evolved mechanism for protein synthesis.

Within the field of protein polymers, elastomeric proteins have stood out as useful archetypes for the design of elastic, mechanically tough materials. These proteins are naturally repetitive, highly disordered polypeptide chains that have rubber-like properties when cross-linked into networks. Furthermore, the ability to genetically engineer bioactivity directly into the polypeptide has made these

macromolecules valuable precursors for tissue engineering applications. Sequences derived from the protein elastomer, resilin, have been applied in the development of a number of biomaterials. Previous work by our laboratory has demonstrated that a resilin sequence derived from a *Drosophila melanogaster* gene has led to recombinant proteins with excellent rubber elasticity and cytocompatibility. As cross-linked hydrogels, these resilin-like polypeptides exhibited the same elastomeric behavior of natural resilin.

This dissertation describes work that builds upon our previous studies by introducing resilin-PEG hybrid hydrogels. These hybrid materials combine the advantages of biosynthetic proteins with the chemical flexibility of synthetic polymers. Resilin-PEG networks may be cross-linked using Michael-type addition or thiol-ene photoinitiated step polymerization. Both cross-linking chemistries lead to elastic hydrogel networks with outstanding cytocompatibility. **Chapter 2** described the genetic engineering, expression and purification of high molecular weight RLPs based upon the RLP12 gene. The RLP12 protein was the first recombinant resilin-like polypeptide to be constructed for tissue engineering applications and was the Kiick laboratory's first foray into the development of elastomeric materials. Recursive ligation of the RLP12 gene was used to construct the high molecular weight RLPs which were then expressed using Studier autoinduction methods. The purification of the RLPs was optimized through the introduction of a heating step that selectively precipitated contaminating bacterial proteins. Purified high molecular weight RLPs (RLP24, RLP36, and RLP48) were reduced and desalted to create precursors with the ability to cross-link with vinyl sulfone terminated PEG macromers. These reactions created elastic hydrogels whose gelation and mechanical properties could be assessed

through oscillatory rheology. Unfortunately, the high molecular weight RLPs were not found to enhance the elasticity of the RLP-PEG hydrogels. The culprit was likely the negligible change in cross-linking density between the different molecular weight RLPs. Nevertheless, RLP-PEG hydrogels were found to successfully encapsulate and culture human aortic adventitial fibroblasts in three dimensional matrices. More importantly, these cells were found to form spindle-like structures within the gels. This initial work demonstrated the success of a hybrid material approach. The reaction between vinyl sulfone moieties and free thiol on the polypeptide was only feasible through the inclusion of a synthetic PEG macromer. Additionally, the hybrid gels facilitated cell-matrix interaction in a way not previously identified in other RLP hydrogels. The only spreading behavior prior to the RLP-PEG hydrogels experiments occurred in two dimensional cultures on RLP12 films. By enabling these cell-matrix interactions in 3D, the hybrid hydrogels more closely mimic the native microenvironment of tissue.

In **Chapter 3**, a more thorough analysis of the mechanical and biological properties of RLP-PEG hydrogels was reported. Oscillatory rheology revealed that the elasticity of RLP24-PEG hydrogels could be modulated by altering the cross-linking ratio of vinyl sulfone to cysteine thiol and tensile testing provided crucial measurements that confirmed the resilience of these materials. Additionally, the engineered degradation domains of the RLP24 protein were found to be specifically cleaved by matrix metalloproteinase enzymes. The RLP24-PEG hydrogels were found to be similarly degradable by MMP. These studies supported previous reports that these matrices were interactive with cells and that they could be remodeled by cell-directed degradation. The encapsulation and 3D culture of hMSCs demonstrated that

RLP24-PEG hydrogels were compatible with stem cells. The hMSCs were viable within the hybrid hydrogels and even demonstrated proliferation. Finally, the hybrid materials demonstrated interesting liquid-liquid partitioning behavior which created a heterogeneous gel microstructure. If the experiments in **Chapter 2** introduced the idea of RLP-PEG hydrogels as potential tissue engineering scaffolds, then the experiments in **Chapter 3** confirmed this potential through the demonstration of mechanical resilience, degradability and stem cell cytocompatibility.

In **Chapter 4**, photoinitiated cross-linking, widely applied in synthetic hydrogels, was utilized with recombinant RLP and PEG to form hybrid materials. The RLPX protein was functionalized through lysine residues with photoreactive norbornene acid using HATU coupling. The degree of functionalization was controllable and could be assessed using  $^1\text{H}$  NMR. The resulting RLPXN was then photocross-linked with thiol-terminated PEG in the presence of light and a photoinitiator. Elastic hydrogels were created through this thiol-ene step polymerization. Furthermore, these hydrogels were found to encapsulate and culture viable hMSCs for up to four weeks. The application of click chemistry to recombinant protein polymers was a significant departure from the normal design of protein hydrogels. However, the work presented in **Chapter 4** illustrated the feasibility of this approach. It demonstrated that the spatiotemporal control over cross-linking that is characteristic of many synthetic polymer hydrogels can be equally applied to systems which utilized biosynthetic proteins.

Hybrid hydrogels are an interesting class of materials that ought to have greater application in tissue engineering. Here, two systems were developed and characterized, but there is significant potential for the design of other hybrid systems.

There is a wealth of biology present in the extracellular matrix and a vast array of chemistry at the disposal of the polymer scientist. Combining the advantages of the two different macromolecules into single material is a valuable paradigm for tissue engineers that could be greatly expanded upon as more is discovered about the process of tissue regeneration.

## **5.2 Future Directions**

Throughout the project, potential future investigations did not go unnoticed and several prospective areas of research are discussed in the following sections.

### **5.2.1 Expression and Purification of RLPs**

One of the major limitations concerning the development of RLPs for biomaterials is the current production level of the polypeptides. The RLPX protein and the RLP12 family of proteins are produced at much lower rates than other RLPs.<sup>[144, 166, 168, 174]</sup> For example, a successful RLPX expression and purification provides only 135 mg of protein for several days' worth of labor (4.5L at 30 mg/L of expression culture). To obtain RLP in quantity, a significant amount of time is devoted to the expression and purification of the protein. This is time and labor that may be better spent on experiments and investigations with higher value in the biomaterial field. Furthermore, as the number of batches increase the potential for variability increases as well. This is a huge concern with respect to troubleshooting experiments and reproducing results.

To address these issues, large scale production of the RLPs is absolutely necessary. Other laboratories that have utilized fermentation technology to produce RLPs have had great success increasing productivity and creating large quantities of

the protein. Also, the use of a two-step induction protocol where IPTG ‘primes’ an expression culture has proven to be highly effective at increasing expression yields.<sup>[144, 166, 168, 174]</sup> Replicating those procedures with RLPX or the RLP12 family of proteins might provide a facile approach to improving protein production.

Additionally, small changes in the purification process may eliminate bottlenecks that hamper the production of RLP. For example, sonication is currently used as the primary method of membrane disruption, but it is a low through-put method as only a few hundred milliliters of cell lysate can be processed at a time. A high pressure homogenizer could substitute for sonication as the processing capacity is much greater. Bench-top homogenizers can disrupt 1-5 liters of cell lysate per hour. Alternatively, it may be worth revisiting the buffer composition and switching to a denaturing protocol. As an intrinsically disordered protein, there is little concern related to maintaining the secondary or tertiary structure of RLP. Therefore, chemical lysis of cell pellets in denaturants such as urea or guanidine hydrochloride may offer a simple alternative to recovery of protein. Large quantity of cell pellet may be easily lysed in 6 or 8 M urea overnight and quickly purified the following day.

Future application of the RLPs will rely on the development of methods that ensure the production of non-immunogenic protein. Bacterial expression is easy to perform, but there is a risk of contamination by immunostimulatory components of bacteria such as lipopolysaccharide. Another consideration is the presence of N-formylmethionine in bacterial proteins which may be used by eukaryotes to distinguish from non-self.<sup>[307, 308]</sup> Incomplete or non-removal of this chemical group from the N-terminus of RLP may have an immunogenic effect, especially when the RLP is cross-linked at high concentrations into hydrogels. Expression of RLP in

alternative host organisms may be a longer-term project, but it would have benefits for the application of the material.

### **5.2.2 *In vivo* Experiments and Immunogenicity**

The RLP-PEG hydrogels performed uniquely well with respect to cell encapsulation and 3D culture. While this *in vitro* testing is important in determining compatibility with biological systems, it is no substitute for the complexity of natural tissue. The subcutaneous injection or implantation of RLP-PEG hydrogels will provide valuable data as to whether the materials elicit a response from the host immune system. A degree of immune stimulation may be desirable for wound healing, but prolonged inflammation would be damaging and unproductive.

To quickly assess the immunogenicity of the RLP-PEG hydrogels, macrophages (or some similar immune cell) may be seeded onto the gels and measured for stimulatory cytokine secretion. In a previous study, hydrogels had been seeded with J774 mouse peritoneal macrophages and the secretion of TNF- $\alpha$  was measured via ELISA.<sup>[309]</sup> These experiments are not as informative as *in vivo* testing, but they are less complicated to perform. Furthermore, a wider range of RLP-PEG compositions may be analyzed using this method as compared to *in vivo* experiments, which are limited by the number of host animals available for experimentation.

### **5.2.3 Expanded Analysis of RLPXN-PEGSH Hydrogels**

The successful functionalization and cross-linking of norbornene conjugated RLPX only provided a glimpse into the potential of this material. The RLPXN-PEGSH hydrogels were elastic networks with demonstrable cytocompatibility, but unfortunately displayed limited cell-matrix interaction. Furthermore, the functionality

of RLPXN was easily varied, but only a single construct was explored for cross-linking into hydrogels. Further analysis of this system would be highly beneficial and could take the following forms.

#### **5.2.3.1 ECM Biomimicry**

The RLP12 family of polypeptides did not have an effective ‘control’ for different experiments concerning the biological domains. These domains conferring heparin binding, cell adhesion and MMP degradation were *fixed* in the gene sequence and could not be easily removed nor their ratio easily changed. However, the RLPX system is perfectly suited for the differential analysis of biomimetic domains. The flexibility of the RLPX gene sequence allows for the incorporation of multiple and different biomimetic sequences. Effectively, one could create a library of RLPs (*see Figure 5.1*) with different biological domains that could be mixed in various concentrations to create hydrogels with tailored properties.<sup>[101]</sup>

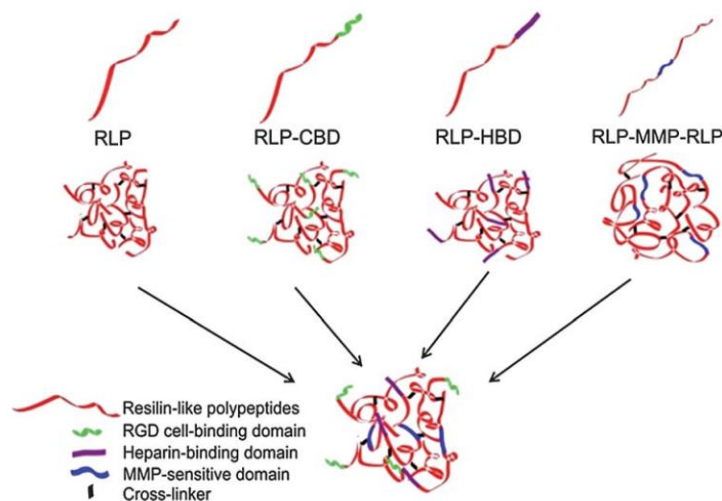


**Figure 5.1** Schematic illustrating the different RLPs in the RLPX system and the ability to tailor the biological properties of the final hydrogels. Reproduced from Ref. [101] with permission from The Royal Society of Chemistry.

Work performed by Li *et al.* has already demonstrated that the incorporation of RGD or MMP cleavage sequences contributes to the cell-matrix interactivity of the small molecule cross-linked RLPX hydrogels.<sup>[101]</sup> Therefore, there is good reason to create photocross-linkable RLPs containing these same biological domains to try to impart the hybrid hydrogels with enhanced bioactivity. Additionally, other biomimetic domains, such as growth factor mimetic domains, may further enhance the potential of these materials as tissue engineering scaffolds.

### 5.2.3.2 Photopatterning

Admittedly, one important and yet largely unexplored aspect of the RLPXN-PEGSH hydrogels was the ability to spatial control the photocross-linking. A few attempts, not presented here, were made to try to pattern the hydrogels with

fluorescent molecules. Unfortunately, these investigations were not optimized and remained inconclusive. Further research ought to take advantage of collimated UV irradiation and thinner RLP-PEG hydrogels. In addition, two-photon laser scanning lithographic techniques have been applied in the patterning of PEG hydrogels and may also have application in this photocross-linkable system.<sup>[280]</sup>

### **5.2.3.3 Solubility and Liquid-Liquid Partitioning Analysis**

The RLPXN polypeptide functionalized with 9.1 norbornenes displayed greater solubility than the more highly functional conjugate. Based upon this observation, most of the experiments in **Chapter 4** were carried out using that version of RLPXN. It would be interesting to revisit the other versions of RLPXN to more thoroughly investigate their solubility as well as their ability to cross-link with PEG.

The solubility of RLPXN appeared to have larger implications for material than initially anticipated. Similar to the RLP24-PEG hydrogels, the RLPXN-PEGSH hydrogels also partitioned, but it was dependent on the buffer composition. The hydrogels presented in **Chapter 4** were created in PBS buffer; a condition that was chosen for the cell encapsulation experiments. However, if the protein was dissolved in pure water containing only a small concentration of NaOH the protein did not partition when PEG was introduced. The result was that the mechanical properties of these hydrogels were far higher than what was reported in the PBS buffered gels. **Figure 5.2** depicts the results of oscillatory rheology on RLPXN-PEGSH hydrogels that did partition. This was an interesting discovery because it meant that the buffer composition of the solution was affecting the solubility characteristics of the protein and its ability to cross-link. A more thorough analysis of this behavior may lead to a

better understanding of RLP-PEG partitioning as well as the effect it has on the material properties of these hydrogels.

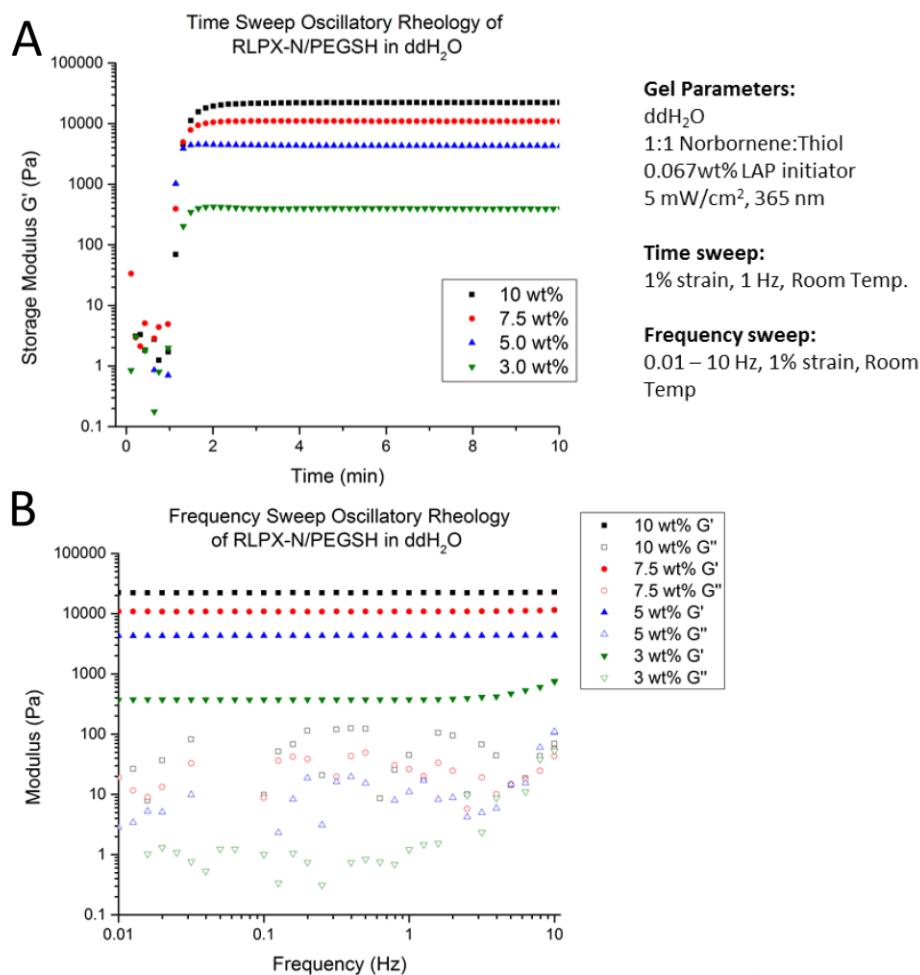


**Figure 5.2** Depicts the oscillatory time sweep (**A**) and frequency sweep (**B**) of RLPXN-PEGSH hydrogels dissolved in pure water. The mechanical properties of these hydrogels were greater than for RLPXN-PEGSH gels dissolved in PBS.

#### **5.2.4 Liquid-Liquid Partitioning of RLP-PEG Hydrogels**

The partitioning behavior of the RLP-PEG mixtures and formation of heterogeneous structures within the hydrogels is another important area of future research. This dissertation provided clear evidence that partitioning occurred and that it became ‘fixed’ as the hydrogels cross-linked. However, the exact mechanisms for this behavior and whether it may be controlled are still under investigation. Control over the size and distribution of the microstructure within the phase-separated gels may be another important tool in the design of tissue engineering scaffolds, especially if it influences cell behavior.

To determine whether the heterogeneity facilitates cell spreading and migration, cell encapsulation needs to be performed on RLP hydrogels that do not partition. Recently, these experiments have been attempted, but not with any success. RLP24 was cross-linked with a vinyl sulfone PEG macromer with a 2 kDa molecular weight and in a separate experiment RLP24 was cross-linked with the amine-reactive small molecule, THP. Partitioning did not occur in either of the systems as the molecular weights of cross-linkers were too small. Unfortunately, the RLP24-PEG(2kDa) mixtures did not form elastic hydrogels during cell encapsulation and the THP cross-linked gels resulted in a high rate of cell death. Further optimization will be necessary to perform these studies.

#### **5.2.5 A New RLP Family**

Due to the ‘fixed’ nature of the RLP12 family of proteins, it would be difficult to use the polypeptides in future tissue engineering applications. However, there were important lessons learned from the RLP24-PEG gels that might be applied to a revised RLP gene. For instance, the Michael-type addition chemistry proved to be highly

effective at cross-linking RLP into hydrogels under relatively mild conditions. Cysteines are easy functional group to incorporate into biosynthetic polypeptides and may be utilized in a number of cytocompatible cross-linking chemistries. In addition to the Michael-type addition reaction, thiol containing RLPs may be cross-linked in a thiol-ene photopolymerization with RLPXN. A revised design of the RLPX gene might swap the lysine residues for cysteines and reduce the overall functionality from 15 reactive groups to five. One criticism of the RLPX protein is that the number and distribution of the lysine residues creates hydrogels that are cross-linked too tightly. Fewer cross-linking groups would potentially create a more ‘open’ hydrogel with a larger mesh size that facilitates diffusion and cell-material interaction.

A new cysteine bearing RLP with facile gene editing would be one way to apply the findings of this dissertation to a new generation of elastomeric biomaterials. As with other technologies, successive iterations of biomaterial design will bring to light new ideas and new discoveries that further enrich the field and expand its utility. The mechanically resilient, cytocompatible RLP-PEG hybrid hydrogels described in this work represent one step towards the development of materials that regenerate damaged tissue and restore health to dysfunctional organs.

## REFERENCES

- [1] Lanza, R., Langer, R., Vacanti, J. P., *Principles of Tissue Engineering*. Elsevier Science: 2013.
- [2] Meyer, U., Meyer, T., Handschel, J., Wiesmann, H. P., *Fundamentals of Tissue Engineering and Regenerative Medicine*. Springer: 2009.
- [3] Langer, R., Vacanti, J., Tissue engineering. *Science* **1993**, 260, (5110), 920.
- [4] Vacanti, J. P., Langer, R., Tissue engineering: the design and fabrication of living replacement devices for surgical reconstruction and transplantation. *The Lancet* **1999**, 354, S32.
- [5] Bianco, P., Robey, P. G., Stem cells in tissue engineering. *Nature* **2001**, 414, (6859), 118.
- [6] Lutolf, M. P., Hubbell, J. A., Synthetic biomaterials as instructive extracellular microenvironments for morphogenesis in tissue engineering. *Nature Biotechnology* **2005**, 23, (1), 47.
- [7] Hubbell, J. A., Materials as morphogenetic guides in tissue engineering. *Current Opinion in Biotechnology* **2003**, 14, (5), 551.
- [8] Zhu, J., Bioactive modification of poly(ethylene glycol) hydrogels for tissue engineering. *Biomaterials* **2010**, 31, (17), 4639.
- [9] Lee, K. Y., Mooney, D. J., Hydrogels for tissue engineering. *Chemical Reviews* **2001**, 101, (7), 1869.
- [10] Drury, J. L., Mooney, D. J., Hydrogels for tissue engineering: scaffold design variables and applications. *Biomaterials* **2003**, 24, (24), 4337.
- [11] Hoffman, A. S., Hydrogels for biomedical applications. *Advanced Drug Delivery Reviews* **2002**, 54, (1), 3.
- [12] Nguyen, K. T., West, J. L., Photopolymerizable hydrogels for tissue engineering applications. *Biomaterials* **2002**, 23, (22), 4307.
- [13] Lee, C. H., Singla, A., Lee, Y., Biomedical applications of collagen. *International Journal of Pharmaceutics* **2001**, 221, (1–2), 1.
- [14] Ma, P. X., Biomimetic materials for tissue engineering. *Advanced Drug Delivery Reviews* **2008**, 60, (2), 184.
- [15] Kharkar, P. M., Kiick, K. L., Kloxin, A. M., Designing degradable hydrogels for orthogonal control of cell microenvironments. *Chemical Society Reviews* **2013**, 42, (17), 7335.
- [16] Alcantar, N. A., Aydil, E. S., Israelachvili, J. N., Polyethylene glycol-coated biocompatible surfaces. *Journal of biomedical materials research* **2000**, 51, (3), 343.

- [17] Peppas, N. A., Keys, K. B., Torres-Lugo, M., Lowman, A. M., Poly (ethylene glycol)-containing hydrogels in drug delivery. *Journal of controlled release* **1999**, 62, (1), 81.
- [18] Fairbanks, B. D., Schwartz, M. P., Halevi, A. E., Nuttelman, C. R., Bowman, C. N., Anseth, K. S., A versatile synthetic extracellular matrix mimic via thiol-norbornene photopolymerization. *Advanced Materials* **2009**, 21, (48), 5005.
- [19] Alge, D. L., Azagarsamy, M. A., Donohue, D. F., Anseth, K. S., Synthetically tractable click hydrogels for three-dimensional cell culture formed using tetrazine-norbornene chemistry. *Biomacromolecules* **2013**, 14, (4), 949.
- [20] Hahn, M. S., Miller, J. S., West, J. L., Three-dimensional biochemical and biomechanical patterning of hydrogels for guiding cell behavior. *Advanced Materials* **2006**, 18, (20), 2679.
- [21] Polizzotti, B. D., Fairbanks, B. D., Anseth, K. S., Three-dimensional biochemical patterning of click-based composite hydrogels via thiol-ene photopolymerization. *Biomacromolecules* **2008**, 9, (4), 1084.
- [22] Malkoch, M., Vestberg, R., Gupta, N., Mespouille, L., Dubois, P., Mason, A. F., Hedrick, J. L., Liao, Q., Frank, C. W., Kingsbury, K., Hawker, C. J., Synthesis of well-defined hydrogel networks using Click chemistry. *Chemical Communications* **2006**, (26), 2774.
- [23] DeLong, S. A., Moon, J. J., West, J. L., Covalently immobilized gradients of bFGF on hydrogel scaffolds for directed cell migration. *Biomaterials* **2005**, 26, (16), 3227.
- [24] Lee, S.-H., Moon, J. J., West, J. L., Three-dimensional micropatterning of bioactive hydrogels via two-photon laser scanning photolithography for guided 3D cell migration. *Biomaterials* **2008**, 29, (20), 2962.
- [25] Ehrbar, M., Rizzi, S. C., Schoenmakers, R. G., San Miguel, B., Hubbell, J. A., Weber, F. E., Lutolf, M. P., Biomolecular hydrogels formed and degraded via site-specific enzymatic reactions. *Biomacromolecules* **2007**, 8, (10), 3000.
- [26] Yamaguchi, N., Zhang, L., Chae, B.-S., Palla, C. S., Furst, E. M., Kiick, K. L., Growth factor mediated assembly of cell receptor-responsive hydrogels. *Journal of the American Chemical Society* **2007**, 129, (11), 3040.
- [27] Yamaguchi, N., Kiick, K. L., Polysaccharide–poly(ethylene glycol) star copolymer as a scaffold for the production of bioactive hydrogels. *Biomacromolecules* **2005**, 6, (4), 1921.
- [28] Peppas, N. A., Sefton, M. V., *Molecular and Cellular Foundations of Biomaterials*. Elsevier: 2004.
- [29] Fisher, J. P., Mikos, A. G., Bronzino, J. D., Peterson, D. R., *Tissue Engineering: Principles and Practices*. Taylor & Francis: 2012.
- [30] Jensen, L. T., Høst, N. B., Collagen: scaffold for repair or execution. *Cardiovascular research* **1997**, 33, (3), 535.
- [31] Huttenlocher, A., Sandborg, R. R., Horwitz, A. F., Adhesion in cell migration. *Current opinion in cell biology* **1995**, 7, (5), 697.

- [32] Humphires, M. J., Newham, P., The structure of cell-adhesion molecules. *Trends in cell biology* **1998**, 8, (2), 78.
- [33] Chatzizacharias, N. A., Kouraklis, G. P., Theocharis, S. E., The role of focal adhesion kinase in early development. *Histology and histopathology* **2010**, 25, (8), 1039.
- [34] Ruoslahti, E., Pierschbacher, M. D., New perspectives in cell adhesion: RGD and integrins. *Science* **1987**, 238, (4826), 491.
- [35] Haas, T. A., Plow, E. F., Integrin-ligand interactions: a year in review. *Current opinion in cell biology* **1994**, 6, (5), 656.
- [36] Chen, W., Chang, C.-e., Gilson, M. K., Concepts in receptor optimization: targeting the RGD peptide. *Journal of the American Chemical Society* **2006**, 128, (14), 4675.
- [37] Woods, A., Couchman, J. R., Integrin modulation by lateral association. *Journal of Biological Chemistry* **2000**, 275, (32), 24233.
- [38] Woods, A., Oh, E.-S., Couchman, J. R., Syndecan proteoglycans and cell adhesion. *Matrix biology* **1998**, 17, (7), 477.
- [39] Katz, B.-Z., Zamir, E., Bershadsky, A., Kam, Z., Yamada, K. M., Geiger, B., Physical state of the extracellular matrix regulates the structure and molecular composition of cell-matrix adhesions. *Molecular Biology of the Cell* **2000**, 11, (3), 1047.
- [40] Webb, D. J., Parsons, J. T., Horwitz, A. F., Adhesion assembly, disassembly and turnover in migrating cells—over and over and over again. *Nature cell biology* **2002**, 4, (4), E97.
- [41] Du, J., Chen, X., Liang, X., Zhang, G., Xu, J., He, L., Zhan, Q., Feng, X.-Q., Chien, S., Yang, C., Integrin activation and internalization on soft ECM as a mechanism of induction of stem cell differentiation by ECM elasticity. *Proceedings of the National Academy of Sciences* **2011**, 108, (23), 9466.
- [42] Hersel, U., Dahmen, C., Kessler, H., RGD modified polymers: biomaterials for stimulated cell adhesion and beyond. *Biomaterials* **2003**, 24, (24), 4385.
- [43] Cai, L., Dinh, C. B., Heilshorn, S. C., One-pot synthesis of elastin-like polypeptide hydrogels with grafted VEGF-mimetic peptides. *Biomaterials science* **2014**, 2, (5), 757.
- [44] He, X., Ma, J., Jabbari, E., Effect of grafting RGD and BMP-2 protein-derived peptides to a hydrogel substrate on osteogenic differentiation of marrow stromal cells. *Langmuir* **2008**, 24, (21), 12508.
- [45] Ruoslahti, E., RGD and recognition sequences for integrins. *Annual Review of Cell and Developmental Biology* **1996**, 12, (1), 697.
- [46] Massia, S. P., Hubbell, J. A., An RGD spacing of 440 nm is sufficient for integrin alpha V beta 3-mediated fibroblast spreading and 140 nm for focal contact and stress fiber formation. *The Journal of Cell Biology* **1991**, 114, (5), 1089.
- [47] Metters, A. T., Anseth, K. S., Bowman, C. N., Fundamental studies of a novel, biodegradable PEG-b-PLA hydrogel. *Polymer* **2000**, 41, (11), 3993.

- [48] Bryant, S. J., Anseth, K. S., Controlling the spatial distribution of ECM components in degradable PEG hydrogels for tissue engineering cartilage. *Journal of Biomedical Materials Research Part A* **2003**, 64A, (1), 70.
- [49] Kharkar, P. M., Kloxin, A. M., Kiick, K. L., Dually degradable click hydrogels for controlled degradation and protein release. *Journal of Materials Chemistry B* **2014**, 2, (34), 5511.
- [50] Baldwin, A. D., Kiick, K. L., Reversible maleimide-thiol adducts yield glutathione-sensitive poly(ethylene glycol)-heparin hydrogels. *Polymer Chemistry* **2013**, 4, (1), 133.
- [51] Mann, B. K., Gobin, A. S., Tsai, A. T., Schmedlen, R. H., West, J. L., Smooth muscle cell growth in photopolymerized hydrogels with cell adhesive and proteolytically degradable domains: synthetic ECM analogs for tissue engineering. *Biomaterials* **2001**, 22, (22), 3045.
- [52] Lutolf, M. P., Lauer-Fields, J. L., Schmoekel, H. G., Metters, A. T., Weber, F. E., Fields, G. B., Hubbell, J. A., Synthetic matrix metalloproteinase-sensitive hydrogels for the conduction of tissue regeneration: Engineering cell-invasion characteristics. *Proceedings of the National Academy of Sciences of the United States of America* **2003**, 100, (9), 5413.
- [53] Aimetti, A. A., Machen, A. J., Anseth, K. S., Poly(ethylene glycol) hydrogels formed by thiol-ene photopolymerization for enzyme-responsive protein delivery. *Biomaterials* **2009**, 30, (30), 6048.
- [54] Ellis, V., Murphy, G., Cellular strategies for proteolytic targeting during migration and invasion. *FEBS letters* **2001**, 506, (1), 1.
- [55] Murphy, G., Gavrilovic, J., Proteolysis and cell migration: creating a path? *Current opinion in cell biology* **1999**, 11, (5), 614.
- [56] Birkedal-Hansen, H., Proteolytic remodeling of extracellular matrix. *Current opinion in cell biology* **1995**, 7, (5), 728.
- [57] Gobin, A. S., West, J. L., Cell migration through defined, synthetic extracellular matrix analogues. *Faseb Journal* **2002**, 16, (3), 751.
- [58] Patterson, J., Hubbell, J. A., Enhanced proteolytic degradation of molecularly engineered PEG hydrogels in response to MMP-1 and MMP-2. *Biomaterials* **2010**, 31, (30), 7836.
- [59] Lee, K., Silva, E. A., Mooney, D. J., Growth factor delivery-based tissue engineering: general approaches and a review of recent developments. *Journal of The Royal Society Interface* **2011**, 8, (55), 153.
- [60] Babensee, J. E., McIntire, L. V., Mikos, A. G., Growth factor delivery for tissue engineering. *Pharmaceutical research* **2000**, 17, (5), 497.
- [61] Silva, A. K. A., Richard, C., Bessodes, M., Scherman, D., Merten, O.-W., Growth factor delivery approaches in hydrogels. *Biomacromolecules* **2008**, 10, (1), 9.
- [62] Whitelock, J. M., Murdoch, A. D., Iozzo, R. V., Underwood, P. A., The degradation of human endothelial cell-derived perlecan and release of bound basic fibroblast growth factor by stromelysin, collagenase, plasmin, and heparanases. *Journal of Biological Chemistry* **1996**, 271, (17), 10079.

- [63] Tayalia, P., Mooney, D. J., Controlled growth factor delivery for tissue engineering. *Advanced Materials* **2009**, 21, (32-33), 3269.
- [64] Ferrara, N., Gerber, H.-P., LeCouter, J., The biology of VEGF and its receptors. *Nature medicine* **2003**, 9, (6), 669.
- [65] Lee, S., Jilani, S. M., Nikolova, G. V., Carpizo, D., Iruela-Arispe, M. L., Processing of VEGF-A by matrix metalloproteinases regulates bioavailability and vascular patterning in tumors. *The Journal of Cell Biology* **2005**, 169, (4), 681.
- [66] Ehrbar, M., Metters, A., Zammaretti, P., Hubbell, J. A., Zisch, A. H., Endothelial cell proliferation and progenitor maturation by fibrin-bound VEGF variants with differential susceptibilities to local cellular activity. *Journal of controlled release* **2005**, 101, (1), 93.
- [67] Ehrbar, M., Djonov, V. G., Schnell, C., Tschanz, S. A., Martiny-Baron, G., Schenk, U., Wood, J., Burri, P. H., Hubbell, J. A., Zisch, A. H., Cell-demanded liberation of VEGF121 from fibrin implants induces local and controlled blood vessel growth. *Circulation research* **2004**, 94, (8), 1124.
- [68] Zisch, A. H., Lutolf, M. P., Ehrbar, M., Raeber, G. P., Rizzi, S. C., Davies, N., Schmökel, H., Bezuidenhout, D., Djonov, V., Zilla, P., Cell-demanded release of VEGF from synthetic, biointeractive cell ingrowth matrices for vascularized tissue growth. *The FASEB journal* **2003**, 17, (15), 2260.
- [69] Fischbach, C., Mooney, D. J., Polymers for pro-and anti-angiogenic therapy. *Biomaterials* **2007**, 28, (12), 2069.
- [70] Ozawa, C. R., Banfi, A., Glazer, N. L., Thurston, G., Springer, M. L., Kraft, P. E., McDonald, D. M., Blau, H. M., Microenvironmental VEGF concentration, not total dose, determines a threshold between normal and aberrant angiogenesis. *Journal of Clinical Investigation* **2004**, 113, (4), 516.
- [71] Leslie-Barbick, J. E., Saik, J. E., Gould, D. J., Dickinson, M. E., West, J. L., The promotion of microvasculature formation in poly(ethylene glycol) diacrylate hydrogels by an immobilized VEGF-mimetic peptide. *Biomaterials* **2011**, 32, (25), 5782.
- [72] Nie, T., Baldwin, A., Yamaguchi, N., Kiick, K. L., Production of heparin-functionalized hydrogels for the development of responsive and controlled growth factor delivery systems. *Journal of controlled release* **2007**, 122, (3), 287.
- [73] Nie, T., Akins Jr, R. E., Kiick, K. L., Production of heparin-containing hydrogels for modulating cell responses. *Acta biomaterialia* **2009**, 5, (3), 865.
- [74] Kiick, K. L., Biosynthetic methods for the production of advanced protein-based materials. *Polymer Reviews* **2007**, 47, (1), 1.
- [75] McGrath, K., Kaplan, D., *Protein-based materials*. Springer: 1997.
- [76] Rodríguez-Cabello, J. C., Martín, L., Alonso, M., Arias, F. J., Testera, A. M., "Recombinamers" as advanced materials for the post-oil age. *Polymer* **2009**, 50, (22), 5159.
- [77] Haider, M., Megeed, Z., Ghandehari, H., Genetically engineered polymers: status and prospects for controlled release. *Journal of controlled release* **2004**, 95, (1), 1.

- [78] Werkmeister, J. A., Ramshaw, J. A. M., Recombinant protein scaffolds for tissue engineering. *Biomedical Materials* **2012**, 7, (1).
- [79] Gomes, S., Leonor, I. B., Mano, J. F., Reis, R. L., Kaplan, D. L., Natural and genetically engineered proteins for tissue engineering. *Progress in Polymer Science* **2012**, 37, (1), 1.
- [80] Yang, C. L., Hillas, P. J., Baez, J. A., Nokelainen, M., Balan, J., Tang, J., Spiro, R., Polarek, J. W., The application of recombinant human collagen in tissue engineering. *Biodrugs* **2004**, 18, (2), 103.
- [81] Ito, H., Steplewski, A., Alabyeva, T., Fertala, A., Testing the utility of rationally engineered recombinant collagen-like proteins for applications in tissue engineering. *Journal of Biomedical Materials Research Part A* **2006**, 76A, (3), 551.
- [82] Willard, J. J., Drexler, J. W., Das, A., Roy, S., Shilo, S., Shoseyov, O., Powell, H. M., Plant-derived human collagen scaffolds for skin tissue engineering. *Tissue Engineering Part A* **2013**, 19, (13-14), 1507.
- [83] Shoseyov, O., Posen, Y., Grynspan, F., Human recombinant type I collagen produced in plants. *Tissue Engineering Part A* **2013**, 19, (13-14), 1527.
- [84] Gomes, S. C., Leonor, I. B., Mano, J. F., Reis, R. L., Kaplan, D. L., Antimicrobial functionalized genetically engineered spider silk. *Biomaterials* **2011**, 32, (18), 4255.
- [85] Kundu, B., Kurland, N. E., Bano, S., Patra, C., Engel, F. B., Yadavalli, V. K., Kundu, S. C., Silk proteins for biomedical applications: Bioengineering perspectives. *Progress in Polymer Science* **2014**, 39, (2), 251.
- [86] Spiess, K., Lammel, A., Scheibel, T., Recombinant spider silk proteins for applications in biomaterials. *Macromolecular Bioscience* **2010**, 10, (9), 998.
- [87] van Eldijk, M., McGann, C., Kiick, K., van Hest, J. M., Elastomeric polypeptides. In *Peptide-Based Materials*, Deming, T., Ed. Springer Berlin Heidelberg: 2012; Vol. 310, pp 71.
- [88] Annabi, N., Mithieux, S. M., Camci-Unal, G., Dokmeci, M. R., Weiss, A. S., Khademhosseini, A., Elastomeric recombinant protein-based biomaterials. *Biochemical Engineering Journal* **2013**, 77, (0), 110.
- [89] Nettles, D. L., Chilkoti, A., Setton, L. A., Applications of elastin-like polypeptides in tissue engineering. *Advanced Drug Delivery Reviews* **2010**, 62, (15), 1479.
- [90] Lim, D. W., Nettles, D. L., Setton, L. A., Chilkoti, A., Rapid cross-linking of elastin-like polypeptides with (hydroxymethyl)phosphines in aqueous solution. *Biomacromolecules* **2007**, 8, (5), 1463.
- [91] Rico, P., González-García, C., Petrie, T. A., García, A. J., Salmerón-Sánchez, M., Molecular assembly and biological activity of a recombinant fragment of fibronectin (FNIII<sub>7-10</sub>) on poly (ethyl acrylate). *Colloids and Surfaces B: Biointerfaces* **2010**, 78, (2), 310.
- [92] Cutler, S. M., Garcia, A. J., Engineering cell adhesive surfaces that direct integrin  $\alpha(5)\beta(1)$  binding using a recombinant fragment of fibronectin. *Biomaterials* **2003**, 24, (10), 1759.

- [93] Straley, K. S., Heilshorn, S. C., Independent tuning of multiple biomaterial properties using protein engineering. *Soft Matter* **2009**, 5, (1), 114.
- [94] Heilshorn, S. C., DiZio, K. A., Welsh, E. R., Tirrell, D. A., Endothelial cell adhesion to the fibronectin CS5 domain in artificial extracellular matrix proteins. *Biomaterials* **2003**, 24, (23), 4245.
- [95] Halstenberg, S., Panitch, A., Rizzi, S., Hall, H., Hubbell, J. A., Biologically engineered protein-graft-poly(ethylene glycol) hydrogels: A cell adhesive and plasm in-degradable biosynthetic material for tissue repair. *Biomacromolecules* **2002**, 3, (4), 710.
- [96] Rizzi, S. C., Ehrbar, M., Halstenberg, S., Raeber, G. P., Schmoekel, H. G., Hagenmuller, H., Muller, R., Weber, F. E., Hubbell, J. A., Recombinant protein-co-PEG networks as cell-adhesive and proteolytically degradable hydrogel matrixes. Part II: Biofunctional characteristics. *Biomacromolecules* **2006**, 7, (11), 3019.
- [97] Rizzi, S. C., Hubbell, J. A., Recombinant protein-co-PEG networks as cell-adhesive and proteolytically degradable hydrogel matrixes. Part 1: Development and physicochemical characteristics. *Biomacromolecules* **2005**, 6, (3), 1226.
- [98] Sengupta, D., Heilshorn, S. C., Protein-engineered biomaterials: highly tunable tissue engineering scaffolds. *Tissue Engineering Part B-Reviews* **2010**, 16, (3), 285.
- [99] Renner, J. N., Cherry, K. M., Su, R. S. C., Liu, J. C., Characterization of resilin-based materials for tissue engineering applications. *Biomacromolecules* **2012**, 13, (11), 3678.
- [100] Charati, M. B., Ifkovits, J. L., Burdick, J. A., Linhardt, J. G., Kiick, K. L., Hydrophilic elastomeric biomaterials based on resilin-like polypeptides. *Soft Matter* **2009**, 5, (18), 3412.
- [101] Li, L., Tong, Z., Jia, X., Kiick, K. L., Resilin-like polypeptide hydrogels engineered for versatile biological function. *Soft Matter* **2013**, 9, (3), 665.
- [102] Whittaker, J., Balu, R., Choudhury, N. R., Dutta, N. K., Biomimetic protein-based elastomeric hydrogels for biomedical applications. *Polymer International* **2014**, 63, (9), 1545.
- [103] Tatham, A. S., Shewry, P. R., Elastomeric proteins: biological roles, structures and mechanisms. *Trends in Biochemical Sciences* **2000**, 25, (11), 567.
- [104] McGann, C. L., Levenson, E. A., Kiick, K. L., Resilin-based hybrid hydrogels for cardiovascular tissue engineering. *Macromolecular Chemistry and Physics* **2013**, 214, (2), 203.
- [105] Li, L., Teller, S., Clifton, R. J., Jia, X., Kiick, K. L., Tunable mechanical stability and deformation response of a resilin-based elastomer. *Biomacromolecules* **2011**, 12, (6), 2302.
- [106] Li, L., Kiick, K. L., Resilin-based materials for biomedical applications. *ACS Macro Letters* **2013**, 2, (8), 635.
- [107] Li, L., Charati, M. B., Kiick, K. L., Elastomeric polypeptide-based biomaterials. *Polymer Chemistry* **2010**, 1, (8), 1160.
- [108] Moore, J., Overhill, R., *An Introduction to the Invertebrates*. Cambridge University Press: 2001.

- [109] Weis-Fogh, T., A Rubber-Like Protein in Insect Cuticle. *Journal of Experimental Biology* **1960**, 37, (4), 889.
- [110] Andersen, S. O., Weis-Fogh, T., Resilin. A rubberlike protein in arthropod cuticle. In *Advances in Insect Physiology*, J.W.L. Beament, J.E.T. and Wigglesworth, V.B., Eds. Academic Press: 1964; Vol. Volume 2, pp 1.
- [111] Andersen, S. O., Structure and function of resilin. In *Elastomeric proteins: structures, biomechanical properties, and biological roles.*, Shewry, P.R., Tatham, A.S., Bailey, A.J., Ed. Cambridge University Press: Cambridge, 2003; pp 259.
- [112] Bailey, K., Weis-Fogh, T., Amino acid composition of a new rubber-like protein, resilin. *Biochimica et biophysica acta* **1961**, 48, (3), 452.
- [113] Bennet-Clark, H. C., The first description of resilin. *Journal of Experimental Biology* **2007**, 210, (22), 3879.
- [114] Jensen, M., Weis-Fogh, T., Biology and physics of locust flight. V. Strength and elasticity of locust cuticle. *Philosophical Transactions of the Royal Society of London. Series B, Biological Sciences* **1962**, 245, (721), 137.
- [115] Bennet-Clark, H. C., Negative pressures produced in pharyngeal pump of blood-sucking bug, *Rhodnius prolixus*. *Journal of Experimental Biology* **1963**, 40, (1), 223.
- [116] Rice, M. J., Function of resilin in tsetse fly feeding mechanism. *Nature* **1970**, 228, (5278), 1337.
- [117] Edwards, H. A., Occurrence of resilin in elastic structures in the food-pump of reduviid bugs. *Journal of Experimental Biology* **1983**, 105, (1), 407.
- [118] Hermann, H. R., Willer, D. E., Resilin distribution and its function in the venom apparatus of the honey bee, *Apis mellifera* L. (Hymenoptera : Apidae). *International Journal of Insect Morphology and Embryology* **1986**, 15, (1–2), 107.
- [119] Young, D., Bennet-Clark, H. C., The role of the tymbal in cicada sound production. *The Journal of experimental biology* **1995**, 198, (4), 1001.
- [120] Skals, N., Surlykke, A., Sound production by abdominal tymbal organs in two moth species: the green silver-line and the scarce silver-line (Noctuoidea: Nolidae: Chloephorinae). *The Journal of experimental biology* **1999**, 202, (21), 2937.
- [121] Scott, J., Resilin in the sound-organs of Pyralidae and Cicadidae (Lepidoptera; Homoptera). *Pan pacific Entomol* **1970**.
- [122] Nahirney, P. C., Forbes, J. G., Morris, H. D., Chock, S. C., Wang, K., What the buzz was all about: superfast song muscles rattle the tymbals of male periodical cicadas. *The FASEB journal* **2006**, 20, (12), 2017.
- [123] Fonseca, P. J., Bennet-Clark, H. C., Asymmetry of tymbal action and structure in a cicada: A possible role in the production of complex songs. *Journal of Experimental Biology* **1998**, 201, (5), 717.
- [124] Bennet-Clark, H. C., Tymbal mechanics and the control of song frequency in the cicada *Cyclochila australasiae*. *Journal of Experimental Biology* **1997**, 200, (11), 1681.
- [125] Gorb, S. N., Serial elastic elements in the damselfly wing: Mobile vein joints contain resilin. *Naturwissenschaften* **1999**, 86, (11), 552.

- [126] Haas, F., Gorb, S., Blickhan, R., The function of resilin in beetle wings. *Proceedings of the Royal Society B-Biological Sciences* **2000**, 267, (1451), 1375.
- [127] Haas, F., Gorb, S., Wootton, R. J., Elastic joints in dermapteran hind wings: materials and wing folding. *Arthropod Structure & Development* **2000**, 29, (2), 137.
- [128] Bennet-Clark, H. C., Lucey, E. C. A., Jump of flea - a study of energetics and a model of mechanism. *Journal of Experimental Biology* **1967**, 47, (1), 59.
- [129] Burrows, M., How fleas jump. *Journal of Experimental Biology* **2009**, 212, (18), 2881.
- [130] Rothschild, M., Schlein, Y., Parker, K., Neville, C., Sternberg, S., Flying leap of flea. *Scientific American* **1973**, 229, (5), 92.
- [131] Rothschild, M., Schlein, Y., Sternberg, S., Parker, K., Jump of oriental rat flea *Xenopsylla cheopis* (Roths.). *Nature* **1972**, 239, (5366), 45.
- [132] Rothschild, M., Schlein, J., Jumping mechanism of *Xenopsylla cheopis* 1. Exoskeletal structures and musculature. *Philosophical Transactions of the Royal Society of London Series B-Biological Sciences* **1975**, 271, (914), 457.
- [133] Rothschild, M., Schlein, J., Parker, K., Neville, C., Sternberg, S., Jumping mechanism of *Xenopsylla cheopis* 3. Execution of jump and activity. *Philosophical Transactions of the Royal Society of London Series B-Biological Sciences* **1975**, 271, (914), 499.
- [134] Alexander, R. M., Bennet-Clark, H. C., Storage of elastic strain energy in muscle and other tissues. *Nature* **1977**, 265, (5590), 114.
- [135] Bennet-Clark, H. C., The energetics of the jump of the locust *Schistocerca gregaria*. *Journal of Experimental Biology* **1975**, 63, (1), 53.
- [136] Gorb, S. N., The jumping mechanism of cicada *Cercopis vulnerata* (Auchenorrhyncha, Cercopidae): skeleton–muscle organisation, frictional surfaces, and inverse-kinematic model of leg movements. *Arthropod Structure & Development* **2004**, 33, (3), 201.
- [137] Varman, A. R., Resilin in the abdominal cuticle of workers of the honey-ants, *Myrmecocystus mexicanus*. *Journal of the Georgia Entomological Society* **1981**, 16, (1), 11.
- [138] Balu, R., Whittaker, J., Dutta, N. K., Elvin, C. M., Choudhury, N. R., Multi-responsive biomaterials and nanobioconjugates from resilin-like protein polymers. *Journal of Materials Chemistry B* **2014**, 2, (36), 5936.
- [139] Lombardi, E. C., Kaplan, D. L., Preliminary characterization of resilin isolated from the cockroach, *Periplaneta americana*. In *Biomolecular Materials*, Viney, C., Case, S.T. and Waite, J.H., Eds. Materials Research Soc: Pittsburgh, 1993; Vol. 292, pp 3.
- [140] Ardell, D. H., Andersen, S. O., Tentative identification of a resilin gene in *Drosophila melanogaster*. *Insect Biochemistry and Molecular Biology* **2001**, 31, (10), 965.
- [141] Rebers, J. E., Riddiford, L. M., Structure and expression of a *Manduca sexta* larval cuticle gene homologous to *Drosophila* cuticle genes. *Journal of Molecular Biology* **1988**, 203, (2), 411.

- [142] Elvin, C. M., Carr, A. G., Huson, M. G., Maxwell, J. M., Pearson, R. D., Vuocolo, T., Liyou, N. E., Wong, D. C. C., Merritt, D. J., Dixon, N. E., Synthesis and properties of crosslinked recombinant pro-resilin. *Nature* **2005**, 437, (7051), 999.
- [143] Lyons, R. E., Wong, D. C. C., Kim, M., Lekieffre, N., Huson, M. G., Vuocolo, T., Merritt, D. J., Nairn, K. M., Dudek, D. M., Colgrave, M. L., Elvin, C. M., Molecular and functional characterisation of resilin across three insect orders. *Insect Biochemistry and Molecular Biology* **2011**, 41, (11), 881.
- [144] Lyons, R. E., Nairn, K. M., Huson, M. G., Kim, M., Dumsday, G., Elvin, C. M., Comparisons of recombinant resilin-like proteins: repetitive domains are sufficient to confer resilin-like properties. *Biomacromolecules* **2009**, 10, (11), 3009.
- [145] Andersen, S. O., Characterization of a new type of cross-linkage in resilin, a rubber-like protein. *Biochimica et biophysica acta* **1963**, 69, 249.
- [146] Andersen, S. O., 2 Fluorescent amino acids which function as cross-linkages between peptide chains in resilin, a rubber-like protein. *Acta Chemica Scandinavica* **1963**, 17, (3), 869.
- [147] Andersen, S. O., Kristens.B, Incorporation of phenylalanine and tyrosine in cross-linkages of a protein, resilin. *Acta Physiologica Scandinavica* **1963**, 59, 15.
- [148] Andersen, S. O., The cross-links in resilin identified as dityrosine and trityrosine. *Biochimica et Biophysica Acta (BBA)-General Subjects* **1964**, 93, (1), 213.
- [149] Gross, A. J., Sizer, I. W., The oxidation of tyramine, tyrosine, and related compounds by peroxidase. *Journal of Biological Chemistry* **1959**, 234, (6), 1611.
- [150] Aeschbach, R., Amadoò, R., Neukom, H., Formation of dityrosine cross-links in proteins by oxidation of tyrosine residues. *Biochimica et Biophysica Acta (BBA)-Protein Structure* **1976**, 439, (2), 292.
- [151] Kristensen, B. I., Time course of incorporation of tyrosine into rubber-like cuticle of locusts. *Journal of Insect Physiology* **1968**, 14, (8), 1135.
- [152] Kristensen, B. I., Incorporation of tyrosine into the rubber-like cuticle of locusts studied by autoradiography. *Journal of Insect Physiology* **1966**, 12, (2), 173.
- [153] Neville, A., Growth and deposition of resilin and chitin in locust rubber-like cuticle. *Journal of Insect Physiology* **1963**, 9, (3), 265.
- [154] Coles, G., Studies on resilin biosynthesis. *Journal of Insect Physiology* **1966**, 12, (6), 679.
- [155] Gosline, J., Lillie, M., Carrington, E., Guerette, P., Ortlepp, C., Savage, K., Elastic proteins: biological roles and mechanical properties. *Philosophical Transactions of the Royal Society of London. Series B: Biological Sciences* **2002**, 357, (1418), 121.
- [156] Elliott, G., Huxley, A., Weis-Fogh, T., On the structure of resilin. *Journal of Molecular Biology* **1965**, 13, (3), 791.
- [157] Weis-Fogh, T., Thermodynamic properties of resilin, a rubber-like protein. *Journal of Molecular Biology* **1961**, 3, (5), 520.
- [158] Rubinstein, M., Colby, R. H., *Polymer Physics*. OUP Oxford: 2003.
- [159] Andersen, S. O., Studies on resilin-like gene products in insects. *Insect Biochemistry and Molecular Biology* **2010**, 40, (7), 541.

- [160] Kim, W., Conticello, V. P., Protein engineering methods for investigation of structure-function relationships in protein-based elastomeric materials. *Polymer Reviews* **2007**, 47, (1), 93.
- [161] Tatham, A. S., Shewry, P. R., Comparative structures and properties of elastic proteins. *Philosophical Transactions of the Royal Society of London Series B-Biological Sciences* **2002**, 357, (1418), 229.
- [162] Urry, D. W., Hugel, T., Seitz, M., Gaub, H. E., Sheiba, L., Dea, J., Xu, J., Parker, T., Elastin: a representative ideal protein elastomer. *Philosophical Transactions of the Royal Society of London Series B-Biological Sciences* **2002**, 357, (1418), 169.
- [163] Nairn, K. M., Lyons, R. E., Mulder, R. J., Mudie, S. T., Cookson, D. J., Lesieur, E., Kim, M., Lau, D., Scholes, F. H., Elvin, C. M., A synthetic resilin is largely unstructured. *Biophysical Journal* **2008**, 95, (7), 3358.
- [164] Tamburro, A. M., Panariello, S., Santopietro, V., Bracalello, A., Bochicchio, B., Pepe, A., Molecular and supramolecular structural studies on significant repetitive sequences of resilin. *Chembiochem* **2010**, 11, (1), 83.
- [165] Rauscher, S., Baud, S., Miao, M., Keeley, F. W., Pomes, R., Proline and glycine control protein self-organization into elastomeric or amyloid fibrils. *Structure* **2006**, 14, (11), 1667.
- [166] Kim, M., Elvin, C., Brownlee, A., Lyons, R., High yield expression of recombinant pro-resilin: Lactose-induced fermentation in *E. coli* and facile purification. *Protein Expression and Purification* **2007**, 52, (1), 230.
- [167] Studier, F. W., Protein production by auto-induction in high-density shaking cultures. *Protein Expression and Purification* **2005**, 41, (1), 207.
- [168] Lyons, R. E., Lesieur, E., Kim, M., Wong, D. C., Huson, M. G., Nairn, K. M., Brownlee, A. G., Pearson, R. D., Elvin, C. M., Design and facile production of recombinant resilin-like polypeptides: gene construction and a rapid protein purification method. *Protein Engineering Design and Selection* **2007**, 20, (1), 25.
- [169] Qin, G., Lapidot, S., Numata, K., Hu, X., Meirovitch, S., Dekel, M., Podoler, I., Shoseyov, O., Kaplan, D. L., Expression, cross-linking, and characterization of recombinant chitin binding resilin. *Biomacromolecules* **2009**, 10, (12), 3227.
- [170] Qin, G., Rivkin, A., Lapidot, S., Hu, X., Preis, I., Arinus, S. B., Dgany, O., Shoseyov, O., Kaplan, D. L., Recombinant exon-encoded resilins for elastomeric biomaterials. *Biomaterials* **2011**, 32, (35), 9231.
- [171] Qin, G., Hu, X., Cebe, P., Kaplan, D. L., Mechanism of resilin elasticity. *Nature Communications* **2012**, 3, 1003.
- [172] Gedde, U., *Polymer Physics*. Springer: 1995.
- [173] Dutta, N. K., Truong, M. Y., Mayavan, S., Choudhury, N. R., Elvin, C. M., Kim, M., Knott, R., Nairn, K. M., Hill, A. J., A genetically engineered protein responsive to multiple stimuli. *Angewandte Chemie-International Edition* **2011**, 50, (19), 4428.
- [174] Lyons, R. E., Elvin, C. M., Taylor, K., Lekieffre, N., Ramshaw, J. A. M., Purification of recombinant protein by cold-coacervation of fusion constructs

- incorporating resilin-inspired polypeptides. *Biotechnology and Bioengineering* **2012**, 109, (12), 2947.
- [175] Hassouneh, W., Christensen, T., Chilkoti, A., Elastin-Like Polypeptides as a Purification Tag for Recombinant Proteins. In *Current Protocols in Protein Science*, John Wiley & Sons, Inc.: 2001.
- [176] Dutta, N. K., Choudhury, N. R., Truong, M. Y., Kim, M., Elvin, C. M., Hill, A. J., Physical approaches for fabrication of organized nanostructure of resilin-mimetic elastic protein rec1-resilin. *Biomaterials* **2009**, 30, (28), 4868.
- [177] Truong, M. Y., Dutta, N. K., Choudhury, N. R., Kim, M., Elvin, C. M., Hill, A. J., Thierry, B., Vasilev, K., A pH-responsive interface derived from resilin-mimetic protein Rec1-resilin. *Biomaterials* **2010**, 31, (15), 4434.
- [178] Vashi, A. V., Ramshaw, J. A. M., Glattauer, V., Elvin, C. M., Lyons, R. E., Werkmeister, J. A., Controlled surface modification of tissue culture polystyrene for selective cell binding using resilin-inspired polypeptides. *Biofabrication* **2013**, 5, (3), 9.
- [179] Renner, J. N., Kim, Y., Cherry, K. M., Liu, J. C., Modular cloning and protein expression of long, repetitive resilin-based proteins. *Protein Expression and Purification* **2012**, 82, (1), 90.
- [180] Lv, S., Dudek, D. M., Cao, Y., Balamurali, M. M., Gosline, J., Li, H. B., Designed biomaterials to mimic the mechanical properties of muscles. *Nature* **2010**, 465, (7294), 69.
- [181] Wang, H. Y., Cai, L., Paul, A., Enejder, A., Heilshorn, S. C., Hybrid elastin-like polypeptide-polyethylene glycol (ELP-PEG) hydrogels with improved transparency and independent control of matrix mechanics and cell ligand density. *Biomacromolecules* **2014**, 15, (9), 3421.
- [182] Alwan, A., *Global status report on noncommunicable diseases 2010*. World Health Organization: 2011.
- [183] Mendis, S., Puska, P., Norrving, B., *Global atlas on cardiovascular disease prevention and control*. World Health Organization: 2011.
- [184] Mathers, C. D., Loncar, D., Projections of global mortality and burden of disease from 2002 to 2030. *Plos Medicine* **2006**, 3, (11).
- [185] Sur, S., Sugimoto, J. T., Agrawal, D. K., Coronary artery bypass graft: why is the saphenous vein prone to intimal hyperplasia? *Canadian Journal of Physiology and Pharmacology* **2014**, 92, (7), 531.
- [186] Wang, Y., Hu, J., Jiao, J., Liu, Z., Zhou, Z., Zhao, C., Chang, L.-J., Chen, Y. E., Ma, P. X., Yang, B., Engineering vascular tissue with functional smooth muscle cells derived from human iPS cells and nanofibrous scaffolds. *Biomaterials* **2014**, 35, (32), 8960.
- [187] L'Heureux, N., Dusserre, N., Konig, G., Victor, B., Keire, P., Wight, T. N., Chronos, N. A. F., Kyles, A. E., Gregory, C. R., Hoyt, G., Robbins, R. C., McAllister, T. N., Human tissue-engineered blood vessels for adult arterial revascularization. *Nature medicine* **2006**, 12, (3), 361.

- [188] Samuel, R., Daheron, L., Liao, S., Vardam, T., Kamoun, W. S., Batista, A., Buecker, C., Schäfer, R., Han, X., Au, P., Scadden, D. T., Duda, D. G., Fukumura, D., Jain, R. K., Generation of functionally competent and durable engineered blood vessels from human induced pluripotent stem cells. *Proceedings of the National Academy of Sciences* **2013**, 110, (31), 12774.
- [189] Fernandez, C. E., Achneck, H. E., Reichert, W. M., Truskey, G. A., Biological and engineering design considerations for vascular tissue engineered blood vessels (TEBVs). *Current Opinion in Chemical Engineering* **2014**, 3, (0), 83.
- [190] Long, J. L., Tranquillo, R. T., Elastic fiber production in cardiovascular tissue-equivalents. *Matrix biology* **2003**, 22, (4), 339.
- [191] Mitchell, S. L., Niklason, L. E., Requirements for growing tissue-engineered vascular grafts. *Cardiovascular Pathology* **2003**, 12, (2), 59.
- [192] Patel, A., Fine, B., Sandig, M., Mequanint, K., Elastin biosynthesis: The missing link in tissue-engineered blood vessels. *Cardiovascular research* **2006**, 71, (1), 40.
- [193] Silver, F. H., Snowhill, P. B., Foran, D. J., Mechanical behavior of vessel wall: A comparative study of aorta, vena cava, and carotid artery. *Annals of Biomedical Engineering* **2003**, 31, (7), 793.
- [194] Maskarinec, S. A., Tirrell, D. A., Protein engineering approaches to biomaterials design. *Current Opinion in Biotechnology* **2005**, 16, (4), 422.
- [195] Romano, N. H., Sengupta, D., Chung, C., Heilshorn, S. C., Protein-engineered biomaterials: Nanoscale mimics of the extracellular matrix. *Biochimica Et Biophysica Acta-General Subjects* **2011**, 1810, (3), 339.
- [196] Daamen, W. F., Veerkamp, J. H., van Hest, J. C. M., van Kuppevelt, T. H., Elastin as a biomaterial for tissue engineering. *Biomaterials* **2007**, 28, (30), 4378.
- [197] Lim, D. W., Nettles, D. L., Setton, L. A., Chilkoti, A., In situ cross-linking of elastin-like polypeptide block copolymers for tissue repair. *Biomacromolecules* **2008**, 9, (1), 222.
- [198] McHale, M. K., Setton, L. A., Chilkoti, A., Synthesis and in vitro evaluation of enzymatically cross-linked elastin-like polypeptide gels for cartilaginous tissue repair. *Tissue Engineering* **2005**, 11, (11-12), 1768.
- [199] Nettles, D. L., Kitaoka, K., Hanson, N. A., Flahiff, C. M., Mata, B. A., Hsu, E. W., Chilkoti, A., Setton, L. A., In situ crosslinking elastin-like polypeptide gels for application to articular cartilage repair in a goat osteochondral defect model. *Tissue Engineering Part A* **2008**, 14, (7), 1133.
- [200] Weis-Fogh, T., Molecular interpretation of elasticity of resilin, a rubber-like protein. *Journal of Molecular Biology* **1961**, 3, (5), 648.
- [201] Mayavan, S., Dutta, N. K., Choudhury, N. R., Kim, M., Elvin, C. M., Hill, A. J., Self-organization, interfacial interaction and photophysical properties of gold nanoparticle complexes derived from resilin-mimetic fluorescent protein rec1-resilin. *Biomaterials* **2011**, 32, (11), 2786.
- [202] Truong, M. Y., Dutta, N. K., Choudhury, N. R., Kim, M., Elvin, C. M., Nairn, K. M., Hill, A. J., The effect of hydration on molecular chain mobility and the

- viscoelastic behavior of resilin-mimetic protein-based hydrogels. *Biomaterials* **2011**, 32, (33), 8462.
- [203] Cui, J., Lackey, M. A., Madkour, A. E., Saffer, E. M., Griffin, D. M., Bhatia, S. R., Crosby, A. J., Tew, G. N., Synthetically simple, highly resilient hydrogels. *Biomacromolecules* **2012**, 13, (3), 584.
- [204] Lutolf, M. P., Tirelli, N., Cerritelli, S., Cavalli, L., Hubbell, J. A., Systematic modulation of Michael-type reactivity of thiols through the use of charged amino acids. *Bioconjugate Chemistry* **2001**, 12, (6), 1051.
- [205] Chawla, K., Yu, T. B., Liao, S. W., Guan, Z. B., Biodegradable and Biocompatible Synthetic Saccharide-Peptide Hydrogels for Three-Dimensional Stem Cell Culture. *Biomacromolecules* **2011**, 12, (3), 560.
- [206] Dobner, S., Bezuidenhout, D., Govender, P., Zilla, P., Davies, N., A synthetic non-degradable polyethylene glycol hydrogel retards adverse post-infarct left ventricular remodeling. *Journal of Cardiac Failure* **2009**, 15, (7), 629.
- [207] Hiemstra, C., van der Aa, L. J., Zhong, Z. Y., Dijkstra, P. J., Feijen, J., Rapidly in situ-forming degradable hydrogels from dextran thiols through michael addition. *Biomacromolecules* **2007**, 8, (5), 1548.
- [208] Hiemstra, C., van der Aa, L. J., Zhong, Z. Y., Dijkstra, P. J., Feijen, J., Novel in situ forming, degradable dextran hydrogels by Michael addition chemistry: Synthesis, rheology, and degradation. *Macromolecules* **2007**, 40, (4), 1165.
- [209] Hiemstra, C., Zhong, Z. Y., van Steenberg, M. J., Hennink, W. E., Feijen, J., Release of model proteins and basic fibroblast growth factor from in situ forming degradable dextran hydrogels. *Journal of controlled release* **2007**, 122, (1), 71.
- [210] Jeong, K. J., Panitch, A., Interplay between Covalent and Physical Interactions within Environment Sensitive Hydrogels. *Biomacromolecules* **2009**, 10, (5), 1090.
- [211] Jin, R., Teixeira, L. S. M., Krouwels, A., Dijkstra, P. J., van Blitterswijk, C. A., Karperien, M., Feijen, J., Synthesis and characterization of hyaluronic acid-poly(ethylene glycol) hydrogels via Michael addition: An injectable biomaterial for cartilage repair. *Acta biomaterialia* **2010**, 6, (6), 1968.
- [212] Kraehenbuehl, T. P., Ferreira, L. S., Hayward, A. M., Nahrendorf, M., van der Vlies, A. J., Vasile, E., Weissleder, R., Langer, R., Hubbell, J. A., Human embryonic stem cell-derived microvascular grafts for cardiac tissue preservation after myocardial infarction. *Biomaterials* **2011**, 32, (4), 1102.
- [213] Liu, Y., Liu, B., Riesberg, J. J., Shen, W., In Situ Forming Physical Hydrogels for Three-dimensional Tissue Morphogenesis. *Macromolecular Bioscience* **2011**, 11, (10), 1325.
- [214] Lutolf, M. P., Raeber, G. P., Zisch, A. H., Tirelli, N., Hubbell, J. A., Cell-responsive synthetic hydrogels. *Advanced Materials* **2003**, 15, (11), 888.
- [215] Pratt, A. B., Weber, F. E., Schmoekel, H. G., Muller, R., Hubbell, J. A., Synthetic extracellular matrices for in situ tissue engineering. *Biotechnology and Bioengineering* **2004**, 86, (1), 27.

- [216] Raeber, G. P., Lutolf, M. P., Hubbell, J. A., Molecularly engineered PEG hydrogels: A novel model system for proteolytically mediated cell migration. *Biophysical Journal* **2005**, 89, (2), 1374.
- [217] Seliktar, D., Zisch, A. H., Lutolf, M. P., Wrana, J. L., Hubbell, J. A., MMP-2 sensitive, VEGF-bearing bioactive hydrogels for promotion of vascular healing. *Journal of Biomedical Materials Research Part A* **2004**, 68A, (4), 704.
- [218] Zustiak, S. P., Leach, J. B., Hydrolytically Degradable Poly(Ethylene Glycol) Hydrogel Scaffolds with Tunable Degradation and Mechanical Properties. *Biomacromolecules* **2010**, 11, (5), 1348.
- [219] Ehrbar, M., Sala, A., Lienemann, P., Ranga, A., Mosiewicz, K., Bittermann, A., Rizzi, S. C., Weber, F. E., Lutolf, M. P., Elucidating the Role of Matrix Stiffness in 3D Cell Migration and Remodeling. *Biophysical Journal* **2011**, 100, (2), 284.
- [220] Ehrbar, M., Rizzi, S. C., Hlushchuk, R., Djonov, V., Zisch, A. H., Hubbell, J. A., Weber, F. E., Lutolf, M. P., Enzymatic formation of modular cell-instructive fibrin analogs for tissue engineering. *Biomaterials* **2007**, 28, (26), 3856.
- [221] Bott, K., Upton, Z., Schrobback, K., Ehrbar, M., Hubbell, J. A., Lutolf, M. P., Rizzi, S. C., The effect of matrix characteristics on fibroblast proliferation in 3D gels. *Biomaterials* **2010**, 31, (32), 8454.
- [222] Anderson, S. B., Lin, C.-C., Kuntzler, D. V., Anseth, K. S., The performance of human mesenchymal stem cells encapsulated in cell-degradable polymer-peptide hydrogels. *Biomaterials* **2011**, 32, (14), 3564.
- [223] Lindeman, J. H. N., Ashcroft, B. A., Beenakker, J. W. M., van Es, M., Koekkoek, N. B. R., Prins, F. A., Tielemans, J. F., Abdul-Hussien, H., Bank, R. A., Oosterkamp, T. H., Distinct defects in collagen microarchitecture underlie vessel-wall failure in advanced abdominal aneurysms and aneurysms in Marfan syndrome. *Proceedings of the National Academy of Sciences of the United States of America* **2010**, 107, (2), 862.
- [224] Sambrook, J., Russell, D. W., *Molecular Cloning: A Laboratory Manual*. Cold Spring Harbor Laboratory Press: 2001.
- [225] Bulaj, G., Kortemme, T., Goldenberg, D. P., Ionization-reactivity relationships for cysteine thiols in polypeptides. *Biochemistry* **1998**, 37, (25), 8965.
- [226] Interchim Quantitation of sulfhydryls DTNB, Ellman's reagent. <http://www.interchim.fr/ft/0/01566H.pdf> (July 2012),
- [227] Nagase, H., Fields, G. B., Human matrix metalloproteinase specificity studies using collagen sequence-based synthetic peptides. *Biopolymers* **1996**, 40, (4), 399.
- [228] Zhang, L., Furst, E. M., Kiick, K. L., Manipulation of hydrogel assembly and growth factor delivery via the use of peptide-polysaccharide interactions. *Journal of controlled release* **2006**, 114, (2), 130.
- [229] Chow, D. C., Dreher, M. R., Trabbic-Carlson, K., Chilkoti, A., Ultra-high expression of a thermally responsive recombinant fusion protein in E-coli. *Biotechnology Progress* **2006**, 22, (3), 638.

- [230] Metters, A., Hubbell, J., Network formation and degradation behavior of hydrogels formed by Michael-type addition reactions. *Biomacromolecules* **2005**, 6, (1), 290.
- [231] Wagenseil, J. E., Mecham, R. P., Vascular Extracellular Matrix and Arterial Mechanics. *Physiological Reviews* **2009**, 89, (3), 957.
- [232] Benton, J. A., Fairbanks, B. D., Anseth, K. S., Characterization of valvular interstitial cell function in three dimensional matrix metalloproteinase degradable PEG hydrogels. *Biomaterials* **2009**, 30, (34), 6593.
- [233] Gonen-Wadmany, M., Oss-Ronen, L., Seliktar, D., Protein-polymer conjugates for forming photopolymerizable biomimetic hydrogels for tissue engineering. *Biomaterials* **2007**, 28, (26), 3876.
- [234] Shapira-Schweitzer, K., Seliktar, D., Matrix stiffness affects spontaneous contraction of cardiomyocytes cultured within a PEGylated fibrinogen biomaterial. *Acta biomaterialia* **2007**, 3, (1), 33.
- [235] Gonen-Wadmany, M., Goldshmid, R., Seliktar, D., Biological and mechanical implications of PEGylating proteins into hydrogel biomaterials. *Biomaterials* **2011**, 32, (26), 6025.
- [236] Peyton, S. R., Kim, P. D., Ghajar, C. M., Seliktar, D., Putnam, A. J., The effects of matrix stiffness and RhoA on the phenotypic plasticity of smooth muscle cells in a 3-D biosynthetic hydrogel system. *Biomaterials* **2008**, 29, (17), 2597.
- [237] Robinson, K. G., Nie, T., Baldwin, A. D., Yang, E. C., Kiick, K. L., Akins, R. E., Differential effects of substrate modulus on human vascular endothelial, smooth muscle, and fibroblastic cells. *Journal of Biomedical Materials Research Part A* **2012**, 100A, (5), 1356.
- [238] Li, L., Kiick, K., Transient dynamic mechanical analysis of resilin-based elastomeric hydrogels. *Frontiers in Chemistry* **2014**, 2.
- [239] Gustafson, J. A., Price, R. A., Frandsen, J., Henak, C. R., Cappello, J., Ghandehari, H., Synthesis and characterization of a matrix-metalloproteinase responsive silk-elastinlike protein polymer. *Biomacromolecules* **2013**, 14, (3), 618.
- [240] Turk, B. E., Huang, L. L., Piro, E. T., Cantley, L. C., Determination of protease cleavage site motifs using mixture-based oriented peptide libraries. *Nature Biotechnology* **2001**, 19, (7), 661.
- [241] Vu, T. H., Werb, Z., Matrix metalloproteinases: effectors of development and normal physiology. *Genes & Development* **2000**, 14, (17), 2123.
- [242] Chamberlain, G., Fox, J., Ashton, B., Middleton, J., Concise Review: Mesenchymal Stem Cells: Their Phenotype, Differentiation Capacity, Immunological Features, and Potential for Homing. *STEM CELLS* **2007**, 25, (11), 2739.
- [243] Au, P., Tam, J., Fukumura, D., Jain, R. K., *Bone marrow-derived mesenchymal stem cells facilitate engineering of long-lasting functional vasculature*. 2008; Vol. 111, p 4551.
- [244] Davani, S., Marandin, A., Mersin, N., Royer, B., Kantelip, B., Hervé, P., Etievent, J.-P., Kantelip, J.-P., Mesenchymal Progenitor Cells Differentiate into an

- Endothelial Phenotype, Enhance Vascular Density, and Improve Heart Function in a Rat Cellular Cardiomyoplasty Model. *Circulation* **2003**, 108, (10 suppl 1), II.
- [245] Nagaya, N., Fujii, T., Iwase, T., Ohgushi, H., Itoh, T., Uematsu, M., Yamagishi, M., Mori, H., Kangawa, K., Kitamura, S., *Intravenous administration of mesenchymal stem cells improves cardiac function in rats with acute myocardial infarction through angiogenesis and myogenesis*. 2004; Vol. 287, p H2670.
- [246] Baskir, J. N., Hatton, T. A., Suter, U. W., Protein partitioning in two-phase aqueous polymer systems. *Biotechnology and Bioengineering* **1989**, 34, (4), 541.
- [247] Albertsson, P. A., *Partition of Cell Particles and Macromolecules*. Wiley: 1986.
- [248] Ausubel, F. M., Brent, R., Kingston, R. E., Moore, D. D., Seidman, J. G., Smith, J. A., Struhl, K., *Short Protocols in Molecular Biology*. Wiley: 2002.
- [249] Liu, S. C., Zhou, F. Y., Hook, M., Carson, D. D., A heparin-binding synthetic peptide of heparin/heparan sulfate-interacting protein modulates blood coagulation activities. *Proceedings of the National Academy of Sciences of the United States of America* **1997**, 94, (5), 1739.
- [250] Han, J. C., Han, G. Y., A procedure for the quantitative determination of tris(2-carboxyethyl)phosphine, an odorless reducing agent more stable and effective than dithiothreitol. *Analytical Biochemistry* **1994**, 220, (1), 5.
- [251] Chambon, F., Winter, H. H., Linear viscoelasticity at the gel point of a crosslinking PDMS with imbalanced stoichiometry. *Journal of Rheology (1978-present)* **1987**, 31, (8), 683.
- [252] Winter, H. H., Morganelli, P., Chambon, F., Stoichiometry effects on rheology of model polyurethanes at the gel point. *Macromolecules* **1988**, 21, (2), 532.
- [253] Mubeen, A., *Mechanics of Solids*. Pearson Education: 2002.
- [254] Mott, P. H., Roland, C. M., Limits to Poisson's ratio in isotropic materials. *Physical Review B* **2009**, 80, (13).
- [255] Wu, X., Sallach, R. E., Caves, J. M., Conticello, V. P., Chaikof, E. L., Deformation responses of a physically cross-linked high molecular weight elastin-like protein polymer. *Biomacromolecules* **2008**, 9, (7), 1787.
- [256] Sallach, R. E., Cui, W., Wen, J., Martinez, A., Conticello, V. P., Chaikof, E. L., Elastin-mimetic protein polymers capable of physical and chemical crosslinking. *Biomaterials* **2009**, 30, (3), 409.
- [257] Krishna, U. M., Martinez, A. W., Caves, J. M., Chaikof, E. L., Hydrazone self-crosslinking of multiphase elastin-like block copolymer networks. *Acta biomaterialia* **2012**, 8, (3), 988.
- [258] Teng, W., Cappello, J., Wu, X., Recombinant Silk-Elastinlike Protein Polymer Displays Elasticity Comparable to Elastin. *Biomacromolecules* **2009**, 10, (11), 3028.
- [259] Qiu, W., Huang, Y., Teng, W., Cohn, C. M., Cappello, J., Wu, X., Complete Recombinant Silk-Elastinlike Protein-Based Tissue Scaffold. *Biomacromolecules* **2010**, 11, (12), 3219.
- [260] Bellingham, C. M., Lillie, M. A., Gosline, J. M., Wright, G. M., Starcher, B. C., Bailey, A. J., Woodhouse, K. A., Keeley, F. W., Recombinant human elastin

- polypeptides self-assemble into biomaterials with elastin-like properties. *Biopolymers* **2003**, 70, (4), 445.
- [261] Naficy, S., Brown, H. R., Razal, J. M., Spinks, G. M., Whitten, P. G., Progress Toward Robust Polymer Hydrogels. *Australian Journal of Chemistry* **2011**, 64, (8), 1007.
- [262] Huang, N. F., Li, S., Mesenchymal stem cells for vascular regeneration. *Regenerative Medicine* **2008**, 3, (6), 877.
- [263] Beijerinck, M. W., *Kolloidz* **1910**, 7, 16.
- [264] Walter, H., *Partitioning In Aqueous Two – Phase System: Theory, Methods, Uses, And Applications To Biotechnology*. Elsevier Science: 2012.
- [265] Flory, P. J., *Principles of Polymer Chemistry*. Cornell University Press: 1953.
- [266] McPherson, A., A brief-history of protein crystal-growth. *Journal of Crystal Growth* **1991**, 110, (1-2), 1.
- [267] Hedrich, H. C., Spener, F., Menge, U., Hecht, H.-J., Schmid, R. D., Large-scale purification, enzymic characterization, and crystallization of the lipase from *Geotrichum candidum*. *Enzyme and Microbial Technology* **1991**, 13, (10), 840.
- [268] Diederich, P., Amrhein, S., Hämmerling, F., Hubbuch, J., Evaluation of PEG/phosphate aqueous two-phase systems for the purification of the chicken egg white protein avidin by using high-throughput techniques. *Chemical Engineering Science* **2013**, 104, (0), 945.
- [269] Lima, Á. S., Alegre, R. M., Meirelles, A. J. A., Partitioning of pectinolytic enzymes in polyethylene glycol/potassium phosphate aqueous two-phase systems. *Carbohydrate Polymers* **2002**, 50, (1), 63.
- [270] Hatti-Kaul, R., Mattiasson, B., *Isolation and Purification of Proteins*. Taylor & Francis: 2003.
- [271] Annunziata, O., Asherie, N., Lomakin, A., Pande, J., Ogun, O., Benedek, G. B., Effect of polyethylene glycol on the liquid–liquid phase transition in aqueous protein solutions. *Proceedings of the National Academy of Sciences* **2002**, 99, (22), 14165.
- [272] Atha, D. H., Ingham, K. C., Mechanism of precipitation of proteins by polyethylene glycols. Analysis in terms of excluded volume. *Journal of Biological Chemistry* **1981**, 256, (23), 12108.
- [273] DeForest, C. A., Polizzotti, B. D., Anseth, K. S., Sequential click reactions for synthesizing and patterning three-dimensional cell microenvironments. *Nature Materials* **2009**, 8, (8), 659.
- [274] Nemir, S., Hayenga, H. N., West, J. L., PEGDA hydrogels with patterned elasticity: Novel tools for the study of cell response to substrate rigidity. *Biotechnology and Bioengineering* **2010**, 105, (3), 636.
- [275] Rueggeberg, F. A., State-of-the-art: dental photocuring—a review. *Dental Materials* **2011**, 27, (1), 39.
- [276] Maffezzoli, A., Pietra, A. D., Rengo, S., Nicolais, L., Valletta, G., Photopolymerization of dental composite matrices. *Biomaterials* **1994**, 15, (15), 1221.

- [277] Burdick, J. A., Anseth, K. S., Photoencapsulation of osteoblasts in injectable RGD-modified PEG hydrogels for bone tissue engineering. *Biomaterials* **2002**, 23, (22), 4315.
- [278] Bryant, S. J., Nuttelman, C. R., Anseth, K. S., Cytocompatibility of UV and visible light photoinitiating systems on cultured NIH/3T3 fibroblasts in vitro. *Journal of Biomaterials Science-Polymer Edition* **2000**, 11, (5), 439.
- [279] Carrico, I. S., Maskarinec, S. A., Heilshorn, S. C., Mock, M. L., Liu, J. C., Nowatzki, P. J., Franck, C., Ravichandran, G., Tirrell, D. A., Lithographic patterning of photoreactive cell-adhesive proteins. *Journal of the American Chemical Society* **2007**, 129, (16), 4874.
- [280] Culver, J. C., Hoffmann, J. C., Poché, R. A., Slater, J. H., West, J. L., Dickinson, M. E., Three-dimensional biomimetic patterning in hydrogels to guide cellular organization. *Advanced Materials* **2012**, 24, (17), 2344.
- [281] Anseth, K. S., Bowman, C. N., Brannon-Peppas, L., Mechanical properties of hydrogels and their experimental determination. *Biomaterials* **1996**, 17, (17), 1647.
- [282] Slaughter, B. V., Khurshid, S. S., Fisher, O. Z., Khademhosseini, A., Peppas, N. A., Hydrogels in Regenerative Medicine. *Advanced Materials* **2009**, 21, (32-33), 3307.
- [283] Anseth, K. S., Wang, C. M., Bowman, C. N., Reaction behaviour and kinetic constants for photopolymerizations of multi(meth)acrylate monomers. *Polymer* **1994**, 35, (15), 3243.
- [284] Raphael, J., Parisi-Amon, A., Heilshorn, S. C., Photoreactive elastin-like proteins for use as versatile bioactive materials and surface coatings. *Journal of Materials Chemistry* **2012**, 22, (37), 19429.
- [285] Nagapudi, K., Brinkman, W. T., Leisen, J. E., Huang, L., McMillan, R. A., Apkarian, R. P., Conticello, V. P., Chaikof, E. L., Photomediated solid-state cross-linking of an elastin-mimetic recombinant protein polymer. *Macromolecules* **2002**, 35, (5), 1730.
- [286] Xiao, W., He, J., Nichol, J. W., Wang, L., Hutson, C. B., Wang, B., Du, Y., Fan, H., Khademhosseini, A., Synthesis and characterization of photocrosslinkable gelatin and silk fibroin interpenetrating polymer network hydrogels. *Acta biomaterialia* **2011**, 7, (6), 2384.
- [287] Wang, H., Zhou, L., Liao, J., Tan, Y., Ouyang, K., Ning, C., Ni, G., Tan, G., Cell-laden photocrosslinked GelMA–DexMA copolymer hydrogels with tunable mechanical properties for tissue engineering. *Journal of Materials Science: Materials in Medicine* **2014**, 25, (9), 2173.
- [288] Daniele, M. A., Adams, A. A., Naciri, J., North, S. H., Ligler, F. S., Interpenetrating networks based on gelatin methacrylamide and PEG formed using concurrent thiol click chemistries for hydrogel tissue engineering scaffolds. *Biomaterials* **2014**, 35, (6), 1845.
- [289] Shin, H., Olsen, B. D., Khademhosseini, A., The mechanical properties and cytotoxicity of cell-laden double-network hydrogels based on photocrosslinkable gelatin and gellan gum biomacromolecules. *Biomaterials* **2012**, 33, (11), 3143.

- [290] Hutson, C. B., Nichol, J. W., Aubin, H., Bae, H., Yamanlar, S., Al-Haque, S., Koshy, S. T., Khademhosseini, A., Synthesis and Characterization of Tunable Poly(Ethylene Glycol): Gelatin Methacrylate Composite Hydrogels. *Tissue Engineering Part A* **2011**, 17, (13-14), 1713.
- [291] Nichol, J. W., Koshy, S. T., Bae, H., Hwang, C. M., Yamanlar, S., Khademhosseini, A., Cell-laden microengineered gelatin methacrylate hydrogels. *Biomaterials* **2010**, 31, (21), 5536.
- [292] Albany, L., Seliktar, D., Biosynthetic hydrogel scaffolds made from fibrinogen and polyethylene glycol for 3D cell cultures. *Biomaterials* **2005**, 26, (15), 2467.
- [293] Elvin, C. M., Vuocolo, T., Brownlee, A. G., Sando, L., Huson, M. G., Liyou, N. E., Stockwell, P. R., Lyons, R. E., Kim, M., Edwards, G. A., A highly elastic tissue sealant based on photopolymerised gelatin. *Biomaterials* **2010**, 31, (32), 8323.
- [294] Lee, B. H., Tin, S. P. H., Chaw, S. Y., Cao, Y., Xia, Y., Steele, T. W. J., Seliktar, D., Bianco-Peled, H., Venkatraman, S. S., Influence of soluble PEG-OH incorporation in a 3D cell-laden PEG-fibrinogen (PF) hydrogel on smooth muscle cell morphology and growth. *Journal of Biomaterials Science, Polymer Edition* **2013**, 25, (4), 394.
- [295] Van den Bulcke, A. I., Bogdanov, B., De Rooze, N., Schacht, E. H., Cornelissen, M., Berghmans, H., Structural and rheological properties of methacrylamide modified gelatin hydrogels. *Biomacromolecules* **2000**, 1, (1), 31.
- [296] Benton, J. A., DeForest, C. A., Vivekanandan, V., Anseth, K. S., Photocrosslinking of gelatin macromers to synthesize porous hydrogels that promote valvular interstitial cell function. *Tissue Engineering Part A* **2009**, 15, (11), 3221.
- [297] Dikovsky, D., Bianco-Peled, H., Seliktar, D., The effect of structural alterations of PEG-fibrinogen hydrogel scaffolds on 3-D cellular morphology and cellular migration. *Biomaterials* **2006**, 27, (8), 1496.
- [298] Aubin, H., Nichol, J. W., Hutson, C. B., Bae, H., Sieminski, A. L., Cropek, D. M., Akhyari, P., Khademhosseini, A., Directed 3D cell alignment and elongation in microengineered hydrogels. *Biomaterials* **2010**, 31, (27), 6941.
- [299] Chen, Y.-C., Lin, R.-Z., Qi, H., Yang, Y., Bae, H., Melero-Martin, J. M., Khademhosseini, A., Functional human vascular network generated in photocrosslinkable gelatin methacrylate hydrogels. *Advanced Functional Materials* **2012**, 22, (10), 2027.
- [300] Hoyle, C. E., Bowman, C. N., Thiol–Ene Click Chemistry. *Angewandte Chemie International Edition* **2010**, 49, (9), 1540.
- [301] Lowe, A. B., Bowman, C. N., *Thiol-X Chemistries in Polymer and Materials Science*. Royal Society of Chemistry: 2013.
- [302] Kloxin, A. M., Kloxin, C. J., Bowman, C. N., Anseth, K. S., Mechanical Properties of Cellularly Responsive Hydrogels and Their Experimental Determination. *Advanced Materials* **2010**, 22, (31), 3484.
- [303] Lin, C.-C., Raza, A., Shih, H., PEG hydrogels formed by thiol-ene photo-click chemistry and their effect on the formation and recovery of insulin-secreting cell spheroids. *Biomaterials* **2011**, 32, (36), 9685.

- [304] *The QIAexpressionist*. 5th ed.; QIAGEN, Inc.: 2003.
- [305] Fairbanks, B. D., Schwartz, M. P., Bowman, C. N., Anseth, K. S., Photoinitiated polymerization of PEG-diacrylate with lithium phenyl-2,4,6-trimethylbenzoylphosphinate: polymerization rate and cytocompatibility. *Biomaterials* **2009**, 30, (35), 6702.
- [306] Grillet, A. M., Wyatt, N. B., Gloe, L. M., Polymer Gel Rheology and Adhesion. In *Rheology*, De Vicente, J., Ed. InTech: 2012; pp 59.
- [307] Todd, I., Spickett, G., *Lecture Notes: Immunology*. Wiley: 2011.
- [308] Cruse, J. M., Lewis, R. E., *Atlas of Immunology, Third Edition*. Taylor & Francis: 2010.
- [309] Haines-Butterick, L. A., Salick, D. A., Pochan, D. J., Schneider, J. P., In vitro assessment of the pro-inflammatory potential of  $\beta$ -hairpin peptide hydrogels. *Biomaterials* **2008**, 29, (31), 4164.

## Appendix

### LICENSES FOR COPYRIGHTED MATERIAL

#### CHAPTER 1

Reproduced in part from Ref. [87].

**SPRINGER LICENSE  
TERMS AND CONDITIONS**

Apr 03, 2015

---

---

This is a License Agreement between Christopher L McGann ("You") and Springer ("Springer") provided by Copyright Clearance Center ("CCC"). The license consists of your order details, the terms and conditions provided by Springer, and the payment terms and conditions.

**All payments must be made in full to CCC. For payment instructions, please see information listed at the bottom of this form.**

License Number	3601400472918
License date	Apr 03, 2015
Licensed content publisher	Springer
Licensed content publication	Springer eBook
Licensed content title	Elastomeric Polypeptides
Licensed content author	Mark B. van Eldijk
Licensed content date	Jan 1, 2011
Type of Use	Thesis/Dissertation
Portion	Excerpts
Author of this Springer article	Yes and you are the sole author of the new work
Order reference number	A006
Title of your thesis / dissertation	RESILIN-LIKE POLYPEPTIDE-POLY(ETHYLENE GYLCOL) HYBRID HYDROGELS FOR MECHANICALLY-DEMANDING TISSUE ENGINEERING APPLICATIONS
Expected completion date	May 2015
Estimated size(pages)	200
Total	0.00 USD
Terms and Conditions	

#### Introduction

The publisher for this copyrighted material is Springer Science + Business Media. By clicking "accept" in connection with completing this licensing transaction, you agree that the following terms and conditions apply to this transaction (along with the Billing and Payment terms and conditions established by Copyright Clearance Center, Inc. ("CCC"), at

the time that you opened your Rightslink account and that are available at any time at <http://myaccount.copyright.com>).

#### Limited License

With reference to your request to reprint in your thesis material on which Springer Science and Business Media control the copyright, permission is granted, free of charge, for the use indicated in your enquiry.

Licenses are for one-time use only with a maximum distribution equal to the number that you identified in the licensing process.

This License includes use in an electronic form, provided its password protected or on the university's intranet or repository, including UMI (according to the definition at the Sherpa website: <http://www.sherpa.ac.uk/romeo/>). For any other electronic use, please contact Springer at ([permissions.dordrecht@springer.com](mailto:permissions.dordrecht@springer.com) or [permissions.heidelberg@springer.com](mailto:permissions.heidelberg@springer.com)).

The material can only be used for the purpose of defending your thesis limited to university-use only. If the thesis is going to be published, permission needs to be re-obtained (selecting "book/textbook" as the type of use).

Although Springer holds copyright to the material and is entitled to negotiate on rights, this license is only valid, subject to a courtesy information to the author (address is given with the article/chapter) and provided it concerns original material which does not carry references to other sources (if material in question appears with credit to another source, authorization from that source is required as well).

Permission free of charge on this occasion does not prejudice any rights we might have to charge for reproduction of our copyrighted material in the future.

#### Altering/Modifying Material: Not Permitted

You may not alter or modify the material in any manner. Abbreviations, additions, deletions and/or any other alterations shall be made only with prior written authorization of the author(s) and/or Springer Science + Business Media. (Please contact Springer at ([permissions.dordrecht@springer.com](mailto:permissions.dordrecht@springer.com) or [permissions.heidelberg@springer.com](mailto:permissions.heidelberg@springer.com)))

#### Reservation of Rights

Springer Science + Business Media reserves all rights not specifically granted in the combination of (i) the license details provided by you and accepted in the course of this licensing transaction, (ii) these terms and conditions and (iii) CCC's Billing and Payment terms and conditions.

#### Copyright Notice:Disclaimer

You must include the following copyright and permission notice in connection with any reproduction of the licensed material: "Springer and the original publisher /journal title, volume, year of publication, page, chapter/article title, name(s) of author(s), figure number(s), original copyright notice) is given to the publication in which the material was originally published, by adding; with kind permission from Springer Science and Business Media"

Warranties: None

Example 1: Springer Science + Business Media makes no representations or warranties with respect to the licensed material.

Example 2: Springer Science + Business Media makes no representations or warranties with respect to the licensed material and adopts on its own behalf the limitations and disclaimers established by CCC on its behalf in its Billing and Payment terms and conditions for this licensing transaction.

#### Indemnity

You hereby indemnify and agree to hold harmless Springer Science + Business Media and CCC, and their respective officers, directors, employees and agents, from and against any and all claims arising out of your use of the licensed material other than as specifically authorized pursuant to this license.

#### No Transfer of License

This license is personal to you and may not be sublicensed, assigned, or transferred by you to any other person without Springer Science + Business Media's written permission.

#### No Amendment Except in Writing

This license may not be amended except in a writing signed by both parties (or, in the case of Springer Science + Business Media, by CCC on Springer Science + Business Media's behalf).

#### Objection to Contrary Terms

Springer Science + Business Media hereby objects to any terms contained in any purchase order, acknowledgment, check endorsement or other writing prepared by you, which terms are inconsistent with these terms and conditions or CCC's Billing and Payment terms and conditions. These terms and conditions, together with CCC's Billing and Payment terms and conditions (which are incorporated herein), comprise the entire agreement between you and Springer Science + Business Media (and CCC) concerning this licensing transaction. In the event of any conflict between your obligations established by these terms and conditions and those established by CCC's Billing and Payment terms and conditions, these

terms and conditions shall control.

#### Jurisdiction

All disputes that may arise in connection with this present License, or the breach thereof, shall be settled exclusively by arbitration, to be held in The Netherlands, in accordance with Dutch law, and to be conducted under the Rules of the 'Netherlands Arbitrage Instituut' (Netherlands Institute of Arbitration).**OR:**

**All disputes that may arise in connection with this present License, or the breach thereof, shall be settled exclusively by arbitration, to be held in the Federal Republic of Germany, in accordance with German law.**

#### Other terms and conditions:

#### v1.3

Questions? [customercare@copyright.com](mailto:customercare@copyright.com) or +1-855-239-3415 (toll free in the US) or +1-978-646-2777.

Gratis licenses (referencing \$0 in the Total field) are free. Please retain this printable license for your reference. No payment is required.

## CHAPTER 2

Reproduced in its entirety from Ref. [104].

### JOHN WILEY AND SONS LICENSE TERMS AND CONDITIONS

Mar 30, 2015

---

---

This Agreement between Christopher L McGann ("You") and John Wiley and Sons ("John Wiley and Sons") consists of your license details and the terms and conditions provided by John Wiley and Sons and Copyright Clearance Center.

License Number	3598920913351
License date	Mar 30, 2015
Licensed Content Publisher	John Wiley and Sons
Licensed Content Publication	Macromolecular Chemistry and Physics
Licensed Content Title	Resilin-Based Hybrid Hydrogels for Cardiovascular Tissue Engineering
Licensed Content Author	Christopher L. McGann, Eric A. Levenson, Kristi L. Kiick
Licensed Content Date	Nov 21, 2012

Pages	11
Type of use	Dissertation/Thesis
Requestor type	Author of this Wiley article
Format	Print and electronic
Portion	Full article
Will you be translating?	No
Order reference number	A006
Title of your thesis / dissertation	RESILIN-LIKE POLYPEPTIDE-POLY(ETHYLENE GYLCOL) HYBRID HYDROGELS FOR MECHANICALLY-DEMANDING TISSUE ENGINEERING APPLICATIONS
Expected completion date	May 2015
Expected size (number of pages)	200
Requestor Location	Christopher L McGann 201 DuPont Hall  Newark, DE 19716 United States Attn: Christopher L McGann
Billing Type	Invoice
Billing Address	Christopher L McGann 201 DuPont Hall  Newark, DE 19716 United States Attn: Christopher L McGann
Total	0.00 USD
Terms and Conditions	

### TERMS AND CONDITIONS

This copyrighted material is owned by or exclusively licensed to John Wiley & Sons, Inc. or one of its group companies (each a "Wiley Company") or handled on behalf of a society with which a Wiley Company has exclusive publishing rights in relation to a particular work (collectively "WILEY"). By clicking  in connection with completing this licensing transaction, you agree that the following terms and conditions apply to this transaction (along with the billing and payment terms and conditions established by the Copyright Clearance Center Inc., ("CCC's Billing and Payment terms and conditions"), at the time that you opened your Rightslink account (these are available at any time at <http://myaccount.copyright.com>).

## Terms and Conditions

- The materials you have requested permission to reproduce or reuse (the "Wiley Materials") are protected by copyright.
- You are hereby granted a personal, non-exclusive, non-sub licensable (on a stand-alone basis), non-transferable, worldwide, limited license to reproduce the Wiley Materials for the purpose specified in the licensing process. This license is for a one-time use only and limited to any maximum distribution number specified in the license. The first instance of republication or reuse granted by this licence must be completed within two years of the date of the grant of this licence (although copies prepared before the end date may be distributed thereafter). The Wiley Materials shall not be used in any other manner or for any other purpose, beyond what is granted in the license. Permission is granted subject to an appropriate acknowledgement given to the author, title of the material/book/journal and the publisher. You shall also duplicate the copyright notice that appears in the Wiley publication in your use of the Wiley Material. Permission is also granted on the understanding that nowhere in the text is a previously published source acknowledged for all or part of this Wiley Material. Any third party content is expressly excluded from this permission.
- With respect to the Wiley Materials, all rights are reserved. Except as expressly granted by the terms of the license, no part of the Wiley Materials may be copied, modified, adapted (except for minor reformatting required by the new Publication), translated, reproduced, transferred or distributed, in any form or by any means, and no derivative works may be made based on the Wiley Materials without the prior permission of the respective copyright owner. You may not alter, remove or suppress in any manner any copyright, trademark or other notices displayed by the Wiley Materials. You may not license, rent, sell, loan, lease, pledge, offer as security, transfer or assign the Wiley Materials on a stand-alone basis, or any of the rights granted to you hereunder to any other person.
- The Wiley Materials and all of the intellectual property rights therein shall at all times remain the exclusive property of John Wiley & Sons Inc, the Wiley Companies, or their respective licensors, and your interest therein is only that of having possession of and the right to reproduce the Wiley Materials pursuant to Section 2 herein during the continuance of this Agreement. You agree that you own no right, title or interest in or to the Wiley Materials or any of the intellectual property rights therein. You shall have no rights hereunder other than the license as provided for above in Section 2. No right, license or interest to any trademark, trade name, service mark or other branding ("Marks") of WILEY or its licensors is granted hereunder, and you agree that you shall not assert any such right, license or

interest with respect thereto.

- NEITHER WILEY NOR ITS LICENSORS MAKES ANY WARRANTY OR REPRESENTATION OF ANY KIND TO YOU OR ANY THIRD PARTY, EXPRESS, IMPLIED OR STATUTORY, WITH RESPECT TO THE MATERIALS OR THE ACCURACY OF ANY INFORMATION CONTAINED IN THE MATERIALS, INCLUDING, WITHOUT LIMITATION, ANY IMPLIED WARRANTY OF MERCHANTABILITY, ACCURACY, SATISFACTORY QUALITY, FITNESS FOR A PARTICULAR PURPOSE, USABILITY, INTEGRATION OR NON-INFRINGEMENT AND ALL SUCH WARRANTIES ARE HEREBY EXCLUDED BY WILEY AND ITS LICENSORS AND WAIVED BY YOU
- WILEY shall have the right to terminate this Agreement immediately upon breach of this Agreement by you.
- You shall indemnify, defend and hold harmless WILEY, its Licensors and their respective directors, officers, agents and employees, from and against any actual or threatened claims, demands, causes of action or proceedings arising from any breach of this Agreement by you.
- IN NO EVENT SHALL WILEY OR ITS LICENSORS BE LIABLE TO YOU OR ANY OTHER PARTY OR ANY OTHER PERSON OR ENTITY FOR ANY SPECIAL, CONSEQUENTIAL, INCIDENTAL, INDIRECT, EXEMPLARY OR PUNITIVE DAMAGES, HOWEVER CAUSED, ARISING OUT OF OR IN CONNECTION WITH THE DOWNLOADING, PROVISIONING, VIEWING OR USE OF THE MATERIALS REGARDLESS OF THE FORM OF ACTION, WHETHER FOR BREACH OF CONTRACT, BREACH OF WARRANTY, TORT, NEGLIGENCE, INFRINGEMENT OR OTHERWISE (INCLUDING, WITHOUT LIMITATION, DAMAGES BASED ON LOSS OF PROFITS, DATA, FILES, USE, BUSINESS OPPORTUNITY OR CLAIMS OF THIRD PARTIES), AND WHETHER OR NOT THE PARTY HAS BEEN ADVISED OF THE POSSIBILITY OF SUCH DAMAGES. THIS LIMITATION SHALL APPLY NOTWITHSTANDING ANY FAILURE OF ESSENTIAL PURPOSE OF ANY LIMITED REMEDY PROVIDED HEREIN.
- Should any provision of this Agreement be held by a court of competent jurisdiction to be illegal, invalid, or unenforceable, that provision shall be deemed amended to achieve as nearly as possible the same economic effect as the original provision, and the legality, validity and enforceability of the remaining provisions of this Agreement shall not be affected or impaired thereby.
- The failure of either party to enforce any term or condition of this Agreement shall not constitute a waiver of either party's right to enforce each and every term and

condition of this Agreement. No breach under this agreement shall be deemed waived or excused by either party unless such waiver or consent is in writing signed by the party granting such waiver or consent. The waiver by or consent of a party to a breach of any provision of this Agreement shall not operate or be construed as a waiver of or consent to any other or subsequent breach by such other party.

- This Agreement may not be assigned (including by operation of law or otherwise) by you without WILEY's prior written consent.
- Any fee required for this permission shall be non-refundable after thirty (30) days from receipt by the CCC.
- These terms and conditions together with CCC's Billing and Payment terms and conditions (which are incorporated herein) form the entire agreement between you and WILEY concerning this licensing transaction and (in the absence of fraud) supersedes all prior agreements and representations of the parties, oral or written. This Agreement may not be amended except in writing signed by both parties. This Agreement shall be binding upon and inure to the benefit of the parties' successors, legal representatives, and authorized assigns.
- In the event of any conflict between your obligations established by these terms and conditions and those established by CCC's Billing and Payment terms and conditions, these terms and conditions shall prevail.
- WILEY expressly reserves all rights not specifically granted in the combination of (i) the license details provided by you and accepted in the course of this licensing transaction, (ii) these terms and conditions and (iii) CCC's Billing and Payment terms and conditions.
- This Agreement will be void if the Type of Use, Format, Circulation, or Requestor Type was misrepresented during the licensing process.
- This Agreement shall be governed by and construed in accordance with the laws of the State of New York, USA, without regards to such state's conflict of law rules. Any legal action, suit or proceeding arising out of or relating to these Terms and Conditions or the breach thereof shall be instituted in a court of competent jurisdiction in New York County in the State of New York in the United States of America and each party hereby consents and submits to the personal jurisdiction of such court, waives any objection to venue in such court and consents to service of process by registered or certified mail, return receipt requested, at the last known address of such party.

## WILEY OPEN ACCESS TERMS AND CONDITIONS

Wiley Publishes Open Access Articles in fully Open Access Journals and in Subscription journals offering Online Open. Although most of the fully Open Access journals publish open access articles under the terms of the Creative Commons Attribution (CC BY) License only, the subscription journals and a few of the Open Access Journals offer a choice of Creative Commons Licenses:: Creative Commons Attribution (CC-BY) license [Creative Commons Attribution Non-Commercial \(CC-BY-NC\) license](#) and [Creative Commons Attribution Non-Commercial-NoDerivs \(CC-BY-NC-ND\) License](#). The license type is clearly identified on the article.

Copyright in any research article in a journal published as Open Access under a Creative Commons License is retained by the author(s). Authors grant Wiley a license to publish the article and identify itself as the original publisher. Authors also grant any third party the right to use the article freely as long as its integrity is maintained and its original authors, citation details and publisher are identified as follows: [Title of Article/Author/Journal Title and Volume/Issue. Copyright (c) [year] [copyright owner as specified in the Journal]. Links to the final article on Wiley's website are encouraged where applicable.

### The Creative Commons Attribution License

The [Creative Commons Attribution License \(CC-BY\)](#) allows users to copy, distribute and transmit an article, adapt the article and make commercial use of the article. The CC-BY license permits commercial and non-commercial re-use of an open access article, as long as the author is properly attributed.

The Creative Commons Attribution License does not affect the moral rights of authors, including without limitation the right not to have their work subjected to derogatory treatment. It also does not affect any other rights held by authors or third parties in the article, including without limitation the rights of privacy and publicity. Use of the article must not assert or imply, whether implicitly or explicitly, any connection with, endorsement or sponsorship of such use by the author, publisher or any other party associated with the article.

For any reuse or distribution, users must include the copyright notice and make clear to others that the article is made available under a Creative Commons Attribution license, linking to the relevant Creative Commons web page.

To the fullest extent permitted by applicable law, the article is made available as is and without representation or warranties of any kind whether express, implied, statutory or otherwise and including, without limitation, warranties of title, merchantability, fitness for a particular purpose, non-infringement, absence of defects, accuracy, or the presence or

absence of errors.

### **Creative Commons Attribution Non-Commercial License**

The [Creative Commons Attribution Non-Commercial \(CC-BY-NC\) License](#) permits use, distribution and reproduction in any medium, provided the original work is properly cited and is not used for commercial purposes.(see below)

### **Creative Commons Attribution-Non-Commercial-NoDerivs License**

The [Creative Commons Attribution Non-Commercial-NoDerivs License](#) (CC-BY-NC-ND) permits use, distribution and reproduction in any medium, provided the original work is properly cited, is not used for commercial purposes and no modifications or adaptations are made. (see below)

### **Use by non-commercial users**

For non-commercial and non-promotional purposes, individual users may access, download, copy, display and redistribute to colleagues Wiley Open Access articles, as well as adapt, translate, text- and data-mine the content subject to the following conditions:

- The authors' moral rights are not compromised. These rights include the right of "paternity" (also known as "attribution" - the right for the author to be identified as such) and "integrity" (the right for the author not to have the work altered in such a way that the author's reputation or integrity may be impugned).
- Where content in the article is identified as belonging to a third party, it is the obligation of the user to ensure that any reuse complies with the copyright policies of the owner of that content.
- If article content is copied, downloaded or otherwise reused for non-commercial research and education purposes, a link to the appropriate bibliographic citation (authors, journal, article title, volume, issue, page numbers, DOI and the link to the definitive published version on **Wiley Online Library**) should be maintained. Copyright notices and disclaimers must not be deleted.
- Any translations, for which a prior translation agreement with Wiley has not been agreed, must prominently display the statement: "This is an unofficial translation of an article that appeared in a Wiley publication. The publisher has not endorsed this translation."

### **Use by commercial "for-profit" organisations**

Use of Wiley Open Access articles for commercial, promotional, or marketing purposes requires further explicit permission from Wiley and will be subject to a fee. Commercial purposes include:

- Copying or downloading of articles, or linking to such articles for further redistribution, sale or licensing;
- Copying, downloading or posting by a site or service that incorporates advertising with such content;
- The inclusion or incorporation of article content in other works or services (other than normal quotations with an appropriate citation) that is then available for sale or licensing, for a fee (for example, a compilation produced for marketing purposes, inclusion in a sales pack)
- Use of article content (other than normal quotations with appropriate citation) by for-profit organisations for promotional purposes
- Linking to article content in e-mails redistributed for promotional, marketing or educational purposes;
- Use for the purposes of monetary reward by means of sale, resale, licence, loan, transfer or other form of commercial exploitation such as marketing products
- Print reprints of Wiley Open Access articles can be purchased from: [corporatesales@wiley.com](mailto:corporatesales@wiley.com)

Further details can be found on Wiley Online

Library <http://olabout.wiley.com/WileyCDA/Section/id-410895.html>

Other Terms and Conditions:

**v1.9**

**Questions? [customercare@copyright.com](mailto:customercare@copyright.com) or +1-855-239-3415 (toll free in the US) or +1-978-646-2777.**

**Gratis licenses (referencing \$0 in the Total field) are free. Please retain this printable license for your reference. No payment is required.**



**TABLE 1.1** Reproduced from Ref. [15]. Published by The Royal Society of Chemistry. This article is licensed under a Creative Commons Attribution-NonCommercial 3.0 Unported Licence. Material from this article can be used in other publications provided that the correct acknowledgement is given with the reproduced material and it is not used for commercial purposes.

**TABLE 1.2** Reproduced from Ref. [112].

**ELSEVIER LICENSE  
TERMS AND CONDITIONS**

Apr 06, 2015

---

---

This is a License Agreement between Christopher L McGann ("You") and Elsevier ("Elsevier") provided by Copyright Clearance Center ("CCC"). The license consists of your order details, the terms and conditions provided by Elsevier, and the payment terms and conditions.

**All payments must be made in full to CCC. For payment instructions, please see information listed at the bottom of this form.**

Supplier	Elsevier Limited The Boulevard, Langford Lane Kidlington, Oxford, OX5 1GB, UK
Registered Company Number	1982084
Customer name	Christopher L McGann
Customer address	201 DuPont Hall Newark, DE 19716
License number	3603161322901
License date	Apr 06, 2015
Licensed content publisher	Elsevier
Licensed content publication	Biochimica et Biophysica Acta
Licensed content title	Amino acid composition of a new rubber-like protein, resilin

Licensed content author	Kenneth Bailey,Torkel Weis-Fogh
Licensed content date	15 April 1961
Licensed content volume number	48
Licensed content issue number	3
Number of pages	8
Start Page	452
End Page	459
Type of Use	reuse in a thesis/dissertation
Portion	figures/tables/illustrations
Number of figures/tables/illustrations	1
Format	both print and electronic
Are you the author of this Elsevier article?	No
Will you be translating?	No
Order reference number	A008
Original figure numbers	Table 1
Title of your thesis/dissertation	RESILIN-LIKE POLYPEPTIDE-POLY(ETHYLENE GLYCOL) HYBRID HYDROGELS FOR MECHANICALLY-DEMANDING TISSUE ENGINEERING APPLICATIONS
Expected completion date	May 2015
Estimated size (number of pages)	200
Elsevier VAT number	GB 494 6272 12
Permissions price	0.00 USD
VAT/Local Sales Tax	0.00 USD / 0.00 GBP
Total	0.00 USD
Terms and Conditions	

## **INTRODUCTION**

1. The publisher for this copyrighted material is Elsevier. By clicking "accept" in connection with completing this licensing transaction, you agree that the following terms and conditions apply to this transaction (along with the Billing and Payment terms and conditions established by Copyright Clearance Center, Inc. ("CCC"), at the time that you opened your Rightslink account and that are available at any time at <http://myaccount.copyright.com>).

## GENERAL TERMS

2. Elsevier hereby grants you permission to reproduce the aforementioned material subject to the terms and conditions indicated.

3. Acknowledgement: If any part of the material to be used (for example, figures) has appeared in our publication with credit or acknowledgement to another source, permission must also be sought from that source. If such permission is not obtained then that material may not be included in your publication/copies. Suitable acknowledgement to the source must be made, either as a footnote or in a reference list at the end of your publication, as follows:

"Reprinted from Publication title, Vol /edition number, Author(s), Title of article / title of chapter, Pages No., Copyright (Year), with permission from Elsevier [OR APPLICABLE SOCIETY COPYRIGHT OWNER]." Also Lancet special credit - "Reprinted from The Lancet, Vol. number, Author(s), Title of article, Pages No., Copyright (Year), with permission from Elsevier."

4. Reproduction of this material is confined to the purpose and/or media for which permission is hereby given.

5. Altering/Modifying Material: Not Permitted. However figures and illustrations may be altered/adapted minimally to serve your work. Any other abbreviations, additions, deletions and/or any other alterations shall be made only with prior written authorization of Elsevier Ltd. (Please contact Elsevier at [permissions@elsevier.com](mailto:permissions@elsevier.com))

6. If the permission fee for the requested use of our material is waived in this instance, please be advised that your future requests for Elsevier materials may attract a fee.

7. Reservation of Rights: Publisher reserves all rights not specifically granted in the combination of (i) the license details provided by you and accepted in the course of this licensing transaction, (ii) these terms and conditions and (iii) CCC's Billing and Payment terms and conditions.

8. License Contingent Upon Payment: While you may exercise the rights licensed immediately upon issuance of the license at the end of the licensing process for the transaction, provided that you have disclosed complete and accurate details of your proposed use, no license is finally effective unless and until full payment is received from you (either by publisher or by CCC) as provided in CCC's Billing and Payment terms and conditions. If full payment is not received on a timely basis, then any license preliminarily granted shall be deemed automatically revoked and shall be void as if never granted. Further, in the event that you breach any of these terms and conditions or any of

CCC's Billing and Payment terms and conditions, the license is automatically revoked and shall be void as if never granted. Use of materials as described in a revoked license, as well as any use of the materials beyond the scope of an unrevoked license, may constitute copyright infringement and publisher reserves the right to take any and all action to protect its copyright in the materials.

9. Warranties: Publisher makes no representations or warranties with respect to the licensed material.

10. Indemnity: You hereby indemnify and agree to hold harmless publisher and CCC, and their respective officers, directors, employees and agents, from and against any and all claims arising out of your use of the licensed material other than as specifically authorized pursuant to this license.

11. No Transfer of License: This license is personal to you and may not be sublicensed, assigned, or transferred by you to any other person without publisher's written permission.

12. No Amendment Except in Writing: This license may not be amended except in a writing signed by both parties (or, in the case of publisher, by CCC on publisher's behalf).

13. Objection to Contrary Terms: Publisher hereby objects to any terms contained in any purchase order, acknowledgment, check endorsement or other writing prepared by you, which terms are inconsistent with these terms and conditions or CCC's Billing and Payment terms and conditions. These terms and conditions, together with CCC's Billing and Payment terms and conditions (which are incorporated herein), comprise the entire agreement between you and publisher (and CCC) concerning this licensing transaction. In the event of any conflict between your obligations established by these terms and conditions and those established by CCC's Billing and Payment terms and conditions, these terms and conditions shall control.

14. Revocation: Elsevier or Copyright Clearance Center may deny the permissions described in this License at their sole discretion, for any reason or no reason, with a full refund payable to you. Notice of such denial will be made using the contact information provided by you. Failure to receive such notice will not alter or invalidate the denial. In no event will Elsevier or Copyright Clearance Center be responsible or liable for any costs, expenses or damage incurred by you as a result of a denial of your permission request, other than a refund of the amount(s) paid by you to Elsevier and/or Copyright Clearance Center for denied permissions.

#### **LIMITED LICENSE**

The following terms and conditions apply only to specific license types:

**15. Translation:** This permission is granted for non-exclusive world **English** rights only unless your license was granted for translation rights. If you licensed translation rights you may only translate this content into the languages you requested. A professional translator must perform all translations and reproduce the content word for word preserving the integrity of the article. If this license is to re-use 1 or 2 figures then permission is granted for non-exclusive world rights in all languages.

**16. Posting licensed content on any Website:** The following terms and conditions apply as follows: Licensing material from an Elsevier journal: All content posted to the web site must maintain the copyright information line on the bottom of each image; A hyper-text must be included to the Homepage of the journal from which you are licensing at <http://www.sciencedirect.com/science/journal/xxxxx> or the Elsevier homepage for books at <http://www.elsevier.com>; Central Storage: This license does not include permission for a scanned version of the material to be stored in a central repository such as that provided by Heron/XanEdu.

Licensing material from an Elsevier book: A hyper-text link must be included to the Elsevier homepage at <http://www.elsevier.com>. All content posted to the web site must maintain the copyright information line on the bottom of each image.

**Posting licensed content on Electronic reserve:** In addition to the above the following clauses are applicable: The web site must be password-protected and made available only to bona fide students registered on a relevant course. This permission is granted for 1 year only. You may obtain a new license for future website posting.

**17. For journal authors:** the following clauses are applicable in addition to the above:

**Preprints:**

A preprint is an author's own write-up of research results and analysis, it has not been peer-reviewed, nor has it had any other value added to it by a publisher (such as formatting, copyright, technical enhancement etc.).

Authors can share their preprints anywhere at any time. Preprints should not be added to or enhanced in any way in order to appear more like, or to substitute for, the final versions of articles however authors can update their preprints on arXiv or RePEc with their Accepted Author Manuscript (see below).

If accepted for publication, we encourage authors to link from the preprint to their formal

publication via its DOI. Millions of researchers have access to the formal publications on ScienceDirect, and so links will help users to find, access, cite and use the best available version. Please note that Cell Press, The Lancet and some society-owned have different preprint policies. Information on these policies is available on the journal homepage.

**Accepted Author Manuscripts:** An accepted author manuscript is the manuscript of an article that has been accepted for publication and which typically includes author-incorporated changes suggested during submission, peer review and editor-author communications.

Authors can share their accepted author manuscript:

- – immediately
  - via their non-commercial person homepage or blog
  - by updating a preprint in arXiv or RePEc with the accepted manuscript
  - via their research institute or institutional repository for internal institutional uses or as part of an invitation-only research collaboration work-group
  - directly by providing copies to their students or to research collaborators for their personal use
  - for private scholarly sharing as part of an invitation-only work group on commercial sites with which Elsevier has an agreement
- – after the embargo period
  - via non-commercial hosting platforms such as their institutional repository
  - via commercial sites with which Elsevier has an agreement

In all cases accepted manuscripts should:

- – link to the formal publication via its DOI
- – bear a CC-BY-NC-ND license - this is easy to do
- – if aggregated with other manuscripts, for example in a repository or other site, be shared in alignment with our hosting policy not be added to or enhanced in any way to appear more like, or to substitute for, the published journal article.

**Published journal article (JPA):** A published journal article (PJA) is the definitive final record of published research that appears or will appear in the journal and embodies all value-adding publishing activities including peer review co-ordination, copy-editing, formatting, (if relevant) pagination and online enrichment.

Policies for sharing publishing journal articles differ for subscription and gold open access

articles:

**Subscription Articles:** If you are an author, please share a link to your article rather than the full-text. Millions of researchers have access to the formal publications on ScienceDirect, and so links will help your users to find, access, cite, and use the best available version.

Theses and dissertations which contain embedded PJAs as part of the formal submission can be posted publicly by the awarding institution with DOI links back to the formal publications on ScienceDirect.

If you are affiliated with a library that subscribes to ScienceDirect you have additional private sharing rights for others' research accessed under that agreement. This includes use for classroom teaching and internal training at the institution (including use in course packs and courseware programs), and inclusion of the article for grant funding purposes.

**Gold Open Access Articles:** May be shared according to the author-selected end-user license and should contain a [CrossMark logo](#), the end user license, and a DOI link to the formal publication on ScienceDirect.

Please refer to Elsevier's [posting policy](#) for further information.

18. **For book authors** the following clauses are applicable in addition to the above: Authors are permitted to place a brief summary of their work online only. You are not allowed to download and post the published electronic version of your chapter, nor may you scan the printed edition to create an electronic version. **Posting to a repository:** Authors are permitted to post a summary of their chapter only in their institution's repository.

19. **Thesis/Dissertation:** If your license is for use in a thesis/dissertation your thesis may be submitted to your institution in either print or electronic form. Should your thesis be published commercially, please reapply for permission. These requirements include permission for the Library and Archives of Canada to supply single copies, on demand, of the complete thesis and include permission for Proquest/UMI to supply single copies, on demand, of the complete thesis. Should your thesis be published commercially, please reapply for permission. Theses and dissertations which contain embedded PJAs as part of the formal submission can be posted publicly by the awarding institution with DOI links back to the formal publications on ScienceDirect.

## **Elsevier Open Access Terms and Conditions**

You can publish open access with Elsevier in hundreds of open access journals or in nearly 2000 established subscription journals that support open access publishing. Permitted third party re-use of these open access articles is defined by the author's choice of Creative Commons user license. See our [open access license policy](#) for more information.

### **Terms & Conditions applicable to all Open Access articles published with Elsevier:**

Any reuse of the article must not represent the author as endorsing the adaptation of the article nor should the article be modified in such a way as to damage the author's honour or reputation. If any changes have been made, such changes must be clearly indicated.

The author(s) must be appropriately credited and we ask that you include the end user license and a DOI link to the formal publication on ScienceDirect.

If any part of the material to be used (for example, figures) has appeared in our publication with credit or acknowledgement to another source it is the responsibility of the user to ensure their reuse complies with the terms and conditions determined by the rights holder.

### **Additional Terms & Conditions applicable to each Creative Commons user license:**

**CC BY:** The CC-BY license allows users to copy, to create extracts, abstracts and new works from the Article, to alter and revise the Article and to make commercial use of the Article (including reuse and/or resale of the Article by commercial entities), provided the user gives appropriate credit (with a link to the formal publication through the relevant DOI), provides a link to the license, indicates if changes were made and the licensor is not represented as endorsing the use made of the work. The full details of the license are available at <http://creativecommons.org/licenses/by/4.0>.

**CC BY NC SA:** The CC BY-NC-SA license allows users to copy, to create extracts, abstracts and new works from the Article, to alter and revise the Article, provided this is not done for commercial purposes, and that the user gives appropriate credit (with a link to the formal publication through the relevant DOI), provides a link to the license, indicates if changes were made and the licensor is not represented as endorsing the use made of the work. Further, any new works must be made available on the same conditions. The full details of the license are available at <http://creativecommons.org/licenses/by-nc-sa/4.0>.

**CC BY NC ND:** The CC BY-NC-ND license allows users to copy and distribute the

Article, provided this is not done for commercial purposes and further does not permit distribution of the Article if it is changed or edited in any way, and provided the user gives appropriate credit (with a link to the formal publication through the relevant DOI), provides a link to the license, and that the licensor is not represented as endorsing the use made of the work. The full details of the license are available at <http://creativecommons.org/licenses/by-nc-nd/4.0>. Any commercial reuse of Open Access articles published with a CC BY NC SA or CC BY NC ND license requires permission from Elsevier and will be subject to a fee.

Commercial reuse includes:

- – Associating advertising with the full text of the Article
- – Charging fees for document delivery or access
- – Article aggregation
- – Systematic distribution via e-mail lists or share buttons

Posting or linking by commercial companies for use by customers of those companies.

## 20. Other Conditions:

Questions? [customer@copyright.com](mailto:customer@copyright.com) or +1-855-239-3415 (toll free in the US) or +1-978-646-2777.

**Gratis licenses (referencing \$0 in the Total field) are free. Please retain this printable license for your reference. No payment is required.**

**TABLE 1.3 & TABLE 1.4** Reproduced from Ref. [87].

### **SPRINGER LICENSE TERMS AND CONDITIONS**

Mar 30, 2015

---

---

This is a License Agreement between Christopher L McGann ("You") and Springer ("Springer") provided by Copyright Clearance Center ("CCC"). The license consists of your order details, the terms and conditions provided by Springer, and the payment terms and conditions.

**All payments must be made in full to CCC. For payment instructions, please see**

**information listed at the bottom of this form.**

License Number	3598900102158
License date	Mar 30, 2015
Licensed content publisher	Springer
Licensed content publication	Springer eBook
Licensed content title	Elastomeric Polypeptides
Licensed content author	Mark B. van Eldijk
Licensed content date	Jan 1, 2011
Type of Use	Thesis/Dissertation
Portion	Figures
Author of this Springer article	Yes and you are the sole author of the new work
Order reference number	A002
Original figure numbers	Table 2 and Table 4
Title of your thesis / dissertation	RESILIN-LIKE POLYPEPTIDE-POLY(ETHYLENE GLYCOL) HYBRID HYDROGELS FOR MECHANICALLY-DEMANDING TISSUE ENGINEERING APPLICATIONS
Expected completion date	May 2015
Estimated size(pages)	200
Total	0.00 USD

**Terms and Conditions**

**Introduction**

The publisher for this copyrighted material is Springer Science + Business Media. By clicking "accept" in connection with completing this licensing transaction, you agree that the following terms and conditions apply to this transaction (along with the Billing and Payment terms and conditions established by Copyright Clearance Center, Inc. ("CCC"), at the time that you opened your Rightslink account and that are available at any time at <http://myaccount.copyright.com>).

**Limited License**

With reference to your request to reprint in your thesis material on which Springer Science and Business Media control the copyright, permission is granted, free of charge, for the use indicated in your enquiry.

Licenses are for one-time use only with a maximum distribution equal to the number that you identified in the licensing process.

This License includes use in an electronic form, provided its password protected or on the

university's intranet or repository, including UMI (according to the definition at the Sherpa website: <http://www.sherpa.ac.uk/romeo/>). For any other electronic use, please contact Springer at ([permissions.dordrecht@springer.com](mailto:permissions.dordrecht@springer.com) or [permissions.heidelberg@springer.com](mailto:permissions.heidelberg@springer.com)).

The material can only be used for the purpose of defending your thesis limited to university-use only. If the thesis is going to be published, permission needs to be re-obtained (selecting "book/textbook" as the type of use).

Although Springer holds copyright to the material and is entitled to negotiate on rights, this license is only valid, subject to a courtesy information to the author (address is given with the article/chapter) and provided it concerns original material which does not carry references to other sources (if material in question appears with credit to another source, authorization from that source is required as well).

Permission free of charge on this occasion does not prejudice any rights we might have to charge for reproduction of our copyrighted material in the future.

#### Altering/Modifying Material: Not Permitted

You may not alter or modify the material in any manner. Abbreviations, additions, deletions and/or any other alterations shall be made only with prior written authorization of the author(s) and/or Springer Science + Business Media. (Please contact Springer at ([permissions.dordrecht@springer.com](mailto:permissions.dordrecht@springer.com) or [permissions.heidelberg@springer.com](mailto:permissions.heidelberg@springer.com)))

#### Reservation of Rights

Springer Science + Business Media reserves all rights not specifically granted in the combination of (i) the license details provided by you and accepted in the course of this licensing transaction, (ii) these terms and conditions and (iii) CCC's Billing and Payment terms and conditions.

#### Copyright Notice:Disclaimer

You must include the following copyright and permission notice in connection with any reproduction of the licensed material: "Springer and the original publisher /journal title, volume, year of publication, page, chapter/article title, name(s) of author(s), figure number(s), original copyright notice) is given to the publication in which the material was originally published, by adding; with kind permission from Springer Science and Business Media"

#### Warranties: None

Example 1: Springer Science + Business Media makes no representations or warranties

with respect to the licensed material.

Example 2: Springer Science + Business Media makes no representations or warranties with respect to the licensed material and adopts on its own behalf the limitations and disclaimers established by CCC on its behalf in its Billing and Payment terms and conditions for this licensing transaction.

#### Indemnity

You hereby indemnify and agree to hold harmless Springer Science + Business Media and CCC, and their respective officers, directors, employees and agents, from and against any and all claims arising out of your use of the licensed material other than as specifically authorized pursuant to this license.

#### No Transfer of License

This license is personal to you and may not be sublicensed, assigned, or transferred by you to any other person without Springer Science + Business Media's written permission.

#### No Amendment Except in Writing

This license may not be amended except in a writing signed by both parties (or, in the case of Springer Science + Business Media, by CCC on Springer Science + Business Media's behalf).

#### Objection to Contrary Terms

Springer Science + Business Media hereby objects to any terms contained in any purchase order, acknowledgment, check endorsement or other writing prepared by you, which terms are inconsistent with these terms and conditions or CCC's Billing and Payment terms and conditions. These terms and conditions, together with CCC's Billing and Payment terms and conditions (which are incorporated herein), comprise the entire agreement between you and Springer Science + Business Media (and CCC) concerning this licensing transaction. In the event of any conflict between your obligations established by these terms and conditions and those established by CCC's Billing and Payment terms and conditions, these terms and conditions shall control.

#### Jurisdiction

All disputes that may arise in connection with this present License, or the breach thereof, shall be settled exclusively by arbitration, to be held in The Netherlands, in accordance with Dutch law, and to be conducted under the Rules of the 'Netherlands Arbitrage Instituut' (Netherlands Institute of Arbitration).**OR:**

**All disputes that may arise in connection with this present License, or the breach thereof, shall be settled exclusively by arbitration, to be held in the Federal Republic**

of Germany, in accordance with German law.

**Other terms and conditions:**

v1.3

Questions? [customercare@copyright.com](mailto:customercare@copyright.com) or +1-855-239-3415 (toll free in the US) or +1-978-646-2777.

**Gratis licenses (referencing \$0 in the Total field) are free. Please retain this printable license for your reference. No payment is required.**

---

---

FIGURE 1.3 Reproduced from Ref. [138].

**ROYAL SOCIETY OF CHEMISTRY LICENSE  
TERMS AND CONDITIONS**

Mar 30, 2015

---

---

This is a License Agreement between Christopher L McGann ("You") and Royal Society of Chemistry ("Royal Society of Chemistry") provided by Copyright Clearance Center ("CCC"). The license consists of your order details, the terms and conditions provided by Royal Society of Chemistry, and the payment terms and conditions.

**All payments must be made in full to CCC. For payment instructions, please see information listed at the bottom of this form.**

License Number	3598890217268
License date	Mar 30, 2015
Licensed content publisher	Royal Society of Chemistry
Licensed content publication	Journal of Materials Chemistry B
Licensed content title	Multi-responsive biomaterials and nanobioconjugates from resilin-like protein polymers
Licensed content author	Rajkamal Balu, Jasmin Whittaker, Naba K. Dutta, Christopher M. Elvin, Namita R. Choudhury
Licensed content date	Jun 25, 2014
Volume number	2
Issue number	36
Type of Use	Thesis/Dissertation

Requestor type	academic/educational
Portion	figures/tables/images
Number of figures/tables/images	1
Format	print and electronic
Distribution quantity	1000
Will you be translating?	no
Order reference number	A001
Title of the thesis/dissertation	RESILIN-LIKE POLYPEPTIDE-POLY(ETHYLENE GLYCOL) HYBRID HYDROGELS FOR MECHANICALLY-DEMANDING TISSUE ENGINEERING APPLICATIONS
Expected completion date	May 2015
Estimated size	200
Total	0.00 USD

#### Terms and Conditions

This License Agreement is between {Requestor Name} ("You") and The Royal Society of Chemistry ("RSC") provided by the Copyright Clearance Center ("CCC"). The license consists of your order details, the terms and conditions provided by the Royal Society of Chemistry, and the payment terms and conditions.

### RSC / TERMS AND CONDITIONS

#### INTRODUCTION

The publisher for this copyrighted material is The Royal Society of Chemistry. By clicking "accept" in connection with completing this licensing transaction, you agree that the following terms and conditions apply to this transaction (along with the Billing and Payment terms and conditions established by CCC, at the time that you opened your RightsLink account and that are available at any time at .

#### LICENSE GRANTED

The RSC hereby grants you a non-exclusive license to use the aforementioned material anywhere in the world subject to the terms and conditions indicated herein. Reproduction of the material is confined to the purpose and/or media for which permission is hereby given.

#### RESERVATION OF RIGHTS

The RSC reserves all rights not specifically granted in the combination of (i) the license details provided by your and accepted in the course of this licensing transaction; (ii) these terms and conditions; and (iii) CCC's Billing and Payment terms and conditions.

#### REVOCATION

The RSC reserves the right to revoke this license for any reason, including, but not limited to, advertising and promotional uses of RSC content, third party usage, and incorrect source figure attribution.

#### THIRD-PARTY MATERIAL DISCLAIMER

If part of the material to be used (for example, a figure) has appeared in the RSC publication with credit to another source, permission must also be sought from that source. If the other source is another RSC publication these details should be included in your RightsLink request. If the other source is a third party, permission must be obtained from the third party. The RSC disclaims any responsibility for the reproduction you make of items owned by a third party.

#### PAYMENT OF FEE

If the permission fee for the requested material is waived in this instance, please be advised that any future requests for the reproduction of RSC materials may attract a fee.

#### ACKNOWLEDGEMENT

The reproduction of the licensed material must be accompanied by the following acknowledgement:

Reproduced (“Adapted” or “in part”) from {Reference Citation} (or Ref XX) with permission of The Royal Society of Chemistry.

If the licensed material is being reproduced from New Journal of Chemistry (NJC), Photochemical & Photobiological Sciences (PPS) or Physical Chemistry Chemical Physics (PCCP) you must include one of the following acknowledgements:

For figures originally published in NJC:

Reproduced (“Adapted” or “in part”) from {Reference Citation} (or Ref XX) with permission of The Royal Society of Chemistry (RSC) on behalf of the European Society for Photobiology, the European Photochemistry Association and the RSC.

For figures originally published in PPS:

Reproduced (“Adapted” or “in part”) from {Reference Citation} (or Ref XX) with permission of The Royal Society of Chemistry (RSC) on behalf of the Centre National de la Recherche Scientifique (CNRS) and the RSC.

For figures originally published in PCCP:

Reproduced (“Adapted” or “in part”) from {Reference Citation} (or Ref XX) with

permission of the PCCP Owner Societies.

#### **HYPertext LINKS**

With any material which is being reproduced in electronic form, you must include a hypertext link to the original RSC article on the RSC's website. The recommended form for the hyperlink is <http://dx.doi.org/10.1039/DOI> suffix, for example in the link <http://dx.doi.org/10.1039/b110420a> the DOI suffix is 'b110420a'. To find the relevant DOI suffix for the RSC article in question, go to the Journals section of the website and locate the article in the list of papers for the volume and issue of your specific journal. You will find the DOI suffix quoted there.

#### **LICENSE CONTINGENT ON PAYMENT**

While you may exercise the rights licensed immediately upon issuance of the license at the end of the licensing process for the transaction, provided that you have disclosed complete and accurate details of your proposed use, no license is finally effective unless and until full payment is received from you (by CCC) as provided in CCC's Billing and Payment terms and conditions. If full payment is not received on a timely basis, then any license preliminarily granted shall be deemed automatically revoked and shall be void as if never granted. Further, in the event that you breach any of these terms and conditions or any of CCC's Billing and Payment terms and conditions, the license is automatically revoked and shall be void as if never granted. Use of materials as described in a revoked license, as well as any use of the materials beyond the scope of an unrevoked license, may constitute copyright infringement and the RSC reserves the right to take any and all action to protect its copyright in the materials.

#### **WARRANTIES**

The RSC makes no representations or warranties with respect to the licensed material.

#### **INDEMNITY**

You hereby indemnify and agree to hold harmless the RSC and the CCC, and their respective officers, directors, trustees, employees and agents, from and against any and all claims arising out of your use of the licensed material other than as specifically authorized pursuant to this licence.

#### **NO TRANSFER OF LICENSE**

This license is personal to you or your publisher and may not be sublicensed, assigned, or transferred by you to any other person without the RSC's written permission.

#### **NO AMENDMENT EXCEPT IN WRITING**

This license may not be amended except in a writing signed by both parties (or, in the case of "Other Conditions, v1.2", by CCC on the RSC's behalf).

## OBJECTION TO CONTRARY TERMS

You hereby acknowledge and agree that these terms and conditions, together with CCC's Billing and Payment terms and conditions (which are incorporated herein), comprise the entire agreement between you and the RSC (and CCC) concerning this licensing transaction, to the exclusion of all other terms and conditions, written or verbal, express or implied (including any terms contained in any purchase order, acknowledgment, check endorsement or other writing prepared by you). In the event of any conflict between your obligations established by these terms and conditions and those established by CCC's Billing and Payment terms and conditions, these terms and conditions shall control.

## JURISDICTION

This license transaction shall be governed by and construed in accordance with the laws of the District of Columbia. You hereby agree to submit to the jurisdiction of the courts located in the District of Columbia for purposes of resolving any disputes that may arise in connection with this licensing transaction.

## LIMITED LICENSE

The following terms and conditions apply to specific license types:

### Translation

This permission is granted for non-exclusive world English rights only unless your license was granted for translation rights. If you licensed translation rights you may only translate this content into the languages you requested. A professional translator must perform all translations and reproduce the content word for word preserving the integrity of the article.

### Intranet

If the licensed material is being posted on an Intranet, the Intranet is to be password-protected and made available only to bona fide students or employees only. All content posted to the Intranet must maintain the copyright information line on the bottom of each image. You must also fully reference the material and include a hypertext link as specified above.

### Copies of Whole Articles

All copies of whole articles must maintain, if available, the copyright information line on the bottom of each page.

### Other Conditions

v1.2

Gratis licenses (referencing \$0 in the Total field) are free. Please retain this printable license for your reference. No payment is required.

If you would like to pay for this license now, please remit this license along with your payment made payable to "COPYRIGHT CLEARANCE CENTER" otherwise you will be invoiced within 48 hours of the license date. Payment should be in the form of a check or money order referencing your account number and this invoice number (Invoice Number).

Once you receive your invoice for this order, you may pay your invoice by credit card.

Please follow instructions provided at that time.

Make Payment To:  
Copyright Clearance Center  
Dept 001  
P.O. Box 843006  
Boston, MA 02284-3006

For suggestions or comments regarding this order, contact Rightslink Customer Support: [customercare@copyright.com](mailto:customercare@copyright.com) or +1-855-239-3415 (toll free in the US) or +1-978-646-2777.

**Questions? [customercare@copyright.com](mailto:customercare@copyright.com) or +1-855-239-3415 (toll free in the US) or +1-978-646-2777.**

**Gratis licenses (referencing \$0 in the Total field) are free. Please retain this printable license for your reference. No payment is required.**

**FIGURE 1.5** Reproduced from Ref. [169].

Copyright Clearance Center  
**RightsLink**<sup>®</sup>  
Home Account Info Help

ACS Publications Title: Expression, Cross-Linking, and Characterization of Recombinant Chitin Binding Resilin  
Author: Guokui Qin, Shaul Lapidot, Keiji Numata, et al  
Publication: Biomacromolecules  
Publisher: American Chemical Society  
Date: Dec 1, 2009  
Copyright © 2009, American Chemical Society

Logged in as:  
Christopher McGann  
Account #: 3000309309  
LOGOUT

**PERMISSION/LICENSE IS GRANTED FOR YOUR ORDER AT NO CHARGE**

This type of permission/license, instead of the standard Terms & Conditions, is sent to you because no fee is being charged for your order. Please note the following:

- Permission is granted for your request in both print and electronic formats, and translations.
- If figures and/or tables were requested, they may be adapted or used in part.
- Please print this page for your records and send a copy of it to your publisher/graduate school.
- Appropriate credit for the requested material should be given as follows: "Reprinted (adapted) with permission from (COMPLETE REFERENCE CITATION). Copyright (YEAR) American Chemical Society." Insert appropriate information in place of the capitalized words.
- One-time permission is granted only for the use specified in your request. No additional uses are granted (such as derivative works or other editions). For any other uses, please submit a new request.

If credit is given to another source for the material you requested, permission must be obtained from that source.

BACK

CLOSE WINDOW

Copyright © 2015 Copyright Clearance Center, Inc. All Rights Reserved. [Privacy statement](#). [Terms and Conditions](#).  
Comments? We would like to hear from you. E-mail us at [customercare@copyright.com](mailto:customercare@copyright.com)

**FIGURE 1.6** Reproduced from Ref. [174].

**JOHN WILEY AND SONS LICENSE  
TERMS AND CONDITIONS**

Mar 30, 2015

---

---

This Agreement between Christopher L McGann ("You") and John Wiley and Sons

("John Wiley and Sons") consists of your license details and the terms and conditions provided by John Wiley and Sons and Copyright Clearance Center.

License Number

3598901356461

License date

Mar 30, 2015

Licensed Content Publisher

John Wiley and Sons

Licensed Content Publication

Biotechnology & Bioengineering

Licensed Content Title

Purification of recombinant protein by cold-coacervation of fusion constructs incorporating resilin-inspired polypeptides

Licensed Content Author

Russell E. Lyons, Christopher M. Elvin, Karin Taylor, Nicolas Lekieffre, John A.M. Ramshaw

Licensed Content Date

Jun 11, 2012

Pages

8

Type of use

Dissertation/Thesis

Requestor type

University/Academic

Format

Print and electronic

Portion

Figure/table

Number of figures/tables

1

Original Wiley figure/table number(s)

Figure 4

Will you be translating?

No

Order reference number

A003

Title of your thesis / dissertation

RESILIN-LIKE POLYPEPTIDE-POLY(ETHYLENE GLYCOL) HYBRID HYDROGELS FOR  
MECHANICALLY-DEMANDING TISSUE ENGINEERING APPLICATIONS

Expected completion date

May 2015

Expected size (number of pages)

200

Requestor Location

Christopher L McGann  
201 DuPont Hall

Newark, DE 19716  
United States  
Attn: Christopher L McGann

Billing Type

Invoice

Billing Address

Christopher L McGann  
201 DuPont Hall

Newark, DE 19716  
United States  
Attn: Christopher L McGann

Total

0.00 USD

[Terms and Conditions](#)

## TERMS AND CONDITIONS

This copyrighted material is owned by or exclusively licensed to John Wiley & Sons, Inc. or one of its group companies (each a "Wiley Company") or handled on behalf of a society with which a Wiley Company has exclusive publishing rights in relation to a particular work (collectively "WILEY"). By clicking  accept  in connection with completing this licensing transaction, you agree that the following terms and conditions apply to this transaction (along with the billing and payment terms and conditions established by the Copyright Clearance Center Inc., ("CCC's Billing and Payment terms and conditions"), at the time that you opened your Rightslink account (these are available at any time at <http://myaccount.copyright.com>).

### Terms and Conditions

- The materials you have requested permission to reproduce or reuse (the "Wiley Materials") are protected by copyright.
- You are hereby granted a personal, non-exclusive, non-sub licensable (on a stand-alone basis), non-transferable, worldwide, limited license to reproduce the Wiley Materials for the purpose specified in the licensing process. This license is for a one-time use only and limited to any maximum distribution number specified in the license. The first instance of republication or reuse granted by this licence must be completed within two years of the date of the grant of this licence (although copies prepared before the end date may be distributed thereafter). The Wiley Materials shall not be used in any other manner or for any other purpose, beyond what is granted in the license. Permission is granted subject to an appropriate acknowledgement given to the author, title of the material/book/journal and the publisher. You shall also duplicate the copyright notice that appears in the Wiley publication in your use of the Wiley Material. Permission is also granted on the understanding that

nowhere in the text is a previously published source acknowledged for all or part of this Wiley Material. Any third party content is expressly excluded from this permission.

- With respect to the Wiley Materials, all rights are reserved. Except as expressly granted by the terms of the license, no part of the Wiley Materials may be copied, modified, adapted (except for minor reformatting required by the new Publication), translated, reproduced, transferred or distributed, in any form or by any means, and no derivative works may be made based on the Wiley Materials without the prior permission of the respective copyright owner. You may not alter, remove or suppress in any manner any copyright, trademark or other notices displayed by the Wiley Materials. You may not license, rent, sell, loan, lease, pledge, offer as security, transfer or assign the Wiley Materials on a stand-alone basis, or any of the rights granted to you hereunder to any other person.
- The Wiley Materials and all of the intellectual property rights therein shall at all times remain the exclusive property of John Wiley & Sons Inc, the Wiley Companies, or their respective licensors, and your interest therein is only that of having possession of and the right to reproduce the Wiley Materials pursuant to Section 2 herein during the continuance of this Agreement. You agree that you own no right, title or interest in or to the Wiley Materials or any of the intellectual property rights therein. You shall have no rights hereunder other than the license as provided for above in Section 2. No right, license or interest to any trademark, trade name, service mark or other branding ("Marks") of WILEY or its licensors is granted hereunder, and you agree that you shall not assert any such right, license or interest with respect thereto.
- NEITHER WILEY NOR ITS LICENSORS MAKES ANY WARRANTY OR REPRESENTATION OF ANY KIND TO YOU OR ANY THIRD PARTY, EXPRESS, IMPLIED OR STATUTORY, WITH RESPECT TO THE MATERIALS OR THE ACCURACY OF ANY INFORMATION CONTAINED IN THE MATERIALS, INCLUDING, WITHOUT LIMITATION, ANY IMPLIED WARRANTY OF MERCHANTABILITY, ACCURACY, SATISFACTORY QUALITY, FITNESS FOR A PARTICULAR PURPOSE, USABILITY, INTEGRATION OR NON-INFRINGEMENT AND ALL SUCH WARRANTIES ARE HEREBY EXCLUDED BY WILEY AND ITS LICENSORS AND WAIVED BY YOU
- WILEY shall have the right to terminate this Agreement immediately upon breach of this Agreement by you.
- You shall indemnify, defend and hold harmless WILEY, its Licensors and their respective directors, officers, agents and employees, from and against any

actual or threatened claims, demands, causes of action or proceedings arising from any breach of this Agreement by you.

- IN NO EVENT SHALL WILEY OR ITS LICENSORS BE LIABLE TO YOU OR ANY OTHER PARTY OR ANY OTHER PERSON OR ENTITY FOR ANY SPECIAL, CONSEQUENTIAL, INCIDENTAL, INDIRECT, EXEMPLARY OR PUNITIVE DAMAGES, HOWEVER CAUSED, ARISING OUT OF OR IN CONNECTION WITH THE DOWNLOADING, PROVISIONING, VIEWING OR USE OF THE MATERIALS REGARDLESS OF THE FORM OF ACTION, WHETHER FOR BREACH OF CONTRACT, BREACH OF WARRANTY, TORT, NEGLIGENCE, INFRINGEMENT OR OTHERWISE (INCLUDING, WITHOUT LIMITATION, DAMAGES BASED ON LOSS OF PROFITS, DATA, FILES, USE, BUSINESS OPPORTUNITY OR CLAIMS OF THIRD PARTIES), AND WHETHER OR NOT THE PARTY HAS BEEN ADVISED OF THE POSSIBILITY OF SUCH DAMAGES. THIS LIMITATION SHALL APPLY NOTWITHSTANDING ANY FAILURE OF ESSENTIAL PURPOSE OF ANY LIMITED REMEDY PROVIDED HEREIN.
- Should any provision of this Agreement be held by a court of competent jurisdiction to be illegal, invalid, or unenforceable, that provision shall be deemed amended to achieve as nearly as possible the same economic effect as the original provision, and the legality, validity and enforceability of the remaining provisions of this Agreement shall not be affected or impaired thereby.
- The failure of either party to enforce any term or condition of this Agreement shall not constitute a waiver of either party's right to enforce each and every term and condition of this Agreement. No breach under this agreement shall be deemed waived or excused by either party unless such waiver or consent is in writing signed by the party granting such waiver or consent. The waiver by or consent of a party to a breach of any provision of this Agreement shall not operate or be construed as a waiver of or consent to any other or subsequent breach by such other party.
- This Agreement may not be assigned (including by operation of law or otherwise) by you without WILEY's prior written consent.
- Any fee required for this permission shall be non-refundable after thirty (30) days from receipt by the CCC.
- These terms and conditions together with CCC's Billing and Payment terms and conditions (which are incorporated herein) form the entire agreement between you and WILEY concerning this licensing transaction and (in the

absence of fraud) supersedes all prior agreements and representations of the parties, oral or written. This Agreement may not be amended except in writing signed by both parties. This Agreement shall be binding upon and inure to the benefit of the parties' successors, legal representatives, and authorized assigns.

- In the event of any conflict between your obligations established by these terms and conditions and those established by CCC's Billing and Payment terms and conditions, these terms and conditions shall prevail.
- WILEY expressly reserves all rights not specifically granted in the combination of (i) the license details provided by you and accepted in the course of this licensing transaction, (ii) these terms and conditions and (iii) CCC's Billing and Payment terms and conditions.
- This Agreement will be void if the Type of Use, Format, Circulation, or Requestor Type was misrepresented during the licensing process.
- This Agreement shall be governed by and construed in accordance with the laws of the State of New York, USA, without regards to such state's conflict of law rules. Any legal action, suit or proceeding arising out of or relating to these Terms and Conditions or the breach thereof shall be instituted in a court of competent jurisdiction in New York County in the State of New York in the United States of America and each party hereby consents and submits to the personal jurisdiction of such court, waives any objection to venue in such court and consents to service of process by registered or certified mail, return receipt requested, at the last known address of such party.

## **WILEY OPEN ACCESS TERMS AND CONDITIONS**

Wiley Publishes Open Access Articles in fully Open Access Journals and in Subscription journals offering Online Open. Although most of the fully Open Access journals publish open access articles under the terms of the Creative Commons Attribution (CC BY) License only, the subscription journals and a few of the Open Access Journals offer a choice of Creative Commons Licenses: Creative Commons Attribution (CC-BY) license [Creative Commons Attribution Non-Commercial \(CC-BY-NC\) license](#) and [Creative Commons Attribution Non-Commercial-NoDerivs \(CC-BY-NC-ND\) License](#). The license type is clearly identified on the article.

Copyright in any research article in a journal published as Open Access under a Creative Commons License is retained by the author(s). Authors grant Wiley a license to publish the article and identify itself as the original publisher. Authors also grant any third party the right to use the article freely as long as its integrity is maintained and its original authors, citation details and publisher are identified as follows: [Title

of Article/Author/Journal Title and Volume/Issue. Copyright (c) [year] [copyright owner as specified in the Journal]. Links to the final article on Wiley's website are encouraged where applicable.

### **The Creative Commons Attribution License**

The [Creative Commons Attribution License \(CC-BY\)](#) allows users to copy, distribute and transmit an article, adapt the article and make commercial use of the article. The CC-BY license permits commercial and non-commercial re-use of an open access article, as long as the author is properly attributed.

The Creative Commons Attribution License does not affect the moral rights of authors, including without limitation the right not to have their work subjected to derogatory treatment. It also does not affect any other rights held by authors or third parties in the article, including without limitation the rights of privacy and publicity. Use of the article must not assert or imply, whether implicitly or explicitly, any connection with, endorsement or sponsorship of such use by the author, publisher or any other party associated with the article.

For any reuse or distribution, users must include the copyright notice and make clear to others that the article is made available under a Creative Commons Attribution license, linking to the relevant Creative Commons web page.

To the fullest extent permitted by applicable law, the article is made available as is and without representation or warranties of any kind whether express, implied, statutory or otherwise and including, without limitation, warranties of title, merchantability, fitness for a particular purpose, non-infringement, absence of defects, accuracy, or the presence or absence of errors.

### **Creative Commons Attribution Non-Commercial License**

The [Creative Commons Attribution Non-Commercial \(CC-BY-NC\) License](#) permits use, distribution and reproduction in any medium, provided the original work is properly cited and is not used for commercial purposes.(see below)

### **Creative Commons Attribution-Non-Commercial-NoDerivs License**

The [Creative Commons Attribution Non-Commercial-NoDerivs License](#) (CC-BY-NC-ND) permits use, distribution and reproduction in any medium, provided the original work is properly cited, is not used for commercial purposes and no modifications or adaptations are made. (see below)

### **Use by non-commercial users**

For non-commercial and non-promotional purposes, individual users may access, download, copy, display and redistribute to colleagues Wiley Open Access articles, as well as adapt, translate, text- and data-mine the content subject to the following conditions:

- The authors' moral rights are not compromised. These rights include the right of "paternity" (also known as "attribution" - the right for the author to be identified as such) and "integrity" (the right for the author not to have the work altered in such a way that the author's reputation or integrity may be impugned).
- Where content in the article is identified as belonging to a third party, it is the obligation of the user to ensure that any reuse complies with the copyright policies of the owner of that content.
- If article content is copied, downloaded or otherwise reused for non-commercial research and education purposes, a link to the appropriate bibliographic citation (authors, journal, article title, volume, issue, page numbers, DOI and the link to the definitive published version on **Wiley Online Library**) should be maintained. Copyright notices and disclaimers must not be deleted.
- Any translations, for which a prior translation agreement with Wiley has not been agreed, must prominently display the statement: "This is an unofficial translation of an article that appeared in a Wiley publication. The publisher has not endorsed this translation."

### **Use by commercial "for-profit" organisations**

Use of Wiley Open Access articles for commercial, promotional, or marketing purposes requires further explicit permission from Wiley and will be subject to a fee. Commercial purposes include:

- Copying or downloading of articles, or linking to such articles for further redistribution, sale or licensing;
- Copying, downloading or posting by a site or service that incorporates advertising with such content;
- The inclusion or incorporation of article content in other works or services (other than normal quotations with an appropriate citation) that is then available for sale or licensing, for a fee (for example, a compilation produced for marketing purposes, inclusion in a sales pack)

- Use of article content (other than normal quotations with appropriate citation) by for-profit organisations for promotional purposes
- Linking to article content in e-mails redistributed for promotional, marketing or educational purposes;
- Use for the purposes of monetary reward by means of sale, resale, licence, loan, transfer or other form of commercial exploitation such as marketing products
- Print reprints of Wiley Open Access articles can be purchased from: [corporatesales@wiley.com](mailto:corporatesales@wiley.com)

Further details can be found on Wiley Online

Library <http://olabout.wiley.com/WileyCDA/Section/id-410895.html>

Other Terms and Conditions:

**v1.9**

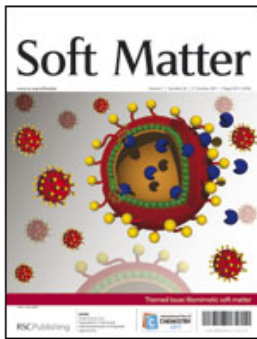
**Questions? [customercare@copyright.com](mailto:customercare@copyright.com) or +1-855-239-3415 (toll free in the US) or +1-978-646-2777.**

**Gratis licenses (referencing \$0 in the Total field) are free. Please retain this printable license for your reference. No payment is required.**

FIGURE 1.8 Reproduced from Ref. [100].

Copyright Clearance Center RightsLink®

Home Account Info Help



**Title:** Hydrophilic elastomeric biomaterials based on resilin-like polypeptides

**Author:** Manoj B. Charati, Jamie L. Ifkovits, Jason A. Burdick, Jeffery G. Linhardt, Kristi L. Kiick

**Publication:** Soft Matter

**Publisher:** Royal Society of Chemistry

**Date:** Aug 5, 2009

Copyright © 2009, Royal Society of Chemistry

Logged in as:  
Christopher McGann  
Account #:  
3000309309

LOGOUT

This reuse request is free of charge. Please review guidelines related to author permissions here:  
<http://www.rsc.org/AboutUs/Copyright/Permissionrequests.asp>

BACK

CLOSE WINDOW

Copyright © 2015 Copyright Clearance Center, Inc. All Rights Reserved. [Privacy statement](#). [Terms and Conditions](#).  
Comments? We would like to hear from you. E-mail us at [customercare@copyright.com](mailto:customercare@copyright.com)

FIGURE 1.9 Reproduced from Ref. [105].



The screenshot shows the Copyright Clearance Center RightsLink interface. At the top left is the Copyright Clearance Center logo. To its right is the RightsLink logo. Further right are three navigation buttons: Home, Account Info, and Help. Below the logos is the ACS Publications logo with the tagline "Most Trusted. Most Cited. Most Read." The main content area displays the following information:

- Title:** Tunable Mechanical Stability and Deformation Response of a Resilin-Based Elastomer
- Author:** Linqing Li, Sean Teller, Rodney J. Clifton, et al
- Publication:** Biomacromolecules
- Publisher:** American Chemical Society
- Date:** Jun 1, 2011

At the bottom of this section is the text "Copyright © 2011, American Chemical Society". On the right side of the interface, there is a user login box showing "Logged in as: Christopher McGann" and "Account #: 3000309309". Below this is a blue "LOGOUT" button.

**PERMISSION/LICENSE IS GRANTED FOR YOUR ORDER AT NO CHARGE**

This type of permission/license, instead of the standard Terms & Conditions, is sent to you because no fee is being charged for your order. Please note the following:

- Permission is granted for your request in both print and electronic formats, and translations.
- If figures and/or tables were requested, they may be adapted or used in part.
- Please print this page for your records and send a copy of it to your publisher/graduate school.
- Appropriate credit for the requested material should be given as follows: "Reprinted (adapted) with permission from (COMPLETE REFERENCE CITATION). Copyright (YEAR) American Chemical Society." Insert appropriate information in place of the capitalized words.
- One-time permission is granted only for the use specified in your request. No additional uses are granted (such as derivative works or other editions). For any other uses, please submit a new request.

If credit is given to another source for the material you requested, permission must be obtained from that source.

BACK

CLOSE WINDOW

Copyright © 2015 Copyright Clearance Center, Inc. All Rights Reserved. [Privacy statement](#). [Terms and Conditions](#). Comments? We would like to hear from you. E-mail us at [customer@copyright.com](mailto:customer@copyright.com)

FIGURE 1.10 Reproduced from Ref. [180].

**NATURE PUBLISHING GROUP LICENSE  
TERMS AND CONDITIONS**

Mar 30, 2015

---

This is a License Agreement between Christopher L McGann ("You") and Nature

Publishing Group ("Nature Publishing Group") provided by Copyright Clearance Center ("CCC"). The license consists of your order details, the terms and conditions provided by Nature Publishing Group, and the payment terms and conditions.

**All payments must be made in full to CCC. For payment instructions, please see information listed at the bottom of this form.**

License Number	3598911412410
License date	Mar 30, 2015
Licensed content publisher	Nature Publishing Group
Licensed content publication	Nature
Licensed content title	Designed biomaterials to mimic the mechanical properties of muscles
Licensed content author	Shanshan Lv, Daniel M. Dudek, Yi Cao, M. M. Balamurali, John Gosline, Hongbin Li
Licensed content date	May 6, 2010
Volume number	465
Issue number	7294
Type of Use	reuse in a dissertation / thesis
Requestor type	academic/educational
Format	print and electronic
Portion	figures/tables/illustrations
Number of figures/tables/illustrations	1
High-res required	no
Figures	Figure 1
Author of this NPG article	no
Your reference number	A004
Title of your thesis / dissertation	RESILIN-LIKE POLYPEPTIDE-POLY(ETHYLENE GLYCOL) HYBRID HYDROGELS FOR MECHANICALLY-DEMANDING TISSUE ENGINEERING APPLICATIONS
Expected completion date	May 2015
Estimated size (number of pages)	200
Total	0.00 USD
Terms and Conditions	

Terms and Conditions for Permissions

Nature Publishing Group hereby grants you a non-exclusive license to reproduce this material for this purpose, and for no other use, subject to the conditions below:

1. NPG warrants that it has, to the best of its knowledge, the rights to license reuse of this material. However, you should ensure that the material you are requesting is original to Nature Publishing Group and does not carry the copyright of another entity (as credited in the published version). If the credit line on any part of the material you have requested indicates that it was reprinted or adapted by NPG with permission from another source, then you should also seek permission from that source to reuse the material.
2. Permission granted free of charge for material in print is also usually granted for any electronic version of that work, provided that the material is incidental to the work as a whole and that the electronic version is essentially equivalent to, or substitutes for, the print version. Where print permission has been granted for a fee, separate permission must be obtained for any additional, electronic re-use (unless, as in the case of a full paper, this has already been accounted for during your initial request in the calculation of a print run). NB: In all cases, web-based use of full-text articles must be authorized separately through the 'Use on a Web Site' option when requesting permission.
3. Permission granted for a first edition does not apply to second and subsequent editions and for editions in other languages (except for signatories to the STM Permissions Guidelines, or where the first edition permission was granted for free).
4. Nature Publishing Group's permission must be acknowledged next to the figure, table or abstract in print. In electronic form, this acknowledgement must be visible at the same time as the figure/table/abstract, and must be hyperlinked to the journal's homepage.
5. The credit line should read:  
Reprinted by permission from Macmillan Publishers Ltd: [JOURNAL NAME] (reference citation), copyright (year of publication)  
For AOP papers, the credit line should read:  
Reprinted by permission from Macmillan Publishers Ltd: [JOURNAL NAME], advance online publication, day month year (doi: 10.1038/sj.[JOURNAL ACRONYM].XXXXX)

**Note: For republication from the *British Journal of Cancer*, the following credit lines apply.**

Reprinted by permission from Macmillan Publishers Ltd on behalf of Cancer Research UK: [JOURNAL NAME] (reference citation), copyright (year of publication) For AOP papers, the credit line should read:  
Reprinted by permission from Macmillan Publishers Ltd on behalf of Cancer Research UK: [JOURNAL NAME], advance online publication, day month year (doi: 10.1038/sj.[JOURNAL ACRONYM].XXXXX)

6. Adaptations of single figures do not require NPG approval. However, the adaptation should be credited as follows:  
  
Adapted by permission from Macmillan Publishers Ltd: [JOURNAL NAME] (reference citation), copyright (year of publication)

**Note: For adaptation from the *British Journal of Cancer*, the following credit line applies.**

Adapted by permission from Macmillan Publishers Ltd on behalf of Cancer Research UK: [JOURNAL NAME] (reference citation), copyright (year of publication)

7. Translations of 401 words up to a whole article require NPG approval. Please visit <http://www.macmillanmedicalcommunications.com> for more information. Translations of up to a 400 words do not require NPG approval. The translation should be credited as follows:

Translated by permission from Macmillan Publishers Ltd: [JOURNAL NAME] (reference citation), copyright (year of publication).

**Note: For translation from the *British Journal of Cancer*, the following credit line applies.**

Translated by permission from Macmillan Publishers Ltd on behalf of Cancer Research UK: [JOURNAL NAME] (reference citation), copyright (year of publication)

We are certain that all parties will benefit from this agreement and wish you the best in the use of this material. Thank you.

Special Terms:

v1.1

Questions? [customercare@copyright.com](mailto:customercare@copyright.com) or +1-855-239-3415 (toll free in the US) or +1-978-646-2777.

**Gratis licenses (referencing \$0 in the Total field) are free. Please retain this printable license for your reference. No payment is required.**

---

---

**FIGURE 5.1** Reproduced from Ref. [101].

**ROYAL SOCIETY OF CHEMISTRY LICENSE  
TERMS AND CONDITIONS**

Mar 30, 2015

---

---

This is a License Agreement between Christopher L McGann ("You") and Royal Society of Chemistry ("Royal Society of Chemistry") provided by Copyright Clearance Center ("CCC"). The license consists of your order details, the terms and conditions provided by

Royal Society of Chemistry, and the payment terms and conditions.

**All payments must be made in full to CCC. For payment instructions, please see information listed at the bottom of this form.**

License Number	3598920404734
License date	Mar 30, 2015
Licensed content publisher	Royal Society of Chemistry
Licensed content publication	Soft Matter
Licensed content title	Resilin-like polypeptide hydrogels engineered for versatile biological function
Licensed content author	Linqing Li,Zhixiang Tong,Xinqiao Jia,Kristi L. Kiick
Licensed content date	Nov 2, 2012
Volume number	9
Issue number	3
Type of Use	Thesis/Dissertation
Requestor type	academic/educational
Portion	figures/tables/images
Number of figures/tables/images	1
Format	print and electronic
Distribution quantity	1000
Will you be translating?	no
Order reference number	A005
Title of the thesis/dissertation	RESILIN-LIKE POLYPEPTIDE-POLY(ETHYLENE GLYCOL) HYBRID HYDROGELS FOR MECHANICALLY-DEMANDING TISSUE ENGINEERING APPLICATIONS
Expected completion date	May 2015
Estimated size	200
Total	0.00 USD

#### Terms and Conditions

This License Agreement is between {Requestor Name} ("You") and The Royal Society of Chemistry ("RSC") provided by the Copyright Clearance Center ("CCC"). The license consists of your order details, the terms and conditions provided by the Royal Society of Chemistry, and the payment terms and conditions.

#### RSC / TERMS AND CONDITIONS

#### INTRODUCTION

The publisher for this copyrighted material is The Royal Society of Chemistry. By clicking “accept” in connection with completing this licensing transaction, you agree that the following terms and conditions apply to this transaction (along with the Billing and Payment terms and conditions established by CCC, at the time that you opened your RightsLink account and that are available at any time at .

#### LICENSE GRANTED

The RSC hereby grants you a non-exclusive license to use the aforementioned material anywhere in the world subject to the terms and conditions indicated herein. Reproduction of the material is confined to the purpose and/or media for which permission is hereby given.

#### RESERVATION OF RIGHTS

The RSC reserves all rights not specifically granted in the combination of (i) the license details provided by your and accepted in the course of this licensing transaction; (ii) these terms and conditions; and (iii) CCC’s Billing and Payment terms and conditions.

#### REVOCATION

The RSC reserves the right to revoke this license for any reason, including, but not limited to, advertising and promotional uses of RSC content, third party usage, and incorrect source figure attribution.

#### THIRD-PARTY MATERIAL DISCLAIMER

If part of the material to be used (for example, a figure) has appeared in the RSC publication with credit to another source, permission must also be sought from that source. If the other source is another RSC publication these details should be included in your RightsLink request. If the other source is a third party, permission must be obtained from the third party. The RSC disclaims any responsibility for the reproduction you make of items owned by a third party.

#### PAYMENT OF FEE

If the permission fee for the requested material is waived in this instance, please be advised that any future requests for the reproduction of RSC materials may attract a fee.

#### ACKNOWLEDGEMENT

The reproduction of the licensed material must be accompanied by the following acknowledgement:

Reproduced (“Adapted” or “in part”) from {Reference Citation} (or Ref XX) with permission of The Royal Society of Chemistry.

If the licensed material is being reproduced from New Journal of Chemistry (NJC),

Photochemical & Photobiological Sciences (PPS) or Physical Chemistry Chemical Physics (PCCP) you must include one of the following acknowledgements:

For figures originally published in NJC:

Reproduced (“Adapted” or “in part”) from {Reference Citation} (or Ref XX) with permission of The Royal Society of Chemistry (RSC) on behalf of the European Society for Photobiology, the European Photochemistry Association and the RSC.

For figures originally published in PPS:

Reproduced (“Adapted” or “in part”) from {Reference Citation} (or Ref XX) with permission of The Royal Society of Chemistry (RSC) on behalf of the Centre National de la Recherche Scientifique (CNRS) and the RSC.

For figures originally published in PCCP:

Reproduced (“Adapted” or “in part”) from {Reference Citation} (or Ref XX) with permission of the PCCP Owner Societies.

#### **HYPertext LINKS**

With any material which is being reproduced in electronic form, you must include a hypertext link to the original RSC article on the RSC’s website. The recommended form for the hyperlink is <http://dx.doi.org/10.1039/DOI suffix>, for example in the link <http://dx.doi.org/10.1039/b110420a> the DOI suffix is ‘b110420a’. To find the relevant DOI suffix for the RSC article in question, go to the Journals section of the website and locate the article in the list of papers for the volume and issue of your specific journal. You will find the DOI suffix quoted there.

#### **LICENSE CONTINGENT ON PAYMENT**

While you may exercise the rights licensed immediately upon issuance of the license at the end of the licensing process for the transaction, provided that you have disclosed complete and accurate details of your proposed use, no license is finally effective unless and until full payment is received from you (by CCC) as provided in CCC's Billing and Payment terms and conditions. If full payment is not received on a timely basis, then any license preliminarily granted shall be deemed automatically revoked and shall be void as if never granted. Further, in the event that you breach any of these terms and conditions or any of CCC's Billing and Payment terms and conditions, the license is automatically revoked and shall be void as if never granted. Use of materials as described in a revoked license, as well as any use of the materials beyond the scope of an unrevoked license, may constitute copyright infringement and the RSC reserves the right to take any and all action to protect

its copyright in the materials.

#### WARRANTIES

The RSC makes no representations or warranties with respect to the licensed material.

#### INDEMNITY

You hereby indemnify and agree to hold harmless the RSC and the CCC, and their respective officers, directors, trustees, employees and agents, from and against any and all claims arising out of your use of the licensed material other than as specifically authorized pursuant to this licence.

#### NO TRANSFER OF LICENSE

This license is personal to you or your publisher and may not be sublicensed, assigned, or transferred by you to any other person without the RSC's written permission.

#### NO AMENDMENT EXCEPT IN WRITING

This license may not be amended except in a writing signed by both parties (or, in the case of "Other Conditions, v1.2", by CCC on the RSC's behalf).

#### OBJECTION TO CONTRARY TERMS

You hereby acknowledge and agree that these terms and conditions, together with CCC's Billing and Payment terms and conditions (which are incorporated herein), comprise the entire agreement between you and the RSC (and CCC) concerning this licensing transaction, to the exclusion of all other terms and conditions, written or verbal, express or implied (including any terms contained in any purchase order, acknowledgment, check endorsement or other writing prepared by you). In the event of any conflict between your obligations established by these terms and conditions and those established by CCC's Billing and Payment terms and conditions, these terms and conditions shall control.

#### JURISDICTION

This license transaction shall be governed by and construed in accordance with the laws of the District of Columbia. You hereby agree to submit to the jurisdiction of the courts located in the District of Columbia for purposes of resolving any disputes that may arise in connection with this licensing transaction.

#### LIMITED LICENSE

The following terms and conditions apply to specific license types:

##### Translation

This permission is granted for non-exclusive world English rights only unless your license was granted for translation rights. If you licensed translation rights you may only translate this content into the languages you requested. A professional translator must perform all

translations and reproduce the content word for word preserving the integrity of the article.

#### Intranet

If the licensed material is being posted on an Intranet, the Intranet is to be password-protected and made available only to bona fide students or employees only. All content posted to the Intranet must maintain the copyright information line on the bottom of each image. You must also fully reference the material and include a hypertext link as specified above.

#### Copies of Whole Articles

All copies of whole articles must maintain, if available, the copyright information line on the bottom of each page.

#### Other Conditions

v1.2

Gratis licenses (referencing \$0 in the Total field) are free. Please retain this printable license for your reference. No payment is required.

If you would like to pay for this license now, please remit this license along with your payment made payable to "COPYRIGHT CLEARANCE CENTER" otherwise you will be invoiced within 48 hours of the license date. Payment should be in the form of a check or money order referencing your account number and this invoice number {Invoice Number}.

Once you receive your invoice for this order, you may pay your invoice by credit card.

Please follow instructions provided at that time.

#### Make Payment To:

Copyright Clearance Center  
Dept 001  
P.O. Box 843006  
Boston, MA 02284-3006

For suggestions or comments regarding this order, contact Rightslink Customer Support: [customercare@copyright.com](mailto:customercare@copyright.com) or +1-855-239-3415 (toll free in the US) or +1-978-646-2777.

**Questions? [customercare@copyright.com](mailto:customercare@copyright.com) or +1-855-239-3415 (toll free in the US) or +1-978-646-2777.**

**Gratis licenses (referencing \$0 in the Total field) are free. Please retain this printable**

**license for your reference. No payment is required.**